MECHANISTIC INSIGHT INTO MALABARICONE C INDUCED CANCER CELL DEATH

By

MRITYUNJAY TYAGI

(LIFE01201104003)

Bhabha Atomic Research Centre, Mumbai

A thesis submitted to the

Board of Studies in Life Sciences

In partial fulfillment of requirements

For the Degree of

DOCTOR OF PHILOSOPHY

of

HOMI BHABHA NATIONAL INSTITUTE

July, 2016

STATEMENT BY AUTHOR

This dissertation has been submitted in partial fulfillment of requirements for an advanced degree at Homi Bhabha National Institute (HBNI) and is deposited in the library to be made available to borrowers under rules of the HBNI.

Brief quotations from this dissertation are allowable without special permission, provided that accurate acknowledgement of source is made. Requests for permission for extended quotation from or reproduction of this manuscript in whole or in partmay be granted by the Competent Authority of HBNI when in his or her judgment the proposed use of the material is in the interests of scholarship. In all other instances, however, permission must be obtained from the author.

(Mrityunjay Tyagi)

DECLARATION

I, hereby declare that the investigation presented in the thesis has been carried out by me. The work is original and has not been submitted earlier as a whole or in part for a degree / diploma at this or any other Institution / University.

(Mrityunjay Tyagi)

List of Publications arising from the thesis

Journal

1. “DNA damage dependent activation of checkpoint kinase-1 and mitogen-activated protein kinase-p38 are required in malabaricone C-induced mitochondrial cell death”, **M. Tyagi**, R. Bhattacharyya, A. K. Bauri, B. S. Patro and S. Chattopadhyay. BiochimicaBiophysicaActa (BBA) - General Subjects,**2014**, 840(3), 1014–1027.
2. “Mechanism of the malabaricone C-induced toxicity to the MCF-7 cell line”, **M. Tyagi**, B. S. Patro and S. Chattopadhyay, Free Radical Research, **2014**, 48(4), 466–477.

Conferences

1. International Conference on recent trends in therapeutic advancement of free radical science and 10^{th} annual meeting of the SFRR-India -2011 (Chennai, TN) – Poster Presentation.
2. International Conference on recent trends in free radical and antioxidant research and 13^{th} annual meeting of the SFRR-India-2014(Lonavala, MH) - Poster Presentation.

Others

1. **Awtar Krishan Award** by International Society for Advancement of Cytometry during Indo US workshop and The Cytometry Society-India conference-2012 (Kolkata, WB).

ACKNOWLEDGEMENTS

I am deeply indebted to my guide **Dr. B. S. Patro** for his continuous encouragement, kind support, careful nurturing and wise advice throughout the period of my PhD study.

I wish to convey my immense gratitude to **Dr. Subrata Chattopadhyay**, Group Director, BSG, BARC, for extending whole hearted support, enthusiasm and encourage to complete my Ph.D. work.

I thank Dr. A. K. Bauri for providing malabaricones as and when needed for completing the study.

Sincere appreciation is also extended to Dr. Biswanath Maity, Dr. Biplab Adhikary, Dr. Sudhir K. Yadav, Mr. Rahul Bhattacharyya, Dr. Mahesh S. Dr. Jitesh S. Rathee, Mr. Saikat Chakraborty, Mr. Bhaskar Saha and Ms. Pooja Gupta for their constant help in day to day experiments in lab. I also wish to express my thanks to the numerous other persons who have helped in some way or the other during the tenure, whose names have been omitted inadvertently.

I would like to thank BARC, Mumbai for providing me the premises and facilitiesto carry out the experiments.

Last but not least, I would like to extend my heartfelt gratitude to my family for their unfailing love and support.

CONTENTS

Homi Bhabha National Institute

Ph. D. PROGRAMME

1. Name of the Student: MRITYUNJAY TYAGI

2. Name of the Constituent Institution: BHABHA ATOMIC RESEARCH CENTRE

3. Enrolment No. : LIFE01201104003

4. Title of the Thesis: MECHANISTIC INSIGHT INTO MALABARICONE C INDUCED CANCER CELL DEATH

5. Board of Studies: LIFE SCIENCES

PREAMBLE

Cancer is a multi-step process, where gene mutations lead to defective protein expression that are unable to perform the same functions as their normal counterpart and thus leads to uncontrolled cell growth. It is a leading cause of death in both developed and developing countries. From the age when surgery and radiotherapy were the only effective way to fight tumor growth, today we reached an era of treatment modalities like chemotherapy, endocrine therapy, virotherapy and photodynamic therapy where molecular features of tumor seem to be the foundation. Despite the intensive efforts and substantial advances on improving treatments, systemic toxicity/side-effect and cancer recurrence remains a major issue. Considering a report from GLOBOCAN 2000; lifestyle, environmental factors and diet influence cancer prevalence [1]. Consumption of spice rich food has been found to play an important role in suppressing the transformative, hyperproliferative and inflammatory processes that initiate carcinogenesis. Of late, research on phytochemicals gained a tremendous attention to fight against

cancer. Currently, there are more than 600 anti-cancer clinical studies registered with www.clinicaltrials.gov involving dietary supplements or phytochemicals. Phytochemicals are small small organic molecules derived from plants/spices and are considered to fall in a safe/non-toxic category of edible compounds. These phytochemicals can be drugged in larger amount to attain increased efficacy, prevent recurrence and also as adjuvants, to potentiate other chemotherapeutic agents as well as radio-therapeutic protocols to minimize chemotherapy and radiotherapy induced toxicity. Some of the extensively studied anti-cancer phytochemicals include curcumin from tumeric, genistein from soybean, sulforaphane from broccoli, isothiocyanates from cruciferous vegetables, lycopene from tomato, apigenin from parsley, and gingerol from gingers and many more [2].

The fruit rind of *Myristica malabarica* (Myristicaceae) (popularly known as rampatri, Bombay mace or false nutmeg) is used as an exotic spice in various Indian cuisines. It is credited with hepatoprotective and antithrombotic properties, and also used in ayurvedic preparations as pasupasi and Muthu-Marunthu. Several herbal formulations containing *M. malabarica* are also claimed to possess antitumor effect [3]. However, nothing much is known about its active constituents and mechanism of its action in cancer cells. We prepared different solvent extracts from fruit rind of *M. malabarica* to isolate active constituents e.g., malabaricones and identify their anti-tumor potential. This project was undertaken to understand the mechanism of action and in establishing malabaricones, especially malabaricone C, as anticancer drugs. Further, with the backdrop of established mechanism of anti-cancer action of malabaricone C, a new therapeutic strategy was devised to augment mal C mediated cancer cell killing.

OBJECTIVES OF THE PRESENT STUDY:

1) To explore the anticancer potential of malabaricones against multiple cancer cell lines.
2) To investigate the underlying molecular mechanism of action of the highly effective malabaricones in killing cancer cells.
3) To elucidate the role of highly potential malabaricone in sensitizing cancer cells to apoptosis in response to chemotherapeutic drugs, radiation or other adjuvants.

4) To evaluate the *in vivo* anticancer ability of highly potential malabaricone in mice.

ORGANISATION OF THE THESIS. The undertaken investigation was categorized into following chapters: (1) General introduction and Review of literature

(2) Materials and Methods

(3) Results

(4) Discussion and Conclusions

(5) Bibliography

CHAPTER 1. GENERAL INTRODUCTION AND REVIEW OF LITERATURE:

This chapter gives an introduction to the research problem and relevant literature in the field of cancer. It begins with a brief introduction on cancer statistics, types of cancer, available treatment modalities and natural/synthetic anticancer drugs. Later, a detailed literature survey on targets for killing cancer cells, modes of cell death, different proteins involved in inducing apoptosis and role of glutathione and glutathionylation will be discussed. At last, history of *Myristica malabarica*, (malbaricones) in relation to health benefits will be covered.

Cancer is a complex disease involving multi-step process. It begins with initiation, followed by promotion and progression. Each year globally, 12.7 million people learn they have cancer, and 7.6 million people die from the disease. Amongst different types of cancer, the cancer that causes the most deaths overall is lung cancer, followed by stomach and liver cancer in men, while, breast cancer is the leading cause of death in women worldwide. Currently, chemotherapy, immunotherapy as well as surgery and radiation, are important clinical methods used to successfully treat cancers. Detailed pros and cons of each modality will be discussed in the thesis. Overall, conventional chemotherapy suffers high toxicity to normal/healthy cells, restricting the dosage of the drugs. Additionally, relapse of cancer is an extremely serious issue, where poor prognosis is largely attributable to the inherent or acquired resistance in cancer cells. Here, deregulated apoptotic pathways, improved DNA repair, drug transport and detoxification are the major causes of drug resistance. A section in this chapter will be especially devoted to discuss different cancer cell death evading mechanisms.

Considering the above mentioned problems with conventional chemotherapeutics, there is a burgeoning interest in finding/discovering small organic molecules (natural/synthetic), capable of killing cancer cells specifically and entrusting normal/healthy cells unharmed. Literature survey to this end show, approximately 25% of the molecules currently used in chemotherapy are plant products while another 25% are derivatives of plant products and rests are artificial (synthetically designed) molecules [4]. Further, as adjuvants, plant derived phytochemicals are proposed to potentiate the efficacy of many chemotherapeutic drugs as well as radio-therapeutic protocols to minimize chemotherapy and radiotherapy induced toxicity.

Earlier, we have found that amongst the four malabaricones A–D (designated as mal A–D), isolated from methanolic extract of fruit rind of *Myristica malabarica*, mal B and mal C possess superior antioxidant, anti-inflammatory, and anti-ulcer properties [6]. Interestingly, mal C, containing a B-ring catechol moiety showed significantly better Cu(II)-dependent nuclease activity and toxicity against MCF-7 human breast cancer cell line [7]. Based on these preliminary findings, the main objectives of this doctoral work is to evaluate the anti-cancer potential of malabaricones (especially malabaricone C), by modulating several molecular targets in cancer cell lines.

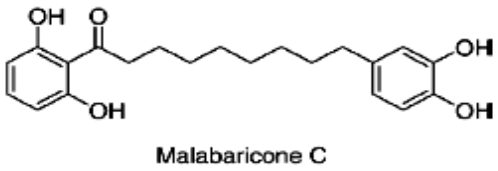

Fig. 1: Chemical structure of mal C

CHAPTER 2. MATERIALS AND METHODS:

All the cell lines used were purchased from National Centre For Cell Science, Pune. The malabaricones were isolated, purified and characterized as per the previous reports [6,8]. All other chemicals and biochemical assays kits were purchased from reputed manufacturers. MTT assay was used for initial screening of malabaricones (mal A-D) and calculating 50% or half maximal inhibitory concentration (IC_{50}). Subsequently, clonogenic and sub-G1 assay were used for quantifying reproductive capacity and cellular defragmentation respectively. Phase contrast microscopy, histone bound DNA ELISA and

Annexin V-FITC were used for quantifying apoptosis. Involvement of caspases was confirmed by both western blotting and caspase-activity assay kit. Flouorescent dyes like JC-1, 2', 7' –dichlorofluorescin diacetate (DCFDA), dihydroethidium (DHE), monobromobimane were used to study mitochondrial membrane integrity, oxidative stress, superoxide generation, and intracellular GSH respectively. Western blotting was used for quantifying different protein expressions and post-translational modifications. We also used reverse transcriptase-PCR to quantify mRNA expression of various genes relevant to the current study. Cytoplasmic, nuclear and chromatin lysates were prepared as per previous report to study subcellular localization of proteins. For *in vivo* experiments, SCID mice, purchased from Vivo Biotech, Hyderabad and C57BL/6 male mice bred at the BARC Laboratory Animal House Facility, Mumbai, India, were used after obtaining clearance from the BARC Animal Ethics Committee (BAEC, BAEC/08/13 and BAEC/06/15). The data were analyzed by paired t-test and one-way analysis of variance (ANOVA). A *p*-value of <0.05 was considered statistically significant.

CHAPTER 3. RESULTS:

3. 1. Evaluating anticancer potential of malabaricones against multiple cancer cell lines:

This chapter deals with experiments, results and analysis on the anticancer potential of malabaricones (especially mal B and mal C) in different cancer cell lines. It describes the preliminary results of two highly potential malabaricones, mal B and mal C, on A549 lung carcinoma cells wherein caspase activation, dependence on p53 etc. were analyzed.

Initially, anticancer potential of malabaricones (mal A-D) was tested against three human cancer cell lines (MCF-7, A549, and HCT-15) where in, mal B and C showed good anticancer potential and hence selected for a detailed study. Further, MTT assay was performed on total 13 cancer cell lines of human origin to calculate IC_{50} (half maximal Inhibitory Concentration) for mal B and mal C (Table 1). Our results showed mal C was slightly better than mal B when compared w.r.t IC_{50} values, derived in MTT assay.

Table 1: Anti-cancer potential of mal B and mal C. Respective cancer cells were incubated with different concentration of mal B and mal C for 48 h. IC_{50} (half maximal Inhibitory Concentration) values were obtained from conventional MTT assay.

Cell lines	Mal C (IC50/μM)	Mal B (IC50/μM)
MCF-7 (Breast Cancer)	6.9±1.2	8.8±2.2
MDA-MB-231 (p53, Missense)	7.0±1.4	8.6±1.5
HCT15 (Colon cancer) (p53, wt/mutant, missense)	8.8±1.6	9.9±2.0
A549 (Lung Cancer)	6.4±1.8	8.6±1.6
NCI-H460	7.1±2.0	9.4±1.4
NCI-H522 (p53, deletion)	7.5±1.5	8.0±1.3
NCI-H23 (p53, missense)	8.1±2.1	9.2±1.9
U2OS (Osteosarcoma)	7.2±1.7	8.2±1.5
A375 (human melanoma)	12.1±2.7	16.8±2.6
A498 (Kidney)	11.4±1.1	15.9±1.3
A431 (Skin carcinoma) (p53, Missense)	7.3±1.6	9.6±1.6
SH-SY5Y (Neuroblastoma)	6.8±1.3	9.3±2.0
IMR-32	7.6±1.4	9.8±2.1
B16F10 (mouse melanoma)	6.2±1.3	----

Further, our investigation showed that both mal B and mal C follow a different mechanism of action. Owing to minor changes in molecular scaffolds, both mal B and mal C kills cancer cells by differentially modulating p53, DNA damage, redox status and several signaling events. With the aim to elucidate a detailed mechanistic study, rest of the thesis work is exclusively focused on highly effective anti-cancer malabaricone, mal C. Further, to find if mal C is selective to cancer cells or not, we performed MTT assay in normal counterparts (L132 and WI-38) of lung cancer tissues also. Here, mal C showed ~3 fold higher cytotoxic potential against lung cancer cells (A549, NCI-H460, NCI-H522, and NCI-H23) compared to their normal counterparts (L132 and WI-38). Beside, a detailed investigation was carried out to show that mal C does not get precipitated in media and its less cytotoxicity to normal cells *vis-à-vis* cancer cells is due to reduced uptake in normal cell. To this end, various results and analyses will be included in this chapter.

3. 2. Molecular mechanism of mal C-induced cell death in A549 (lung cancer) cell line:

Malabaricone C (mal C)-induced cell death followed apoptotic route of programmed cell death (PCD), as quantified by Annexin-V-FITC, histone bound DNA through ELISA, and sub-G1 assays. We also

checked for autophagy (another PCD) but could not detect any significant activation of autophagy related proteins. Also, our experiments excluded any significant necrosis in mal C-treated A549 cells. Induction of different caspases in mal C-treated A549 cells confirmed apoptosis to be the preferred mode of cell death. Earlier, mal C has been shown to interact with plasmid DNA and generate reactive oxygen species (ROS) *in vitro* [7]. Here we found that mal C can also enter nucleus of living cell and bind DNA. This allowed mal C to induce DNA-damage as quantified by γ-H2AX formation and comet assay. Kinetics of mal C-induced DNA damage by comet assay (both alkaline and neutral) and γ-H2AX formation indicated for single strand breaks (SSB) generation which was later converted into double strand breaks (DSBs). DSB generation in mal C-treated cells was paralleled by the induction of ATM- and ATR-mediated CHK1 phosphorylation, later causing p38-MAPK activation, imbalance in BAX/BCL2 expression, mitochondrial dysfunction and cytochrome-c release. Mitochondria depletion and p38-MAPK inhibition made A549 cells resistant, but BCL2 knock-down partially sensitized the cells to mal C treatment. ATM silencing and ATR inhibition partially attenuated the mal C-induced p38-MAPK activation, CHK1 phosphorylation and apoptosis, which were completely suppressed by CHK1 inhibition. Further, combination of mal C with different chemotheraputic agents like topotecan, etoposide, mitomycin C and radiation for sensitizing A549 cells were also evaluated but no significant synergistic effect was observed.

3. 3. Molecular mechanism of mal C-induced cell death in MCF-7 (breast cancer) cell line:

A differential mode of cell killing by mal C was observed in caspase-3 deficient human breast cancer cells i.e., MCF7. To this end, a detail mechanism of action of mal C was deciphered. Here, we found that Ca^{2+} -modulators BAPTA-AM and Ru360 can partially abrogate mal C-induced apoptosis. We also detected signifcant activation of calpain in mal C-treated MCF-7 cells but its activation is indpendent of apoptosis induction. Treatment with mal C induced a marked lysosomal membrane permeabilization (LMP), along with release of cathepsin B, concomitant BID-cleavage and its translocation to mitochondria. All these results and experimental part will be discussed in thesis.

3. 4. Thiol harboring antioxidants ameliorates mal C induced apoptosis in lung carcinoma cells:

This chapter deals and starts with a novel observation that thiol antioxidants (NAC, GSH) robustly enhance mal C-induced cell death. Here, the mechanism by which thiol antioxidants inhibit mal-C induced survival factors and sequester several transcription factors in the cytoplasm to switch from the conventional transcription to death process will be discussed. The role of S-glutathionylation in above process will also be highlighted in this chapter.

Induction of DNA damage by mal C involves intracellular oxidative stress and decrease in GSH content (quantified by increase in DCF fluorescence and decrease in monobromobimane fluorescence). Presences of antioxidants (both thiols and non-thiols) were able to decrease mal C-induced intracellular ROS production. Intriguingly, non-thiol antioxidants failed to protect cancer cells from mal C-induced cell death. In contrast, thiol antioxidants like NAC and GSH enhance the apoptotic process induced by mal C not only in A549 cells but in other cell lines too (A431, U2OS and B16F10). However, in neuronal cell lines-IMR32 and SHSY5Y, NAC failed to ameliorate mal C-induced cell death process.

Enhancement in apoptosis in the presence of NAC was quantified through Annexin V/PI staining and sub-G1 assay (flow cytometry). For understanding the role of nuclear ROS, increase in the fluorescence of dihydro-ethidium (DHE) dye after mal C-treatment was studied. Our investigation showed that catechol moiety in mal C gets converted to its quinone form, as quantified by increase in λ_{max} at 480 nm. Presence of NAC helped in recycling mal C back to its catechol form, thus leading to further production of nuclear ROS and damaging DNA which subsequently led to cell death.

Mal C-induced oxidative stress also depletes intracellular GSH. Thiol anti-oxidants like NAC can reverse this process and maintains the GSH content (reducing environment) of mal C-treated cells at near normal. Under these cellular conditions (reducing environment) and the stress induced by mal C, S-glutathionylation of different proteins like p53 and p65 increases (as quantified by western blotting and immunoprecipitation). These glutahionylated-p65 and p53 are sequestered in the cytoplasm and hence transcription-mediated expression of several anti-apoptotic/survival factors by p65 and p53 was severely

impeded. In addition, glutathionylated-p53 accumulates in the cytoplasm and its translocation to mitochondria induces further loss of mitochondrial membrane potential (MMP) and activation of caspase-9. Results from the literature pertaining to mechanism of S-glutathionylation and NAC dependent enhancement of cell death process in the presence of other agents like gemcitabine, HEMA, leinamycin etc. will also be discussed in the thesis.

3. 5. Anti-tumor efficacy of malabaricone C in mice models:

After establishing the anticancer potential of mal C in different cell lines, the *in vivo* anti-tumor potential of mal C and NAC (alone as well as in combination) was evaluated in two mice models, SCID (using A549 cells) and C57BL/6 (using B16F10 cells). B16F10 melanoma mouse model was taken to investigate the anti-tumor potential of mal C plus NAC against other cancers. In both the models, tumors formed by respective cells were reduced after mal C (50 or 100 mg/kg, orally) treatment, when compared to vehicle treated mice. This significant reduction in tumor volume/weight was further enhanced when mice were supplemented with 100 mg/kg NAC orally. Here, we documented tumor growth kinetics using caliper and after 30 days, all mice were sacrificed, their tumor was excised, weight was taken and photographed. The results obtained from B16F10 melanoma and lung carcinoma xenograft models in C57Bl/6 and SCID mice respectively, support the potential use of mal C alone or in combination with NAC (thiol antioxidants) in the management of tumors.

CHAPTER 4. DISCUSSION AND CONCLUSIONS:

This chapter summarizes the work presented in the thesis by highlighting the important observations and results. It also enlightens new hypotheses/unanswered questions generated during this course of study. Along with several novel findings reported in the thesis, we established mal C as potential chemo-therapeutic agent against different cancer (especially A549, lung carcinoma) cell lines. Here, we established the signaling pathway of mal C-induced DSB generation in cancer cells, which activates p38 MAPK and p53, leading to BAX translocation, mitochondrial membrane potential collapse, caspase-3 activation and eventual cell death. Our observation with thiol antioxidants (like NAC or GSH) is unique and in this study we established a novel molecular mechanism behind thiol-based enhancement in

anticancer potential of mal C. Further, we provide evidence that inhibiting p65 and p53 transcription dependent survival function through S-glutathionylation can be used as a strategy for increasing the efficacy of mal C. The results obtained in this thesis will be discussed thoroughly in a broader prospective by including various supportive and anomalous reports in literature.

CHAPTER 5. BIBLIOGRAPHY:

[1] Adami, H.-O.; Hunter, D.; Trichopoulos, D. Textbook of cancer epidemiology. Second Edi. Oxford University Press; 2008.

[2] Wang, H.; Khor, T. O.; Shu, L.; Su, Z.; Fuentes, F.; Lee, J.-H.; Tony Ah-Ng, K. Plants Against Cancer: A Review on Natural Phytochemicals in Preventing and Treating Cancers and Their Druggability. *Anticancer Agents Med Chem* **12**: 1281–1305; 2012.

[3] Palani, V.; Senthilkumaran, R. K.; Govindasamy, S. Biochemical evaluation of antitumor effect of Muthu Marunthu (a herbal formulation) on experimental fibrosarcoma in rats. *J. Ethnopharmacol.* **65**: 257–265; 1999.

[4] Amin, A.; Gali-muhtasib, H.; Ocker, M.; Schneider-stock, R. Overview of Major Classes of Plant-Derived Anticancer Drugs. *Int. J. Biomed. Sci.* **5**: 1–11; 2009.

[5] Maity, B.; Yadav, S. K.; Patro, B. S.; Tyagi, M.; Bandyopadhyay, S. K.; Chattopadhyay, S. Molecular mechanism of the anti-inflammatory activity of a natural diarylnonanoid, malabaricone C. *Free Radic. Biol. Med.* **52**: 1680–1691; 2012.

[6] Patro, B. S.; Bauri, A. K.; Mishra, S.; Chattopadhyay, S. Antioxidant activity of Myristica malabarica extracts and their constituents. *J. Agric. Food Chem.* **53**: 6912–6918; 2005.

[7] Patro, B. S.; Mrityunjay, T.; Jayati, S.; Subrata, C. Comparative nuclease and anti-cancer properties of the naturally occurring malabaricones. *Bioorganic Med. Chem.* **18**: 7043–7051; 2010.

[8] Kozhiparambil K. Purushothaman, A. S. and J. D. C. Malabaricones A–D, novel diarylnonanoids from Myristica malabarica Lam (Myristicaceae). *J. Chem. Soc., Perkin Trans.* **6**: 587–588; 1977.

LIST OF Figures

LIST OF TABLES

CHAPTER-I

INTRODUCTION

AND

REVIEW OF

LITERATURE

1. 1. Cancer Incidence

Cancer is a complex disease with major public health problem worldwide wherein millions of new cancer patients are diagnosed each year and many deaths results from this disease [1]. It is associated with almost 200 types of disorders that are normally tied in with a wide range of escalating effects both at the molecular and cellular levels. In the case of cancer, an old saying "Prevention is better than cure" holds true where cure, if at all possible, is associated with high cytotoxicity to normal tissues and/or invasive procedures [2].

Each year globally, 12.7 million people learn they have cancer, and 7.6 million people die from the disease [3]. The deaths from cancer worldwide are projected to increase to more than 15 million, with an estimated 12 million deaths in 2020 [4]. According to the World Health Organization (WHO), the numbers of new cancer cases is expected to rise by about 70% over the next 20 years [3]. Talking about the worldwide stats, estimated new cases in males are predominant for lung cancer (16.7%) followed by prostate (14.9%), colon (10%), stomach (8.5%), and liver (7.4%) while in females breast cancer (25%) is predominant followed by colon (9.2%), lung (8.7%), cervix (7.9%) and stomach (4.8%) [1,5]. Estimated deaths in males worldwide are caused by lung (23.6%), liver (11.1%), stomach (10.1%), colon (8%) and prostate (6.5%) cancer, while in females it's due to breast (14.7%), lung (13.8%), colon (9%), cervix (7.5%), stomach (7.1%) and liver (6.3%) cancer [1,5]. With reference to India, NDTV reported a rise in cancer incidence to five-fold by 2025 [6]. Other agencies like GLOBOCON 2012 and Indian Council of Medical Research (ICMR) also published their stats online on developing country like India. According to the data of the National Cancer Registry Programme of the India Council of Medical Research (ICMR), the estimated mortality rate due to cancer saw an increase of six per cent approximately between 2012 and 2014. Total of 4,91,598 people died in 2014 out

of 28,20,179 cases, while in 2013 it was 4,78,180 deaths out of 29,34,314 cases reported and in 2012, around 4,65,169 people lost their lives due to the disease when the number of cases stood at 30,16,628. Also, it has been reported that around 1,300 deaths are occurring every day due to cancer [7]. Counting estimated deaths due to different types of cancers in developing countries like India, among males, lung cancer (22.2%) is the predominant site followed by cancers of the liver (14.3%), stomach (11.8%), esophagus (7.3%), colon (6.5%) and prostate (5.3%). In Indian women, breast cancer accounted for 14.3% of the total cancer death followed by cancer of the lung (12.4%), cervix (10.1%), stomach (8.2%), liver (8%) colon (7.2%) and esophagus (4.7%) (Three-year report of population based cancer registries: 2009-2011, national Cancer Registry Programme, ICMR, INDIA, 2013).

1. 2. Introduction to cancer

Cancer is fundamentally a disease of regulation of tissue growth. Cancer is multi-step process characterized by uncontrolled growth and spread of abnormal cells caused by alteration in normal cellular mechanisms that leads to the perturbation of a delicate balance between cell division and cell death to favor cell proliferation [8]. If the spread is not controlled, it can result even in death of the patient.

People suggested that in order for a normal cell to transform into a cancer cell, genes regulating cell growth and differentiation needs be altered [9]. These genetic changes can occur at many levels, from gain or loss of entire chromosomes to a mutation affecting a single DNA nucleotide [9]. Two broad categories of genes affecting these changes have been documented :- 1) Oncogenes (normal genes which are expressed at inappropriately high levels or altered genes which have novel properties). In either case, their expression promotes the malignant phenotype

of cancer cells. 2) Tumor suppressor genes (often disabled by cancer-promoting genetic changes), which inhibit cell division, survival, or other properties of cancer cells. Thus it's the changes in many genes that are required to transform a normal cell into a cancer cell [10].

1. 2. 1. Causes of cancer

Every normal cell in the body follows a path of growth, division, and death, occurring continuously and after a certain number of divisions, cell die though programmed cell death (PCD). Cancers are generated when the cell ceases to die and follow an alternative path to divide. This abnormal behavior of cells is the result of mutations in different regulatory genes (mutation in DNA). These changes may be either inherited genetically from parents or caused by external factors: - chemicals (asbestos, arsenic, alcohol, benzene, pesticides, dioxins, tobacco smoke, and polycyclic aromatic hydrocarbons (PAHs)) and radiation (UV and IR), tobacco and infectious micro-organisms like Human Papilloma Virus (HPV)) and internal factors (hormones, immune conditions, inherited mutations and mutations that occur from metabolism) [11]. Also, free radicals generated by normal physiological processes, including aerobic metabolism and inflammatory responses, to eliminate invading pathogenic microorganisms can also inflict cellular damage thus becoming a cause of cancer initiation [12].

1. 2. 2. The hallmarks of cancer

Decades of research has attempted to characterize complexity of the cancer cells and defined six hallmarks: Sustaining proliferative signaling, evading growth suppressors, resisting cell death, enabling replication immortality, inducing angiogenesis and activating invasion and metastasis [13]. Furthermore, additional hallmarks were added to the existing original six hallmarks: the ability to reprogramming energy metabolism and evading immune destruction [14] (Figure 1.1)

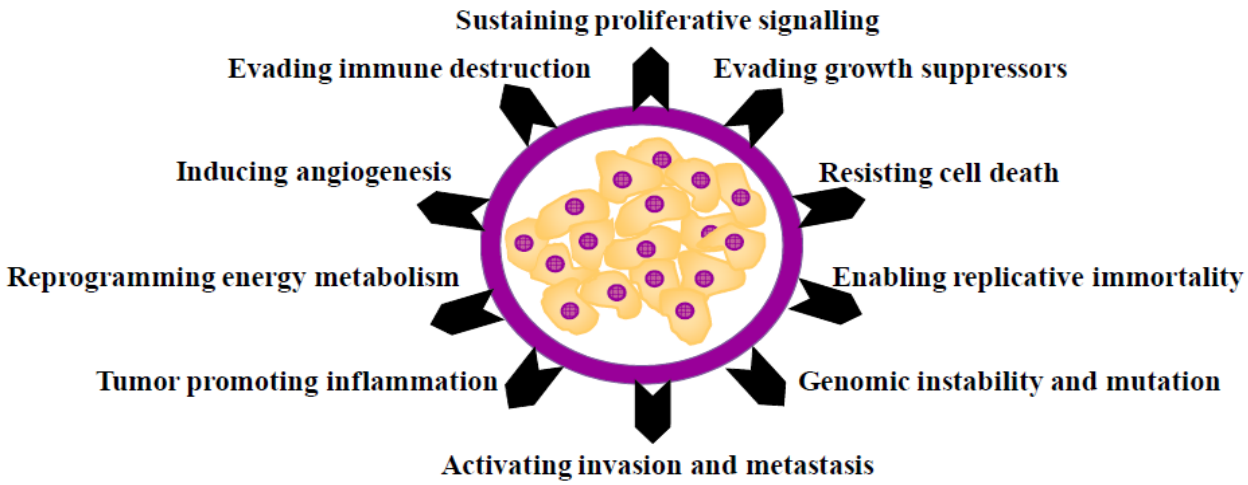

Figure 1. 1. Hallmarks of cancer. Figure showing current view of extended hallmarks and characteristics of cancer (Adapted from Hanahan & Weinberg, 2011).

1. 2. 3. Prevention of cancer

The steps taken to decrease the chances of cancer development are called cancer prevention. Years of research in the field of cancer revealed that cancer is easier to prevent than to treat. It's been found to be affected by multiple factors including our genes, lifestyle and the peripheral environment, which all governs the risk of cancer development. The following measures can be taken to reduce the risk of cancer *e.g.* healthy diet including high intake of antioxidants, less use of tobacco, less exposure to sun, exercise, immunization against viruses and bacteria etc. Vaccines such as the human papilloma virus (HPV) vaccine assist in preventing some cervical, vaginal, vulvar, and oral cancers. A vaccine for hepatitis B can reduce liver cancer risk.

1. 2. 4. Types of cancer

Cancers are broadly named according to either type of tissue in which they originate or the organ in which they are located. Based on type of tissue, below are the five broad groups to classify cancer: -

1) Carcinomas consist of cancer originating at the cells that cover internal and external parts of body. It can be further divided into two major subtypes: **Adenocarcinoma**, developing in an organ or gland, and **Squamous cell carcinoma** originating in the squamous epithelium. Most carcinomas affect organs or glands capable of secretion, such as the breasts, which produce milk, or the lungs, which secrete mucus, or colon or prostate or bladder.

2) Sarcoma refers to the cancer originating in supportive and connective tissues such as bones, tendons, cartilage and muscle.

3) Lymphomas are cancer initiating in the immune system tissues such as lymph nodes.

4) Leukemia refers to the cancers that begin in the bone marrow and often accumulate in the blood stream.

5) Adenomas are the cancers that arise in glandular tissues like thyroid, pituitary, and adrenal glands

1. 2. 5. Cancer treatment modalities

The options for cancer treatment are not limited to single rather a range of options are available which are decided by clinician seeing the stage and origin of cancer. Age, history, and lifestyle of the patient are also the deciding factor for determining the treatment modality. More often various cancer treatments are combined to give the best possible result. Currently, chemotherapy,

immunotherapy as well as surgery and radiation, are important clinical methods used to successfully treat cancers. Recently, newer treatment procedures including targeted therapy lying under personalized medicine are in practice, but they are still under developmental stage. The most popular types of cancer treatment are discussed below:-

1) **Surgery** is the oldest technique to treat cancer. It's been documented to be practice during 7th century by Egyptians to remove breast tumors. Benign tumor, where cancer does not spread around the body, offers biggest chance for cure. However, if the cancer has metastasized to other body parts/ organs, surgery won't be much beneficial.
2) **Radiotherapy or radiation therapy** uses high energy radiations to damage cancerous cells. Almost half of all people with cancer have radiotherapy as part of their treatment plan. It is used not only to cure cancer but is very effective in controlling symptoms of incurable cancers. When used before surgery to shrink a tumour it is known as neoadjuvant treatment, and if used after surgery to destroy small amounts of tumour that may be left it's called adjuvant treatment. Earlier radiotherapy was confined to X-rays and gamma rays but now heavy-ion therapy including carbon ions are also used for treating different types of cancer. If the radiation is delivered from outside the body using a machine, called linear accelerator which focuses high-energy radiation beams onto the area requiring treatment, it is called as external-beam radiation therapy and if the radiation is delivered from radioactive material placed inside the body (temporarily near cancer calls) it is called brachytherapy/internal radiation therapy or the use of a radioactive liquid that's swallowed or injected. External beam radiotherapy usually involves a series of daily treatments over a number of days or weeks. The type of radiotherapy one has to use and the length of treatment depend on the size and type of cancer, and where it is in your body. The radiation either damages DNA directly

or it causes hydrolysis of water generating free radicals inside the cell that end up damaging the DNA, protein or lipid membrane depending on the dose of radiation. Once the DNA is damaged, cancer cell tries to repair and get arrested. If failed to repair, cells enter senescence or eventually die through apoptosis wherein dead cells will be eliminated by body's natural processes. Normal cells also suffer temporary cell damage from radiation, but these cells are usually able to repair the DNA damage and continue growing normally. This temporary DNA damage to the normal tissues is the reason for side effects associated with radiotherapy, varying from person to person and often they are mild. Few of them are – tiredness, feeling sick, problem with eating and drinking, skin reaction, flu-like symptoms, hair loss etc.

3) **Chemotherapy** is the use of chemicals to kill the cancer cells. It can be given with either curative intent (involving combinations of drugs), or it may aim to prolong life by reducing symptoms (palliative chemotherapy). Often these chemicals interferes the process of cell division and is done by damaging DNA, inhibiting spindle fiber formation and polymerization/ depolymerization of tubulin etc. in the cancer cells. The drugs for chemotherapy are often given in combination of two or three at the same time, called regimens. The purpose of each regimen differs according to the type and stage of cancer. For instance, regimens lower the risk of cancer recurrence in early stage breast cancers, while it makes cancer to shrink or disappear during advanced stages. Again, like radiotherapy, chemotherapy not only kills the cancer cells but affects the healthy cells too. Due to the damage induced in blood cells, different side effects including anemia, fatigue, and various kinds of infections may arise. Damage in the cell of mucous membrane can lead to mouth sores and diarrhea while destruction in hair roots and follicles results in loss of hair. Depending on the method of killing cancer cells, different cytotoxic chemotherapy drugs are

classified in following classes: antimetabolites (5-fluorouracil, methotrexate etc.), alkylating agents (cisplatin, cyclophosphamide etc.), anti-microtubule agents (paclitaxel, vincristine etc.) topoisomerase inhibitors (topotecan, etoposide etc.) and antibiotics (doxorubicin, mitomycin, bleomycin etc.) [15].

4) **Hormone therapy** includes use hormones (or corticosteroids) such as prednisone and dexamethasone which, in high doses, can damage lymphoma or lymphocytic leukemia cells.
5) **Targeted Therapy** is a selective way of attacking cancer cells with drugs and generally better tolerated by patients. It has precise method of attacking cells with little damage to normal cells and thus fewer side effects. This therapy focus on proteins involved in cell signaling pathways regulating cellular functions like cell division, movement, responses and cell death. Small-molecule drugs which can diffuse into the cell and act on the specific targets or monoclonal antibodies, directed against the targets outside the cell are the most commonly used targeted therapies [16].
6) **Immunotherapy** is a new type of therapy where body uses its own immune system to fight cancer cells. Immune system comprises of group of cells and organs that work together to defend the body against foreign particles such as bacteria, and viruses including cancer cells. During this defense several kinds of cells like macrophages, lymphocytes, dendritic cells and T lymphocytes take part. These immune cells communicate with each other through cytokines (protein molecules) e.g. interferons, interleukins and tumor necrosis factor (TNF). For immunotherapy treatment, large amount of cytokines (natural, recombinant or synthetic) are injected or infused so that the cells of immune system act more effectively on tumor cells.
7) **Hyperthermia (thermal therapy or thermotherapy)** is a type of cancer treatment in which the temperature of tumor is increased up to 113°F using microwave, radiofrequency, and

ultrasound. This high temperature is capable of killing the cancer cells with minimal injury to normal tissues, also cancer cells become more sensitive to radiation. Hyperthermia kills cancer cells by damaging proteins and structures within cells. It is applied as an adjoining therapy with other established cancer treatments like radiotherapy and chemotherapy. For metastatic spread, whole-body hyperthermia is given by raising the body temperature to 107-108°F using thermal chambers. More recently the concept of intracellular hyperthermia has emerged wherein magnetic particles are concentrated at the tumor site and remotely heated using an applied magnetic field to achieve hyperthermic temperatures (42-45°C) [17].

1. 2. 6. Lung cancer

Lung cancer contributes largest to the mortality among different cancers. A large number of lung cancers are associated with cigarette smoke, while other factors such as environmental influences including radon and nutrition are also involved. Many lung cancer patients are diagnosed at late stages of the disease when surgery is not that effective and hence chemotherapy and radiation therapy, as well as a combination of both therapies, are used to reduce tumor mass and halt disease progression. There are three main types of lung cancer and this categorization helps in deciding treatment options as well as prognosis.

1. **Non-small cell lung cancer** is the most common type of lung cancer, affecting about 85% of total lung cancers patients. Squamous cell carcinoma, adenocarcinoma, and large cell carcinoma are all subtypes of non-small cell lung cancer.
2. **Small cell lung cancer** affects around 10%-15% of lung cancers patients and tends to spread quickly than any other lung cancer.

3. **Lung carcinoid tumor** is also called lung neuroendocrine tumors. They affect fewer than 5% of lung cancers patients and these tumors grow slowly and rarely spread.

Histologically, adenocarcinoma is more common than squamous cell carcinoma in lung cancer patients [18]. Apart from primary lung cancers, secondary lung cancers can originate from primary tumors of different tissue origin including, late stage melanoma [19], which is an aggressive and highly metastatic disease. Lungs are the second most common site for its metastatic spread [20]. The 5-year survival rate is less than 15% in patients with metastatic disease and approximately one-third of all melanoma patients experience disease recurrence [21].

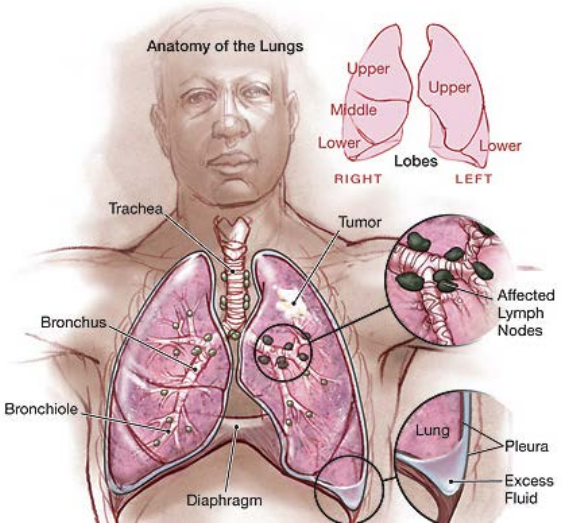

Figure 1. 2. Anatomy of lung showing lung cancer. (Adapted from http://studynursing.blogspot.com/).

Lung cancer cells have acquired numerous characteristic alterations facilitating their oncogenic growth. Accumulating evidence suggests that cancer cells use multiple and perhaps redundant pathways like mitogen-activated protein kinases (MAPK), AKT and NF-κB to maintain survival.

1. 3. Mode of cell death in cancer cells

One born in this world has to die someday. This statement is true for organism, tissue or the normal/ non-cancerous cells but for cancer cells, escaping death is a strategy which they have learnt. Although, during this escape cancer cells acquire lot of mutations, some are even deleterious but for others it gives them a second chance to survive. Once cell dies it can follow either step wise path called as programmed cell death or sudden death discussed as necrosis. Programmed cell death is again divided into many types and subtypes depending on the proteins/organelles involved or the morphological changes it bring about.

The importance of understanding the mechanistic machinery of cell death is vital because it is a component of both healthy and diseased tissue/organ, being initiated by various physiologic and pathologic stimuli. Moreover, the widespread involvement of different modes of cell death in the pathophysiology of various diseases lends itself to therapeutic intervention at many different checkpoints. Thus understanding the mechanism at molecular level provides deeper insight into various disease processes and may thus influence therapeutic strategy. Following are the important modes of cell death and a summary of mechanism described in literature:

1. 3. 1. Apoptosis

John Kerr's coined the term “apoptosis” in the late 1960s which was initially called as "shrinkage necrosis”. The word ‘‘apoptosis’’ comes from the ancient Greek apo´pto´sis, meaning the “falling off of petals from a flower” or “of leaves from a tree in autumn” [22]. Apoptosis is defined as a physiological process of programmed cell death important for normal tissue development and homeostasis, and elimination of virally infected or degenerated cells [23].

Apoptosis is a tightly regulated energy-requiring process that is stimulated by various cellular stresses, such as chemotherapy and oxidative stress [24].

Apoptosis is over 20 times faster than mitosis. Sightings of dying cells in vivo are therefore rare. Apoptotic cells are engulfed and degraded by neighboring cells without a trace. For cell homeostasis to be maintained, a balance between the increase (by differentiation from precursors and by proliferation) and decrease (by further differentiation and cell death) in the number of a cell population has to be neatly balanced. If mitosis proceeded without cell death, an 80-year-old person would have 2 tons of bone marrow and lymph nodes, and a gut 16 km long [25].

1. 3. 1. 1. Morphological changes during apoptosis

Apoptosis is found to be associated with a distinct set of biochemical and physical changes involving the cytoplasm (cell shrinkage), nucleus (nuclear fragmentation, chromatin condensation) and plasma membrane blebbing [26]. With light microscopy, the early process of apoptosis, cell shrinkage and pyknosis (irreversible condensation of chromatin) are visible [23]. With cell shrinkage, the cells become smaller in size, dense cytoplasm and tightly packed organelles. On histological examination with hematoxylin and eosin stain, apoptosis involving single cells or small clusters of cells appears as round or oval mass with dark eosinophilic cytoplasm and dense purple nuclear chromatin fragments [27]. The condensed chromatin aggregates into dense compact masses, and gets fragmented internucleosomally by endonucleases, which are analyzed by the typical ‘‘DNA ladder’’ formation. Extensive plasma membrane blebbing occurs followed by karyorrhexis (fragmentation of the nucleus) and separation of cell fragments into apoptotic bodies during a process called “budding” where the

organelle integrity is still maintained and is enclosed within an intact plasma membrane [28]. These bodies are subsequently phagocytosed by macrophages, parenchyma cells, or neoplastic cells and degraded within phagolysosomes and thus cause no inflammation. Macrophages that engulf and digest apoptotic cells are called “tingible body macrophages” and are frequently found within the reactive germinal centers of lymphoid follicles or occasionally within the thymic cortex. The tingible bodies are the bits of nuclear debris from the apoptotic cells. There is essentially no inflammatory reaction associated neither with the process of apoptosis nor with the removal of apoptotic cells because: (1) Apoptotic cells do not release their cellular constituents into the surrounding interstitial tissue; (2) They are quickly phagocytosed by surrounding cells thus likely preventing secondary necrosis; and, (3) The engulfing cells do not produce anti-inflammatory cytokines (Figure 1. 3) [29].

This form of physiological cell death is morphologically quite different from oncosis, in which the cell swells and disintegrates in an unordered manner eventually leading to the destruction of the cellular organelles and finally rupture of the plasma membrane and leakage of the cell content (necrosis). Necrosis also the final result in situations where there is too much apoptosis occurring for phagocytotic cells to cope with, especially in cell culture, where professional phagocytotic cells are usually lacking [26].

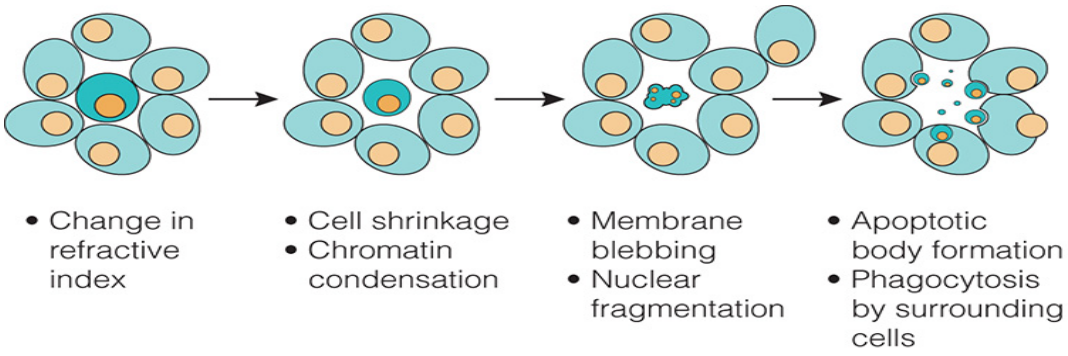

Figure 1. 3. Morphological changes during apoposis. (Adapted from *promegaconnections.com*).

1. 3. 1. 2. Mechanisms of Apoptosis

The mechanisms of apoptosis are highly complex and sophisticated, involving an energy dependent cascade of molecular events divided into two main apoptotic pathways: the extrinsic or death receptor pathway and the intrinsic or mitochondrial pathway. The extrinsic pathway is dependent on death-receptor stimulation, but the intrinsic pathway is activated in response to DNA damage and follows a mitochondrial route to induce cell death [30]. Activation of either pathway leads to activation of caspases, cysteine-dependent aspartic-directed proteases that act as the final executioners of apoptosis by cleaving both nuclear and cytoplasmic substrates. These pathways are initiated by the cleavage of caspase-8 or 9 followed by caspase-3 cleavage and results in DNA fragmentation, degradation of cytoskeletal and nuclear proteins, cross-linking of proteins, formation of apoptotic bodies, expression of ligands for phagocytic cell receptors and finally uptake by phagocytic cells [26]. An additional pathway that involves T-cell mediated cytotoxicity and perforin/granzyme dependent killing of the cell is also reported [31].

1. **Extrinsic Pathway:** The extrinsic signaling pathways that initiate apoptosis involve death receptor-mediated interactions between members of the tumor necrosis factor (TNF) receptor gene super-family [32]. Receptors of TNF family share similar cysteine-rich

extracellular domains and have a cytoplasmic domain of about 80 amino acids called the "death domain" [33]. This death domain plays a critical role in transmitting the death signal from the cell surface to the intracellular signaling proteins activating cascade of pathways. The best-characterized ligands and corresponding death receptors include FasL/FasR, TNF-α/TNFR1, Apo3L/DR3, Apo2L/DR4 and Apo2L/DR5 [34] [35]. For activating extrinsic death pathway, clustering of receptors and binding with the homologous trimeric ligand happens. For example, the binding of Fas ligand to Fas receptor results in the binding of the adapter protein FADD and the binding of TNF ligand to TNF receptor results in the binding of the adapter protein TRADD with recruitment of FADD and RIP [36]. FADD then associates with procaspase-8 via dimerization and death-inducing signaling complex (DISC) is formed, resulting in the auto-catalytic activation of procaspase-8. Once caspase-8 is activated, the execution phase of apoptosis involving caspase-3 activation is triggered [37] . Death receptor mediated apoptosis can be inhibited by a protein called c-FLIP which can bind to FADD and caspase-8, rendering them ineffective (Figure 1. 4) [37].

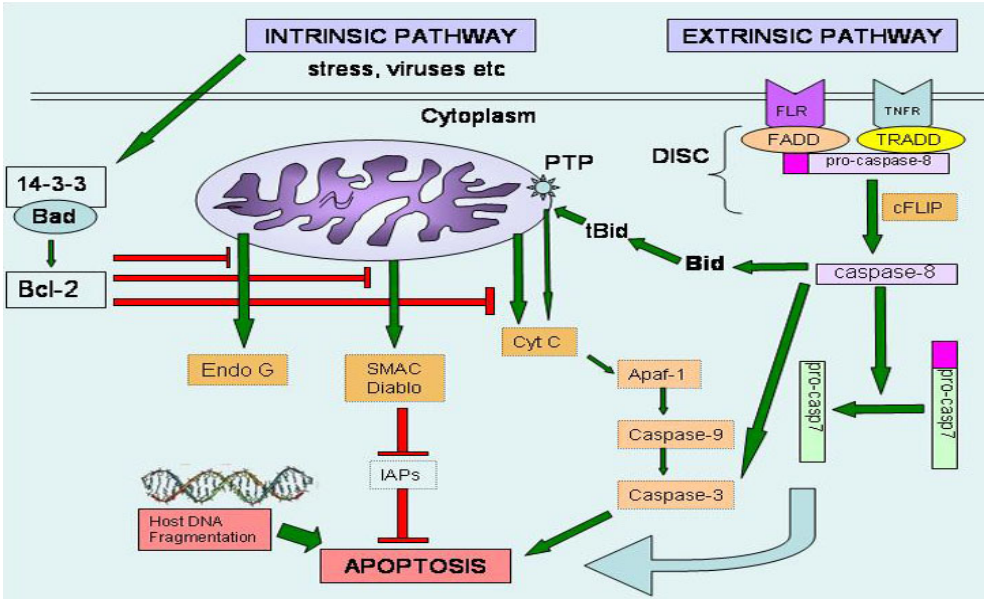

Figure 1. 4. Mechanism of apoptosis. (Adapted from - C*ell Biology of Disease and Excercise*).

2. **Intrinsic Pathway:** The intrinsic apoptosis involves a diverse array of non-receptor-mediated stimuli that produce intracellular signals *via* mitochondrial-initiated events. Intrinsic apoptosis mediated sometimes through negative signals involving absence of certain growth factors, hormones and cytokines that can lead to activation of apoptosis. Other stimuli like radiation, toxins, hypoxia and free radicals act in positive fashion. All of these stimuli cause changes in the inner mitochondrial membrane that results in an opening of the mitochondrial permeability transition (MPT) pore, loss of the mitochondrial transmembrane potential and release of pro-apoptotic proteins from the intermembrane space into the cytosol constituting cytochrome c, Smac/DIABLO, and the serine protease HtrA2/Omi [38,39]. These proteins activate the caspase-dependent mitochondrial pathway. Binding of cytochrome c, Apaf-1 and procaspase-9 forms "apoptosome" thus activating caspase-9 [40]. Smac/DIABLO and HtrA2/Omi are reported to promote apoptosis by inhibiting IAP (inhibitors of apoptosis proteins) activity (**Figure 1. 4)** [41]. Another group of pro-apoptotic proteins like AIF, endonuclease G and CAD (Caspase-Activated DNase), are also released from the mitochondria during late stage of apoptosis. AIF and endonuclease G both function in a caspase-independent manner. AIF translocate to nucleus and causes DNA fragmentation [42] while endonuclease G can cleave nuclear chromatin to produce oligonucleosomal DNA fragments [43]. Subsequently, CAD released from the mitochondria translocates to the nucleus where, cleavage by caspase-3 leads to its activation resulting in oligonucleosomal DNA fragmentation and advanced chromatin condensation [44]. The control of these apoptotic mitochondrial events involves members of the BCL-2 family of proteins [45] and their regulation through tumor suppressor protein p53. Around 25 genes have been identified in the BCL-2 family, including anti-apoptotic proteins like BCL-2, BCL-x, BCL-XL, BCL-XS, BCL-w, BAG, and some of the pro-apoptotic proteins like

BCL-10, BAX, BAK, BID, BAD, BIM, BIK, and BLK *etc.* The main mechanism of action of the BCL-2 family of proteins is the regulation of cytochrome c release from the mitochondria through alteration of mitochondrial membrane permeability. “Cross-talk” between the death-receptor (extrinsic) pathway and the mitochondrial (intrinsic) pathway is also been reported, where BID is been documented to play an important role. Another pro-apoptotic protein, BAD can also hetero-dimerize with BCL-XL or BCL-2, neutralizing their protective effect and promoting cell death. Its regulation is done through phosphorylation, without phosphorylation it interacts with 14-3-3 and remains sequestered in the cytoplasm. Genotoxic damage or oncogene activation of p53-mediated apoptosis can be regulated through pro-apoptotic members of BCL2, PUMA and NOXA. Overexpression of PUMA is accompanied by increased BAX expression, BAX conformational change, translocation to the mitochondria, cytochrome c release and reduction in the mitochondrial membrane potential [46] (Figure 1. 4, 5).

3. **Perforin/granzyme Pathway:** T-cell mediated death of tumor cells and virus-infected cells is reported to occur *via* a novel pathway that involves secretion of the transmembrane pore-forming molecule perforin with a subsequent exophytic release of cytoplasmic granules containing serine proteases granzyme A and granzyme B through the pore and into the target cell [47]. Granzyme B can cleave proteins at aspartate residues including procaspase-10 and factors like ICAD (Inhibitor of Caspase Activated DNAse) [48]. Also, granzyme B can cleave BID and directly activate caspase-3, thus amplifying mitochondrial apoptosis pathway. Granzyme A is also important in cytotoxic T cell induced apoptosis and activates caspase independent DNA nicking via DNAse. This DNAse has an important role in immune surveillance to prevent cancer through the induction of tumor cell apoptosis (Figure 1. 5).

4. **Execution Phase:** At the execution phase, caspases activate cytoplasmic endonuclease, which degrades nuclear material, and proteases that degrade the nuclear and cytoskeletal proteins. Caspase-3, caspase-6, and caspase-7 function as effector or "executioner" caspases, cleaving cytokeratins, PARP, the plasma membrane cytoskeletal proteins and the nuclear protein that ultimately cause the morphological and biochemical changes seen in apoptotic cells. Caspase-3, an important executioner caspase activates the endonuclease CAD. In growing cells CAD is complexed with its inhibitor, ICAD. During apoptosis, activated caspase-3 cleaves ICAD to release CAD followed by chromosomal DNA degradation and chromatin condensation. During cytoskeletal reorganization and disintegration, gelsolin, an actin binding protein, has been identified as one of the key substrates of activated caspase-3. Caspase-3 can cleave gelsolin and the cleaved fragments of gelsolin, in turn can cleave actin filaments in a calcium independent manner [49] (Figure 1. 5).

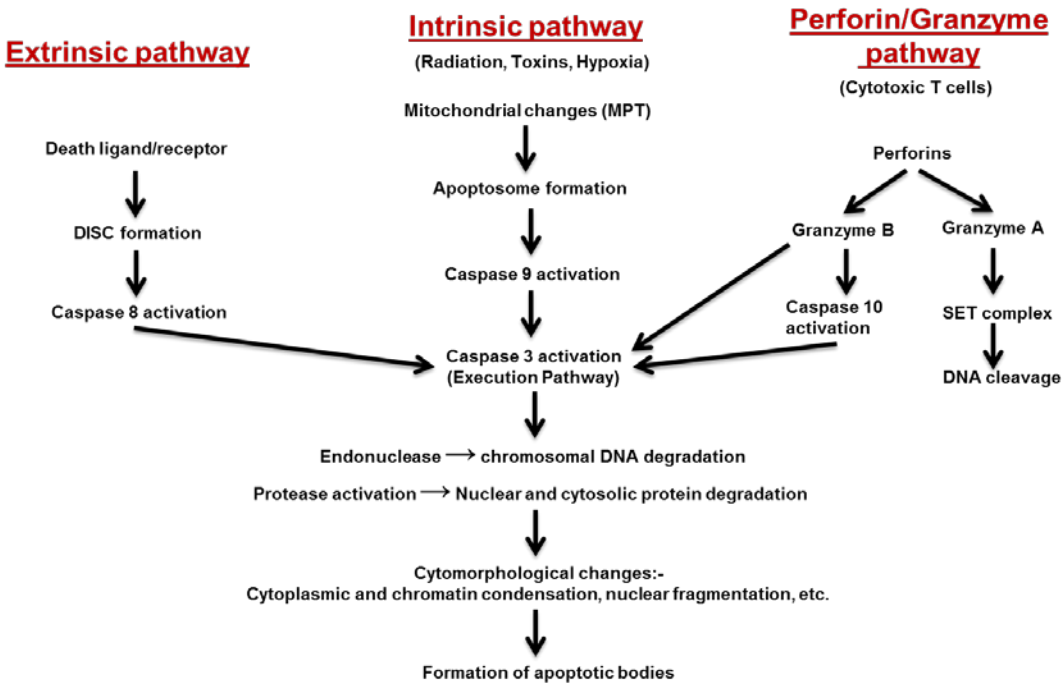

Figure 1. 5. Schematic representation of extrinsic, intrinsic and Perforin/ Granzyme pathway.

Phagocytic uptake of apoptotic cells is the last component of apoptosis. Phospholipid asymmetry and externalization of phosphatidylserine on the surface of apoptotic cells and their fragments is the hallmark of this phase and is associated with loss of aminophospholipid translocase activity and nonspecific flip-flop of phospholipids of various classes [50]. The externalization of phosphotidylserine in apoptotic cells facilitates noninflammatory phagocytic recognition and disposal.

1. 3. 2. Autophagy

Autophagy was discovered way back in 1960's and the term was first coined by Christian de Duve over 40 years ago. It was largely based on the observed degradation of mitochondria and other intra-cellular structures within lysosomes of rat liver perfused with the pancreatic hormone, glucagon [51]. It was only in 1990, when autophagy was recognized as a mode of cell death. Now it is defined as a catabolic process involving degradation of cell's own components through lysosomal machinery, hence also called 'self-eating'. It is a tightly regulated process that controls cell growth homeostasis and development, and assisting to maintain a balance between the synthesis, breakdown and ensuing recycling of cellular products. It is a key mechanism by which a dying cell reorders nutrients from unnecessary processes to important processes. Broadly, autophagy is divided into three types:

1. **Chaperone-mediated autophagy (CMA),** a mechanism that allows degradation of cytosolic proteins containing a particular pentapeptide consensus motif. The cytosolic proteins are recognized after binding to a heat shock cytosolic protein 70 (HSC70) containing chaperon/co-chaperone complex. This substrate-chaperone complex then gets recognized and

translocated across the lysosomal membrane by the lysosomal membrane receptor, lysosomal-associated membrane protein 2A (LAMP-2A), resulting in their unfolding and degradation.

2. **Microautophagy**, a mechanism when lysosomes directly swallow up cytoplasmic content by invagination, protrusion and septation of lysosomal membrane.

3. **Macroautophagy,** where organelle and long-lived proteins are degraded and recycled through double-membrane structures called autophagosomes enclosing cellular material and fusion with lysosomes or vacuoles. The formation of autophagosomes is initiated by class III PI-3 kinase and autophagy-related gene ATG6, also known as Beclin-1. Other structures are composed of ATG8 also known as light chain 3 (LC3), a ubiquitin like protein and ATG4 protease bound to ATG12-AtTG5-ATG-16 complex [52]. The outer membrane of autophagosome fuses with a lysosome in the cytoplasm, forming an autolysosome or autophagolysosome where their contents are degraded via acidic lysosomal hydrolases. Some organelle-specific macroautophagy processes such as mitophagy, pexophagy and ribophagy remove damaged organelles (Figure 1.6) [53].

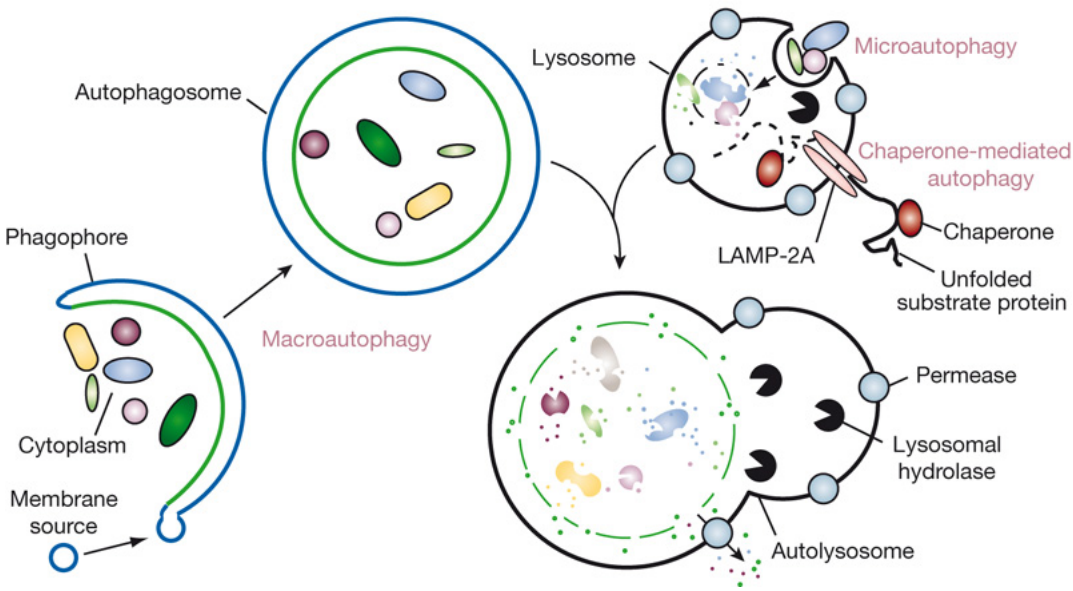

Figure 1. 6. The autophagy pathway. (Adapted from- Mizushima *et.al.*, 2008).

1. 3. 3. Necrosis

It is morphologically characterized by vacuolization of the cytoplasm and breakdown of plasma membrane, thus releasing pro-inflammatory molecules causing inflammation around the cell. Necrotic cells do display modifications in nuclear morphology, but nothing resembles the organized chromatin condensation and fragmentation seen in apoptotic cell death [52]. Recently, cell death research has revitalized the understanding of necrosis towards its programmed or regulated nature [54]. In the nucleus of necrotic cells, irrevocable changes like karyolysis (complete dissolution of the chromatin due to the enzymatic degradation by endonucleases), pyknosis (condensation of chromatin) and karyorrhexis (fragmentation of the nucleus) can be observed [55]. Condensation and severe eosinophilia, loss of structure and disintegration of the cytoplasm can also take place [56]. Recently, the accidental death, necrosis has been shown to follow cascade of signaling events and hence thought to be programmed [57]. Necrotic features are also observed in the cells under the conditions where different apoptotic proteins like caspases are inhibited with non-specific inhibitors such as zVAD-fmk [58] or anti-apoptotic molecules like BCL-XL overexpression that prevent caspase activation [59]. In some cases, caspase-independent necrotic cell death can be activated by antioxidant treatment or by eradicating the activity of the protein kinase receptor interacting protein (RIP) [60]. Initiation of apoptosis can suppress necrosis because activated caspases cleave and inactivate proteins required for programmed necrosis (RIP and PARP) [61]. Recently, caspase 8 catalytic activity has been shown to prevent RIPK3-dependent necrosis without inducing apoptosis by functioning in a proteolytically active complex with FLICE-like inhibitory protein long ($FLIP_L$, also known as CFLAR) [62].

The DNA repair protein PARP was found to initiate programmed necrosis in resonse to DNA damage in proliferating cells. This discernment was accredited to the fact that PARP activation leads to exhaustion of NAD both in nucleus and cytoplasm consequently inhibition of glycolysis. As a result, cells relying on glycolysis for ATP production rapidly become depleted of ATP after PARP activation and then die by necrosis [63]. Cancer cells are reliant on glucose metabolism for ATP production as they make use of amino acids and lipids for protein- and membrane synthesis, respectively. But, quiescent cells can maintain ATP levels by means of oxidative phosphorylation by catabolizing amino and lipids. Here, PARP activation can perform DNA repair without lethally depleting cellular ATP. Additionally, acute and massive DNA damage induces hyperactivation of PARP leading to NAD+/ATP depletion, and thus necrosis [63].

1. 3. 4. Mitotic catastrophe

Mitotic catastrophe has long been considered as a mode of cell death that results from premature or inappropriate entry of cells into mitosis and can be caused by chemical or physical stresses [64]. But now it's been accepted as not a separate mode of cell death, rather a process (prestage) preceding cell death, which can occur through necrosis or apoptosis. The final outcome of mitotic catastrophe depends on the molecular profile of the cell.

Mitotic catastrophe has been described as an aberrant form of mitosis associated with various morphological and biochemical changes (namely mitochondrial membrane permeabilization and caspase activation). The final step of mitotic catastrophe is almost always characterized by the formation of nuclear envelopes around individual clusters of missegregated chromosomes. Mitotic catastrophe is also correlated with incomplete DNA synthesis and

premature chromosome condensation (PCC). Interestingly, the well-defined mode of cell death – apoptosis – is also characterized by chromatin condensation; however, the morphology of apoptosis is distinguished from mitotic catastrophe and illustrated by cytoplasm shrinkage and nuclear fragmentation. However, it is still unclear whether mitotic catastrophe results in death that requires caspase-dependent or caspase-independent mechanisms. In addition, there are several examples that permit to define mitotic catastrophe as a cell survival mechanism of tumors.

Mechanisms of induction of mitotic catastrophe: It can be induced by many factors such as DNA damage, defects in mitotic machinery, checkpoint adaptation and mitotic slippage etc [64]. During DNA damage checkpoint regulations coordinate the response through activation of two protein kinase pathways: the ATM (ataxia-telangiectasia-mutated) and the ATR (ataxia-telangiectasia and Rad3-related). The alert signal is modulated through the action of the so-called checkpoint mediators (adaptors) and further transduced through phosphorylation of effector kinases CHK1 and CHK2. Delay in each cell cycle phase is controlled by group of proteins. The p53/MDM2-p21 controls the G1/S arrest and allows repair to occur before the chromosomal replication. Here, DNA synthesis is blocked by silencing of G1/S promoting cyclin E/Cdk2. Independent of p53, a late G1 arrest may also occur by Cdc25A degradation. S phase arrest controlled by ATM/ATR also involves this Cdc25A degradation. In G2/M arrest cell cycle is halted just before the mitotic entry, preventing the segregation of damaged chromosome. Here cyclin B/CDK1kinase and CDC25C plays an important role. Now the cells with impaired or lost checkpoint enter the mitosis prematurely in the presence of unrepaired DNA and this can lead to mitotic catastrophe in some tumor cells. Dying cells are characterized by multiple mitotic abnormalities, including multipolar meta- or anaphase, lagging telophase, random distribution of

condensed chromosomes throughout the cells, and so on. Thus, the abrogation of G1 and/or G2 checkpoints is essential for mitotic catastrophe.

1. 3. 5. Mechanism of evading cancer cell death and drug resistance

Despite intensive treatment modalities, majority of high-risk lung cancer patients and other type of cancers which were initially sensitive to chemotherapy at diagnosis develop resistance after relapse and their mechanisms are still poorly understood. However, several ideas have been postulated including altered expression of drug resistance genes, most notably involving the presence of p-glycoprotein (Pgp) and increased expression of its multi-drug resistance gene (MDR-1) and MDR related protein (MRP) [65]. Other mechanisms include mutations in the p53 gene affecting downstream effectors such as BAX and Caspase-8 resulting in decreased apoptotic activity [66]. Recently, other pathways including improved DNA repair, drug transport and detoxification, and the presence of cancer 'stem cells' [67] have been also proposed to play an important role in developing resistance. Despite the introduction of newer agents and increasing number of patients whose survival after relapse is prolonged, this remains a sensitive and delicate issue and it is hoped that recent advances in the understanding of molecular biology of different cancers including lung cancer will eventually lead to the discovery of novel therapeutic targets. Some of them are discussed in next section.

1. 4. Proteins regulating DNA damage response and apoptosis

This section gives an introduction to the various proteins (structure, functions and regulations) related to DNA damage and other insults in cancer cells.

1. 4. 1. ATM/ATR

The maintenance of genomic integrity is crucial for the survival of all organisms. This task of safeguarding the genome is accomplished by a number of cellular processes, including DNA replication, DNA repair, senescence and apoptosis. These processes are regulated by the DNA-damage checkpoint, which is a complex signaling network and involves multiple steps initiated through phosphorylation of numerous key players in its various branches. The five most prominent DDR kinases involve ATM (ataxia telangiectasia mutated), ATR (ATM- and Rad3-related), DNA-PK (DNA-dependent protein kinase), CHK1 (Checkpoint kinase 1) and CHK2 (Checkpoint kinase 2). Two phospho-inositide 3-kinase-like protein kinases (PIKKs) – ATM, and ATR – are master regulators of the checkpoint pathways [68]. ATM is primarily activated by DNA double-strand breaks (DSBs), whereas ATR responds to a much broader spectrum of DNA damage, including DSBs, chromatin alterations and many other types of DNA damage including base depurination and deamination that interfere with DNA replication [69]. If not repaired, these DNA lesion leads to generation of mutations leading to cancer.

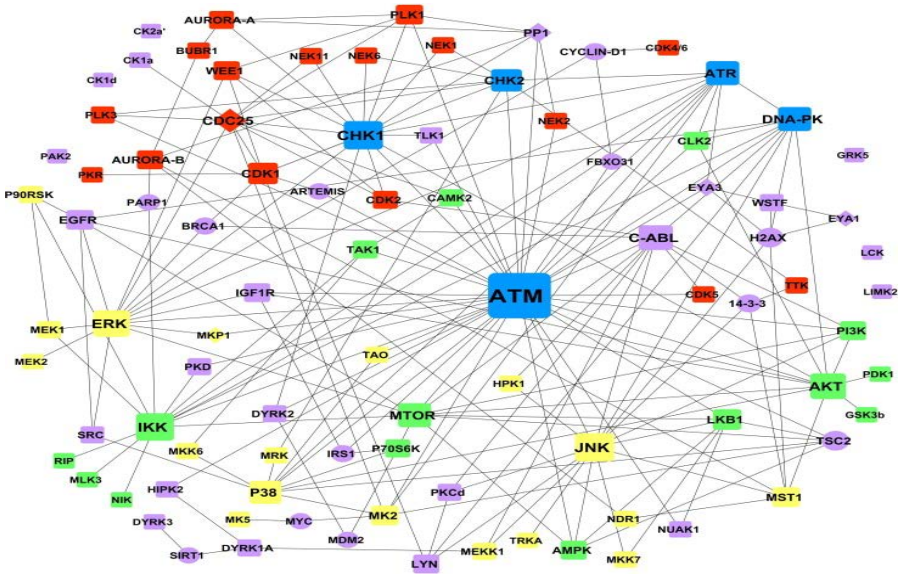

Figure 1. 7. The expanding protein kinase landscape of the DNA damage response.

(Adapted from - Bensimon *et al*. 2011).

Ataxia telangiectasia (AT) is a rare human disease characterized by cellular sensitivity to radiation and a predisposition to cancer. These patients contain mutations in their ATM gene. According to COSMIC (Catalogue Of Somatic Mutations In Cancer) the frequencies with which heterozygous mutations in ATM are found in common cancers include 7.2% among 1,040 lung cancers, 11.1% in 1790 hematopoetic and lymphoid tissue cancers, 4.6% in colon cancers, 2.1% in 847 kidney cancers, 1.9% in 1,120 breast cancers, 0.9% in central nervous system cancers and 0.7% in 713 ovarian cancers.

ATM is a 350 kDa protein consisting of 3056 amino acids and five domains. These are the HEAT repeat domain, the FRAP-ATM-TRRAP (FAT) domain, the kinase domain (KD), the PIKK-regulatory domain (PRD) and the FAT-C-terminal (FATC) domain. ATM is thought to wrap around double-stranded DNA after a conformational change. A complex of three proteins MRE11, RAD50 and NBS1, also known as MRN complex, recruits ATM to double strand breaks (DSBs) and holds the two ends together [70]. ATM directly interacts with the NBS1 subunit and phosphorylates H2AX. The Ser139 phosphorylation on histone variant H2AX generates binding sites for different adaptor proteins. These adaptor proteins with BRCT domain then recruit different factors including the effector protein kinase CHK2, BRCA1, NBS1 and the tumor suppressor p53 (phosphorylating at ser15). P53 also gets phosphorylated, stabilized thus activated by the effector kinase CHK2. Subsequent transcription of numerous p53 target genes including CDK inhibitor p21 lead to long-term cell-cycle arrest or even apoptosis. Although, ATM and ATR share overlapping substrate specificity and thus show functional redundancy; both preferentially phosphorylate serine or threonine residues that are followed by glutamine (“SQ/TQ” motifs) in their substrates. More than 700 proteins containing the ATM/ATR phosphorylation motif (SQ/TQ) that are inducibly phosphorylated in response to IR are been

identified by Matsuoka et al. [71]. Some of the ATM/ATR substrates are themselves protein kinases that target downstream effectors, most notably CHK1 and CHK2 [72]. The activities of both CHK1 and CHK2 are also antagonized their own activities via regulatory feedback loops involving phosphatases and both are promoted to dissociate from the chromatin in response to DNA damage. Till date extensive cross talk between different protein kinase regulated by ATM has been documented (Fig. 1.7) [73]. Also ATM/CHK2, ATR/CHK1, and p38/MK2 pathways converging to control DDR response by inactivation of the CDC25 phosphatases is also reported [74].

ATR is a 301 KDa protein with 2644 amino acids. ATR is activated in response to persistent single-stranded DNA. It works with a partner protein called ATRIP (ATR interacting protein) to recognize single-stranded DNA coated with RPA (Replication protein A). Once activated, it phosphorylates CHK1, and other checkpoint proteins RAD17 and RAD9, as well as tumor suppressor protein BRCA1, initiating a signal transduction cascade that culminates in cell cycle arrest or apoptosis depending on extent and duration of the damage. Mutations in ATR are responsible for Seckel syndrome, a rare human disorder that shares some characteristics with AT patients.

1. 4. 2. MAPK (Mitogen-Activated Protein Kinases)

The MAPKs are a family of serine/threonine kinases with crucial roles in communicating extracellular stimuli such as growth factors, cytokines, hormones and various stresses into a variety of cellular processes affecting cellular growth, proliferation, differentiation, and inflammation. They are classified into three major groups: ERK1/2s (extracellular signal-regulated kinases), JNKs (c-Jun N-terminal kinases) or SAPK group (stress-activated protein

kinase) and the p38 MAPKs family. The involvement of MAPKs in different genotoxic responses have been studied in detail [75].

ERK1/2 gets activated in response to etoposide, adriamycin and IR, in a manner dependent on ATM and the upstream kinase MEK1. Dephosphorylation of ERK1/2 was mediated by an ATM-dependent regulation of the MAPK phosphatase 1 (MKP1) [76]. Inhibition of ERK1/2 was found to impair IR-induced ATR, CHK1 and WEE1 activity, as well as ATM autophosphorylation and homologous recombination (HR) repair [77].

P38 mitogen-activated protein kinases are responsive to stress stimuli, such as cytokines, ultraviolet irradiation, heat shock, and are involved in cell differentiation, apoptosis and autophagy. P38 was found to get induced in response to various DNA damaging agents, including UV, cisplatin and IR. UV irradiation activated p38 was more vigorous than IR and facilitated the initiation of a G2/M checkpoint. Here, p38/MK2 complex undergoes nuclear export into the cytoplasm to phosphorylates different players and stabilize specific mRNAs involved in G2/M checkpoint [78]. Recently, thousand and one amino acid (TAO) kinases (a kind of MAP3Ks) were discovered to activate p38 MAPK during IR treatment. P38 MAPKs which are classically been associated with the induction of apoptosis can also mediate cell survival in specific situations through non –classical pathway in response to DNA damage [79]. P38 has been shown to regulate mitochondrial function by disrupting balance between different pro and anti-apoptotic BCl2 family members [80,81]. Here, phosphorylation of BAX mediated the signaling cascade.

C-Jun N-terminal kinases (JNKs), were originally identified as kinases that bind and phosphorylate c-Jun within its transcriptional activation domain. They also play an important

role in T cell differentiation and the cellular apoptosis pathway. Activation of JNK is done through two MAP kinases, MKK4 and MKK7 and can be inactivated through Ser/Thr and Tyr protein phosphatases. For DNA damage dependent activation of JNK several other proteins like c-Abl, DNA-PK, Lyn tyrosine kinase and protein kinase Cδ (PKCδ) are proposed to play their part [73]. Apoptotic function of JNK by translocating onto phosphorylated H2AX has also been proposed. JNK also controls mitochondrial regulation by phosphorylating BCL2 family member proteins [80].

1. 4. 3. P53

The tumor suppressor p53 is a stress sensor and DNA sequence-specific transcription factor. Upon DNA damage and other stresses like oxidative damage and oncogenic overexpression, p53 is stabilized, binds to chromatin and activates or represses gene expression to regulate cell cycle arrest, DNA repair, senescence and apoptosis [82]. It has been described as "the guardian of the genome" because of its role in conserving stability by preventing genome mutation. The International Cancer Genome Consortium has established that the p53 gene is the most frequently mutated gene (>50%) in human cancer, indicating that the p53 gene plays a crucial role in preventing cancer formation [26]. P53 protein can be understood as having transactivation domain (activating transcription factors) ranging from 1-42 aa, activation domain 2 (AD2) important for apoptotic activity ranging 43-63, proline rich region ranging from 64-92, central DNA binding domain, DBD (rich in arginine amino acids) ranging 102- 292, nuclear localization signals (NLS) from 316-325, homodimerization domain ranging from 307 -355 amino acids and C-terminal regulatory domain (356-393) downregulating the DNA binding of the central region [82] (Figure 1. 8). Mutations that deactivate p53 in cancer usually occur in the DBD.

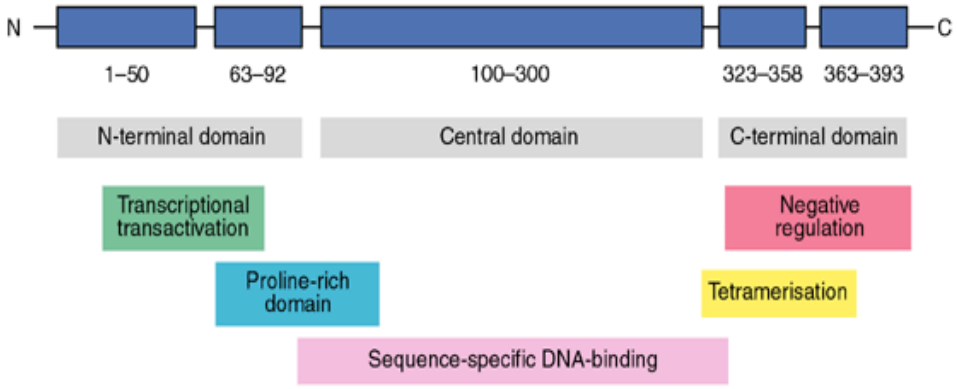

Figure 1. 8. Structure of p53 protein. (Adapted from - http://www.expertreviews.org/).

Dual role p53, survival and death are dependent on cell type and extent of stress induced. Activated p53 binds DNA and activates expression of several genes including microRNA miR-34a, p21 and hundreds of other down-stream genes. p21 binds to the G1-S/CDK (CDK4/CDK6, CDK2, and CDK1) complexes (molecules important for the G1/S transition in the cell cycle) inhibiting their activity. Upon DNA damage, p53 induced p21 helps in arresting the cells, giving them time to repair the damage and avoid mitotic catastrophe [83]. Once repair is finished, cells can re-enter the cell cycle and hence survive [84]. However, persistent or irreparable DNA damage invokes p53-mediated apoptotic cascade involving increase in the expression of BAX and PUMA [85]. Here, conformational changes in BAX proteins are mediated through PUMA to induce mitochondrial pore formation [46]. Recently, a transcriptional independent role of p53 has also been proposed, where both caspase activation and cyt c release has been shown to occur [86].

1. 4. 4. BAX/BCL2

Apoptosis regulator BCL-2 is a family of proteins governing mitochondrial outer membrane permeabilization (MOMP). BCL-2 proto-oncogene, was discovered at the chromosomal

breakpoint of t (14;18) bearing human B-cell lymphomas. In this family, proteins can be either pro-apoptotic (BAX, BAD, BAK and BOK among others) or anti-apoptotic (including BCL-2, BCL-xL, and BCL-w, among an assortment of others). Indeed, the ratio between these two subsets helps determine, in part, the susceptibility of cells to a death signal [45]. Till date, there are a total of 25 genes in the BCL-2 family. BCL-2 family members possess up to four conserved BCL-2 homology (BH) domains designated BH1, BH2, BH3, and BH4 [87]. Mutational studies suggest that BH3 domain serves as a critical death domain in the pro-apoptotic members. This is supported by BH3-domain-only molecule, BIM, BID and BAD. Many BCL-2 family members also contain a carboxy-terminal hydrophobic domain, which in the case of BCL-2 is essential for its targeting to membranes such as the mitochondrial outer membrane [87]. The site of action for the BCL-2 family is mostly on the outer mitochondrial membrane inside which various apoptogenic factors (cytochrome c, Smac/Diablo homolog, Omi) that if released activate the executioners of apoptosis, through caspases [88]. Due to multiple roles played by BCL2 family members and their role in carcinogenesis, pharmacological inhibitors ABT-737 and ABT-263 were also developed to target BCL-2, BCL-xL and BCL-w proteins [89]. These enhanced the effects of apoptotic signals in small-cell lung carcinoma and lymphoma lines and are under clinical trials.

1. 4. 5. NF-κB

Nuclear Factor Kappa B (NF-κB) is a family of dimeric protein complexes which regulate many functions including DNA transcription. All animal cell types have NF-κB expressed in them, it implicates cellular responses to stress, immune and inflammatory processes, and regulation of cell cycle, differentiation, and death. First described as a B-cell factor which interacts with the

immunoglobulin kappa (Igκ) enhancer, it is now known that NF-κB. It has evolved as one of the major molecular targets in cancer research.

The NF-κB family is composed of five proteins, characterised by presence of Rel homology domain (RHD). The five family members are: p50/p105 (NF-κB1), p52/p100 (NF-κB2), c- Rel, RelB, and p65 (RelA) [90]. They can be further classified into two groups based on the C-terminal sequences in the RH domain. The first group (p105 and p100) has long C-terminal domain containing the inhibitor ankyrin. Through limited proteolysis or arrested translation, they become shorter, active DNA-binding proteins p50 and p52 respectively. The transcriptionally active second group (c-Rel, RelB, and p65 (RelA) contains variable transactivation domain (TAD) at the C-terminal [91]. NF-κB binds to κB elements base pair DNA sites (5'-GGGRNYYYCC-3'), also called κB sites, as either homo- or heterodimers. NF-κB generally refers to the p50-p65 (RelA) heterodimer, one of the major Rel complexes in most cells.

1. 4. 5. 1. Mechanism of NF-κB activation

NF-**κ**B is a transcription factor that induces expression of more than 200 genes involved in diverse process such as cell survival, cell adhesion, inflammation, differentiation and growth. NF-**κ**B activation through canonical pathway involves dimers composed of p50 and p65 or c-Rel and is often activated by microbial infections, pro-inflammatory growth factors and cytokines including TNFα. TNFα engagement induces trimerization of TNFα receptor 1 (TNFR1) and recruitment of multiple adaptor proteins and kinases, resulting in the phosphorylation and activation of I**κ**B kinase (IKK) complex [90]. IKKs consist with catalytic subunits IKKα/IKK1, IKKβ/IKK2, and an essential regulatory subunit IKKγ/nuclear factor-**κ**B essential modulator

(NEMO). The activated IKK is switched from the TNFR1 signaling complex to the NF-κB/IκB complex, where IKKβ phosphorylates IκBα, which is then polyubiquitinated followed by 26S proteasome mediated degradation. When NF-κB is freed up from IκBα, the NLS signal on p65 and p50 are exposed, leading to their nuclear translocation and activate expression of different NF-κB target genes, one of which is IκBα. IκBα contains both NLS and nuclear export sequence (NES) and as such, newly synthesised IκBα entering the nucleus can abrogate this signal and remove NF-κB dimers from DNA to the cytoplasm. In the nucleus, NF-κB is also subjected to different modifications like phosphorylation, glutathionylation [92] and acetylation on the p65 subunit, which regulates the localization in the compartments of nucleus, binding to DNA or interaction with transcriptional co-activators such as cAMP response element-binding protein-binding protein (CBP)/p300 [90].

Various DNA damage induced by both radiation and anticancer genotoxic agents activates the IKK-IκB-NF-κB cascade. Here, ataxia telangiectasia mutated (ATM) kinase, activated upon DNA damage phosphorylates the IKK subunit NEMO/IKKγ in a complex in the nucleus called PIDDsome, consisting of RIP1, p53-induced death domain (PIDD) and NEMO [93]. After a series of modifications including phosphorylation and sumolysation, NEMO translocates to the cytoplasm and bind IKKβ to activate it. Then IKKβ phosphorylates IκBα and turns on the canonical NF-κB activation pathway. The noncanonical pathway involves activation by TNF receptor family members such as CD40, lymphotoxin beta (LT beta) and B-cell-activating factor (BAF). With these receptors, NF-κB inducing kinase (NIK) is stabilized and activated by auto-phosphorylation mediating IKKα phosphorylation and subsequently conformational change in p100, which is then cleaved to generate p52 [93]. A functional NF-κB

heterodimer containing p52 and RelB is formed and translocated to the nucleus to turn on the expression of different genes. The canonical and noncanonical pathways are coordinated under some circumstances, which may provide a delicate control of the overall NF-κB activity in the cell. One more pathway called, atypical pathways has also been discovered where, e.g. casein kinase 2 (CK2) rather than IKK is required for short wavelength ultraviolet (UV) light -induced NF-κB activation [94]. In this pathway, calpain-dependent rather than proteasome is involved in IκBα degradation.

1. 4. 5. 2. Functions of NF-κB

NF-kB is known to increase the expression cyclins D and E, factors involved cell cycle progression and thus enhancing the transition from G1 to S phase. Furthermore, NF-κB negatively regulates expression of growth arrest and DNA damage-inducible protein 45 (GADD45), a cell cycle checkpoint protein that keeps cell at the G2/M phase transition. However, under certain conditions, NFκB can function as a transcriptional suppressor. For example, DNA-damage-induced NF-κB suppresses gene transcription [91] involving interactions with transcriptional repressors and tumor suppressors such as p53 and ARF. Thus, it is important to elucidate the transcriptional functions of DNA damaging anticancer drugs-induced NF-κB activation in different cancer cells before applying NF-κB manipulating approaches for sensitizing anticancer chemotherapy. NF-κB also plays a critical role in blocking apoptosis through various mechanisms including induction of anti-apoptotic protein expression such as BCL-XL, cIAP1, cIAP2, XIAP, and c-FLIP, which promote cell survival. NF-κB can also increase the expression of redox enzymes like manganese superoxide dismutase (MnSOD) thus suppressing cellular stress-mediated apoptosis through removal of reactive oxygen species

(ROS). Further, NF-κB also negatively regulates the apoptotic JNK activation. In addition, NF-κB suppresses apoptosis through antagonizing p53, possibly through competition for transcriptional co-activators. Finally, NF-κB down-regulates the expression of phosphatase and tensin homolog (PTEN) to activate AKT to promote cell survival and proliferation.

Proaoptotic role of NF-κB activation has been documented in the case of phorbol ester and ionomycin-induced apoptosis which occurs through up-regulation of the Fas ligand (FasL) [95]. This is supported by Kasibhatla et al. who reported that NF-κB induced proapoptotic FasL protein in response to etoposide or T-cell activation signals [96,97]. NF-κB mediated prevention or promotion of apoptosis is dependent upon stimulus, cell type, and context.

1. 4. 5. 3. NF-κB in lung cancers

NF-κB has been found to be constitutively active in a variety of solid tumors, including prostate, breast, cervical, pancreatic and lung cancer [98]. High levels of NF-κB activation has been documented in both small cell lung cancer (SCLC) and non-small cell lung cancer (NSCLC). Tumor samples obtained from lung cancer patients showed significant association between NF-κB activity, disease advancement and poor prognosis in lung cancer patients [98]. In recent years, NF-κB has become the focus of many cancer researchers, particularly in certain cancer types such as Hodgkin's lymphoma where NF-κB is constitutively active and NF-κB inhibition may have a therapeutic potential. Aspirin, other non-steroidal anti-inflammatory drugs (NSAIDs) and sodium salicylate have been reported to inhibit NF-κB activation by inhibiting ATP-binding to IKK-ß and thereby reducing IKK-ß-dependent phosphorylation and degradation of IκBα. Inhibiting NF-κB with different approaches such as siRNA, IKK inhibitors and IκBα super suppressor have been found to inhibit lung cancer cell's survival and proliferation [90]. Another

approach to suppress NF-κB is by inhibiting ubiquitin-mediated degradation of IκBα by proteasome. Bortezomib (PS-341, Velcade) is a potent and selective proteasome inhibitor, it is shown to sensitise human colorectal cancer cell lines towards camptothecin analogues CPT-11 and SN-38 [99]. Since then, bortezomib has been approved by the FDA for treatment of multiple myeloma. Nevertheless, since proteasome is also involved in other cellular factors such as cyclins, cyclin-dependent kinase inhibitor p21Waf1 and p27Kip1, and p53, its efficacy may not be solely due to inhibition of NF-κB pathway [99,100].

1. 5. Role of glutathione in cellular system

Glutathione (or GSH) is the body's own master antioxidant discovered way back in 1889. It is a small protein molecule composed of 3 amino acids: cysteine, glutamate, and glycine. It acts as a carrier of an active thiol group in the form of cysteine residue. The reduced and oxidized forms of glutathione (GSH and GSSG) act in concert with other redox-active compounds (e.g., NAD(P)H) to regulate and maintain cellular redox status [101]. GSH is synthesized in a two-step process catalyzed by L-glutamate: L-cysteine γ-ligase, (γ-GLCL, EC 6.3.2.2) (also called γ-glutamyl-L-cysteine ligase or γ-glutamylcysteine synthase), and glutathione synthase (GLS, EC 6.3.2.3). GSH is consumed directly through oxidization by ROS and RNS or indirectly during GSH-dependent peroxidase-catalyzed reactions. Conjugation with endogenous and exogenous electrophiles consumes a substantial portion of cellular GSH. In addition, cells may lose GSH due to export of both oxidized and conjugated forms. Due to important physiological functions of GSH, the processes like its production, consumption, and transportation are tightly regulated and the activities of the enzymes involved in GSH metabolism are controlled at transcriptional, translational, and posttranslational levels [102].

1. 5. 1. Functions of GSH

It has been found to perform many functions including, acting as a reserve of cysteine, stores and transports nitric oxide, regulation of cell growth and division, synthesis of DNA and proteins, transport of amino acid, modulating enzyme activity, metabolism of xenobiotics, enhancement of body immune function, resistance to UV radiation and oxy radical damage, recycling of other antioxidants, metabolizing H_2O_2 [102], copper and iron transfer, participation in the maturation of iron-sulfur clusters in proteins and more importantly involved in the operation of certain transcription factors (particularly those involved in redox signaling) by maintaining the essential thiol status of these proteins and other molecules [103].

GSH can directly react with ROS, RNS, and other reactive species, particularly HO•, HOCl, RO•, RO_2•, $^1O_2$, and $ONOO^-$, often resulting in the formation of thiyl radicals (GS•) (Figure 1. 9). This thiyl radicals can also combine with different molecules (forming Protein-SSG, S-glutahionylation), as well as with other thiyl radicals leading to the formation of oxidized glutathione (glutathione disulfide, GSSG). GSSG may be either excreted from the cell, or reduced by glutathione reductase (GR) at the expense of NADPH. Functions of these glutahionylated proteins do not remain same to their normal counterparts and this adds to another type of protein regulation (apart from phosphorylation, sumoylation, acetylation, ubiquitnylation etc.). Recently, significant amount of glutathioinylated proteins have been found in proliferating cells including cancer cells. Due to multiple roles of GSH, it has attracted the attention of pharmacologist as a possible target for medical intervention. Here both decrease and increase in the GSH levels in organisms have been tried. Buthionine sulfoximine (BSO) is probably the most popular approach for depleting GSH while for its enhancement, supplementation with

precursors of mainly cysteine in the form of different esters and NAC (N-Aectyl –L-Cysteine) are been tried.

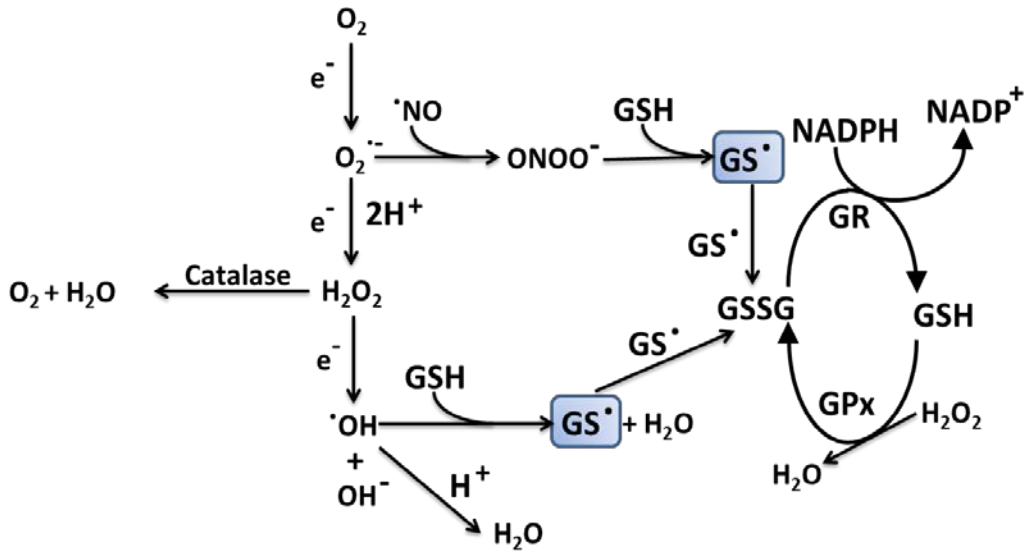

Figure 1. 9. Involvement of glutathione in elimination of reactive oxygen and nitrogen species and generation of thiyl radical.

1. 5. 2. Role of glutathionylation in life and death of cells

Glutathione depletion has been associated with chromosomal DNA fragmentation associated with both apoptosis and necrosis [104]. Here, supplementation with NAC was found to reverse the process. But glutathione depletion is not always reported to be associated with ROS production and is independently controlled [105]. The concentration of glutathione and ROS plays an important role in deciding the fate of cancer cells towards survival or death. Here, the expression levels of glutathione-S-transferase and pattern of S-glutahionylation in different cell types govern the balance [106]. Recently, both reversible and irreversible oxidative post-translational modifications (OPMs) in proteins have been shown to regulate their activity. These include cysteine modifications (nitrosylation-SNO, hydroxylation-SOH, disulphide bond-S-S

and glutahionylation-SSG). Under basal levels also, a significant (1%) proteins are found to be glutathionylated (-SSG) [107]. GSH in the presence of oxidized cysteins (sulfenic acids) can induce glutathionylation as observed under pro-oxidant apoptotic stimuli. Although kinetically GSSG is a poor glutathiolating agent and been documented to fail in glutathiolating proteins with highly reactive cysteines such as calbindin, glycerol-3-phosphate dehydrogenase (G3PDH) and actin [108]. Although glutahionylation of caspases have been documented to decrease the cell death induced by TNF-α [109]. Several groups report whole set of regulation controlled by glutahionylation of different proteins like death receptors (CD95, DR5, TNFR1), STAT3, JNK, ERK, p53, NF-kB(p65) and many more [110]. Gluthionlation of STAT3 decreases its survival function and so does the glutahionylation of p65 and ERK [92]. Glutahionylation of p53 has also been documented to suppress its chromatin binding and transcription functions [111].

1. 6. Drawbacks of current cancer chemotherapy

Chemotherapy is an effective drug treatment designed to kill cancer cells. Chemotherapy, apart from destroying cancer cells can also stop or slow the spread or growth of these cells. Despite the benefits of chemo treatment, there are several disadvantages including, variety of short term symptoms like nausea, vomiting, loss of appetite, constipation or diarrhea which can certainly be severe and painful for the patient. This is attributed to the lack of tumor specificity and more importantly multidrug resistance which later become the reason for cancer recurrence [65]. The aim of ideal cancer chemotherapy is to kill cancer cells specifically, while preventing the normal cells from its action. Although a lot of recent investigations for the advancements in the treatment and control of cancer progression have been carried out, still the scope for improvement remains. Side effects can be targeted with controlled amount of drug entering specific cancer cells and for sufficiently long time. While for preventing cancer recurrence the

drug should have multiple molecular targets and ability to work in synergism with other cancer drugs, in addition to entrusting normal cells of the body [112]. Therefore, in cancer research the search for potent, safe and selective anticancer compounds is crucial for new drug development where natural therapies, such as the use of the plants or plant derived natural products are being investigated to combat cancer.

The first FDA approved chemopreventive agent, tamoxifen citrate, a synthetic antiestrogen was used for reducing the risk of breast cancer in women at high risk. Although it did reduce the breast cancer incidence by 50%, later increased risk of serious side effects such as uterine cancer, blood clots, ocular disturbances, hypercalcemia, and stroke was discovered. Thus, side effects developed by any drug are an important issue of concern when long-term administration of a drug to healthy people who may or may not develop cancer is considered. This clearly adds to the need for agents, which are safe, specific and efficacious in preventing cancer. Diet derived natural products are proposed to be the potential candidates for this purpose [113]. Several classes of anticancer drugs have been developed and some of them are even natural. Further, natural products, due to their structural diversity, provide excellent templates for the construction of novel compounds [114,115].

1. 7. Natural compounds in anticancer research

Because of the growing concern about the side-effects of synthetic substances and chemicals, people often use natural products and plant based remedies in their daily/ routine life According to WHO, in Asia and Africa around 80% of the inhabitants depend on traditional systems (largely plant based) of medicine for their primary health care needs [116]. The Phytochemicals (chemicals produced by plants) have the added advantages of being dietary, simple, effective and

offering a broad spectrum of activity. Currently, research is focused in exploring medicinal plants in detail from last two decades for alleviating ailments of humankind through phytochemicals.

The Indian subcontinent offers a vast repository of medicinal plants that are used in traditional medical treatments [117]. Now westerners have also regarded Indian systems of medicine as a rich source of knowledge for curing various health problems. Almost 20,000 medicinal plants in India have been recorded however traditional communities are using only 7,000 - 7,500 plants for curing different diseases [118]. Even today, different plant and animal products, minerals and metals etc. are used in the preparations of majority of medicines. The plants used in Ayurveda medicine, often are used to provide biologically active molecules and lead structures for the development of modified derivatives with enhanced activity and /or reduced toxicity.

Several studies have been conducted on medicinal herbs, for example, Hartwell has collected data on about 3000 plants, and many of those possess anticancer properties and are subsequently used as potent anticancer drugs [119,120]. Plant are been searched from 1950s for their anti-cancer effects, leading to the discovery and development of drugs like **vinca alkaloids** (vinblastin and vincristine) [121], and the isolation of the cytotoxic **podophyllotoxins** (etoposide and teniposide) [122] and paclitaxel. They were the first agents to advance into clinical use for the treatment of cancer [122]. **Paclitaxel**, a complex taxane diterpene isolated from the bark of *Taxus brevifolia* [123] is used in clinics from last 30 years. Initially, the bark extract was reported to show cytotoxicity in 1963, later Paclitaxel´s in vivo activity against mouse leukemia was discovered in1966 and its structure was elucidated structure in 1971 [124]. Paclitaxel is significantly active against ovarian cancer, advanced breast cancer, small and non-small cell lung

cancer. Vinblastine and vincristine are also used for the treatment of a variety of cancers, including leukemia, lymphomas, advanced testicular cancer, breast and lung cancers. They are often used in combination with other cancer chemotherapeutic drugs [122]. Some of the other plant derived drugs used in clinics are camptothecin derivatives, topotecan and irinotecan, etoposide derived from epipodophyllotoxin, homoharringtonine, teniposide and docetaxel [122,125] etc. Sixty percent of currently used anticancer agents are derived in one way or another from natural sources [126]. Camptothecin, isolated from the Chinese ornamental tree *Camptotheca acuminate* was advanced to clinical trials in 1970s by NCI, but due to severe bladder toxicity, it was dropped. Later, the semi-synthetic derivatives of camptothecin, topotecan and irinotecan were developed and used for the treatment of ovarian and small cell lung cancer, and colorectal cancer, respectively.

In recent years, various plants derived molecules have been studied *in vivo* or *in vitro* for their anticancer property. Some of the these plants like, *Allium sativum* (garlic, lasun), used regularly in Indian diet has **allicin**, ajoene [127] and S-allylcysteine etc. They have been studied for cytotoxic action against Burkitt lymphoma and other transplantable tumors in several animal models [128]. **Rohitukine**, a natural product isolated from ayurvedic plant, *Dysoxylum malabaricum* Bedd., has been studied and one of its derivative flavopiridol, has been found to possess tyrosine kinase activity and thus growth inhibitory action against various breast and lung carcinoma cell lines [129]. **Betulinic acid**, another plant-derived compound from birch tree, *Betula* spp. (Betulaceae), is a lupane-type triterpene associated with replication inhibition of human immunodeficiency virus (HIV), and cytotoxicity against various of cancer cell lines [130]. Significant *in vivo* activity has also been observed in human melanoma xenografts tumor models and thus National Cancer Institute (NCI) is assisting in the development of systemic and

topical formulations for potential clinical trials. **Triterpenoid acids**, such as oleanolic and ursolic acid are common plant constituents which show weak anti-inflammatory and anti-tumor activities. New analogs have been synthesized to increase the potency. In this line 2-cyano-3,12-dioxoolean-1,9-dien-28- oic acid (CDDO) and its methyl ester has been found to exhibit potent in vitro and in vivo anti-tumor activity against a wide range of tumors, including breast carcinomas, leukemias, and pancreatic carcinomas [131]. The most abundant catechin in green tea, **epigallocatechin-3-gallate (EGCG),** has been studied to possess anti-proliferative and anti-tumor activity both in vitro and in animal models [132]. EGCG inhibited DNA methyltransferase activity with reactivation of epigenetically silenced tumor suppressor genes. **Sulforaphane,** an isothiocyanate isolated from broccoli and **pomiferin**, an isoflavone isolated from Osage orange (*Maclura pomifera*) have been identified to show anticancer properties via histone deacetylases inhibition (HDACi) [133]. **Thymoquinone,** a bioactive constituent of the volatile oil of black seed (*Nigella sativa*) have been reported in different animal models to reduce drug toxicity and cause improvement in the drug's anticancer activity. In addition, thymoquinone itself show anticancer potential due to its ability to act as pro-oxidant in human colon cancer cells [134].

Resveratrol is a flavinoid polyphenol found in the skin of red grapes, wine and blueberries [135]. Its possess excellent anti-oxidant property, but can also act as pro-oxidants in cancer cells with already elevated levels of intracellular ROS [136]. Although multiple possible effects of resveratrol have been reported [137], recent studies indicate that resveratrol inhibits synthetic and hydrolytic function of the F1-ATPase, thereby inhibiting mitochondrial ATP synthesis leading to cell death due to ROS over-production. Resveratrol is currently undergoing phase II clinical trials against colorectal cancer [138].

Curcumin (diferuloylmethane) is a polyphenol extracted from turmeric (rhizome of the plant *Curcuma longa*) [139]. Turmeric is a widely used spice in different food preparations as well as Ayurvedic medicine for centuries, as it is nontoxic and has a variety of therapeutic properties including analgesic, anti-inflammatory and antiseptic activity [140]. Curcumin is a potent antioxidant, inhibiting lipid peroxidation and effectively scavenging superoxide radical, the hydroxyl radical and other reactive oxygen species [141]. Its anticancer activities has also been well explored and are due to its effect on variety of pathways involving mutagenesis, cell cycle regulation, apoptosis (activation of caspases and downregulation of antiapoptotic gene products), proliferation (HER-2, EGFR, and AP-1), angiogenesis (VEGF) and inflammation (NF-κB, TNF, IL-6, IL-1 and COX-2) [142]. Using molecular interaction studies, curcumin has also been documented to be multi-targeting in nature [143]. Here, authors showed that curcumin can bind directly to numerous signaling molecules, such as inflammatory molecules, cell survival proteins, protein kinases, xanthine oxidase, proteasome, endoplasmic reticulum Ca^{2+} ATPase, DNA methyltransferases 1, and metal ions like copper and iron [141]. This binding property of curcumin was due to β-diketone moiety undergoing keto–enol tautomerism that has been reported as a favorable state for direct binding through covalent, non-covalent hydrophobic, and hydrogen bonding. Metal curcuminoids, the Cu $(curcumin)_2$ have been shown to be cytotoxic against L929 cells while the 1:1 complex of copper with curcumin exihibit SOD activity [141]. Several phase I and phase II clinical trials indicated that curcumin is quite safe and may exhibit therapeutic efficacy, but its utility is limited by its lack of water solubility and relatively low *in vivo* bioavailability. Furthermore, the ability of curcumin to bind directly to carrier proteins (BSA [144], Fibrinogen, immunoglobulin, casein etc.) improves its solubility and bioavailability [145]. Multiple approaches including nanoparticles, liposomes, micelles and phospholipid

complexes are being sought to overcome the transport and *in vivo* bioavailability. Liposomal curcumin has been shown to suppress pancreatic carcinoma growth in murine xenograft models. With the aim to increase the efficacy, specificity and *in vivo* bioavalability, different stuructural homologues (congeners) of cucumin are also been synthesized and studied for their biological activities [146].

Apart from different compounds/molecules isolated from plants, people also use crude extract of the medicinal plants as medicaments. This knowledge of crude extracts helps in understanding which plants to be used for the isolation and identification of the active principles and if possible the elucidation of the mechanism of action. Understanding the mechanism and structure activity relation is of paramount importance as it assists in modifying the drug for increased efficacy, increased absorbance and decreased side-effects. Understanding the drug targets also help in combining different agents for better therapeutic potential. Hence, work in both crude/mixture of traditional medicine and single active compounds are very important.

Although a number of natural agents/derivatives have entered into clinical trials and terminated due to lack of efficacy or unacceptable toxicity, the search for new plant derived anticancer molecule needs consecrated research and patience. Considering the development of some of most effective anticancer drugs, such as paclitaxel (taxol®) and the camptothecin derivatives, topotecan, and irinotecan which required 20 to 30 years of constant research to ultimately prove their efficacy as clinical drugs, a more intense research is required to this end to develop more effective with relatively safe anti-cancer molecules.

1. 8. Malabaricones

The fruit rind of the plant *Myristica malabarica* (Myristicaceae) (popularly known as rampatri, Bombay mace, or false nutmeg) is used as an exotic spice in various Indian cuisines (Figure 1. 10). It is credited with hepatoprotective, anticarcinogenic and antithrombotic properties, and is found as a constituent in many Ayurvedic preparations such as Muthu Marunthu, a herbal formulation comprising 8 plant ingredients and claimed to have an anticancer effect [147]. The phenolic compounds present in the resin of *M. malabarica* seeds have also been found to prevent the oxidation of various edible oils and fats more efficiently than butylated hydroxytoluene [148]. Although the isolation and characterization of 4 closely related compounds, malabaricones A-D from the plant were performed in 1977 [149], most of the medicinal attributes of the spice have not been adequately substantiated. Crude methanol extract of *M. malabarica* is reported to possess superoxide-scavenging activity and inhibit prolyl endopeptidase [150]. The methanolic extract was found to extract ~29% of the dry weight from fruit rind powder, while individual components were found to be 1.2%, 2.0%, 6.7%, and 8.1% for mal A, B, C and D respectively.

Figure 1. 10. Fruit rind of *M. malabarica.*

Earlier, we have found that amongst the four malabaricones A–D (designated as mal A–D), isolated from methanolic extract of fruit rind of *Myristica malabarica*, mal B and mal C possess superior antioxidant [151] and the gastroprotective properties against indomethacin-

induced stomach ulceration [152,153]. Recently, anti-quorum sensing activity [154], anti-inflammatory properties [155,156] and the anti-proliferative properties [157] of one of its constituent, malabaricone C has also been reported. Interestingly, mal C, containing a B-ring catechol moiety showed significantly better Cu(II)-dependent nuclease activity and toxicity against MCF-7 human breast cancer cell line [158]. In addition, malabaricone A having pro-oxidant activity mediate its cytotoxicity in U937 and MOLT-3 (leukemic) cells via induction of oxidative stress triggering a caspase dependent apoptosis.

Malabaricone C ($C_{21}H_{26}O_5$, Mol.wt. – 358, 1-(2,6-dihydroxyphenyl)-9-(3,4-dihydroxyphenyl)nonan-1-one), Melting Point-119-121°C, is a polyphenol that can interact and interfere with basic cellular mechanisms through their anti-oxidants and pro-oxidant properties (Figure 1. 11) [158]. This compound belongs to the class of organic compounds known as butyrophenones. Metal chelation and radical scavenging are the mechanism for its antioxidant action while binding with transition metals like copper to generate radical species through fenton reaction are the mechanism for pro-oxidant activity [158]. Like any other polyphenol, the chain-breaking ability of malabaricone C is attributed to the ease of donation of the phenolic H-atom to the attacking free radical. Usually with their ant-oxidant potential, risk of developing various types of cancer is significantly reduced. While with pro-oxidant potential they induces high amount of radicals to induce DNA, protein or membrane damage and thus killing cancer cell.

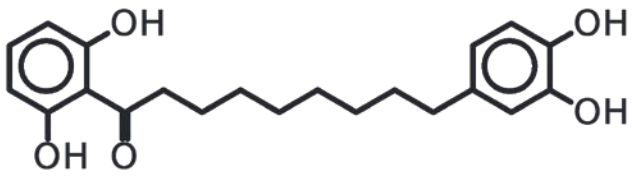

Figure 1. 11. Structure of malabaricones C

Despite the historical medical usage of malabariocnes and the extensive research efforts on its active constituents, identification of the target site and mechanism of actions of malabaricones against cancer cells are not yet explored. Based on these preliminary findings, the main objectives of this doctoral work was focused on to evaluate the anti-cancer potential of malabaricones (especially malabaricone C), by modulating several molecular targets in cancer cell lines. To this end, following objectives were formulated to investigate the efficacy and molecular mechanisms of anti-cancer potentials of malabaricone C:

1) To explore the anticancer potential of malabaricones against multiple cancer cell lines.

2) To investigate the underlying molecular mechanism of action of the highly effective malabaricones in killing cancer cells.

3) To elucidate the role of highly potential malabaricone in sensitizing cancer cells to apoptosis in response to chemotherapeutic drugs, radiation or other adjuvants.

4) To evaluate the *in vivo* anticancer ability of highly potential malabaricone in mice.

CHAPTER-II

MATERIALS

AND

METHODS

All the chemicals, antibodies, cell lines used in this study are listed in the following tables

2. 1. List of Chemicals

Sl. No.	Name of the chemicals	Source of Procurement
1.	VP-16 (Etoposide)	Sigma Chemicals (St. Louis, MO)
2.	3-(4,5-dimethylthiazol-2-yl)-2,5-diphenyltetrazolium bromide (MTT)	Sigma Chemicals (St. Louis, MO)
3.	N-acetylcysteine (NAC)	Sigma Chemicals (St. Louis, MO)
4.	Uridine	Sigma Chemicals (St. Louis, MO)
5.	Ethidium bromide (EtBr)	Sigma Chemicals (St. Louis, MO)
6.	Sodium pyruvate (Pyur-Na)	Sigma Chemicals (St. Louis, MO)
7.	UCN-01	Sigma Chemicals (St. Louis, MO)
8.	Annexin-V kit	Sigma Chemicals (St. Louis, MO)
9.	Kits of caspases-3, -8, -9 activities	Sigma Chemicals (St. Louis, MO)
10.	Dulbecco's modified Eagle's medium (DMEM)	Himedia, Mumbai, India
11.	Fetal bovine serum (FBS)	Gibco Life Technologies (CarlsBAD, CA)
12.	U0126	Calbiochem (Gibbstown, NJ)
13.	KU55933	Calbiochem (Gibbstown, NJ)
14.	SP600125	Calbiochem (Gibbstown, NJ)
15.	SB203580	Calbiochem (Gibbstown, NJ)
16.	Lipofectamine reagent	Invitrogen (CarlsBAD, CA)
17.	Lumi-Light PLUS western blotting kit	Roche Applied Science (BADen-Wurttemberg, Mannheim)
18.	Cell death detection PLUS kit	Roche Applied Science (BADen-Wurttemberg, Mannheim)
19.	Schisandrin B	LKT laboratories (St. Paul, MN, USA)
20.	L-Glutamine	Sigma Chemicals (St. Louis, MO)
21.	Hepes buffer	Sigma Chemicals (St. Louis, MO)
22.	Streptomycin	Sigma Chemicals (St. Louis, MO)
23.	Penicillin	Sigma Chemicals (St. Louis, MO)

24.	Catalase	Sigma Chemicals (St. Louis, MO)
25.	Superoxide dismutase (SOD)	Sigma Chemicals (St. Louis, MO)
26.	NP-40	Sigma Chemicals (St. Louis, MO)
27.	EGTA (ethylene glycol-bis(β-aminoethyl ether)-N,N,N',N'-tetraacetic acid)	Sigma Chemicals (St. Louis, MO)
28.	Ethylenediaminetetraacetic acid (EDTA)	Sarabhai Chemicals, Baroda, India
29.	Curcumin	Aldrich, Milwaukee, WI
30.	Protease Inhibitor Cocktail Tablets	Roche Applied Science (BADen-Wurttemberg, Mannheim)
31.	Z-LEHD-FMK (caspase-9 specific)	Calbiochem (Gibbstown, NJ)
32.	Ac-IETD-CHO (caspase-8 specific)	Calbiochem (Gibbstown, NJ)
33.	Ac-DEVD-CHO (caspase-3 specific)	Calbiochem (Gibbstown, NJ)
34.	Z-VAD-FMK (pan-caspase)	Calbiochem (Gibbstown, NJ)
35.	35% H2O2	Lancaster, Morecambe, UK
36.	Phenylmethylsulfonyl fluoride (PMSF)	Sigma chemicals (St. Luois, MO).
37.	PD150606	Sigma chemicals (St. Luois, MO).
38.	Fura 2-AM	Sigma chemicals (St. Luois, MO).
39.	Thapsigargin,	Sigma chemicals (St. Luois, MO).
40.	RNAse A	Sigma chemicals (St. Luois, MO).
41.	propidium iodide (PI)	Sigma chemicals (St. Luois, MO).
42.	Triton X-100	Sigma chemicals (St. Luois, MO).
43.	Acridine orange (AO)	Sigma chemicals (St. Luois, MO).
44.	Sodium orthovanadate ($NaVO_4$)	Sigma chemicals (St. Luois, MO).
45.	Leupeptin	Sigma chemicals (St. Luois, MO).
46.	Aprotinin	Sigma chemicals (St. Luois, MO).
47.	Hoechst 33342	Molecular Probes Inc. (Eugene, OR)
48.	BAPTA-AM	Molecular Probes, Inc. (Eugene, OR)
49.	Calpain activity assay kit	BioVision (Milpitas, CA)

50.	Nitrocellulose membrane (BioTrace ® NT)	Pall Life Sciences (Easthills, NY)
51.	Ru360	(Calbiochem, Gibbstown, NJ)
52.	2',7'-dichlorodihydrofluorescin diacetate (H2DCFH-DA)	Sigma Chemicals (St. Louis, MO)
53.	Dihydroethidium (DHE)	Sigma Chemicals (St. Louis, MO)
54.	Trolox®	Sigma Chemicals (St. Louis, MO)
55.	Tocopherol	Sigma Chemicals (St. Louis, MO)
56.	PEG-Catalase (PEG-CAT)	Sigma Chemicals (St. Louis, MO)
57.	PEG-SOD	Sigma Chemicals (St. Louis, MO)
58.	Mitochondrial isolation kit	Abcam, USA
59.	Sh-RNA-p53 (scrambled or targeting)	Imgenex, San Diego, CA
60.	Sh-RNA-NEMO (scrambled or targeting)	Imgenex, San Diego, CA
61.	Sh-RNA BCL2 (scrambled or targeting)	Imgenex, San Diego, CA
62.	lentiviral particles encoding shRNA (scrambled or targeting ATM)	Santa Cruz Biotechnology, Santa Cruz, CA
63.	Agarose	Bangalore Genei (P) Ltd., India
64.	Low melting agarose	Sigma Chemicals (St. Louis, MO)
65.	JC-1	Invitrogen (CarlsBAD, CA)
66.	Glutathione (reduced)	Sigma Chemicals (St. Louis, MO)
67.	Ethyl acetate AR grade	S D Fine Chemicals, Mumbai
68.	Chloroform AR grade	S D Fine Chemicals, Mumbai
69.	Methanol AR grade	S D Fine Chemicals, Mumbai
70.	Trizole Reagent	Life Technologies, CarlsBAD, CA
71.	MononbromoBIMane (mBBr) -	Molecular Probes, Inc., Eugene, OR
72.	Bradford Reagent	Sigma Chemicals (St. Louis, MO)
73.	Propidium Iodide	Sigma Chemicals (St. Louis, MO)
74.	Triton™ X-100	Sigma Chemicals (St. Louis, MO)

75.	Sodium Sarcosinate	Sigma Chemicals (St. Louis, MO)
76.	Ethidium Bromide	SRL Pvt., Mumbai, India
		Roche Biochemicals GmbH, Germany

Antibodies

1.	Cytochrome c	Sigma Chemicals (St. Louis, MO)
2.	Caspases-3, -8 and 9	Sigma Chemicals (St. Louis, MO)
3.	BAX	Cell Signaling Technology Inc. (Danvers, MA)
4.	β-actin	Cell Signaling Technology Inc. (Danvers, MA); (Abcam Danvers, MA)
5.	BCL-2	Cell Signaling Technology Inc. (Danvers, MA)
6.	AIF	Sigma chemicals (St. Luois, MO).
7.	Endo G	Sigma chemicals (St. Luois, MO).
8.	BID	(Cell Signaling Technology Inc., Danvers, MA)
9.	COX IV	(Santa Cruz Biotechnology Inc.,Dallas, TX)
10.	p21	Cell Signaling Technology Inc. (Danvers, MA).
11.	P53	Sigma Chemicals (St. Luois, MO)
12.	STAT3	Sigma Chemicals (St. Luois, MO)
13.	XIAP	Sigma Chemicals (St. Luois, MO)
14.	IKBα	Sigma Chemicals (St. Luois, MO)
15.	γ-H2AX	Sigma Chemicals (St. Luois, MO)
16.	H2AX	Abcam, USA
17.	CHK1	Cell Signaling Technology Inc. (Danvers, MA).
18.	ATM	Cell Signaling Technology Inc. (Danvers, MA).
19.	p-ATM	EMD Millipore, KGaA, Germany
20.	p-CHK1	Cell Signaling Technology Inc. (Danvers, MA).
21.	p-p38	Cell Signaling Technology Inc. (Danvers, MA).
22.	p-JNK	Cell Signaling Technology Inc. (Danvers, MA).
23.	p-ERK	Cell Signaling Technology Inc. (Danvers, MA).
24.	P38	Cell Signaling Technology Inc. (Danvers, MA).

25.	JNK	Cell Signaling Technology Inc. (Danvers, MA).
26.	ERK	Cell Signaling Technology Inc. (Danvers, MA).
27.	Beclin-1	Cell Signaling Technology Inc. (Danvers, MA).
28.	ATG5	Cell Signaling Technology Inc. (Danvers, MA).
29.	p-MAPKAPK-2	Cell Signaling Technology Inc. (Danvers, MA).
30.	MAPKAPK-2	Cell Signaling Technology Inc. (Danvers, MA).
31.	P65	(Santa Cruz Biotechnology Inc.,Dallas, TX)
32.	Cathepsin B	(Santa Cruz Biotechnology Inc.,Dallas, TX)
33.	Cathepsin L	(Santa Cruz Biotechnology Inc.,Dallas, TX)
34.	GSH	Abcam, USA
35.	PCNA	(Santa Cruz Biotechnology Inc.,Dallas, TX)

2. 2. List of cell lines

Sl. No.	Name of the cell lines	Details	Source of Procurement
1	HCT-15	Human colon cancer	NCCS, Pune
2	A549	Human lung carcinoma	NCCS, Pune
3	NCI-H23	Human lung adenocarcinoma	NCCS, Pune
4	NCI-H460	Human lung carcinoma	NCCS, Pune
5	NCI-H522	Human lung carcinoma	NCCS, Pune
6	U2OS	Human Osteosarcoma	NCCS, Pune
7	MDA-MB-231	Human breast cancer	NCCS, Pune
8	MCF-7	Human breast cancer	NCCS, Pune
9	A375	Human Melanoma	NCCS, Pune
10	A498	Human kidney carcinoma	NCCS, Pune
11	A431	Human skin carcinoma	NCCS, Pune
12	SH-SY5Y	Human Neuroblastoma	NCCS, Pune
13	IMR-32	Human Neuroblastoma	NCCS, Pune
14	B16F10	Mouse melanoma	NCCS, Pune

2. 3. Sample preparation for malabaricones

Dried fruit rinds of *M. malabarica* (250 g) were successively extracted with ether, methanol, and water (750 ml x 4 with each solvent) at room temperature. The supernatants, in each case were decanted and saved. The entire process was repeated thrice, each of the combined supernatants was filtered through a nylon mesh and evaporated at <40 °C in vacuum to obtain the respective extracts. The methanolic extract (designated as RM, 72.1 g, 28.9%) was stored in a vacuum dessicator. RM (3.7 g) was subjected to partial fractionation over a silica gel (25 g) column, eluting with hexane to collect five 300 ml fractions. These were column chromatographed (silica gel, 0-20% EtOAc/hexane) to isolate the known malabaricones (malabaricones A-D) including malabaricone C (designated as mal C) [149]. Mal C was fully characterized using IR and 1H NMR spectroscopic data. The chemical structures of malabaricones A-D are shown in Fig. 3. 1. 1.

Freshly prepared stock solution of mal A-D (10 mM) in DMSO were diluted with DMEM (without serum) to attain the required concentrations, and used for the cell line studies. For the mice experiments, mal C solutions were prepared in Neobee M5 oil (Sigma) to attain the required concentrations.

2. 4. Cell culture

The cell lines were procured from the National Centre for Cell Science, Pune, India or unless mentioned. The cells were cultured and maintained by standard protocols. Briefly, the cells were routinely seeded at a density of 0.1–3 $x10^6$ cells/ mL in Dulbecco's Modified Eagle Medium (DMEM) or RPMI-1640 medium, supplemented with 10% heat inactivated FBS, 2 mM glutamine, 100 U/mL penicillin and 100 µg/ml streptomycin. The cells were grown at 37 °C under humidified atmosphere of 5% CO_2. Cells were passaged every 3–4 days to maintain at the

level of 80–90% confluency. Sub-culturing was done by trypsinization with 0.25% trypsin in phosphate-buffered saline (PBS).

2. 4. 1. Generation of mitochondria-deficient A549-ρ^o cells

The mitochondria-deficient A549-ρo cells were generated and maintained as described previously with minor modifications [159–161]. Briefly, the A549 cells were cultured in a complete DMEM medium supplemented with 10% FBS and 2 mM L-glutamine, 1 mM sodium pyruvate, 1 mM uridine and 40, 60 and 80 ng/mL of EtBr till 24 passages for 8 weeks with 50 – 70 % confluency. The A549 cells, cultured in medium without EtBr served as the control (wild-type A549-ρ^+). Mitochondria depletion in the A549-ρ^o cells was confirmed by analyzing the loss of mitochondria specific protein, cytochrome oxidase IV. The A549-ρ^o cells also showed a disrupted mitochondrial architecture, as confirmed from the severely low staining by the mitochondria-specific dye, MitoTracker Red. For treatment, A549-ρ^o and A549-ρ^+ cells were treated with EtBr-free ρ^o medium containing pyruvate and uridine as mentioned above.

2. 4. 2. Stable transfection in A549 cells

2. 4. 2. 1. Depletion of BCL2 by shRNA

The A549 cells were transfected with plasmids procured from Imgenex, San Diego, CA, encoding scrambled short-hairpin RNA (shRNA) or shRNA against BCL2 by using lipofectamine 2000 to generate BCL2-WT cells and BCL2 knock down cells (BCL2-KD) respectively. The cells were grown for two weeks in a medium containing G418 (800 μg/ml). Several antibiotic-resistant clones were expanded and screened. The clone with the lowest expression of BCL-2 was selected for the studies and maintained further in the presence of G418 (400 μg/ml).

2. 4. 2. 2. Depletion of ATM by shRNA

The A549 cells were exposed to lentiviral particles (Santa Cruz Biotechnology, Santa Cruz, CA) encoding scrambled shRNA (ATM-WT cells) or targeting ATM to generate ATM-KD cells by using polybrene. The ATM-KD and respective WT cells were grown for two weeks in a medium containing puromycin (1 μg/ml). Several antibiotic-resistant clones were expanded and screened for ATM proteins. The selected clone with lowest expression of ATM was used for further studies and maintained in the presence of puromycin (0.5 μg/ml).

2. 4. 2. 3. Depletion of p53 by shRNA

The A549 cells were transfected with plasmids (Imgenex, San Diego, CA) encoding scrambled short-hairpin RNA (shRNA) and shRNA against p53 using lipofectamine 2000 to generate p53-WT cells and p53 knock down cells (p53-KD) respectively. The cells were grown for two weeks in a medium containing containing G418 (800 μg/ml). Several antibiotic-resistant clones were expanded and screened. The clone with the lowest expression of p53 was selected for the studies and maintained further in the presence of G418 (400 μg/ml).

2. 5. Determination of cell death

Cell death induced by malabaricones and other treatments in different cell lines was determined by using following assays.

2. 5. 1. MTT reduction assay

The MTT, cell proliferation assay measures the cell proliferation rate and conversely, when metabolic events lead to apoptosis or necrosis, the reduction in cell viability. The cytotoxic effects of the malabaricones, curcumin and VP-16 were determined by the MTT reduction assay, as reported earlier [158]. Briefly, cells (5000/well) grown in 96-well plates were incubated overnight at 37 °C under an atmosphere of 5% CO_2. Next day the cells were incubated with vehicle (0.1% DMSO) or various concentrations of the respective compounds for 24 and 48 h.

The cells were washed once with PBS, MTT solution (0.5 mg/mL, 100 μL) was added to each well and kept at 37 °C for 6 h. The formazan crystals in the viable cells were solubilized with 0.01 N HCl (100 μL) containing 10% SDS and the absorbance at 550 nm.

2. 5. 2. Clonogenic survival assay

The cells (500/well) were seeded in 6-well plates and incubated with vehicle (0.1% DMSO) or different concentrations of mal C (0-6 μM) or NAC (5 mM) or in combination or different doses of gamma-radiation at 37 °C for 12 days in the growth media. The colonies were fixed with methanol and stained with 0.5% crystal violet in 1:1:1 acetic acid:methanol:water. Colonies were counted, and images of colonies were scanned. The surviving fractions were determined from the colony counts and corrected for the plating efficiency (75.5%, for A549 lung cancer cell line) of the non-treated controls.

2. 6. Determination of apoptosis

2. 6. 1. Cellular DNA fragmentation through ELISA

Following manufacturer's protocol, the apoptosis induction in the untreated and treated cells was assessed using a cell death ELISA plus kit, which uses a photometric enzyme immunoassay to quantify the accumulation of cytoplasmic histones associated DNA fragments (mono and oligosomes) after the apoptotic cell death. The extent of apoptosis was evaluated by assessing the enrichment of nucleosomes in the cytoplasm. Etoposide (VP16, 25 μM) was used as the positive control.

2. 6. 2. Analysis of annexin V binding

A detail procedure for analysis of apoptosis specific Annexin V binding on cell surface is described in section 2. 7. 3.

2. 6. 3. Caspase activity assays

The assays were performed with a caspase-3 colorimetric kit or caspase-8 and caspase-9 fluorimetric kits according to the manufacturer's protocol. The untreated or mal B or mal C-treated cells (1 x 10^6/well) were incubated for 16 h, and assayed for the individual caspase activity by spectrophotometric detection of the chromatophore p-NA(p-nitroaniline) after cleavage from the respective labeled substrates by caspase-8, caspase-9, and caspase-3. For the caspase inhibition studies, cell lysates were treated with the inhibitory peptides (each 20 μM) Z-LEHDFMK (caspase-9 specific), Ac-DEVD-CHO (caspase-3 specific), and Ac-IETD-CHO (caspase-8 specific) prior to caspase activity assay.

2. 7. Flow Cytometry

All the flow cytometry analyses were carried out with a Partec CyFlow® Space flow cytometer using the FlowJo software. Cellular debris was excluded from the analyses by raising the forward scatter threshold. At least 2 × 10^4 cells of each sample were analyzed at a flow rate of 250–300 cells/s, and the data were registered on a logarithmic scale.

2. 7. 1. Quantification of sub-G1 cells

The hypodiploid DNA content (sub-G1) were analyzed as a marker for apoptosis by flow cytometry. Briefly, the cells (2-3 × 10^5 cells/well) treated with respective compounds for 24 h were collected, washed with cold PBS and incubated in PBS containing Triton X-100 (0.1%), PI (40 μg/ml) and RNAse A (100 μg/ml) for 30 min at 37 ^oC. The cells were then analyzed by flow cytometry. The DNA content of the nuclei (20000 cells) was acquired on a logarithmic scale. The apoptotic nuclei appeared as broad hypodiploid DNA peaks. Similar experiments were also carried out using cells, pretreated with various inhibitors mentioned in respective figures, followed by incubation with mal C (6 μ M) for 24 h.

2. 7. 2. Cell Cycle analysis

Cells were treated as described in the respective figures, washed and fixed with 70% ethanol. Cells were than washed with cold PBS and incubated in PBS containing Triton X-100 (0.1%), PI (40 μg/ml) and RNAse A (100 μg/ml) for 30 min at 37 ^{o}C. The cells were then analyzed by flow cytometry. At least 20000 cells of each sample were analyzed. The DNA content of the nuclei was registered on a linear scale.

2. 7. 3. Analysis of annexin V binding

The flipping of phosphatidyl serine (PS) was assessed by using annexin V/PI apoptosis detection kit, Sigma, as per the manufacturer's instructions. Cells (5×10^5 cells/well) treated with respective concentration of mal C were trypsinized, washed twice and then stained with annexin-V-FITC in binding solution for 20 min. Just before acquiring the cells through flow cytometer, Propidium Iodide (PI) was added to exclude the dead/necrotic/late apoptotic cells.

2. 7. 4. Mitochondrial transmembrane potential (ΔΨm)

The A549 and MCF-7 cells ($1x10^5$ cells/well), cultured in 6-well plate were incubated with mal C (0, 4, and 6 μM) for different time points, washed with PBS, and incubated with JC-1 (20 μM) for 15 min at 37 ° C. The cells were collected, washed once with cold PBS and analyzed for the ΔΨm loss from the shift of emission from green (~ 525 nm) to red (~ 590 nm) with a Pertec CyFlow ® Space flow cytometer using the FlowJo software.

2. 7. 5. Measurement of intra-cellular ROS level using DCFDA and DHE dye

Dichloro-dihydrofluorescein diacetate (H2DCFDA), a lipid soluble membrane permeable dye upon entering cells undergoes deacetylation by intracellular esterases and forms non-fluorescent dye Dichloro-dihydrofluorescein (H2DCF). This is subsequently oxidized by ROS to form a two-electron fluorescent oxidation product, Dichlorofluorescein (DCF); therefore, the

fluorescence generated is directly proportional to the amount of ROS. Another redox sensitive dye, which detects essentially superoxide radicals, is Dihydroethidium (DHE). DHE can freely permeate the cell membrane and upon reaction with superoxide anions forms a red fluorescent product (2-hydroxyethidium) which intercalates with DNA. The ROS levels using DCFDA and DHE in mal C-treated cells were detected as per reported protocol [162,163] with minor modifications. Briefly, A549 cells were loaded with 20 μM oxidation-sensitive H2DCF-DA or 10 μM DHE for 15 min at 37 °C before treated with various concentrations of mal C (0-8 μM) for indicated time periods. The cells were collected by trypsinization, washed two times with PBS, and suspended in PBS. The ROS levels, expressed in arbitrary units were analyzed from the increased green fluorescence (excitation at 480 nm and emission at 530 nm) of oxidized DCFDA by spectro-fluorimeter or in Green channel for DCFDA and red channel for DHE by flow cytometry. Similar experiments were carried out with cells pre-incubated with antioxidants/ROS scavengers for 1h, followed by mal C treatment. H_2O_2 (25 μM) was used as the positive control and incubation was carried out for indicated time periods.

2. 7. 6. Intracellular thiols assay

To measure intracellular glutathione (GSH) concentrations, a non-enzymatically reactive dye monobromoBIMane was used as per reported protocol [164] with minor modifications. Briefly, A549 cells were incubated in the absence or presence of NAC for 1 h, treated with indicated concentrations of mal C (0-8 μM) for 3 h. Cells were washed with PBS, resuspended in PBS and labelled with monobromoBIMane, (mBBr, 40 μM). The fluorescence was recorded using UV laser in the flow cytometer.

2. 8. Comet assay

To measure DNA double strand breaks in cells induced by different treatment, alkaline or neutral comet assay was carried out as per reported protocol [165] with minor modifications. Briefly, untreated and treated cells ($0.5x10^5$) were washed with PBS and suspended in DMEM medium (10 µL). Frosted slides, coated with 80 µL of 0.5% high melting agarose was layered with 100 µL of low melting point (LMP) agarose (0.8% in PBS) containing 0.5×10^5 cells at 40 °C. Cover slips were placed immediately and the slides were placed on ice. After solidification, the cover slips were removed and each slide was coated with another layer of 100 µL LMP (0.8%) and kept at 4 °C as above. After removing the cover slip, the slides were placed in the lysing solution containing 2.5 M NaCl, 100 mM Na_2EDTA and 10 mM Tris–HCl, pH 10.0 with freshly added 1% Triton X-100 and 1% sodium sarcosinate for 1 h at 4 °C. The slides were removed from the lysis solution, washed three times with alkaline electrophoresis buffer and placed on a horizontal electrophoresis tank, filled with freshly prepared alkaline buffer (300 mM NaOH, 1 mM Na2–EDTA, 0.2% DMSO, pH 13.0). The slides were equilibrated in the same buffer for 20 min and subjected to electrophoresis for 25 min at 1 V/cm. The slides were washed gently with 0.4 M Tris–HCl buffer, pH 7.4 to remove alkali, stained by layering on the top with 20 µL of propidium iodide (20 µg/mL), and visualized under Axioskop II Mot plus (Zeiss) microscope (40× optics).

2. 9. Intracellular Ca^{2+} measurement

Cells (1×10^5 cells/ml) in suspension, were stained with Fura-2AM (20 µM) for 30 min, followed by treatment with mal C (0 and 6 µ M) for 0–12 min. Similar experiments were also carried out using cells, pretreated with BAPTA- AM (2 µM) for 1 h, prior to addition of Fura-2AM, followed by incubation with mal C for 0-12 min. The intracellular Ca^{2+} levels were assessed through spectrofluorimetry using excitation at 340 and 380 nm and emission at 510 nm.

2. 10. Calpain activity assay

The intracellular calpain activity was measured using a commercial kit as per manufacturer's protocol (calpain activity kit, Biovision). Briefly, cells (1 x 10^5 cells / well) were incubated with vehicle or mal C (6 μM) for 0–24 h, and extracted in 100 μl of extraction buffer. The samples were gently mixed by tapping several times, centrifuged for 1 min at 10,000 g, the supernatant were transferred to a fresh tube and cooled on an ice bath. The protein concentration was assayed; the cell lysate (100 μg) was diluted to 85 μl with extraction buffer, followed by addition of reaction buffer (10 μl) and the calpain substrate (5 μl). The reaction mixture was incubated at 37 °C for 1 h in the dark. The fluorescence of the samples was read with a fluorimeter, equipped with a 400-nm excitation filter and 505-nm emission filter. The changes in calpain activity of each sample were expressed as relative florescence unit (RFU)/mg protein. Active calpain, provided in the kit was used as the positive control.

2. 11. Whole cell, nuclear and cytosolic extract preparation

The whole cell extracts, nuclear extracts, and chromatin extracts were prepared as per earlier report [166] with minor modifications. The cells (1×10^7 cells/treatment) were grown in 90 or 150-mm petri dishes with 70-80% confluency followed by mal C treatment and scraped into ice-cold phosphate-buffered saline (PBS). Cells were centrifuged at 3000 RPM for 4 min at 4 °C. The whole cell extracts were prepared by lysing the cells in a lysis buffer [Tris (20 mM, pH 7.4), NaCl (250 mM), EDTA (2 mM , pH 8.0), Triton X-100 (0.1%), aprotinin (0.01 μg/ml), leupeptin (0.01 μg/ml), PMSF (0.4 mmol/l), and NaVO4 (4 mmol/l)]. The lysates were spun at 12,000 RPM for 10 min; the supernatants were collected as whole cell lysate and kept at -70 °C. For cytoplasmic, nuclear and chromatin lysates, cells were resuspended in buffer A [HEPES (10 mM, pH 7.9), KCl (10 mM), MgCl2 (1.5 mM), sucrose (0.34 M), glycerol (10%), DTT (1 mM)

and Triton X-100 (0.1%)] supplemented with a mixture of protease inhibitors (Roche Diagnostics) for 5 min on ice. Nuclei were collected in pellet by low-speed centrifugation (4 min, 1,300 x g, 4°C) and the supernatant was kept as cytoplasmic extract. The supernatant was further clarified by high-speed centrifugation (15 min, 13,000 x g, 4°C) to remove cell debris and insoluble aggregates. Nuclei were washed once in buffer A, and then lysed in buffer B [EDTA (3 mM), EGTA (0.2 mM), DTT (1mM) and protease inhibitors as described above). Insoluble chromatin was collected by centrifugation (4 min, 1,700 x g, 4°C), washed once in buffer B, and resuspended in buffer A plus $CaCl_2$ (1 mM) and micrococcal nuclease (0.2 U). After incubation at 37°C for 1 min, centrifuged again under the same conditions. The final chromatin pellet was resuspended in Laemmli buffer and sonicated for 15 s at 33% amplitude and boiled. The chromatin extract. Insoluble proteins were removed by high-speed centrifugation (30 min, 16,000 g, 4°C) and supernatant was treated as chromatin extract. The chromatin, nuclear and cytosolic extracts were subjected to immunoblotting as described below.

2. 12. Immunoblotting

The cell lysates were subjected to 8-15% SDS PAGE gel electrophoresis, and separated proteins were then electro-transferred to nitrocellulose membrane. The membranes were blocked for 1 h at room temperature in TBST buffer Tris (20 mM, pH 7.6), NaCl (137 mM), and Tween-20 (0.1% v/v) containing nonfat milk [2% (w/v)], and then incubated overnight at 4 °C with the required specific primary antibodies. After several washes, HRP-conjugated secondary antibody was added, the membranes were incubated further for 1 h, and the blots were developed using a Lumi-Light PLUS western blotting kit. Protein amounts (arbitrary unit, mean ± SEM) are quantified by ImageJ software, results of three independent experiments were averaged

considering that of untreated control cells as 1, which was quantified after normalizing with respect to the loading controls.

2. 13. Microscopy

2. 13. 1. Phase contrast Microscopy

The A549 or MCF-7 cells (1 x 10^5 cells per well) cultured in 6-well plates, grown on cover slips were incubated with different concentration of mal C (2.5–10 μM) for 24 h. The cells were washed two times with PBS and visualized under a phase contrast microscope. Representative Field of cells were photographed using a Zeiss Axioskop 2 mot plus microscope (40 X objective, 0.65 Ph2), fitted with an Axiocam MRc camera.

2. 13. 2. Fluorescence microscopy

A549 or MCF-7 cells (1 x 10^5 cells/well), cultured on cover slips in 6-well plate were incubated with mal C (0-6 μM) for various periods [6 h for studying ΔΨm loss, 16 h for AIF release, 24 h for chromatin condensation, and 3 h for Lysosomal membrane permeabilization (LMP)]. The cells were stained with Hoechst 33342 (10 μM) or JC-1 (20 μM) or AO (10 μM) for 15 min, washed once with PBS, mounted with glycerol (70%), and analyzed under an Axioskop II Mot plus (Zeiss) microscope (40 X optics) for apoptosis, ΔΨm , and LMP loss, respectively. For detecting AIF release, the cells were washed once with PBS, fixed with 4% paraformaldehyde for 30 min at 4 °C, washed again with PBS, and incubated overnight in PBS containing BSA (5% w/v) and Triton X-100 (0.4% w/v). The cells were subsequently incubated with anti-AIF antibody in PBS containing BSA (2% w/v) and Triton X-100 (0.2% v/v) for 1 h at room temperature. After washing, cells were treated with Alexa Fluor ® 488-linked anti-rabbit secondary antibody in PBS containing BSA (2% w/v) and Triton X-100 (0.2% v/v), incubated

for 1 h at room temperature, washed once with PBS, stained with Hoechst dye 33342, and observed under a fluorescence microscope as above.

2. 13. 3. Confocal microscopy

The A549 cells grown in cover slips, kept in 35 mm petri dishes were treated with mal C and NAC as described in the respective figure legends. After washing, cells were washed with PBS, fixed in paraformaldehyde (4% w/vin PBS) for 20 min at room temperature. Afterwards, the cells were washed twice in PBS. For immunofluorescence staining, cells were permeabilized for 10 min in Triton X-100 (0.25% v/v) in PBS, washed two times in PBS and blocked for 1 h with BSA (5% w/v) in PBS [167]. Antibodies were diluted (1:500) with BSA (5% w/v) in PBS and incubated for 1.5 h at room temperature, washed thrice with PBS and incubated in secondary antibodies for 1 h at room temperature. Finally, stained with Hoechst dye for nuclear visualization, and mounted onto glass slides. Images were captured using LSM780 confocal microscope (Carl Zeiss Microscopy, Jena GmbH, Germany). Acquisition settings were optimized to obtain maximal signal in immunostained cells with minimal background. Overlay images were recorded by superimposing simultaneous images from each channel.

To detect nuclear ROS (superoxide) by using DHE dye, the cells were pre-incubated with DHE (5 μM) for 30 min and then treated with mal C (6 μM) or NAC (5 mM) or in combination for 1 and 3 h. Cells were washed with PBS, fixed with 1% paraformaldehyde for 10 min, permeabilized in PBS containing Triton X-100 (0.5% v/v) for 30 min and then visualized under confocal microscope.

2. 13. 4. Image analysis using ImageJ software

The captured images were analyzed for relative quantification using ImageJ software. A box was positioned over the fluorescent image of each cell, and the average intensity within the selection

(the sum of the intensities of all the pixels in the selection divided by the number of pixels) was measured. At least 100 cells per experiment were analyzed from three independent experiments.

2. 14. S-gluatathionylation assay

S-glutathionylation of proteins was quantified using a reported protocol with minor modifications [92]. The A549 cells were treated with mal C (6 μM) in the presence and absence of NAC (5 mM) for 0-8 h. The cells were washed with PBS and stored at -70 °C till further processing. The cytoplasmic and nuclear extracts were prepared as described above, except for addition of N-ethylmaleimide (NEM, 10 mM) in lysis buffer to block the free thiols. The cytoplastmic extract was subjected to electrophoresis on non-reducing SDS polyacrylamide gel and western blotting. The S-glutathionylated proteins detected with anti-GSH antibody (Abcam, USA) and quantified.

2. 15. Immunoprecipitation

The cells (1×10^7 cells/ group) were incubated in the absence or presence of NAC (5 mM) for 1 h followed by incubation with mal C (6 μM) in the continued absence or presence of NAC 8 h. Subsequently, the cells were washed, scraped, precipitated and lysed in a cytosolic lysis buffer [HEPES (10 mM, pH 7.9), KCl (10 mM), MgCl2 (1.5 mM), sucrose (0.34 M), glycerol (10%), DTT (1 mM) and Triton X-100 (0.1%)] supplemented with a mixture of protease inhibitors and N-ethylmaleimide (NEM, 10 mM) as defined above. 500 μg protein of each sample was immunoprecipitated overnight at 4 °C using 10 μg of rabbit anti-p65 IgG or mouse anti-p53 IgG or control rabbit or mouse IgG antibodies. The antibodies were then pulled by protein G-agarose beads, boiled in 1x loading dye , subjected to electrophoresis on non-reducing SDS polyacrylamide gel, The S-glutathionylated protein detected with anti-GSH antibody (Abcam, USA).

2. 16. Animals

C57BL/6 male mice bred at the BARC laboratory animal house facility, Mumbai, India,, and SCID mice (purchased from VivoBiotech, HyderaBAD) were procured after obtaining clearance from the BARC Animal Ethics Committee (BAEC, BAEC/08/13 and BAEC/06/15). The mice (6 to 8 weeks-old, weighing 20–30 g) were reared on a balanced laboratory diet as per National Institute of Nutrition, HyderaBAD, India, and given tap water ad libitum. Mice were kept in well-ventilated cages at 20 ± 2^{o}C, 65–70% humidity, and day/night cycle (12 h/12 h). All animals were handled following International Animal Ethics Committee Guidelines, and the experiments were conducted with strict adherence to the ethical guidelines laid by the European Convention for the Protection of Vertebrate Animals for experimental and other scientific purposes. In addition, the ethical guidelines for the purpose of control and supervision of experiments on animals, constituted by the Animal Welfare Division, Government of India on the use of animals in scientific research were followed.

2. 17. Anti-tumor studies

Male C57BL/6 and SCID mice, at the age of 6 weeks (mean body weight, 21.2 g), were injected subcutaneously with B16F10 cells and A549 cells on right flank respectively. The B16F10 and A549 cells were grown up to 70% confluency, harvested by trypsinization, washed twice with DMEM media, re-suspended in ice-cold DMEM and kept on ice until transplantation. Right flank region of the male recipient C57BL/6 mice were cleansed with 70% ethanol and subcutaneously injected with B16F10 cells (7.5×10^{4} cells/0.2 ml/mouse) or A549 (8×10^{6} cells/0.2 ml/mouse) [168,169]. After seven days, mice with palpable tumors were randomized and divided into six groups (5 mice/group). The control group received oral dose of vehicle (Neobee M5 oil, 0.2 ml) only throughout the experimental period. The treatment groups received

NAC in Neobee M5 oil (100 mg/ kg); mal C in Neobee M5 oil (50 and 100 mg/kg) and mal C (50 and 100 mg/kg) plus NAC (100 mg/ kg) in combination by oral gavage on alternate days for 21 days. The tumor growth was monitored twice a week by calipers and the tumor volumes calculated according to the formula $0.5236L1(L2)^2$, where L1 and L2 are the long and short axes of the tumor dimension, respectively [170]. The experiments were repeated twice. Four h after the last dose of the treatments on the 30^{th} day of the experiments, the mice were sacrificed after an overdose of thiopental, the tumors were removed and their volumes measured.

2. 18. Irradiation

A549 cells were exposed to different doses of γ irradiation using Gamma Cell 220 irradiator with ^{60}Co as source (Atomic Energy of Canada Ltd), at a dose rate of 3.5 Gy/min in PBS. Cells were then grown in DMEM media containing 10% serum and processed for clonogenic assay.

2. 19. Instrumentation

The absorbance was measured using JASCO V-550 UV/VIS spectrophotometer at 25 °C with wavelength scans in 1 ml quartz cuvette of 1 cm path length. Estimation of mal C and its quinone form, estimation of calcium and ROS (DCFDA) were carried using spectrophotometer or spectrofluorometer. For High Performance Liquid Chromatography (HPLC), a sample of mal C (10 μM) in methanol was injected in C-18 column (reverse phase) as stationary phase and acetonitrile:water (60:40) as mobile phase at a flow rate of 1 ml/min in LC-2000Plus HPLC system. Mal C was detected at 345 nm.

2. 20. Selectivity index (SI)

In the present study, the degree of selectivity (selectivity index) of mal C is expressed as SI = (IC50 of mal C in a normal cell line)/ (IC50 of mal C in cancer cell line), where IC50 is the

concentration required to kill 50% of the cell population.

2. 21. Statistical analysis

The values are expressed as the mean ± standard error of mean (S.E.M). The data were analyzed by paired t-test. Analyses were considered significantly different at $p<0.05$, $p<0.01$, and $p<0.001$.

CHAPTER-III

RESULTS

3. 1. Evaluation of anticancer potential of malabaricones against multiple cancer cell lines

This chapter deals with experiments, results and analyses on the anticancer potential of malabaricones (especially mal B and mal C) in different cancer cell lines. Further, it describes the preliminary results of two highly potential malabaricones, mal B and mal C, on A549 lung carcinoma cells wherein caspase activation, ability to induce DNA damage, dependence on p53 etc. were studied.

3. 1. 1. Cytotoxic potential of malabaricones against three cancer cell lines

We isolated around 10 malabaricones from the methanolic extract of M*yristica malabarica* [151], and found malabaricones (mal A-D, Figure 3. 1. 1A) to possess cytotoxic potential towards cancer cell lines as assessed by MTT assay. Our results revealed that tested malabaricones possess impressive dose-dependent cytotoxic activity against A549 (human lung adenocarcinoma), MCF-7 (mammary gland adenocarcinoma) and HCT-15 (human colorectal adenocarcionoma) after 48 h of incubation. The IC_{50} (half maximal Inhibitory Concentration) value for the cytotoxic activity of mal A, mal B, mal C, mal D, curcumin and etoposide in A549 were 23.1 ± 3.6 μM, 8.3 ± 1.2 μM, 6.9 ± 1.4 μM, 18.1 ± 3.3 μM, 22.4 ± 4.2 μM and 32.4 ± 3.6 μM respectively (Figure 3. 1. 1B). The IC_{50} value for the cytotoxic activity of mal A-D and curcumin on MCF-7 were 21.6 ± 2.6 μM, 6.8 ± 2.6 μM, 5.6 ± 1.2 μM, 15.7 ±2.6 μM and 24.4 ± 3.3 μM, respectively (Figure 3. 1. 1C). The IC_{50} value for the cytotoxic activity of mal A-D and curcumin on HCT-15 were 19.9 ± 4.2 μM, 9.8 ± 1.5 μM, 9.0 ± 1.7 μM, 16.9 ± 4.6 μM and 27.2 ± 5.6 μM, respectively (Figure 3. 1. 1D). From the IC_{50} values (Table 3. 1) of malabaricones in multiple cancer lines, mal B and mal C appear to be highly potent and superior to curcumin and etoposide. Hence further work was carried out with these two highly potential spice molecules.

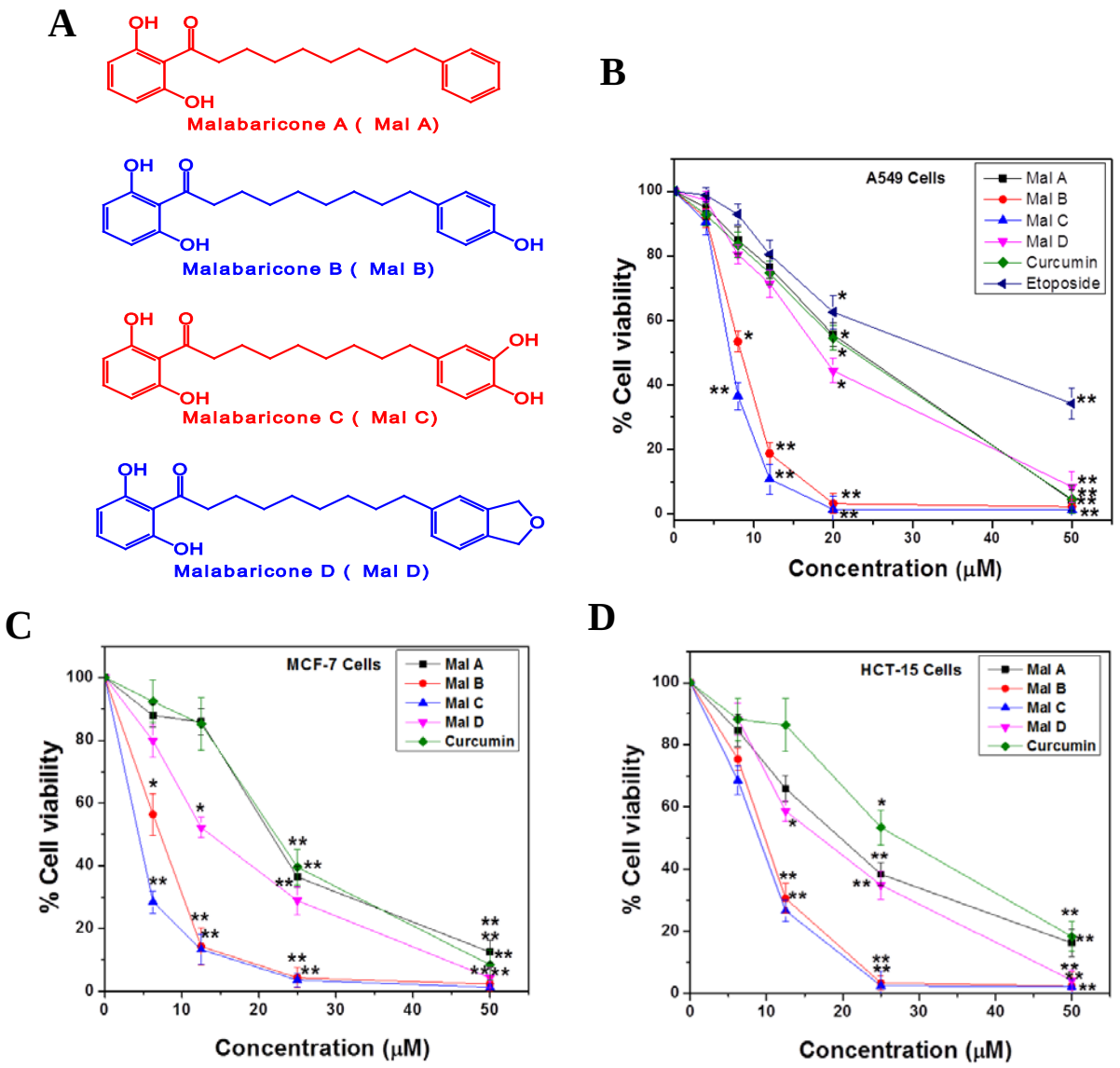

Figure 3. 1. 1. **Malabaricones induced cytotoxicity in multiple cancer cell lines. (A)** Chemical structures of the malabaricones A-D. **(B)** Malabaricones, curcumin and etoposide induced cytotoxicity in human lung carcinoma (A549) cells. **(C)** Malabaricones and curcumin induced cytotoxicity in human breast cancer (MCF-7) cells. **(D)** Malabaricones and curcumin induced cytotoxicity in human colon adenocarcinoma (HCT-15) cells. Cells (5000 cells/well), grown in 96-well plates were treated with vehicle (0.1% DMSO) or increasing concentrations of mal A–D and curcumin. The cell viability was assessed by the MTT assay after 48 h. The results are expressed in percentage survival considering that of the vehicle-treated control cells as 100. The experiments were repeated three times with similar results. All determinations were made in four replicates, and the values are means ± SEM. *p<0.01, **p<0.001 compared to vehicle control.

Table 3. 1. IC_{50} (half maximal inhibitory concentration, μM) for malabaricones against different cancer cell lines

	Mal A	Mal B	Mal C	Mal D
MCF-7	21.8±4.2	6.8±2.2	5.2±1.2	15.7±2.6
HCT15	19.7±5.1	9.7±2.0	8.8±1.6	16.9±3.8
A549	22.5±4.1	7.9±1.6	6.4±1.8	18.3±3.5

3. 1. 2. Comparison of the cytotoxic potential of malabaricone B and C against thirteen cancer cell lines

MTT assay was performed on total 13 cancer cell lines of human origin to calculate IC_{50} for mal B and mal C after 48 h of incubation (Table 3. 2). Our results showed that mal C was better than mal B with lower IC_{50} values against all the 13 tested cancer cells

Table 3. 2. Anti-cancer potential of mal B and mal C. Cells were treated with different concentrations of mal C and mal B, MTT assay was performed and IC50 values were calculated as described in Figure 3. 1. 1.

Human cancer cell lines	Tissue origin	Mal C (IC50/μM)	Mal B (IC50/μM)
MCF-7	Breast Cancer	6.9±1.2	8.8±2.2
MDA-MB-231 (p53, Missense)		7.0±1.4	8.6±1.5
HCT15 (p53, wt/mutant, missense)	Colon cancer	8.8±1.6	9.9±2.0
A549	Lung Cancer	6.4±1.8	8.6±1.6
NCI-H460		7.1±2.0	9.4±1.4
NCI-H522 (p53, deletion)		7.5±1.5	8.0±1.3
NCI-H23 (p53, missense)		8.1±2.1	9.2±1.9
U2OS	Osteosarcoma	7.2±1.7	8.2±1.5
A375	Melanoma	12.1±2.7	16.8±2.6
A498	Kidney	11.4±1.1	15.9±1.3
A431 (p53, Missense)	Skin carcinoma	7.3±1.6	9.6±1.6
SH-SY5Y	Neuroblastoma	6.8±1.3	9.3±2.0
IMR-32		7.6±1.4	9.8±2.1

3. 1. 3. Evaluating the mechanism of mal B and mal C induced cell death in A549 cells

Since, both mal B and mal C are structurally closely similar and showed impressive cytotoxic potential against various cancer cell lines, we sought to understand whether these two molecules function in similar manner. To this end, we have chosen A549 human lung adenocarcinoma cells line to probe the anti-cancer role of mal B *vs.* mal C.

We examined the concentration dependent cytotoxicity of mal B and mal C on A549 cells. The MTT assay as well as phase contrast microscopy revealed a concentration dependent

alteration in cell morphology with increasing number of shrinking cells and membrane blebbing in response to mal B and mal C treatment (Figure 3. 1. 2).

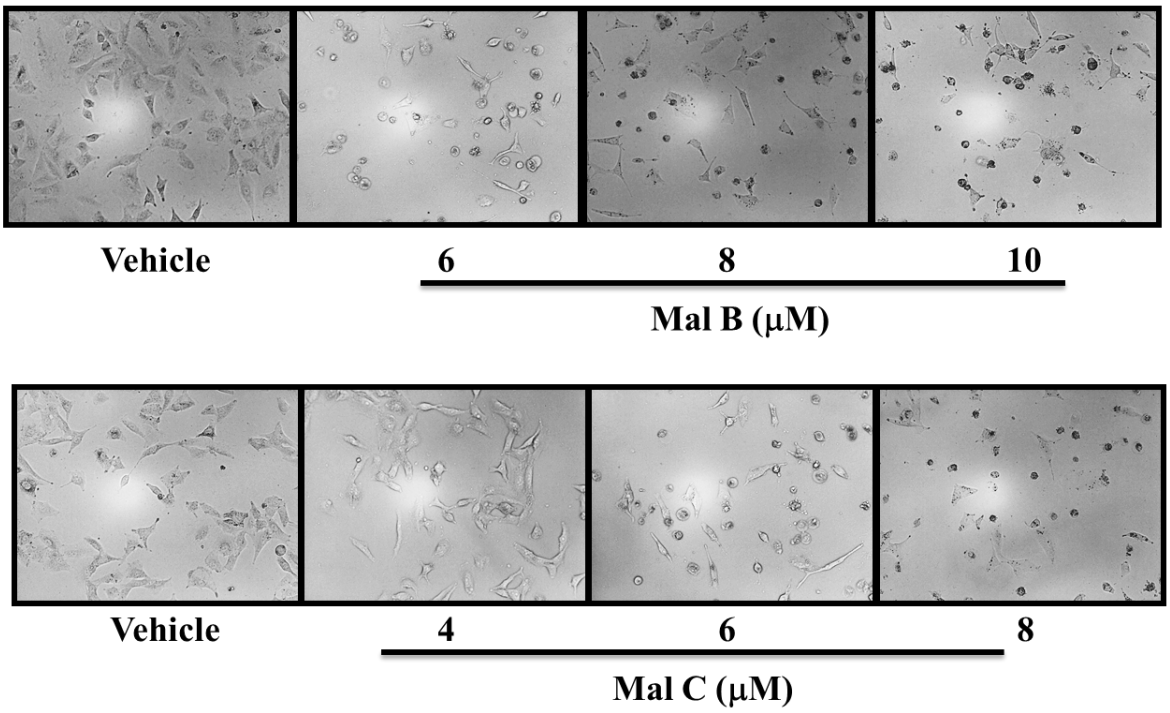

Figure 3. 1. 2. **Mal B and mal C induces morphological changes in A549 cells.** The A549 cells treated with vehicle (0.1% DMSO) or mal B (6, 8and10 μM) or mal C (4, 6 and 8 μM) for 24 h, washed twice with PBS and visualized under a phase contrast microscope.

Increase in the amount of sub-G1 population in both mal B and mal C treated A549 cells indicated that both these molecules induces apoptosis in A549 cancer cells (Figure 3. 1. 3A, B).Interestingly, we observed that mal B *vis-à-vis* mal C treatment induced slightly higher amount of sub-G1 in A549 cancer cells.

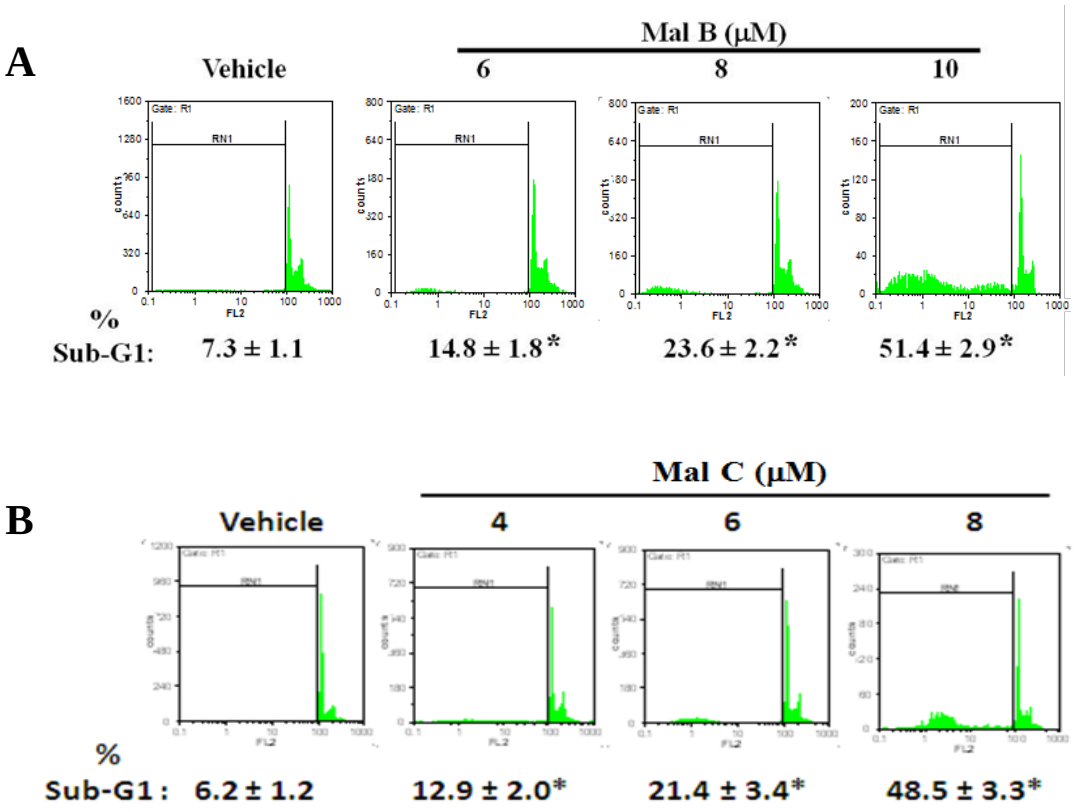

Figure 3. 1. 3. Mal B and mal C induces apoptosis specific sub-G1 population in A549 cells. (A) Flow cytometric analysis of sub-G1 (apoptotic) population in response to mal B treatment. A549 cells were treated with mal B (6, 8 and 10 μM) for 24 h. **(B)** Flow cytometric analysis of sub-G1 (apoptotic) population in response to mal C treatment. A549 cells were treated with mal C (4, 6 and 8 μM) for 24 h. Twenty thousand cells in each treatment were acquired using a flow cytometer. The sub-G1 region (RN1) represents the percentage of cells undergoing apoptosis. The experiments were repeated four times with similar results. All determinations were made in four replicates, and the values are means ± SEM. **p*<0.01 compared to vehicle control.

Various other assays were performed to confirm the involvement of apoptosis in mal B/C induced cell death process. Figure 3. 1. 4A shows percentage of annexin-V positive cells (as quantified through flow cytometer) after 8h of mal B and mal C treatment. Further, mal B and mal C increased apoptosis specific enrichment of cytoplasmic oligonucleosome in a concentration dependent manner in A549 cells. The efficacy of mal B

and mal C, at 5 folds less concentration, was comparable to that of etoposide (25 μM), a clinically used anti-cancer drug (Figure 3. 1. 4B).

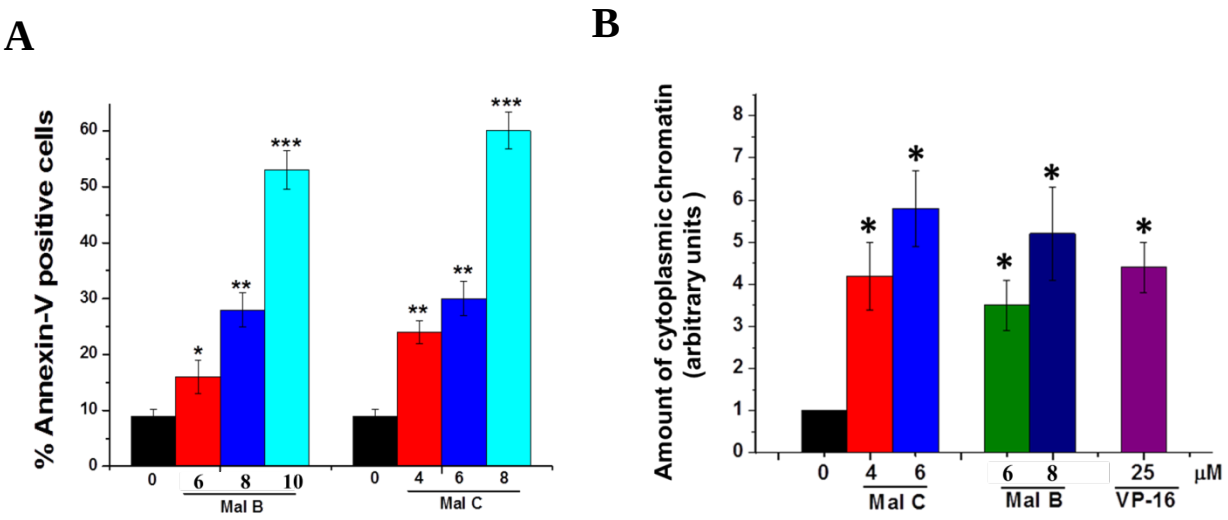

Figure 3. 1. 4. **Mal B and mal C induces cancer cell death through apoptosis. (A)** Annexin-V assay. The A549 cells were treated with vehicle (0.1% DMSO) or mal B (6, 8 and 10 μM) or mal C (4, 6 and 8 μM) for 8 h, increase in annexin-V-positive cells was measured by flow cytometry.All determinations were made in four replicates, and the values are means ± SEM. **p*<0.05, ***p*<0.01 and ****p*<0.001 compared to vehicle control. **(B)** Apoptosis specific enrichment of cytoplasmic oligonucleosomal DNA fragments. The A549 cells were treated with vehicle (0.1% DMSO) or mal B (6 and 8 μM) or mal C (4 and 6 μM) or VP-16 (etoposide, 25 μM) for 16 h. Enrichment of cytoplasmic nuclear DNA was quantified by ELISA assay. All determinations were made in four replicates, and the values are means ± SEM. **p*<0.01 compared to vehicle control.

Next, we investigated whether caspase activation is required for the mal B and/or C-induced apoptosis using their respective IC50 concentration e.g., 8 μM for mal B and 6 μM for mal C. Cells pre-incubated with the pan caspase inhibitor (Z-VAD-FMK) (20 μM) for 1 h prior to mal B (8 μM) treatment showed increase in cell viability (31.6%, *P*<0.01), compared to the only mal B-treated cells (Figure 3. 1. 5A). The final execution of apoptosis is often mediated through caspase-8 and caspase-9 as the initiators, and caspase-3 as the effector. Hence

the effect of specific caspase inhibitors (each 20 μm) on apoptosis induction and cell survival (MTT assay) in the mal B (8 μM)-treated A549 cells were studied at 48 h. Pre-incubation of the cells with specific caspase-9 and caspase-3 inhibitors increased their viability by 60% and 52.6% respectively, compared to the only mal B-treated cells. However, the caspase-8 inhibitor did not show significant effect on the cell survival (Figure 3. 1. 5B).

In contrast to mal B, our results showed an early activation of caspase 3 and -9 while delayed activation of caspase-8 was observed in response to mal C treatment (Figure 3. 1. 5C). Further, specific inhibitor of caspase-3, 8, 9 significantly reduced mal C induced apoptosis suggesting a key role of these caspases in mal C-induced cell death process (Figure 3. 1. 5D).

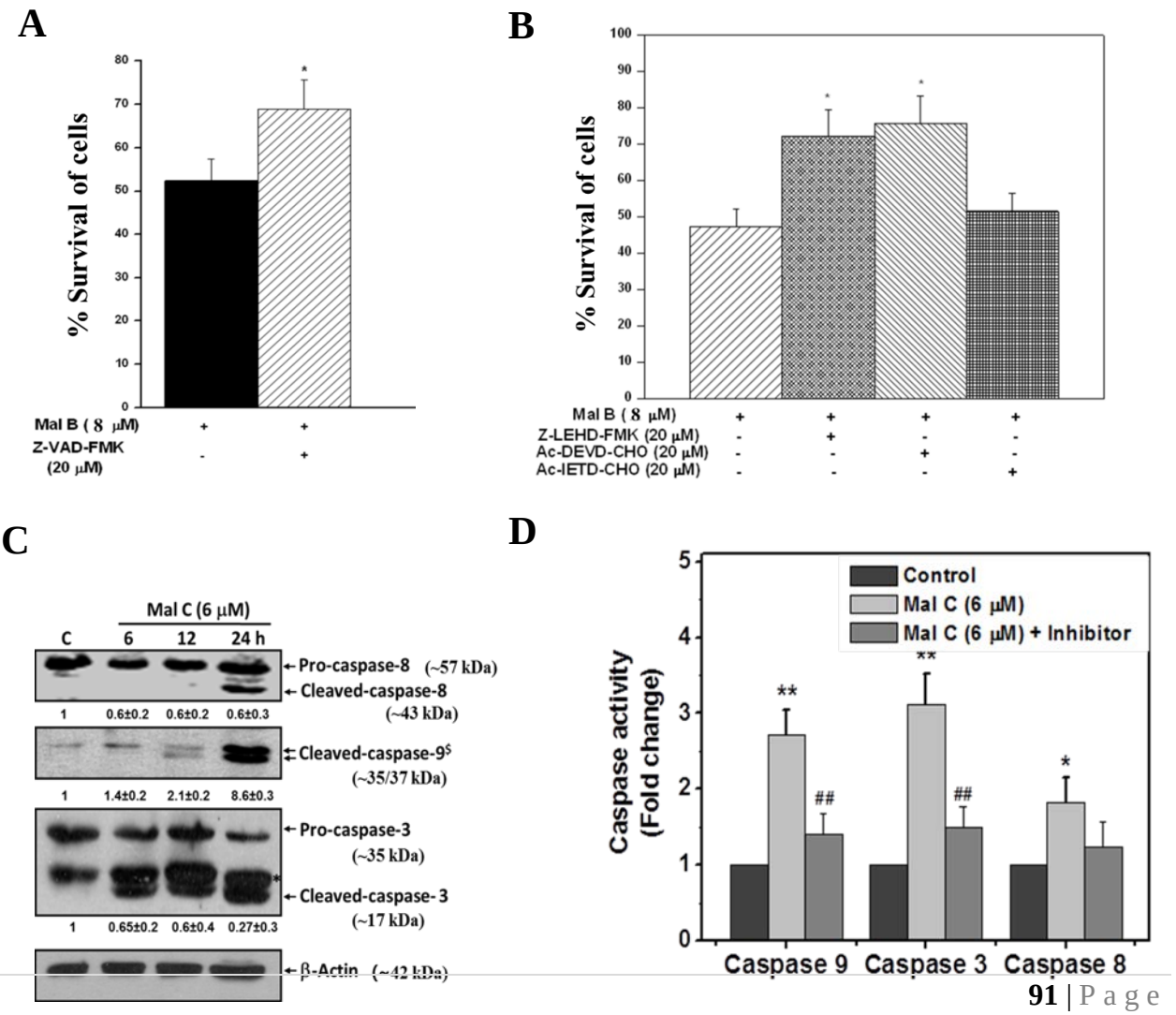

Figure 3. 1. 5. Caspase inhibitors differentially abrogate mal B and mal C induced apoptosis. **(A)** The A549 cells were pre-incubated with or without pan caspase inhibitor (20 μM) prior to mal B (8 μM treatment, after 48h the cell viability was assessed by the MTT assay. **(B)** Effect of individual caspase inhibitor peptides. A549 cells were incubated with or without inhibitory peptides (each 20 μM), Z-LEHD-FMK (caspase-9 specific), Ac-DEVD-CHO (caspase-3 specific) and Ac-IETD-CHO (caspase-8 specific) for 1h followed by mal B (8 μM) treatment, after 48h the cell viability was assessed by the MTT assay and shown in terms of percent survival of cells. **(C)** Expressions of caspases. The A549 cells were incubated with vehicle or mal C (6 μM) for different time periods, and the activation of the caspases were assessed by the appearance of respective cleaved caspases in the whole cell extracts by immunoblots. The experiments were repeated three times with similar results, and a representative images and mean ± SEM of procaspases is shown. *-represents non-specific protein bands in procaspase-3 blot. **$**-represents two cleaved caspase-9 bands, 37 and 35 KD respectively. **(D)** Activities of caspases-9, -3 and -8. The A549 cells (1×10^6 cells/ well) were incubated with vehicle or mal C (6 μM) for 24 h, and the activities of the caspases estimated. The experiments were repeated three times with similar results, all determinations were made in four replicates, and the values are means ± SEM. *p<0.05, **p<0.01 compared to vehicle control, $^{\#\#}p$<0.05 compared to respective mal C-treatment.

Many anticancer agents have profound effects on the cellular redox status, and generation of excess ROS acts as a signal for apoptosis induction. Hence, we used the DCFH-DA assay to see if ROS is a potential factor in the mal B- and mal C-induced apoptosis in A549 cells. Initially, we observed that both mal B and mal C increased ROS generation (oxidative stress) time dependently (Figure 3. 1. 6A) but mal B induced a more robust oxidative burst in comparison to mal C. Mal B and mal C, at their respective IC_{50}, induced ROS generation equivalent to that of 25 μM H_2O_2 treatment in A549 cells. Scavenging ROS with the use of antioxidants has been shown to prevent from the cell death induced by ROS generating agents. Here we used NAC, a thiol antioxidant, and quantified change in cell death induced by mal B and mal C. Pre-incubation of NAC (5 mM) for 1 h completely abrogated mal B-induced cell death (sub-G1), confirming the

role of ROS in mal B-induced apoptosis in A549 cells (Figure 3. 1. 6B). In contrast, the effect of NAC had an opposite effect in mal C-induced cell death. Here, NAC pre-incubation followed by mal C treatment increased the cell death (sub-G1 cells) in A549 cells (Figure 3. 1. 6B).

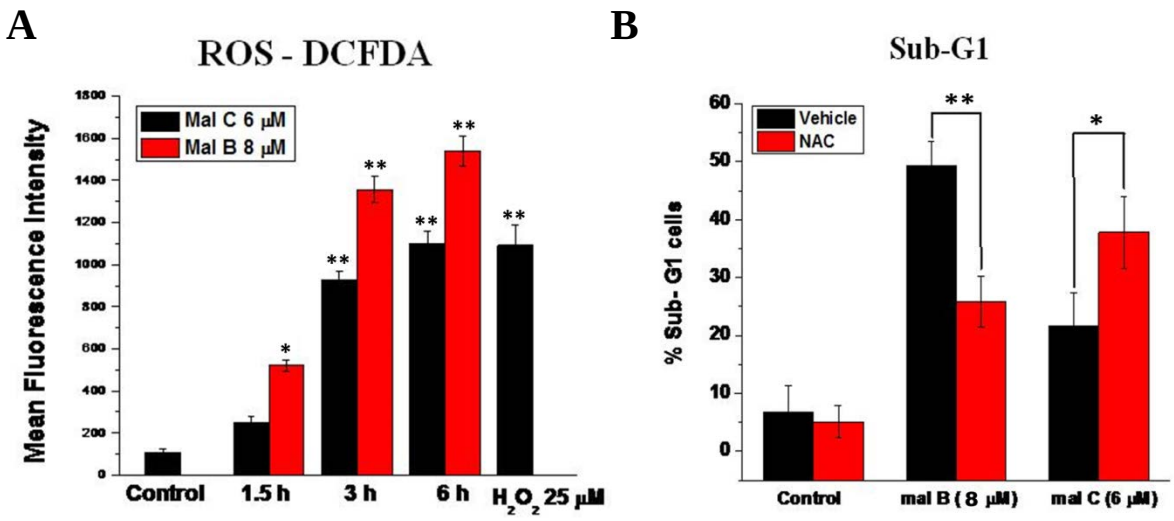

Figure 3. 1. 6. **Role of ROS in mal B and mal C treatment**. **(A)** ROS generation. Cells were treated with mal B (8 μM) or mal C (6 μM) or the positive control, H_2O_2 (25 μM) for 3 h. The amount of ROS generated in the cells was quantified by the DCFDA method as described in materials and methods. The experiments were repeated three times with similar results. *p<0.05, **p<0.01, compared to untreated control cells. **(B)** Effect of NAC on mal B- and mal C-induced cell death. Cells were pre-incubated with NAC (5 mM) for 1h prior to mal B and mal C treatment cell death was assessed by sub-G1 assay using flow cytometry. The experiments were repeated three times with similar results. *p<0.05 and **p<0.01 compared to without NAC treatment.

The oxidative DNA damage by exogenous molecule is an important event in cellular system and if left unrepaired, may lead to cell death. Oxidative DNA damage produced by mal B and mal C in A549 cells was checked by using alkaline comet assay. Comet assay is one of the most sensitive and widely used techniques for detecting damage of cellular DNA. In this assay, the comet tail length indicates the extent of DNA damage, because the cleaved DNA fragments

move faster on the agarose gel. Initial experiments were carried out with alkaline comet assay as it is capable of detecting both single and double strand breaks, compared to neutral comet assay which can detect only double strand breaks. Figure 3. 1. 7 shows the quantification of comet tail length of untreated, mal B (8 μM) and mal C (6 μM)-treated cells. Our results showed that the DNA damage was negligible in untreated (comet tail: 1.3 ± 0.6 μm) and mal B-treated cells (comet tail: 1.5 ± 0.7 μm), while comet tail was significantly long in mal C-treated cells (comet tail: 16.5 ± 3.3 μm, *p<0.01).

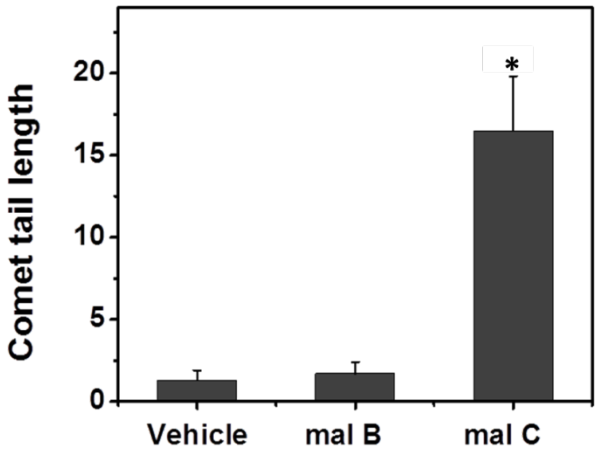

Figure 3. 1. 7. **Induction of DNA single strand breaks (SSB) by mal B and mal C.** A549 cells were treated for 2 h with mal B and mal C, subsequently washed two times with phosphate buffered saline, and processed for the alkaline comet assay (discussed in material and methods). Quantification of comet tail length was plotted in the graph. *p<0.01, compared to vehicle treated cells.

Many anti-cancer agents induce DNA damage that triggers a p53 dependent apoptosis response. To see if p53 protein plays any role in mal B- and mal C-induced killing of the A549 cells, we depleted p53 mRNA in the A549 cells by RNA interference (small hairpin RNA technology) using Lipofectamine® 2000 (described in methods and materials). The respective A549 cells, expressing antisense p53 or scrambled negative control shRNA are designated as A549-p53 or A549-wt cells. The p53 depletion in the transfected cells was confirmed by

immunoblots (Figure 3. 1. 8A). The viability of the A549-wt and p53 knockdown cells (A549-p53) after mal B treatments (respective IC_{50} values of 9.4 ± 1.0 μM and 9.9 ± 1.1 μM) were similar while mal C induced cell death was decreased in A549-p53 cells, compared to A549-wt cells, thus indicating the dependence of mal C-induced cell death on p53 protein (Figure 3. 1. 8B).

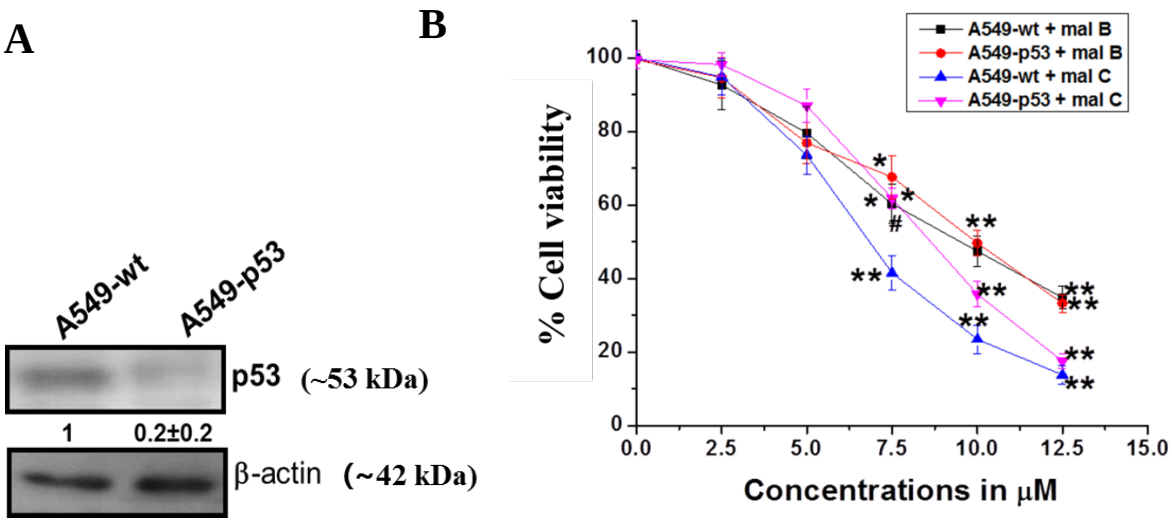

Figure 3. 1. 8. Dependence of mal B- and mal C-induced cell death on p53 protein. (A) A549 cells were transfected with plasmid expressing scrambled shRNA (A549-wt cells) or p53 mRNA targeting shRNA(A549-p53 cells). Antibiotic resistant cells were selected and cell lysates were analysed for expression levels of p53 protein in A549-wt and A549-p53 cells. **(B)** Mal B- and mal C- induced cytotoxicity in A549-wt and A549-p53 cell lines. Cells (6000 cells/well), grown in 96-well plates were treated with vehicle (0.1% DMSO) or increasing concentrations of mal B and mal C. The cell viability was assessed by the MTT assay after 48 h. The results are expressed in percentage survival considering that of the vehicle-treated control cells as 100. The experiments were repeated three times with similar results. All determinations were made in four replicates, and the values are means ± SEM. *p<0.01 compared to vehicle control, **p<0.001 compared to vehicle control, $^{\#}p$<0.05 compared to respective mal C treatment.

To compare the mode of actions of mal B and mal C, all the above results were summarized in the Table. 3. 3. In this table, we also included results of differential expression of p21, gH2AX and DSB induction (neutral comet assay) in A549 cells treated with mal B and mal

C respectively (data not shown). Altogether, our initial extensive investigations on mal B and mal C suggested that these two molecules are highly effective anti-cancer polyphenols but their mode of anti-cancer actions were drastically different.

Table 3. 3. Mode of action of mal B and mal C against A549 cells.

Parameters studied	**Mal C**	**Mal B**
IC_{50}	6.4 ± 1.8 μM	8.6 ± 1.6 μM
P53 dependency	Dependent	Independent
p21 expression	Increase	No change
DNA damage (*in vitro*)	Yes	No
DNA damage (*cellular*)	Yes	No
SSB (Alk. comet)	Yes	No
DSB (Neut. comet)	Yes	No
ROS	Yes	Yes
Role of Thiol antioxidants	Sensitizing	Protection
γ-H2AX foci formation	Yes	No

Since the mode of action of mal B and mal C followed a different route, rest of the thesis is exclusively focussed onto unravel the mechanism of action of mal C in killing cancer cells. Mal C was chosen for further study because:

1) Anti-cancer potential of mal C is far better than mal B treatment against many cancer cells (Table 3. 1, 3. 2).

2) Better DNA damaging ability of mal C than mal B.

3) Non classical ROS-mediated cell death by mal C.

4) Higher natural abundance of mal C in the dried fruit rind of *Myristica malabarica*.

However, prior to a detailed investigation on anti-cancer mechanism of mal C, several key issues as mentioned below were addressed:

1) Stability of mal C in cell culture medium.

2) Mal C is less toxic to normal cells than cancer cells.

3. 2 Stability of malabaricone C in cell culture medium

Stability of mal C was investigated in cell culture medium. This was done to overrule the possibility of attributing any action of precipitated mal C in killing cancer cells. Figure 3. 2. 1A demonstrates the procedure followed to check the above hypothesis. To this end, mal C was added to DMEM medium, incubated for 6 h and extracted with organic solvent like ethyl acetate. Absorption spectra, of ethyl acetate extraction showed mal C was substantially detectable in the soluble fraction even after 6 h of incubation in DMEM medium at 37°C. This showed that mal C does not get precipitated in DMEM media even after 6 h of incubation (Figure 3. 2. 1A, B) and the cytotoxic effects of mal C, as discussed above, was due to soluble form of mal C only.

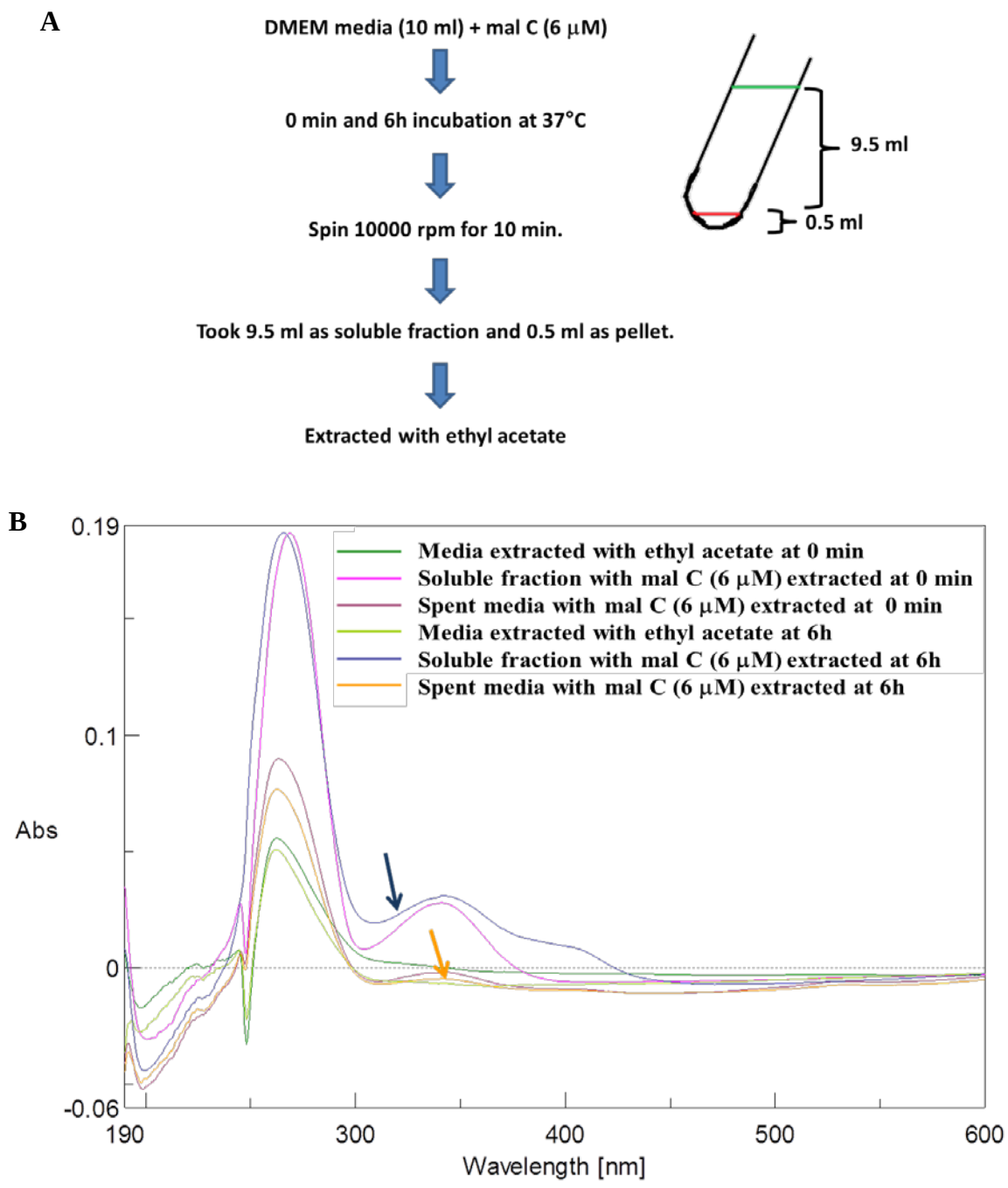

Figure 3. 2. 1. Stability of mal C in cell culture medium. (A) Mal C was added in DMEM media and incubated for different time points (0 and 6 h) and subsequently extracted with ethyl acetate. **(B)** Spectrophotometric absorption spectra of mal C, isolated after different time periods of incubation as mentioned in A. Arrows indicate peaks attributable to presence of mal C.

3. 3. Cytotoxic action of malabaricone C against cancer *vs* normal cells

Cytotoxic effect of mal C on normal/non cancerous cell lines (L132 and WI-38) of human lung origin was also investigated. Normal cell lines, L132 and WI-38 cells showed an IC_{50} value (obtained through MTT assay) of 14.3±1.9 µM and 16.4±2.1 µM respectively after 48 h of mal C treatment while that of the cancer cell line A549 showed IC_{50} of 7.0±1.8 µM (Figure 3. 3. 1). Further, a selective index (SI), as described in material and methods, was calculated to understand the the differential activity of mal C. The selectivity Index (SI) demonstrates the differential activity of a compound, the greater the SI value is, the more selective it is. As per the calculation discussed in material and methods, the selectivity index of mal C was found to be ~2.1.

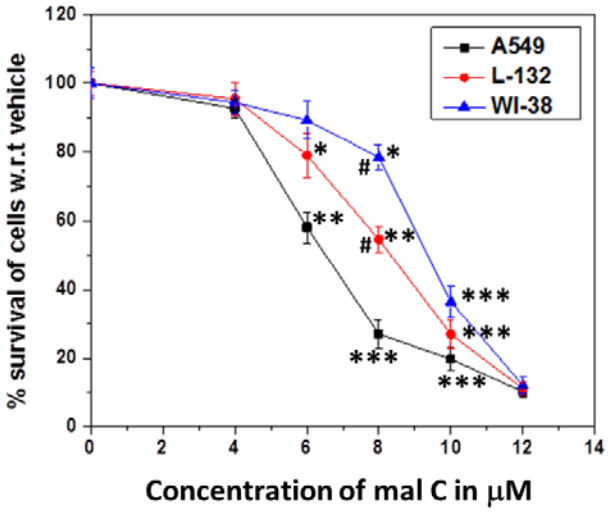

Figure 3. 3. 1. Mal C- induced cytotoxicity in A549, L132 and WI-38 cell lines. Cells (6000 cells/well), grown in 96-well plates were treated with vehicle (0.1% DMSO) or increasing concentrations of mal C. The cell viability was assessed by the MTT assay after 48 h. The results are expressed in percentage survival considering that of the vehicle-treated control cells as 100. The experiments were repeated three times with similar results. All determinations were made in four replicates, and the values

are means ± SEM. *p<0.05, **p<0.01, *p<0.001 compared to vehicle control, #p<0.05 compared to respective treatment in A549 cells.

Further, our results showed that mal C treatment led to a concentration dependent but higher apoptotic induction (sub-G1) in A549 lung carcinoma cell line vis-à-vis normal L132 cell line (Table 3. 4). Together, our result suggested that mal C is less toxic to normal cells than cancer cells.

Table 3. 4. Percent sub-G1 induced by mal C in A549 and L132 cell lines.

Cell line	Vehicle	4 μM	6 μM	8 μM
A549	6.2±1.2	12.9±2.0	21.4±3.4	48.5±3.3
L132	5.6±1.3	6.4±1.1	18.1±1.9	22.9±2.8

Since, mal C induces less cytotoxicity to the normal cells, we sought to know whether lesser uptake of mal C might be less harmful to the normal cells. To this end, uptake of mal C by normal and cancer cell line was studied using absorption spectroscopy. Here respective cells were treated with mal C followed by cytoplasmic and nuclear fraction preparation. The lysates were extracted using ethyl acetate (Figure 3. 3. 2A), subsequently, the presence of mal C in ethyl acetate extracts of various treatments were analyzed by absorption spectrophotometer (Figure 3. 3. 2A, B).

A

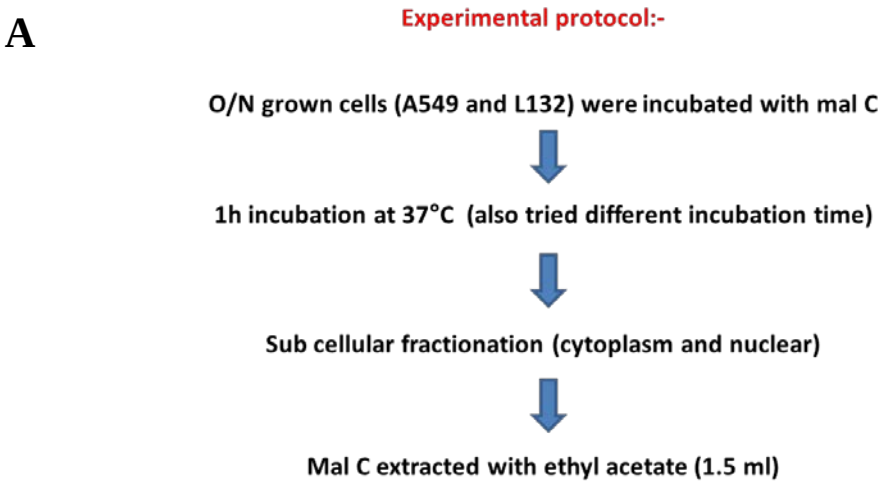

B

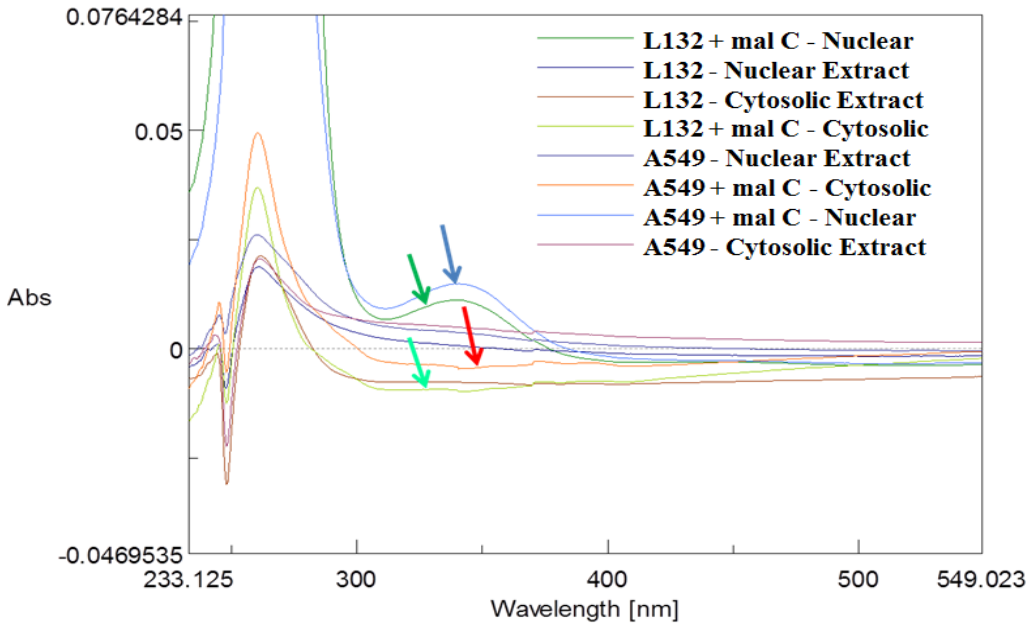

Figure 3. 3. 2. Differential uptake of mal C in normal and cancer cells. (A) Procedure of extracting mal C from different cellular fractions in A549 and L132 cells. **(B)** Absorption spectra of extracts, isolated from cytoplasmic and nuclear fraction, of A549 and L132 cells incubated with mal C for 1 h. Arrows indicate the characteristic λ_{max} absorption of mal C.

Figure 3. 3. 2B showed the presence of mal C in nuclear fraction of both the cells (A549 and L132), but L132 cells showed lesser uptake of mal C compared to A549 cells

(compare dark green arrow vs blue arrow, Figure 3. 3. 2B). Further, the uptake of mal C by normal and cancer cells was also studied using HPLC (High Performance Liquid Chromatography). Here the cells were incubated with mal C, lysed with detergent and then extracted with ethyl acetate. Samples were vaccum evaporated, reconstituted in methanol and run in HPLC with C-18 column (Figure 3. 3. 3).

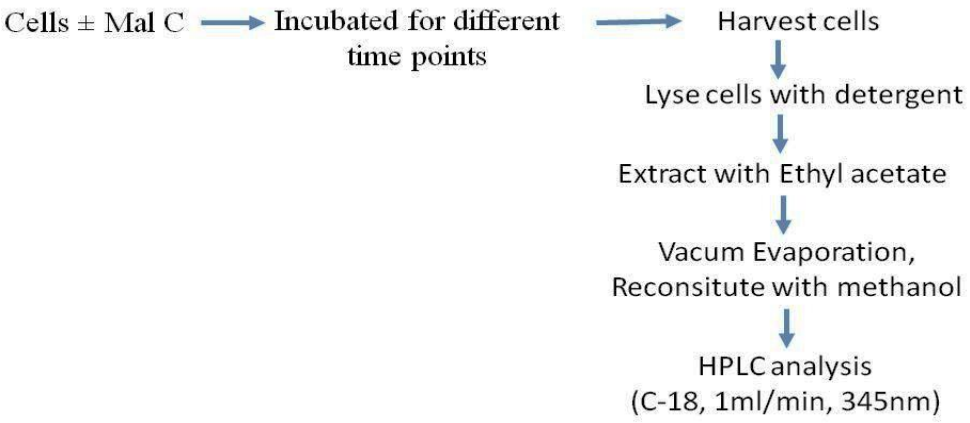

Figure 3. 3. 3. Schematic representation showing the procedure for preparation of cellular fractions for HPLC analysis.

We used two cell lines, A549 as human lung cancer cell line and WI-38 as its normal counterpart. HPLC analysis of mal C from cellular extracts were carried out as per the procedures reported previously [153]. Our HPLC analysis showed that mal C was eluted with a retention time (R_t) 8 min from a standard solution (Figure 3. 3. 4).In corroboration with our spectrophotometric results, HPLC analyses also showed the presence of mal C in celluar extracts of both mal C treated cancer and normal cells. However, the amount of accumulation of mal C in WI-38 cells was lesser (~60%) vis-à-vis A549 cells (Figure 3. 3. 4).

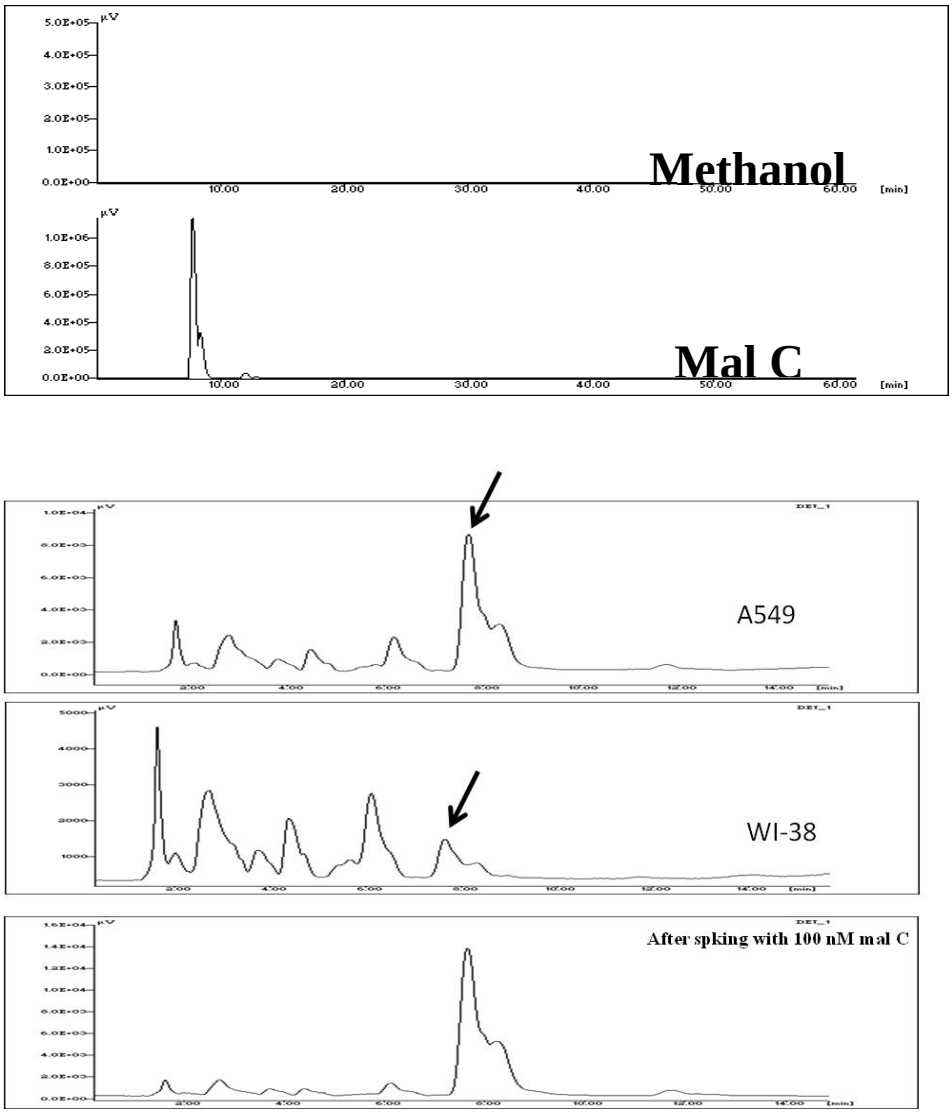

Figure 3. 3. 4. **Differential uptake of mal C by normal and cancer cells.** Indicated cells were treated with mal C (10 μM) for 1 h and solvent extracts were prepared as above. Various untreated and mal C treated cell extracts along with standards were analyzed by HPLC. Arrow indicates the characteristic mal C peak, which was confirmed after spiking with mal C.

Further, we sought to know whether lower uptake of mal C responsible for lesser biological effects e.g., DNA damage, resulting in lesser cytotoxicity towards normal cells. To this end, we investigated mal C-induced DNA damage in normal and cancer cells. Here we found that, mal C-induced DNA damage (γ-H2AX) were less in normal cell line when compared

to its cancer counterpart (Figure 3. 3. 5). Together. Our results suggested that low uptake might be responsible for lesser toxic effect of this natural phenolic towards normal cells.

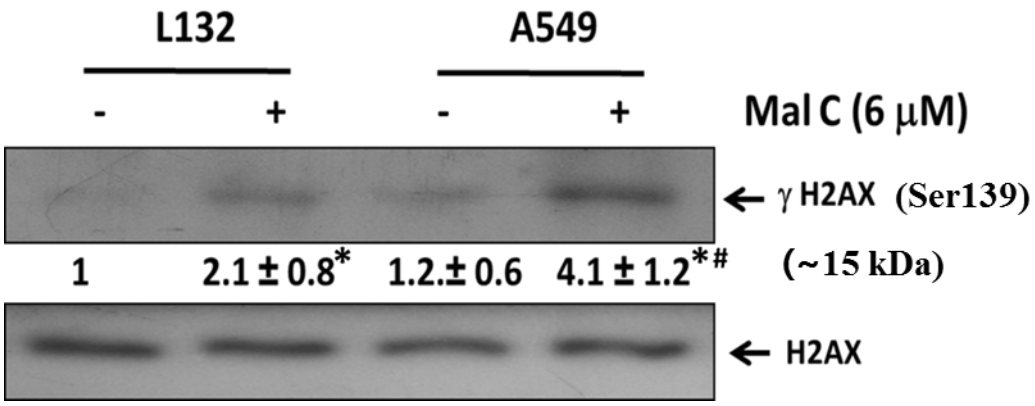

Figure 3. 3. 5. **Mal C induces a differential level of DNA damage in normal and cancer cells.** The L132 and A549 cells were treated with vehicle alone or mal C (6 μM) for 3 h. The γH2AXwas analyzed by immunoblots of the cell lysates. All the experimentswere repeated three times with similar results and the values are means ± SEM. *p<0.05 compared to untreated control, #p<0.05 compared to respective mal C treatment in L132 cells.

3. 4. Molecular mechanism of mal C-induced cell death in A549 (lung cancer) cell line

This section deals with the anticancer mechanism of action of mal C in A549 cells. It describes the involvement of mitochondria, MAPK and DNA damage response proteins in mal C-induced apoptosis.

3. 4. 1. Malabaricone C induces cell death in cancer cells mostly through the apoptosis process

Our previous results showed that mal C induced apoptosis specific increase in sub-G1 population, annexin-V positive (PI negative), cytoplasmic accumulation of DNA bound histones and activation of caspases (caspase-3, -8 and -9) (Figure 3. 1. 3B; 3. 1. 4A, B; 3. 1. 5C, D).

Moreover, cells pre-incubated with the pan caspase inhibitor (20 μM) prior to mal C (8 μM) treatment reduced the sub-G1 cell population (~31%), compared to the only mal C-treated cells (~47%) (Figure 3. 4. 1). Further, our results show that mal C treated cells were not taking up the trypan blue dye up to 24 h, which along with data for Annexin V positive and PI negative suggests mal C induced death process might not be operated through necrotic death process.

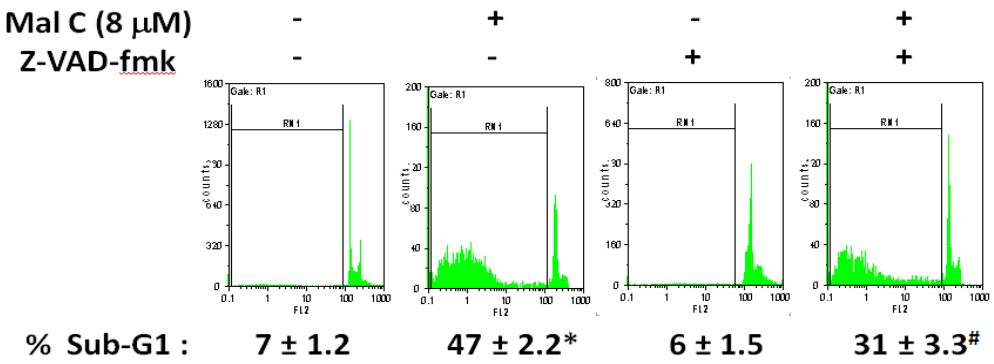

Figure 3. 4. 1. Mal C induced apoptosis was abrogated by pan-caspase inhibitor. A549 cells were treated with mal C (8 μM) in the presence of vehicle or pancaspase inhibitor (20 μM) for 24 h. Twenty thousand cells in each treatment were acquired using a flow cytometer. The sub-G1 region (RN1) represents the percentage of cells undergoing apoptosis. The experiments were repeated four times with similar results and the values are means ± SEM. *p<0.05 compared to without mal C treatment, #p<0.05 compared to respective mal C treated cells.

Autophagy is another mode of cell death wherein cells start eating their own organelles with the help of lysosomal enzymes. Increase in the expression of autophagy related proteins are established indicators for the activation of autophagy. To this end, we used Beclin-1 and ATG5 as reported markers for autophagy. We found that ATG5 and Beclin-1 expression level did not change significantly (up to 16 h) in A549 cells in response to mal C treatment (Figure 3. 4. 2). This results indicated that mal C induced death process might not be mediated through autophagy mode of death process.

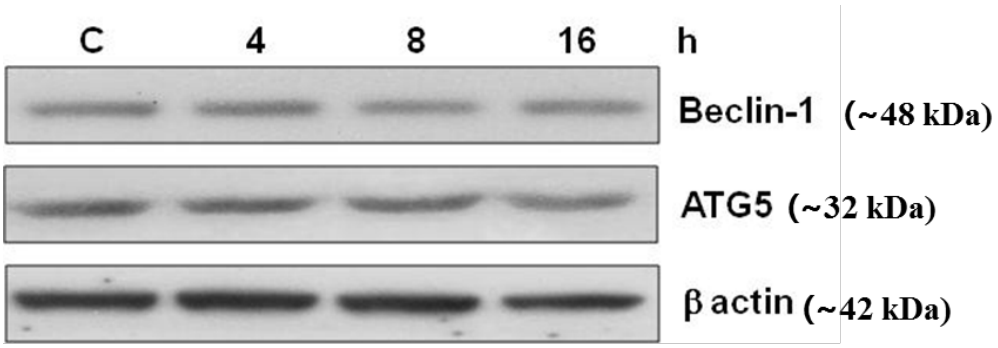

Figure 3. 4. 2. Effects of mal C treatment on the expression level of autophagy regulating proteins in A549 cells. The A549 cells were treated with vehicle alone or mal C (6 μM) for 4, 8 and 16 h. The expression levels of Beclin-1 and ATG5 were analyzed by immunobloting. All the experiments were repeated three times with similar results.

Some of the DNA damaging drugs like etoposide, cisplatin, taxol or nocodazole can induce significant amount of mitotic catastrophe (another mode of cell death) in cancer cells. From a morphologic point of view, mitotic catastrophe is the result of abnormal morphology, exhibiting enlarged, irregular nuclei, multipolar (aberrant) mitoses, or multiple nuclei, which can induce polyploidy and the occurrence of large multinucleated cells and micronucleation. Mal C-treated A549 cells at different time points were checked for mitotic catastrophe using fluorescence microscopy. We did not detect significant number of cells with mitotic catastrophe in mal C treatment. In contrast, all the cells showed nuclear condensation and fragmentation, which are typical characteristic of apoptosis (Figure 3. 2. 3). In addition, DNA damaging drugs showing mitotic catastrophe are found to induce G2/M cell cycle arrest, while mal C have been shown to arrest A549 cells in G1 (Figure 3. 4. 3). Cells were treated with mal C (0-6 μM) and nocodazole (200 ng/ml) for 24 hours and analyzed by FACS. The nocodazole treatment arrests all the cells in G2–M phase, which allows for monitoring G1/S-phase progress within the time of one cell cycle.

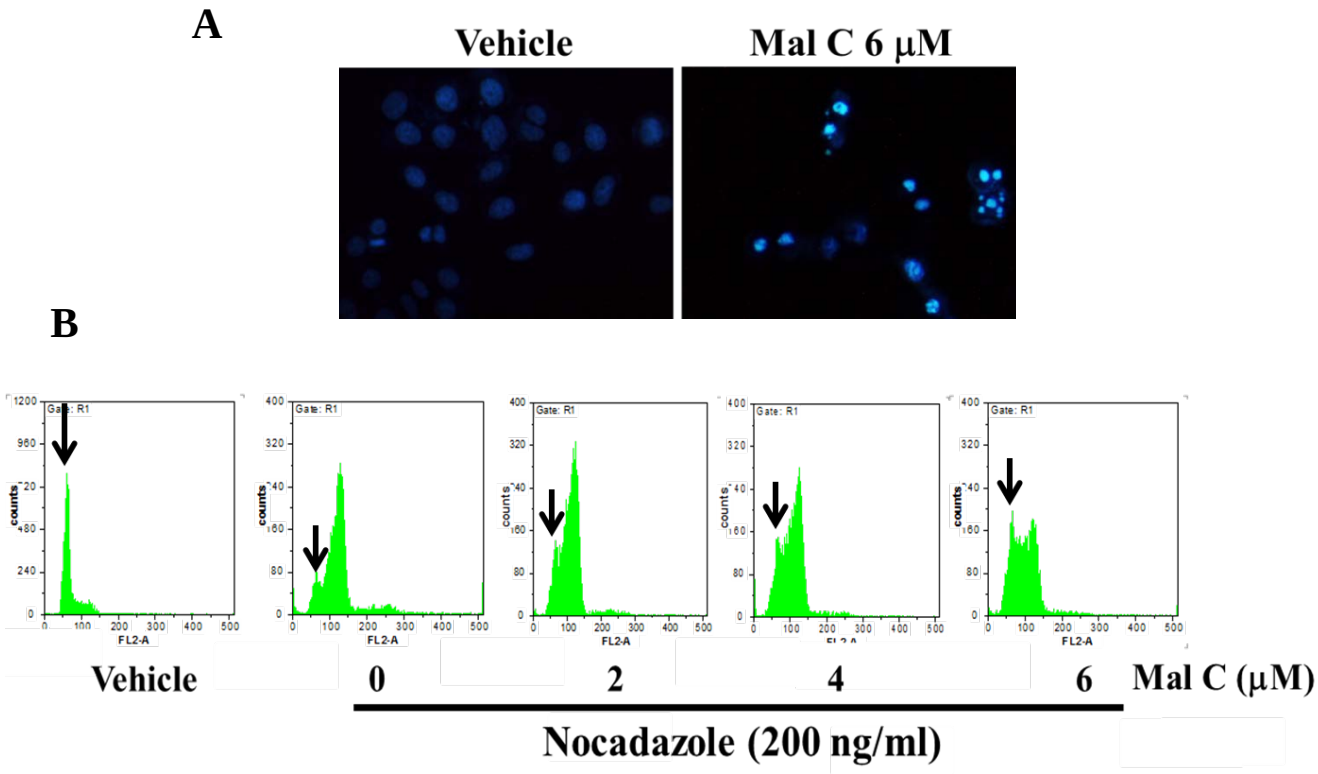

Figure 3. 4. 3. Effect of mal C treatment in inducing mitotic catastrophe. (A) A549 cells were treated with mal C for 24 h, washed with PBS and stained with Hoechst-33342 for 10 min. Cells were visualized under fluorescence microscope to underscore mitotic catastrophe induction. **(B)** A549 cells were treated with mal C; in the presence and absence of nocadazole for 24 h. Cells were washed with PBS, fixed with 70 % alcohol and processed for cell cycle analysis. Arrow indicates for the G1 populations. Twenty thousand cells in each treatment were acquired using a flow cytometer, and the DNA content of the nuclei was registered on a linear scale. Representative images are shown.

All these results confirmed that the cytotoxicity of mal C follows an apoptotic pathway through the activation of caspases-9 and -3 as early events and of caspase-8 later.

3. 4. 2. Mal C perturbs mitochondrial function through BAX/BCL-2 imbalance

To determine whether mitochondrial pathway is involved in the above process,we examined mal C-induced changes in mitochondrial potential (ΔΨm) and release of pro-apoptotic molecules from the mitochondria into cytosol. As shown in Figure 3. 4. 4A, B,

mal C-induced significant loss of ΔΨm and release of cytochrome c into cytosol. The kinetic analysis revealed that the ΔΨm loss (within 1.5 h) preceded the cytochrome c release (4 h) in response to mal C treatment, indicating an initial role of mitochondrial dysfunction in the mal C-induced cell death.

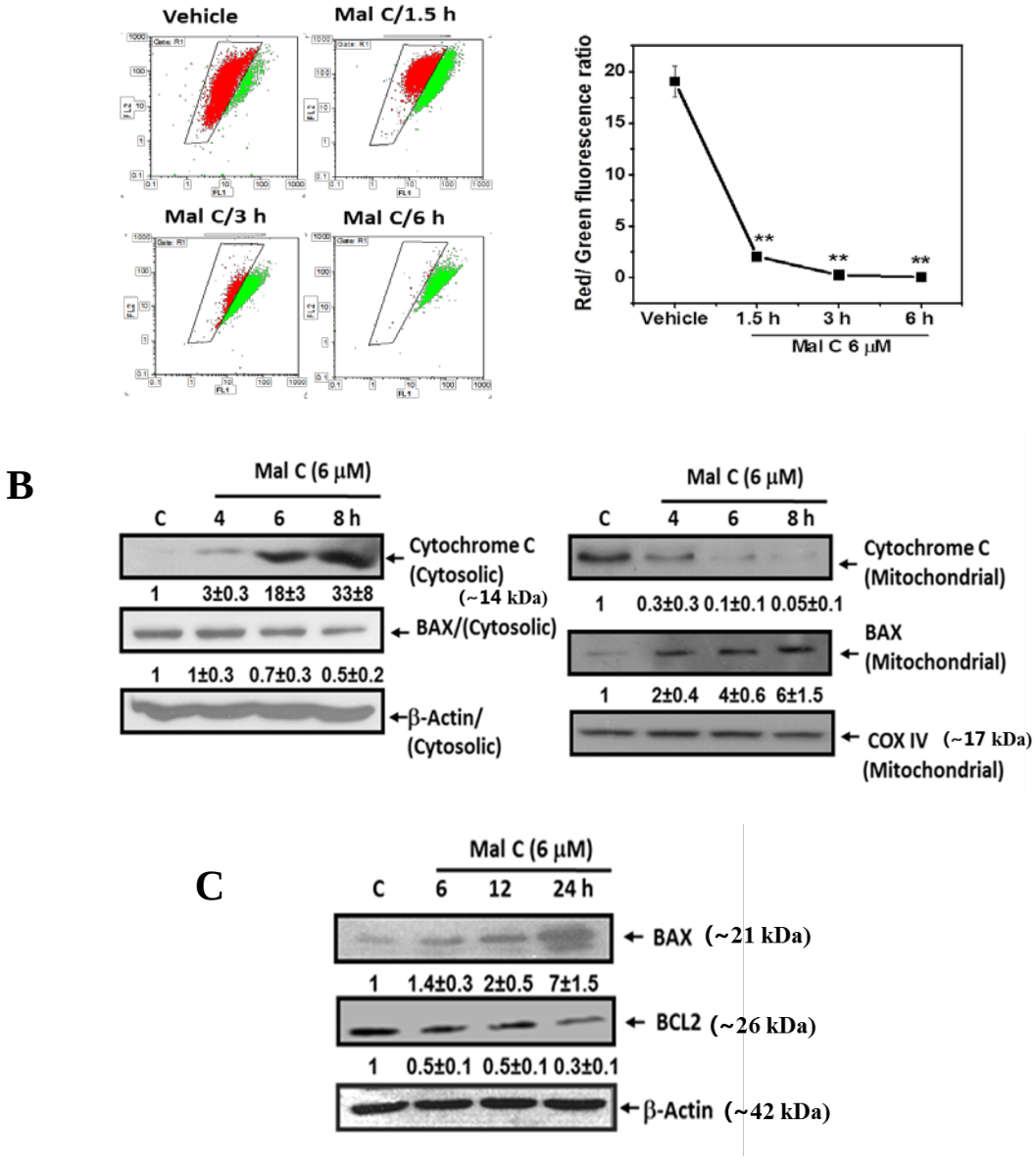

Figure 3. 4. 4. Mal C-induced mitochondrial disruption in A549 cells. (**A)** Mal C-induced ΔΨm loss. Cells (1×10^5 cells/well) were incubated with vehicle or mal C (6 μM) for different time periods. The cells were treated with JC-1 during the last 30 min of the mal C treatment, and ΔΨm were determined by

flow cytometry from the retention of the red fluorescence due to JC-1 aggregates (upper panel). Simultaneously, the ΔΨm loss was also determined by measuring the JC-1 monomer (green fluorescence). The ratio of red/green fluorescence was quantified and shown in the side panel. The abbreviations FL1 and FL2 in the dot plot represent intensities of the green and red fluorescences of JC-1, acquired in the channel 1 and channel 2 respectively. **(B, C)** Translocation and expression of mitochondrial function-related proteins in mal C-treated A549 cells. The cells were treated with vehicle or mal C (6 μM) for different time periods. The expressions of the proteins in the cytosolic, mitochondrial and whole cell extracts were assessed by immunoblotting. The experiments were repeated four times with similar results and the values are means ± SEM. ***p*<0.01 compared to the vehicle.

Because the apoptotic BCL-2 family members, especially BAX and BCL-2 are crucial to the mitochondrial cell death pathway [87], we also analyzed the BAX and BCL-2 expressions in the mal C-treated cells. Within 6 h of treatment, mal C markedly increased the BAX expression (1.4 fold) and its translocation to mitochondria with simultaneous reduction in BCL-2 (0.5 fold) expression (Figure 3. 4. 4B, C).

To further demonstrate the critical role of mitochondria, we analyzed the apoptosis induction in the wild type A549 cells, named as A549-ρ^+cells, and in partially mitochondrial DNA depleted A549 cells, named as A549-ρ^o cells. The A549-ρ^o cells were characterized by the reduced expression (~20%) of the mitochondria-specific protein, COX IV that is an essential component of the mitochondrial respiratory chain (Figure 3. 4. 5D). Moreover, mitochondria-specific fluorescence staining by the MitoTracker® dye showed severe loss of mitochondria in A549-ρ^o cells vis-à-vis the A549-ρ^+ cells (Figure 3. 4. 5A, B). Flow cytometry analysis (sub-G1) revealed that the A549-ρ^o cells were markedly resistant to mal C treatment when compared to A549-ρ^+ cells (Figure 3. 4. 5C, D).

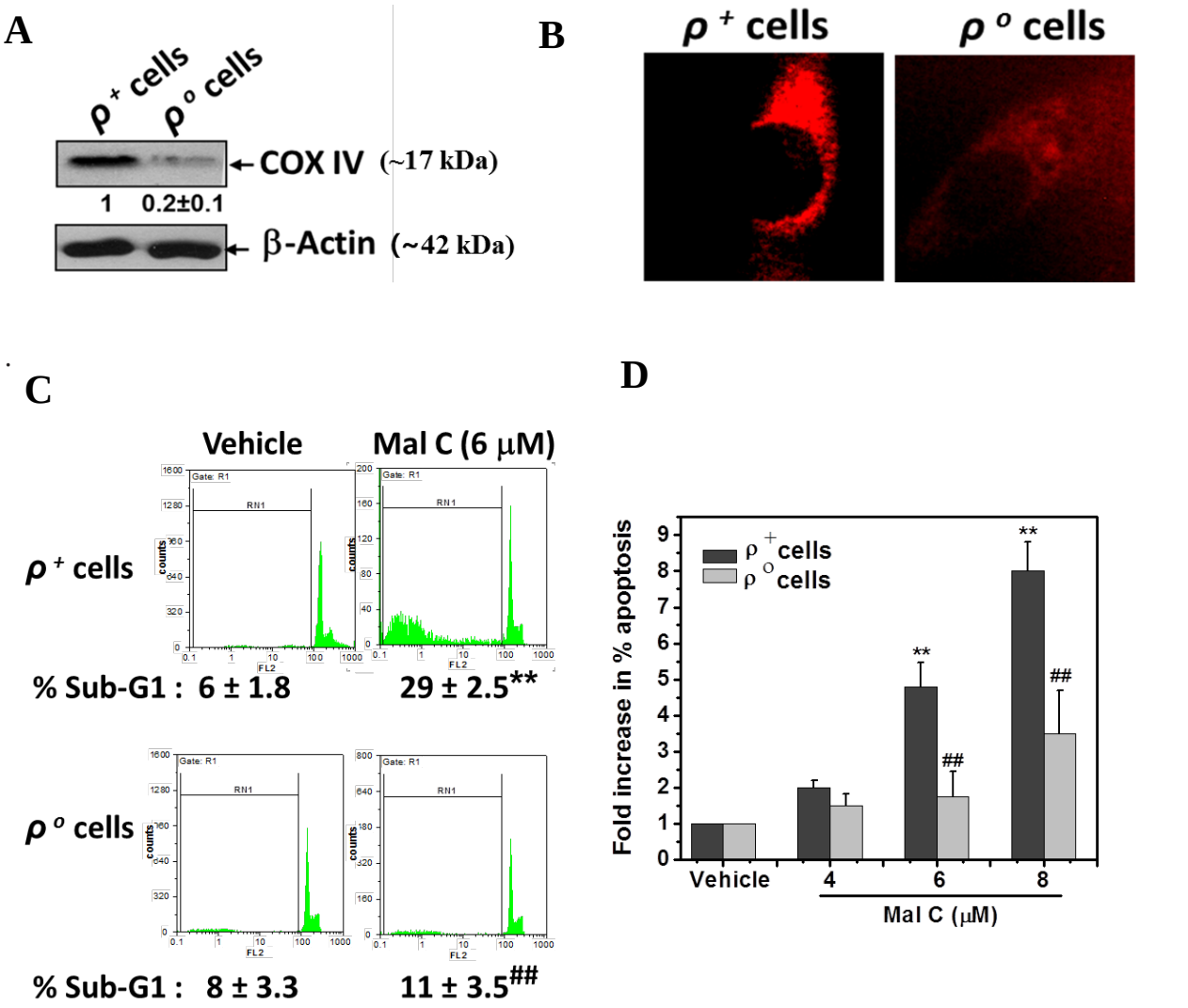

Figure 3. 4. 5. Generation of mitochondrial deficient A549 cells. (A, B) Mitochondria deficiency in A549-ρ^o cells, as assessed by COX IV immunoblottting and fluorescence intensity after labeling with MitoTracker red in the A549-ρ^+ and A549-ρ^o cells. **(C, D)** Concentration-dependent apoptosis induction of mal C in A549-ρ+ and A549-ρo cells. Cells were treated with increasing concentration of mal C and the sub-G1 population was assessed by flow cytometry. The experiments were repeated four times with similar results and the values are means ± SEM. $^{**}p<0.01$ compared to vehicle treated cell, $^{\#\#}p<0.05$ compared to mal C treated A549-ρ+ cell.

Furthermore, shRNA-mediated depletion of the anti-apoptotic BCL-2 protein partially sensitized cell death in response to mal C treatment (Figure 3. 4. 6A, B). These findings provided direct evidence of the essential role of mitochondria in mal C-induced apoptosis.

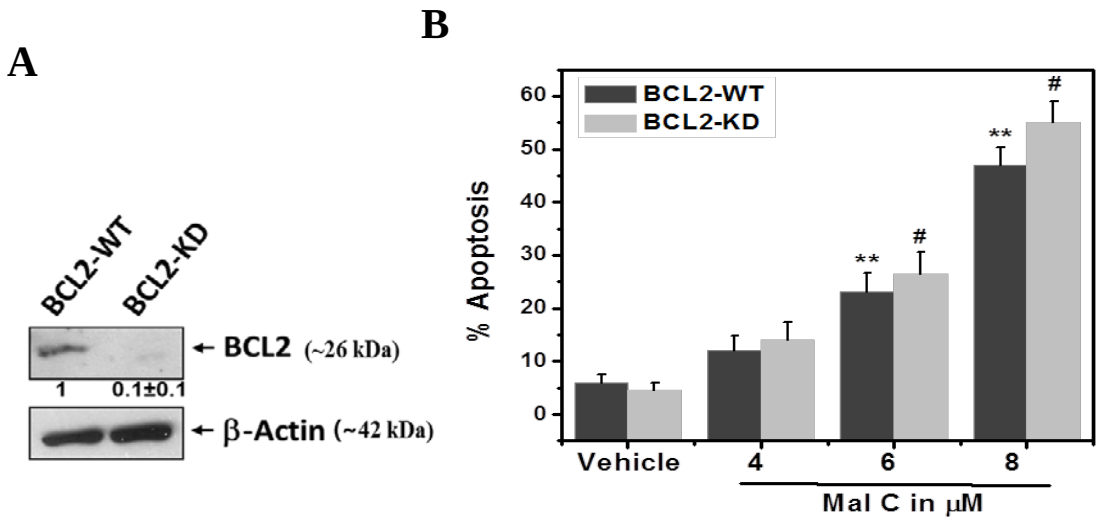

Figure 3. 4. 6. Apoptosis induction by mal C in BCL2 down-regulated cells. (A) Confirmation of BCL2 depletion in BCL2-KD cells by immunoblot. **(B)** The BCL2-WT and BCL2-KD cells were treated with increasing concentration of mal C and the sub-G1 population was assessed through flow cytometry. The experiments were repeated three times with similar results and the values are means ± SEM. ***p*<0.01 compared to vehicle treated cell, #*p*<0.05 compared to mal C treated BCL2-KD cell.

3. 4. 3. P38 MAPK is an important mediator in the mal C-mediated mitochondrial dysfunction and cell death

Treatment of the A549 cells with mal C (6 μM) resulted in a marked time dependent increase in the phosphorylated forms of all the three MAPKs (p38, JNK and ERK), indicating their activation (Figure 3. 4. 7).

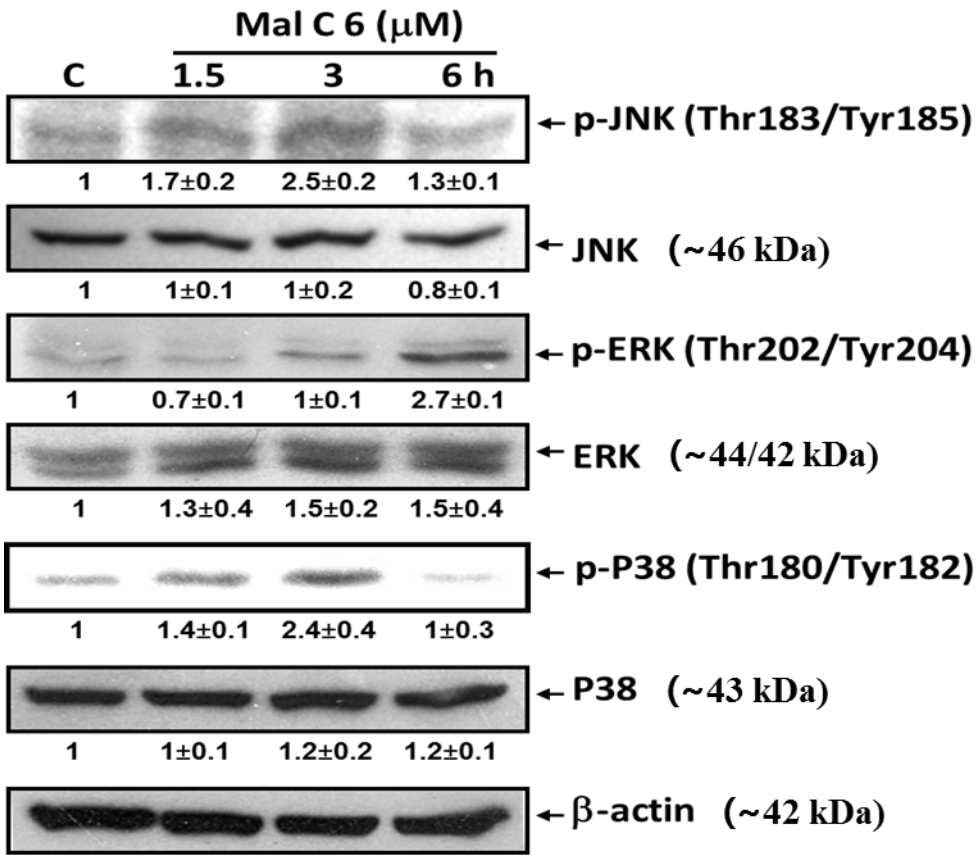

Figure 3. 4. 7. P38 MAPK acts as a critical upstream mediator in mal C-induced mitochondrial cell death. A549 cells were treated with mal C (6 μM) for different time periods. The MAPKs activation in term of phosphorylation of respective proteins in cell lysates was assessed by immunoblotting. The experiments were repeated three times with similar results and the values are means ± SEM.

To investigate the role of individual MAPKs activation, the effects of specific inhibitors such as SB203580 (p38 inhibitor), U0126 (ERK 1/2 inhibitor), and SP600125 (JNK inhibitor) in mal C-induced apoptosis were studied. Initially, we examined the efficacies of the p38 and JNK inhibitors in inhibiting the respective MAPKs at 3 h, as the levels of phospho-p38, andphospho-JNK were reduced at a later time point (6 h). For the ERK inhibitor, this was carried out at 6 h. Furthermore, the effects of the inhibitors on the respective downstream targets of p38 and JNK, such as MAPK activated protein

kinase (MAPKAPK) and c-JUN were also investigated. Normally, p38, JNK and ERK have very low autophosphorylating activity, and their activation is presumed to be dependent mainly on upstream MAPK kinases (MAPKKs) and other kinases. The inhibitors for ERK (U0126), JNK (SP600125) and p38 (SB203580) are known to inhibit the upstream kinases and/or autophosphorylation of the respective MAPKs [75,81]. In our results, the inhibitors for p38 and JNK partially inhibited the p38 and JNK phosphorylation, induced by mal C alone (Figure 3. 4. 8). Further, mal C induced significant phosphorylations of MAPKAPK and c-JUN, which were brought down to the normal levels by these inhibitors (Figure 3. 4. 8). On the other hand, U0126 completely suppressed the endogenous and mal C-induced phosphorylation of ERK (Figure 3. 4. 8). This is possibly due to direct inhibition of upstream MAPKK family members, MEK-1 and MEK-2 by U0126, as reported earlier [171].

Amongst the inhibitors, only SB203580 markedly reduced the mal C-induced apoptosis (Figure 3. 4. 9), indicating the involvement of activated p38 MAPK in the process.

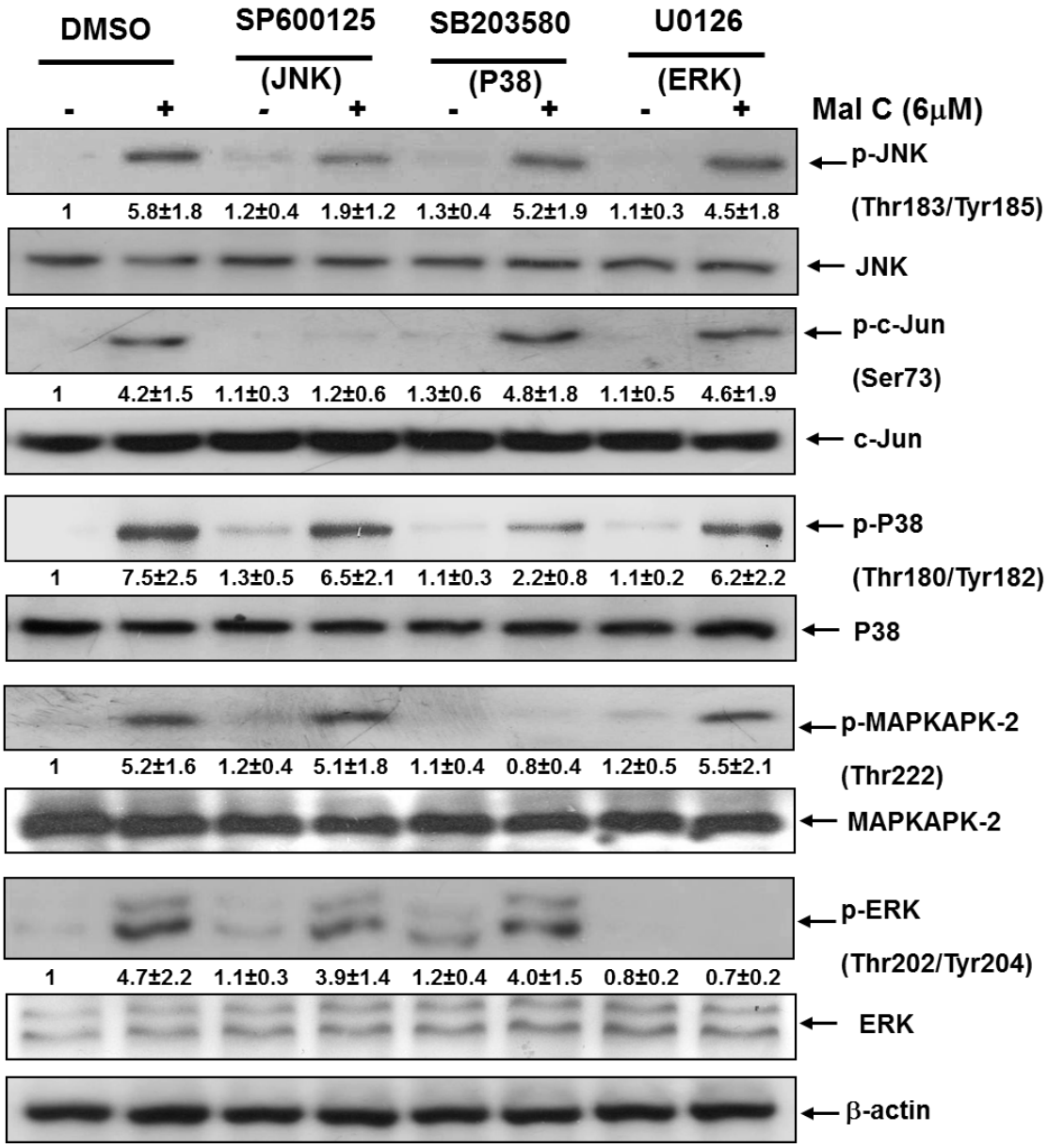

Figure 3. 4. 8. Effect of MAPK inhibitors on MAPK activation in response to mal C. The p38, JNK and ERK inhibitor-pretreated cells were exposed to mal C for 3 h and phosphorylation of MAPKs and their respective downstream proteins were analyzed by immunoblots.

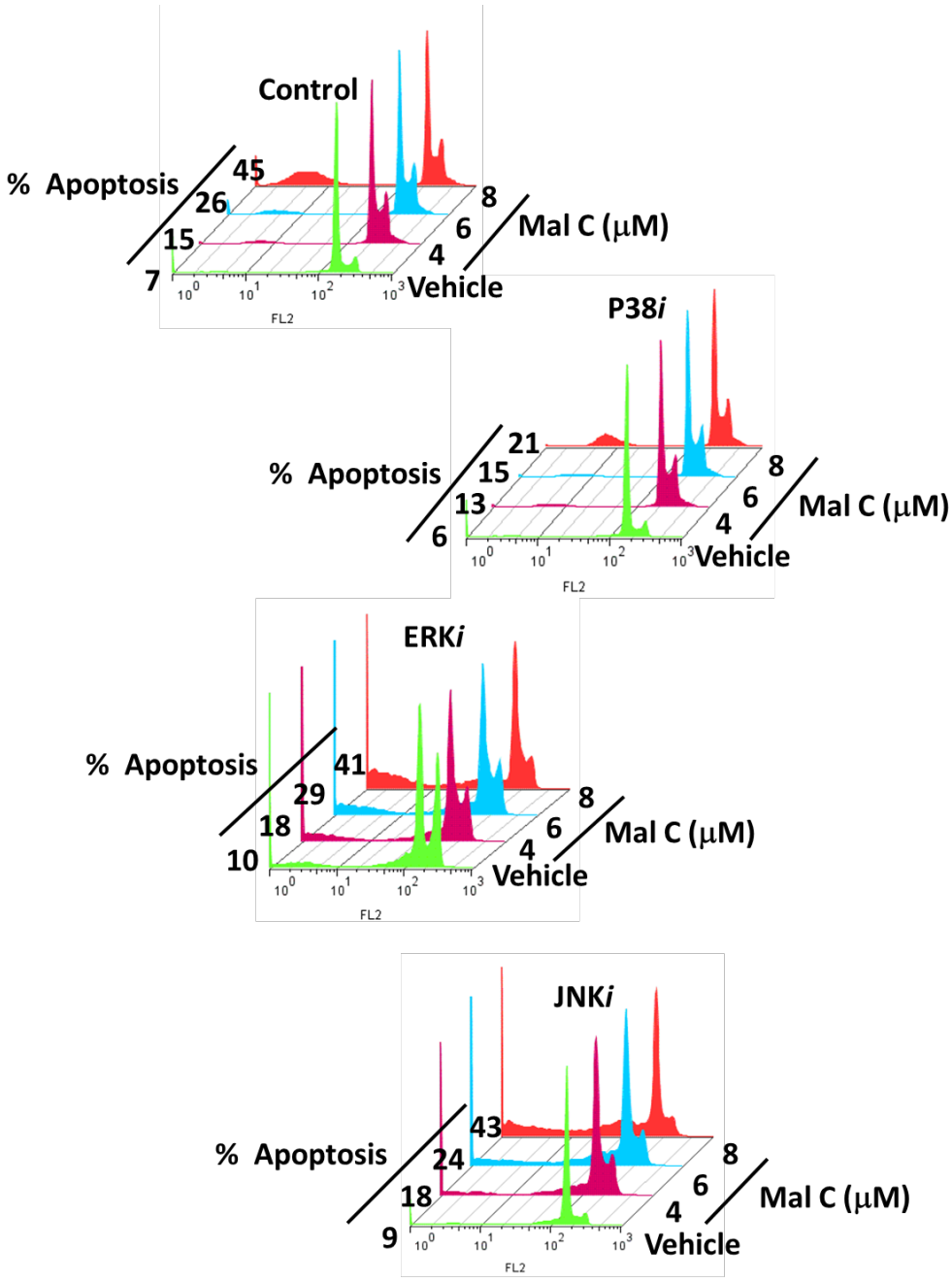

Figure 3. 4. 9: Effect of MAPK inhibitor in mal C induced apoptosis. Cells were pretreated with different MAPK specific inhibitors (each 25 μM) and referred as p38i, JNKi and ERKi cells. Subsequently the cells were incubated with different concentrations of mal C for 24 h and the sub-G1 population was assessed by flow cytometry. The abbreviation FL2 in the histogram represents intensity of the red fluorescence of propidium dye, acquired in channel-2. The values are mean of three experiment.

Interestingly, the mal C-induced p38 MAPK phosphorylation was not affected in the A549-ρ^o and BCL-2 KD cells *vis-à-vis* the respective wild type cells (Figure 3. 4. 10).

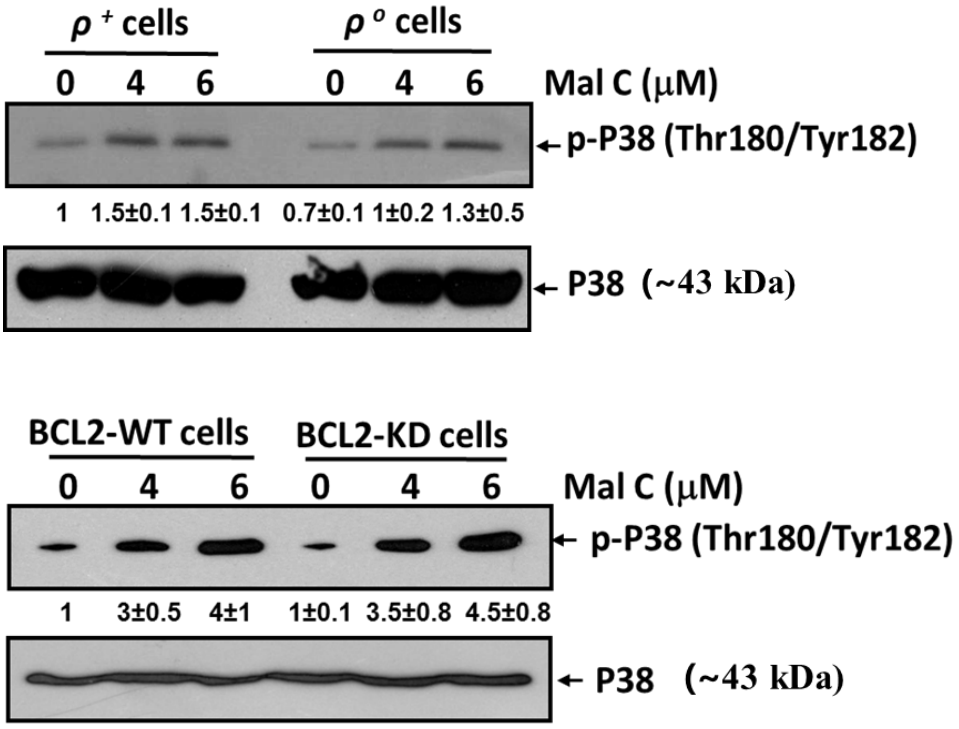

Figure 3. 4. 10. P38 activation in A549-ρ^+, A549-ρ^o, BCL2-WT and BCL2-KD cells. Respective cells were incubated with vehicle alone or mal C (4 and 6 μM) for 3 h and the phospho-p38 (p-p38) levels in the cell lysates were assessed by immunoblots. The experiments were repeated three times with similar results, and representative images are shown. The values are mean ± SEM.

However, pre-treatment of p38 MAPK inhibitor abrogated the mal C-induced ΔΨm loss partially and cytochrome c release into cytosol (Figure 3. 4. 11A, B) . Taken together, these results indicated that p38 activation is the initial event that triggers mitochondrial dysfunction in the mal C-induced cell death.

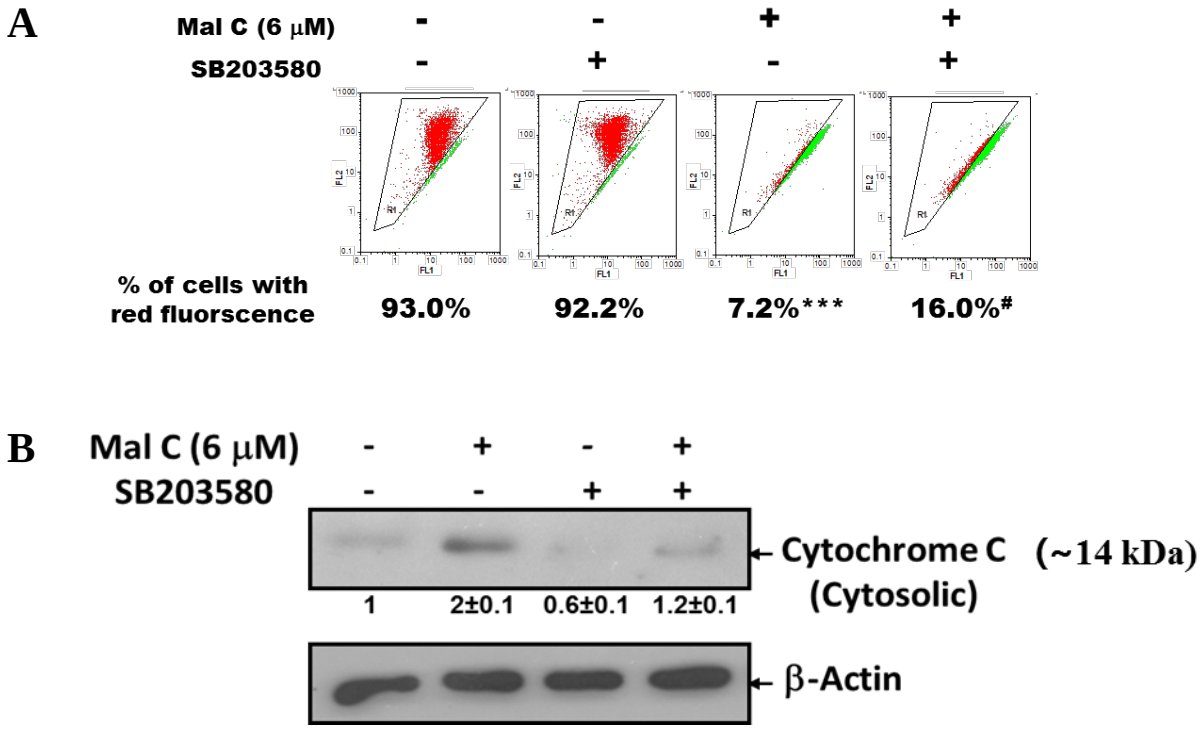

Figure 3. 4. 11. Effect of p38 inhibitor on MMP loss and cytochrome c release. (A) The p38 (SB203580) inhibitor-pretreated cells were exposed to mal C for 3 h and ΔΨm loss was analyzed by flow cytometry using JC-1 dye. **(B)** The p38 inhibitor-pretreated cells were exposed to mal C for 3 h and cytochrome c release into cytoplasm was analyzed by immunoblots. The experiments were repeated three times with similar results, and representative images are shown. The values are mean ± SEM. ***p<0.001 compared to vehicle treated cell, $^{\#}p$<0.05 compared to mal C alone treated A549 cell.

3. 4. 4. Mal C binds to DNA and induces double strand breaks (DSBs) in A549 cancer cells

The DNA repair and replication machinery are known to convert SSBs into the most severe and lethal DSBs, which are powerful apoptosis inducers. Earlier, mal C was found to bind with DNA *in vitro* through minor groove as well as intercalation, and induce SSBs in MCF7 cells [158]. To decipher the initial molecular targets of mal C, the DNA binding and damaging ability of mal C in A549 cells were investigated. Pre-treatment

with mal C reduced the binding of a known DNA binder, Hoechst 33342 (Figure 3. 4.12) in a concentration dependent manner.

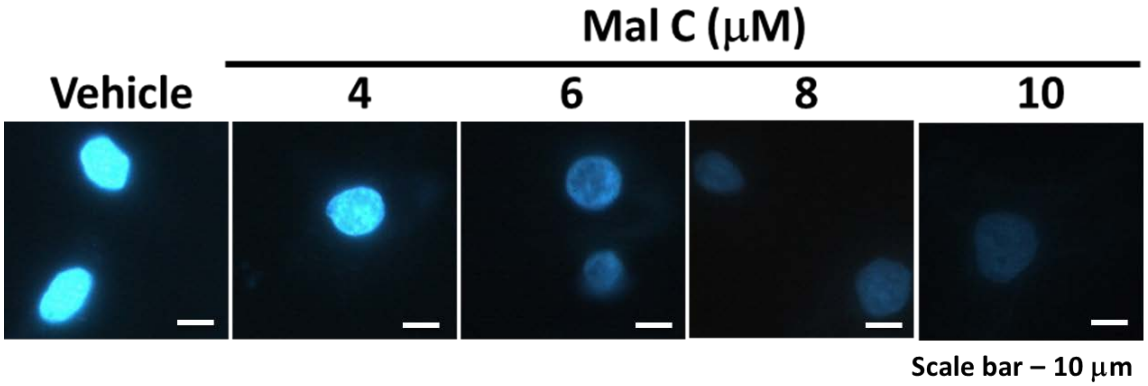

Figure 3. 4. 12. Mal C binds to DNA in A549 cells. The A549 cells were treated with different concentrations of mal C for 1 h. After washing off mal C, cells were labeled with Hoechst 33342, and visualized under an inverted fluorescent microscope. The experiment was repeated three times and the represenative images are shown.

Mal C treatment in A549 cells has also been found to induce DNA damage as quantified by neutral comet assay (data shown as olive tail moment) which showed no or smaller comet tail in the untreated cells, while mal C dose-dependently and time dependently induced longer comet tails in A549 cells (Figure 3. 4. 13A-C). In corroboration with above results, the level of the DSB marker, phosphorylated H2AX (γH2AX) also increased in a time and dose dependent manner in response to mal C treatment (Figure 3. 4. 13D, E).

A

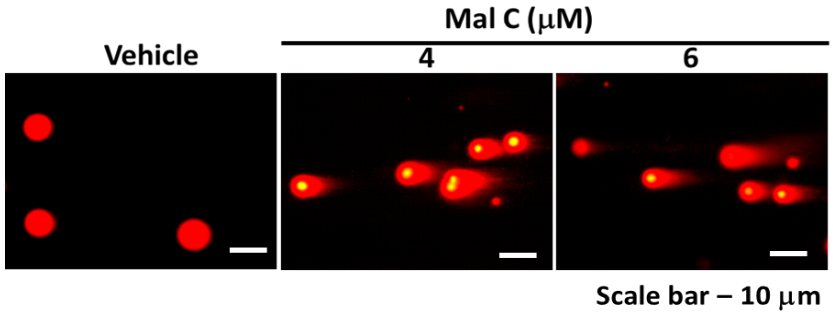

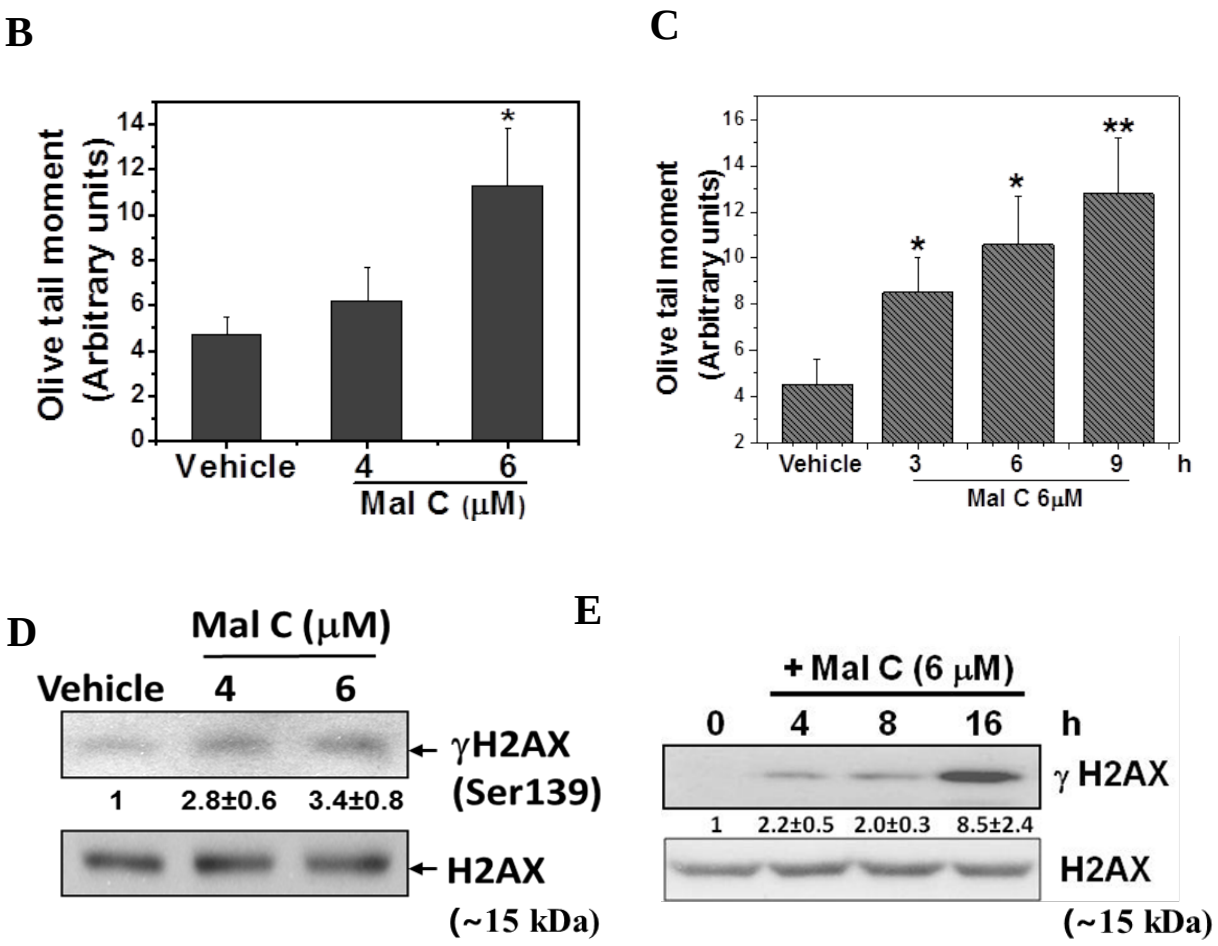

Figure 3. 4. 13. Mal C induces DNA double strand breaks (DSBs). **(A)** A549 cells treated with mal C (4 and 6 μM) for 4 h was analysed through neutral comet assay. **(B)** Quantification of the olive tail moment from the above experiment. (C) Quantification of the olive tail moment in A549 cells treated with mal C (6 μM) for different time periods (3, 6 and 9 h). The experiment was repeated three times with similar results. The values are mean ± SEM. **(C)** The A549 cells were treated with vehicle alone or different concentrations of mal C for 3 h. The γH2AX levels in the cell lysates was analyzed by immunoblots. (**D**) The A549 cells were treated with vehicle alone or mal C (6 μM) for 4, 8 and 16 h. The γH2AX levels in the cell lysates was analyzed by immunoblots. All the experiments were repeated three times with similar results and the values are mean ± SEM. *p<0.05 and **p<0.01 compared to vehicle treated cell.

3. 4. 5. Mal C induces ATM/ATR-mediated DNA damage response and p38MAPK activation

Based on the above results, we hypothesized that the mal C-induced DSBs and putative DNA damage response could lead to the p38 MAPK activation and subsequent mitochondrial death. The ATM and ATR kinases play distinct, but overlapping roles in response to DNA DSBs [172]. To substantiate the hypothesis, auto-phosphorylation at Ser-1981 ATM, and ATR-mediated Ser-345 phosphorylation in CHK1 protein were analyzed [71]. As shown in Figure 3. 4. 14, mal C (6 μM, 3 h)-treatment not only increased phosphorylation of H2AX, but also induced a significant amount of phosphorylation on ATM-Ser1981 and CHK1-Ser345. This suggested a rapid activation of DNA damage response pathway in cancer cells by mal C treatment.

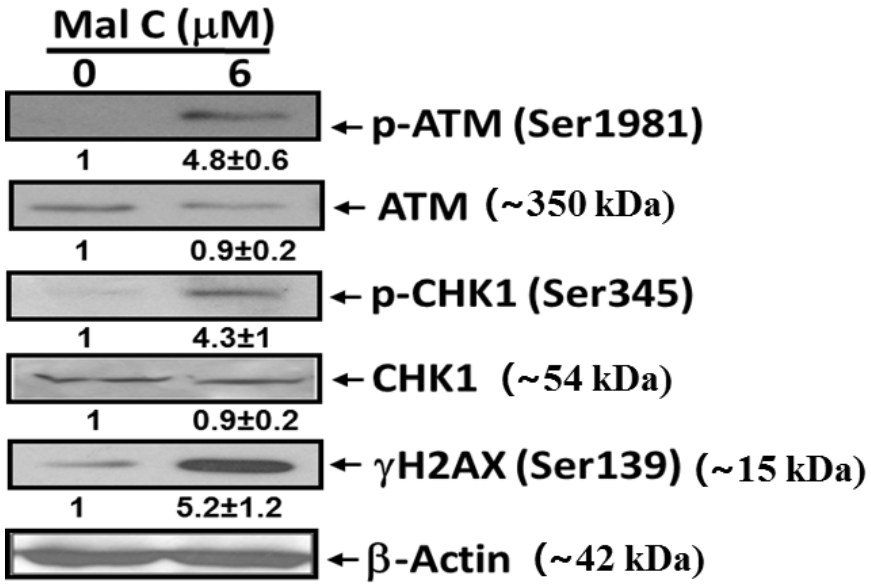

Figure 3. 4. 14. Activation of DNA damage response proteins after mal C treatment. Phosphorylation levels of ATM, CHK1 and H2AX. The A549 cells were treated with vehicle alone or mal C (6 μM) for 3 h and the cell lysates were analyzed for the phosphorylation levels of respective proteins by immunoblots. The values are mean ± SEM. *p<0.01 compared to untreated cell.

Next we determined whether down-regulation of ATM or ATR in the A549 cells impacts p38 MAPK response following mal C treatment. For this, the ATM-depleted cells were generated using ATM mRNA specific shRNA (Figure 3. 4. 15). As ATR is an essential gene, and stable ATR knockdown cells are not viable, we used schisandrin B, a known ATR specific inhibitor to obtain the ATR*i* cells [173]. Next, the activation of ATM and ATR as well as p38 MAPK pathways in ATM-WT (expressing scrambled shRNA control), ATM-KD (expressing ATM shRNA) and ATR*i* cells was evaluated. Mal C (6 μM) treatment markedly induced phosphorylation of ATM, CHK1, H2AX and p38 in ATM-WT cells (Figure 3. 4. 15), suggesting that both ATM and ATR pathways are activated in response to mal C treatment.

However, compared to the wild type cells, phosphorylation of CHK1, H2AX and p38MAPK was significantly reduced in the ATM-KD as well as ATR*i* cells (Figure 3. 4. 15). It is imperative to note that phosphorylation of CHK1; a downstream target of ATR was also abrogated in the ATM-KD cells. Altogether these results suggested a predominant role of both ATM and ATR pathways in p38 MAPK activation by mal C.

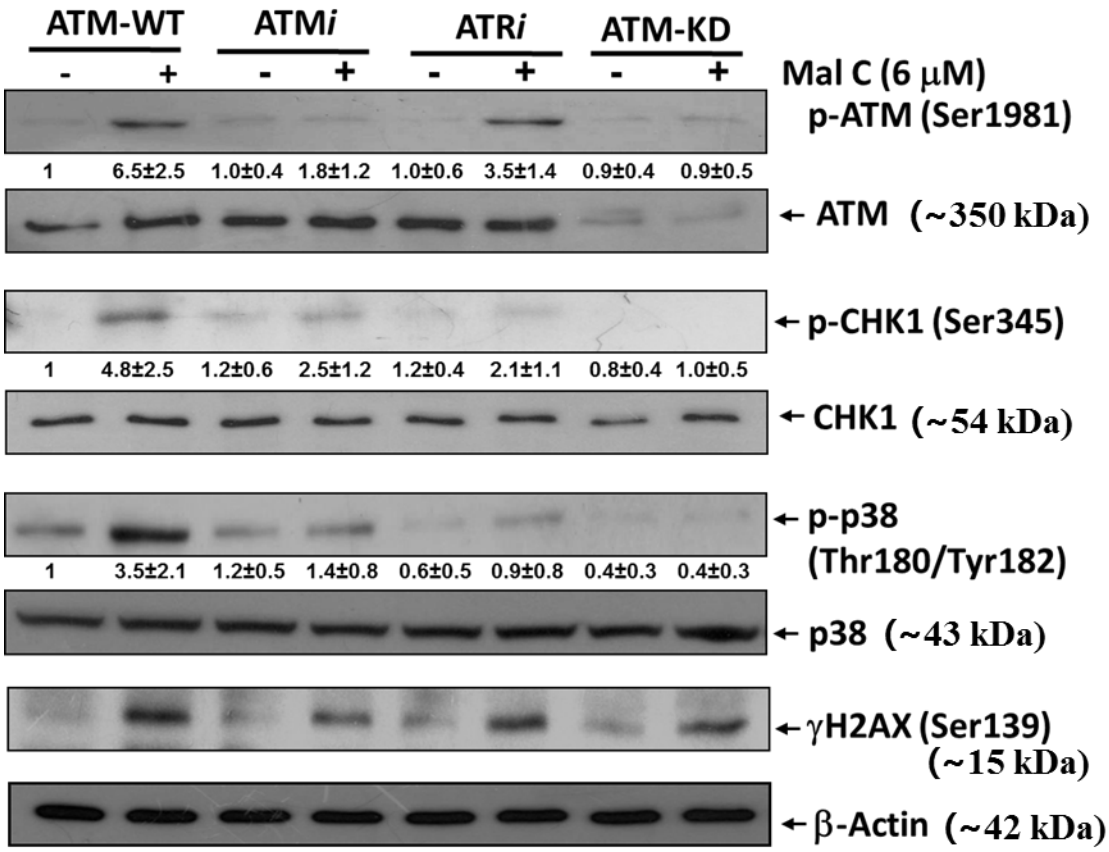

Figure 3. 4. 15: Effects of ATM and ATR downregulation. The ATM-WT, ATM*i*, ATR*i* and ATM-KD cells were treated with vehicle alone or mal C (6 μM) for 3 h and the cell lysates were analyzed for p-ATM, p-CHK1, p-p38 and γH2AX by immunoblots. For ATM*i* and ATR*i*, the respective specific inhibitors, KU55933 (10 μM) and schisandrin B (25 μM) were used. The experiments were repeated three times with similar results, and representative images are shown. The values are mean ± SEM.

3. 4. 6. Inhibition of ATM, ATR or CHK1 proteins leads to abrogation of mal C-induced apoptosis

To probe the participation of ATM-CHK1 in p38MAPK activation and mitochondrial dysfunction, the p38 MAPK phosphorylation and mitochondrial cytochrome c release in the mal C-treated ATM-WT, ATM-KD and CHK1*i* cells were assessed. ATM down regulation as well as CHK1 inhibition, with a CHK1 specific inhibitor, markedly reduced p38 phosphorylation and

mitochondrial release of cytochrome c in the ATM-KD and CHK1*i* cells *vis-à-vis* the ATM-WT cells (Figure 3. 4. 16A). Furthermore, the mal C-induced apoptosis was significantly reduced in CHK1*i* and ATM*i* cells although the ATR inhibitor offered only a marginal protection (Figure 3. 4. 16B). Altogether, these results unraveled the hierarchy of molecular events in which ATM regulates the MAPK cascade that leads to cell death in the mal C-treated A549 cells.

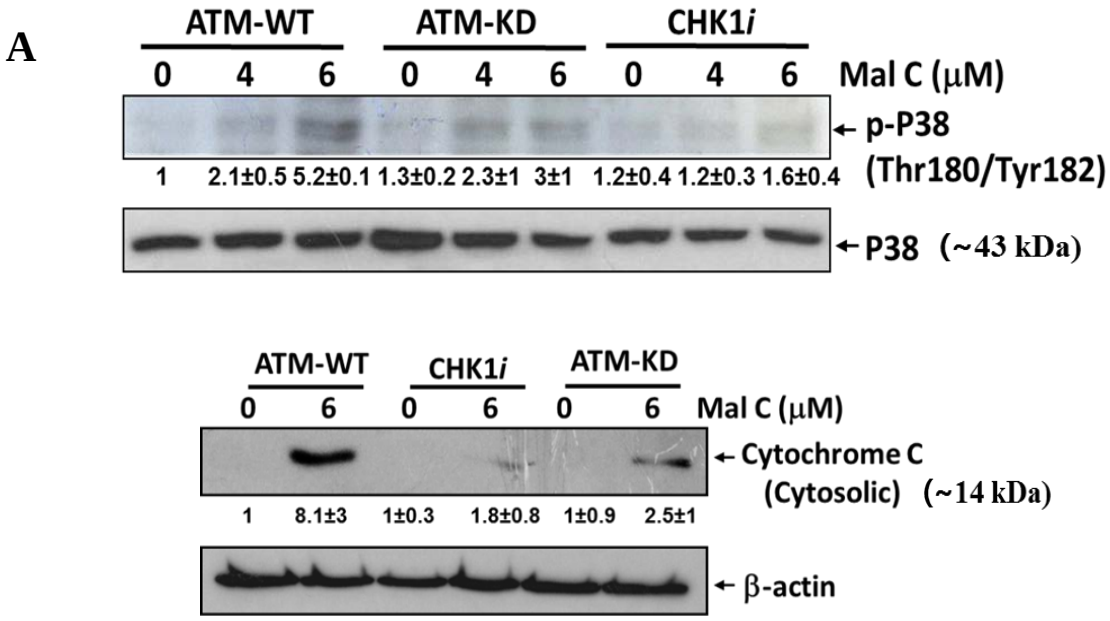

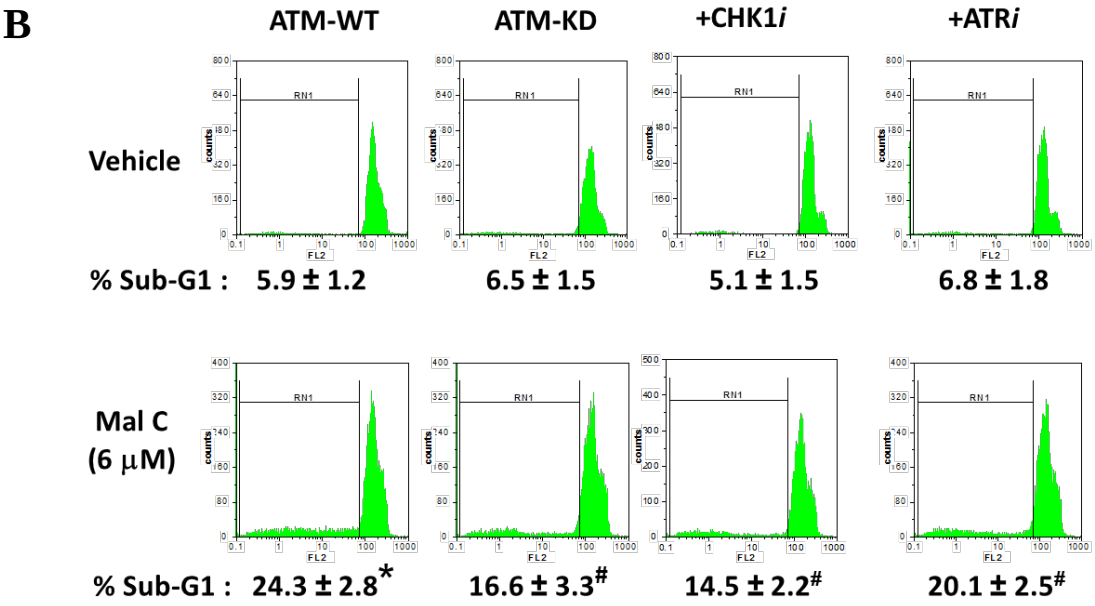

Figure 3. 4. 16. Inhibition of ATM, ATR or CHK1 proteins leads to abrogation of mal C-induced apoptosis. (A) Effect of ATM and CHK1 on p38 phosphorylation and cytochrome c release from mitochondria. The ATM-WT, ATM-KD and CHK1i cells were treated with vehicle alone or different concentrations of mal C and the p-p38 levels in the cell lysates and cytochrome c release into cytosol were analyzed by immunoblots. **(B)** Effect of ATM, ATR or CHK1 on apoptosis induction. The ATM-WT, ATM-KD, ATR*i* and CHK1*i* cells were treated with vehicle alone or mal C (6 μM) for 24 h and the sub-G1 populations were assessed by flow cytometry. For ATR*i* and CHK1*i*, the respective specific inhibitors, schisandrin B (25 μM) and UCN-01 (100 nM) were used. The abbreviation FL2 in the histogram represents intensity of the red fluorescence of propidium dye, acquired in channel-2. The experiments were repeated four times with similar results. All determinations were made in three replicates, and the values are means ± S.E.M. *$p<0.01$ compared to vehicle control, #$p<0.05$ compared to mal C-treated ATM-WT cells.

3. 5. Evaluation of combination treatment of mal C with radiation and other clinically approved cancer therapeutics

As per the objectives of the doctoral work, combination treatment of mal C with other chemotherapeutic drugs and ionising radiation (IR) was tested. For this we used camptothesin (CPT), mitomycin (MMC), topotecan (TPT), etoposide (VP-16) and doxorubicin. MTT assay was used to quantify the loss of cell viability induced by combinations of two different concentrations of mal C and four different concentrations of above mentioned drugs after 48h of incubation. All the above mentioned drugs showed no significant synergism towards the cell death in A549 cells (Figure 3. 5. 1A).

In order to probe radiosensitizing potentials of mal C, A549 cells were exposed to different dose of IR (γ-ray, dose rate: 1.2 Gy/min) and allowed to grow in the presence of vehicle or mal C (3 μM) to assess their clonogenic survival. Our results showed that clonogenic survival of IR treated cells did not change significantly in the presence of mal C (Figure 3. 5. 1B). (Figure 3. 5. 1B).

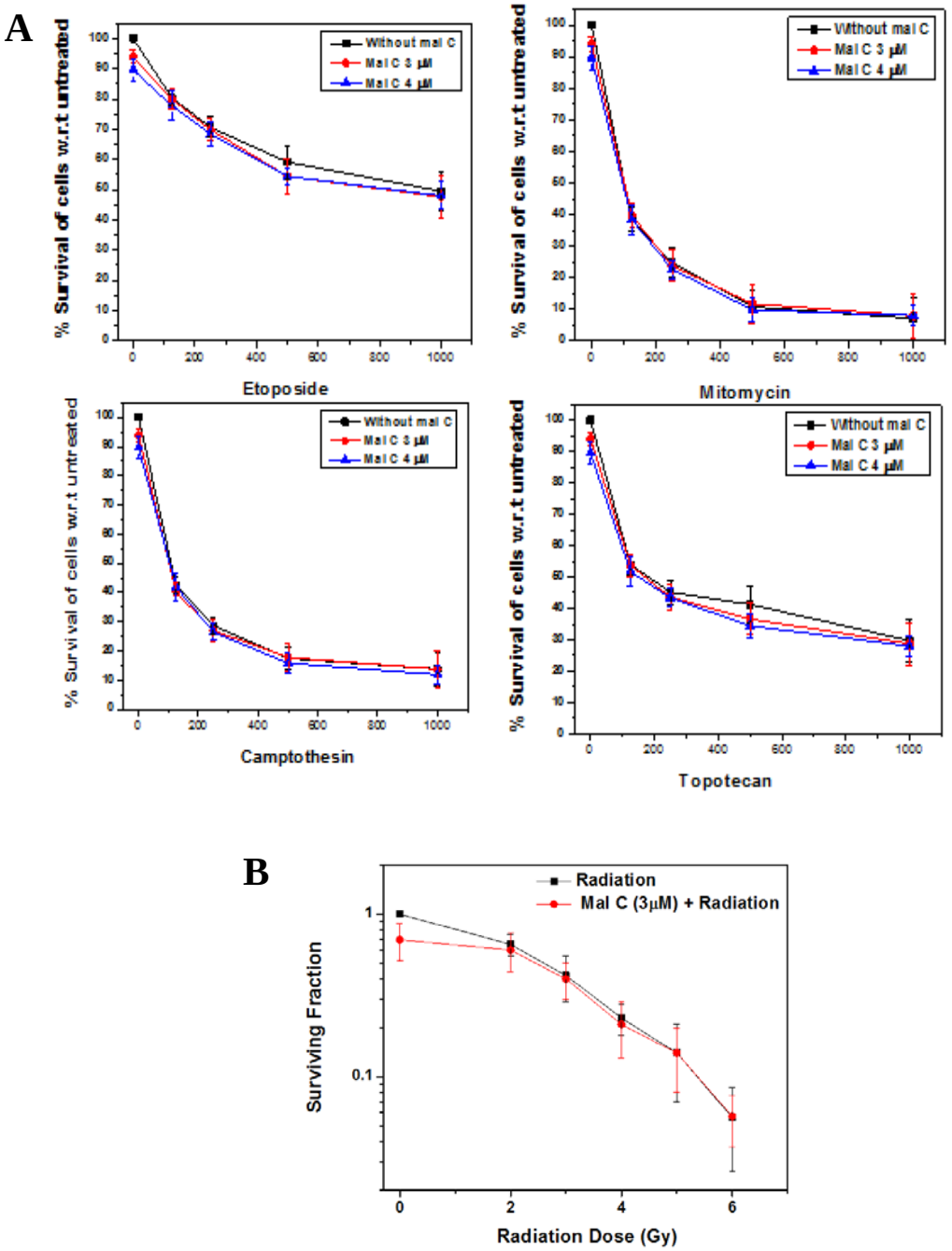

Figure 3. 5. 1. Sensitizing potential of mal C towards chemotherapeutic drugs/radiation induced cell death. (A) A549 cells were treated with mal C (3 and 4 μM) in the absence or presence of indicated concentrations of VP16, MMC, CPT or TPT respectively for 48 h, MTT assay was carried out to assess the cell viability. (B) Radio-sensitizing potential of mal C. A549 cells were exposed to IR (0-6 Gy) and allowed to grow in the presence of vehicle or mal C (3 μM). Further, Clonogenic survival assay was carried out.

3. 6. Molecular mechanism of mal C-induced cell death in MCF-7 (breast cancer) cell line

3. 6. 1. Mal C induces apoptosis in MCF-7 cells

Mal C and the positive control (curcumin) were found to dose-dependently inhibit growth of the MCF-7 cells, with the IC_{50} values of 7.0±1.8 μM and 19.7±2.5 μM respectively after 48 h of incubation. In order to assess whether the cell death induced by the mal C involves apoptosis, we looked for several apoptosis specific parameters: (i) sub G1 population, (ii) enrichment of histone-associated oligo nucleosome (DNA fragments) in the cytoplasm, and (iii) chromatin condensation in the mal C-treated cells. Compared to control, the mal C (4 –10 μM)-treated cells showed significantly increased (up to 64%, $p<0.01$) sub G1 population, while curcumin (50 μM) increased the sub G1 population by ~37% under identical conditions (Figure 3. 6. 1).

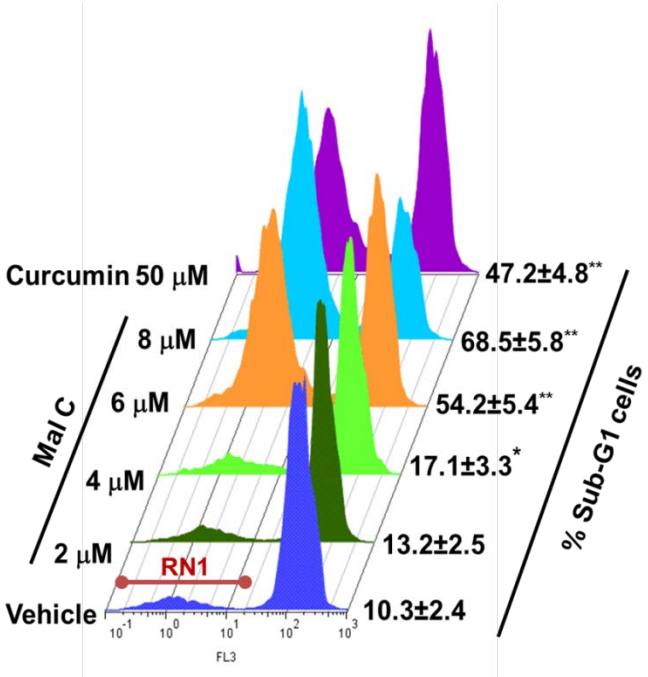

Figure 3. 6. 1. Dose-dependent accumulation of sub-G1 population in MCF7 cells after mal C treatment. The cells were treated with mal C (0–10 μM) for 24 h. Twenty thousand cells in each treatment were acquired using a flow cytometer, and the DNA content of the nuclei was registered on a logarithmic scale. The sub-G1 region (RN1) represents the percentage of cells undergoing apoptosis. All

determinations were made in three replicates, and the values are means ± S.E.M. *p<0.05 **p<0.01 compared to vehicle control.

A similar concentration-dependent enrichment of cytoplasmic oligonucleosome in the MCF-7 cells was induced by mal C. The extents of enrichment (p< 0.01) were 1.7-fold, 4.2-fold, and 6.2-fold, respectively with mal C (4, 6, and 8 μ M), compared to the control (Figure 3. 6. 2A). In comparison, the enrichment (5.5-fold, p<0.01) by the positive control, etoposide (VP16) (25 μM) was less than that by mal C (8 μM). Moreover, our fluorescence microscopy carried out with the Hoechst 33342-stained cells showed brightly fluorescent cells (Figure 3. 6. 2B), revealing chromosomal condensation. Cells, treated with mal C (4 μM) showed condensed nuclei, while the cells, treated with mal C (6 and 8 μM), but not at lower concentrations also induced chromosomal fragmentation and cell shrinkage.

A

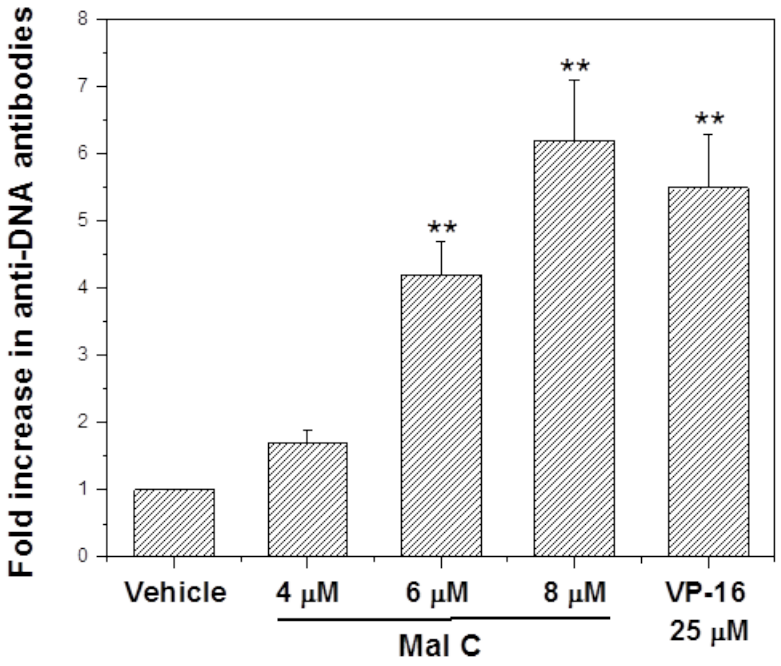

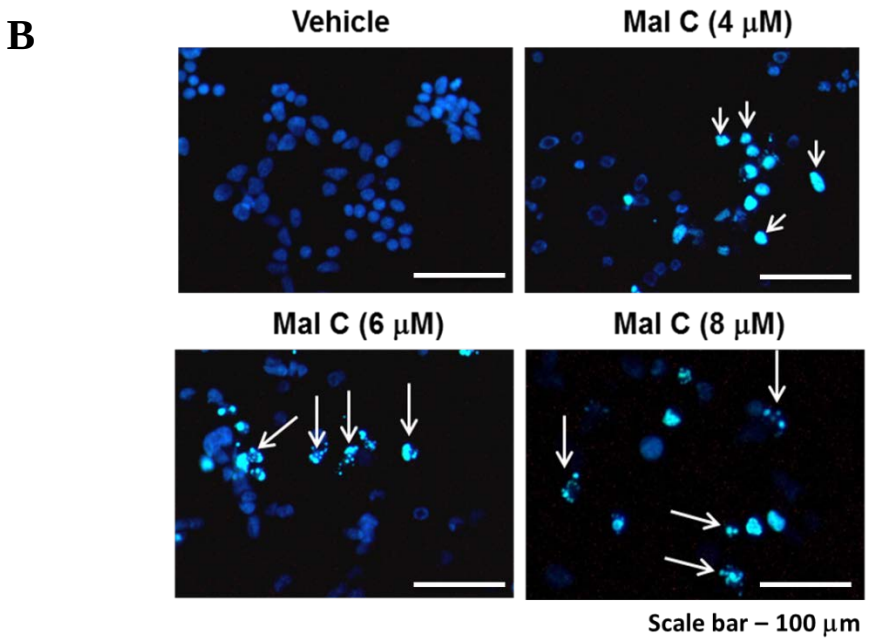

Figure 3. 6. 2. Dose-dependent enhancement of apoptosis in MACF7 cells after mal C treatment. (A) Analysis of enriched nucleosomes in cytoplasm. The cells were treated with mal C (0–8 μM) or VP16 (25 μM) for 24 h. The cytoplasmic histones associated-DNA fragments were assayed by ELISA. **(B)** Chromosomal condensation and fragmentation. The cells were treated with mal C (0, 4, 6, and 8 μ M) for 24 h, stained with Hoechst 33342, and observed under a fluorescence microscope. The experiments were repeated thrice with similar results. All determinations were made in three replicates, and the values are means ± SEM. $**p<0.01$ compared to vehicle control. Representative microscopy images (arrows indicate chromosomal condensation) are shown.

3. 6. 2 Mal C induces $\Delta\Psi_m$ loss to release the death factors in MCF-7 cells

Loss of mitochondrial $\Delta\Psi_m$ is another hallmark of apoptotic initiator signal. Hence, we assessed the dose dependent effect of mal C on $\Delta\Psi_m$ loss in the MCF-7cells, using the fluorescent cationic dye, JC-1 that exhibits potential-dependent accumulation in mitochondria. To this end, the emission shift of JC-1 from red to green post-mal C treatment was monitored by flow cytometry and fluorescent microscopy. Incubation of cells with increasing concentrations of mal C dissipated the $\Delta\Psi_m$. The percentage of green fluorescent cells, shown by gate R1 in Figure 3. 6. 3A increased to 22.1% ($p<0.05$), 67.1% ($p<0.01$) and 72.3% ($p<0.01$) respectively by mal C

(4, 6, and 8 μM), compared to that (1.72%) in the vehicle-treated cells. In fluorescent microscopy, the control cells showed red fluorescence. Exposure to mal C led to a marked increase in green fluorescence in most of the cells and reduced red fluorescence (Figure 3. 6. 3B).

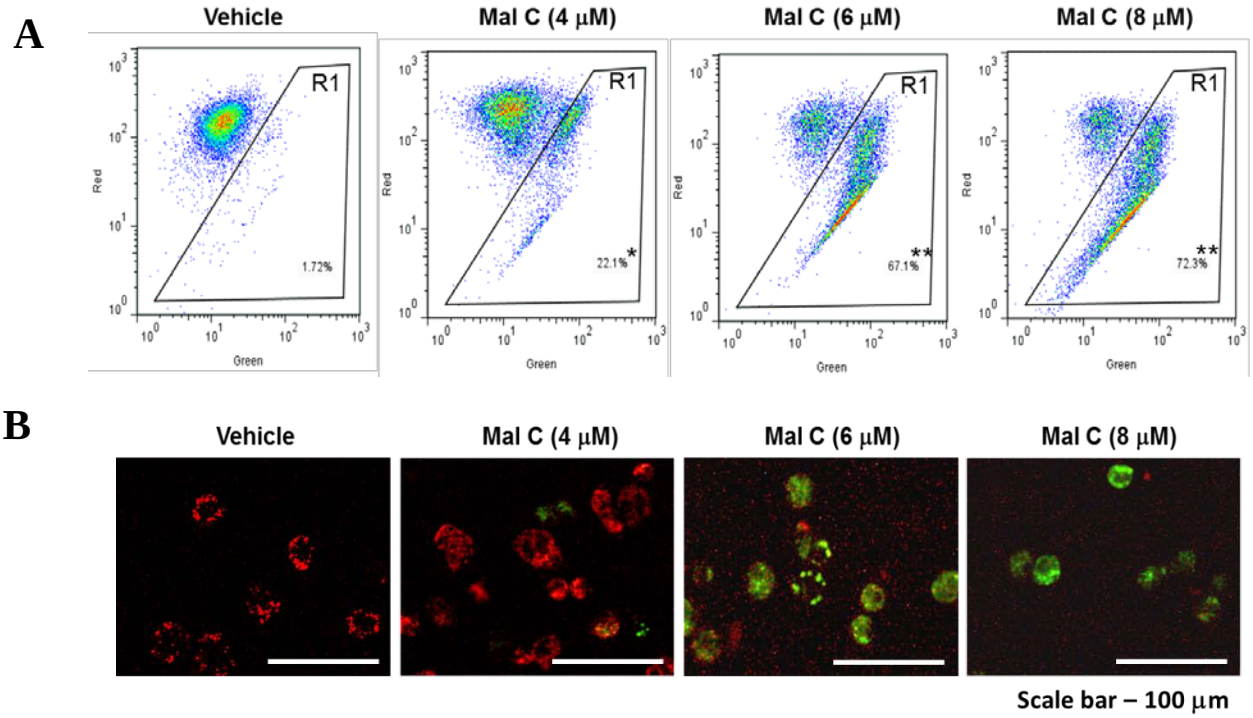

Figure 3. 6. 3. Mal C permeabilizes outer mitochondrial membrane in MCF-7 cells. Loss of $\Delta\Psi_m$ was assessed by (A) flow cytometry, (B) fluorescence microscopy. The cells were incubated for 6 h with mal C (0, 4, 6, and 8 μ M), stained with JC-1 for 15 min, and $\Delta\Psi_m$ loss quantified by flow cytometry from the increased green fluorescent cells, after R1 gating. The JC-1 stained cells were also visualized under a fluorescent microscope. The experiments were repeated three times with similar results. All determinations (shown inside R1 gates) were made in three replicates, and the values are means ± SEM. $*p<0.05$, $**p<0.01$ compared to vehicle control. Representative microscopy images (arrows indicate green fluorescent cells) are shown.

Since MCF-7 is devoid of caspase-3 [174], the two mitochondrial proteins, AIF and endo G can induce apoptosis [28,43]. Hence, we examined the status of these proteins by immunoblots in the mal C-treated cells. The immunoblots of the cytoplasmic fraction of cells showed

increased expressions of endo G (1.3-fold and 2.8-fold) and AIF (1.5-fold and 4.2-fold) at 16 h following mal C (4 and 6 μM, respectively) treatment, compared to that of the control cells (Figure 3. 6. 4A). This was associated with simultaneous reductions of the mitochondrial endo G (0.5-fold) and AIF (0.2-fold and 0.4-fold) expressions in the mal C (4 and 6 μM)-treated cells, compared to that of the control (Figure 3. 6. 4B). The release of AIF in the cytosol was further confirmed by immuno-fluorescence with dual staining. The control cells showed presence of AIF (green fluorescence) outside the nucleus (Figure 3. 4. 4C). However, migration of AIF inside the nucleus (blue fluorescence) was clearly evident following mal C treatment, the effect being more prominent with mal C (6 μM).

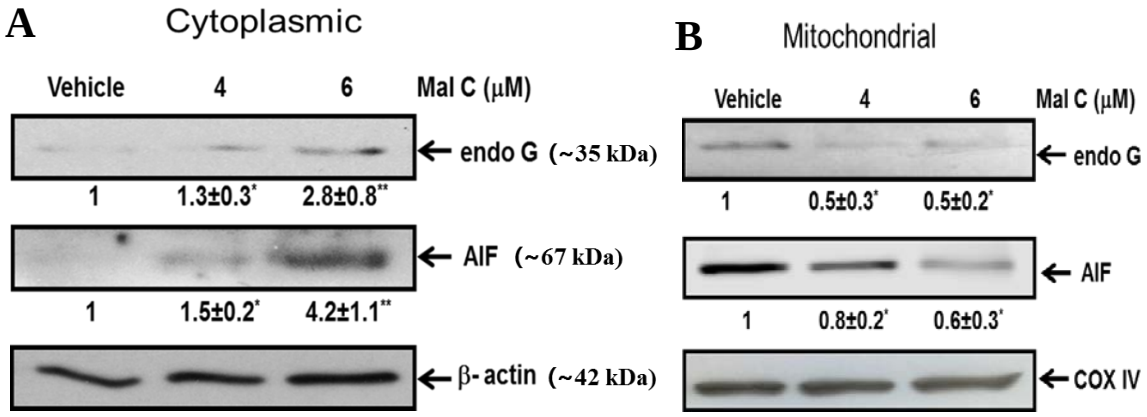

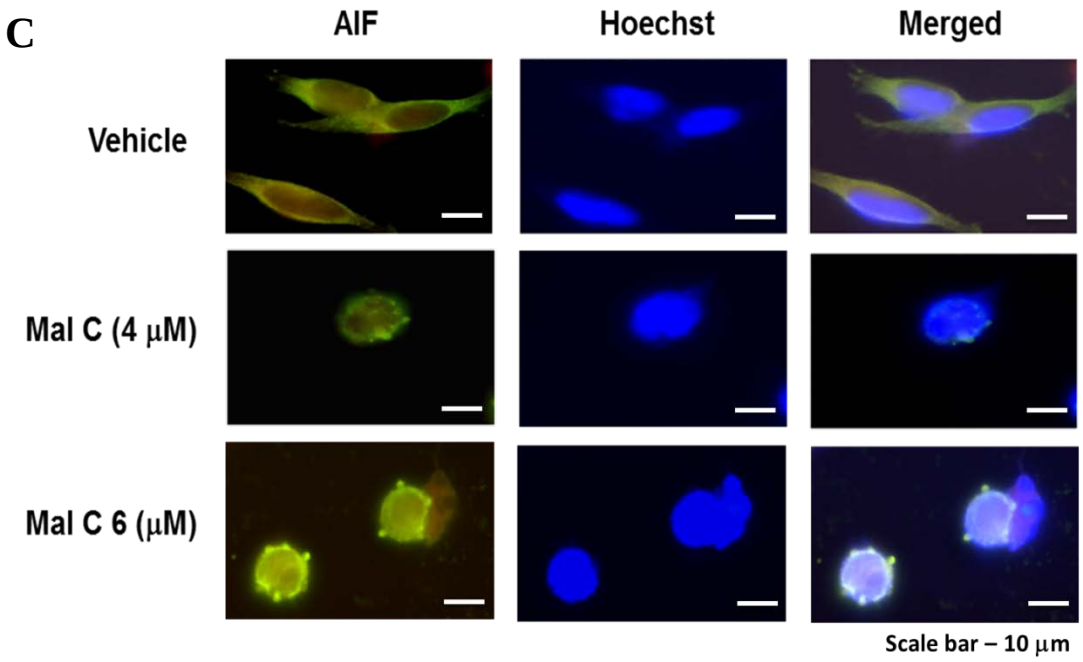

Figure 3. 6. 4. Mal C-induced MMP releases mitochondrial apoptogenic proteins in MCF-7 cells. (A and **B)** Immunoblots of AIF and endo G in the cytoplasmic and mitochondrial fractions. The respective cell extracts were subjected to immunoblotting, using suitable antibodiesagainst AIF and endo G.**(C)** Immunofluorescenceof AIF. The cells were incubated for 16 h with mal C (0, 4, and 6 μ M), treated with AIF antibody or nuclear stain (Hoechst 33342), and cellular localization of AIF examined by immunofluorescence. The experiments were repeated thrice with similar results. The values of the immunoblots are means ± SEM. $*p<0.01$, $**p<0.001$ compared to vehicle control. Representative microscopy images are shown.

3. 6. 3. Mal C increases intracellular Ca^{2+} levels and activates calpain in MCF-7 cells

An early Ca^{2+} influx through plasma membrane channels can activate the intrinsic mitochondria-mediated death cascade in many cases [175]. Furthermore, Ca^{2+}-dependent calpain activation can also induce cell death in a caspase-independent manner. To examine these possibilities, the effect of mal C on intracellular Ca^{2+} levels and calpain activation in the MCF-7 cells were assessed. Six minutes after treatment, mal C increased the Ca^{2+} level by 57%, compared to the vehicle control (Figure 3. 6. 5A). During 9-12 min, the Ca^{2+} level were 2 fold that of the control value.

Pretreatment with the intracellular calcium chelator, BAPTA-AM (2 μM) significantly reduced the peak Ca^{2+} level (12 min) by 37% (Figure 3. 6. 5B). Furthermore, pretreatment of the cells with BAPTA-AM (2 μM) or Ru360 (5 μM), an inhibitor of mitochondrial Ca^{2+} uniporter for 1 h reduced the mal C-induced sub G1 population by 18% and 12% respectively.

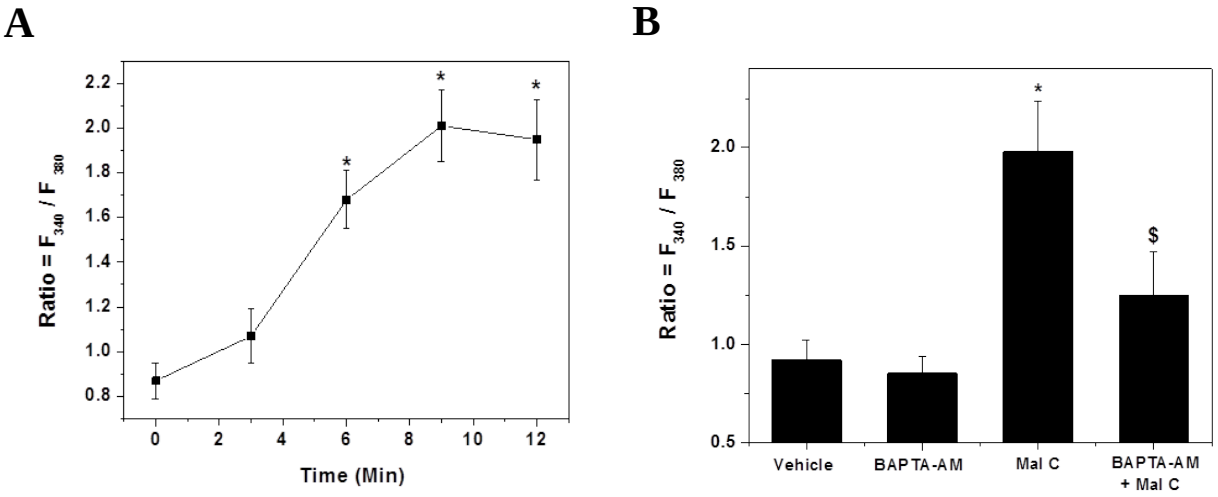

Figure 3. 6. 5. Mal C induces intracellular Ca^{2+} influx in MCF-7 cells. (A) The cells were incubated for 0.5 h with fura-2-AM, followed by treatment with mal C (0 and 6 μ M), and the fluorescence at 510 nm was measured using 340 and 380 nm excitation. **(B)** Ca^{2+} ions release and its attenuation by a Ca^{2+} -specific chelator, BAPTA-AM. Similar experiments were also carried out with cells, pre-incubated with BAPTA-AM for 1 h prior to fura-2-AM treatment and mal C addition. The fluorescence was measured at 9 min post-mal C treatment. The experiments were repeated thrice with similar results. All determinations were made in three replicates, and the values are means ± SEM. $*p<0.01$ compared to vehicle control; $\$p<0.01$ compared to mal C-only treatment.

Regarding calpain activation, a time-dependent analysis revealed that the activation was initiated by mal C (6 μM) at 12 h that increased by 32.2% at 24 h, compared to control (Figure 3. 6. 6A). Mal C (4 μM) did not induce significant calpain activation even at 24 h, which increased significantly with mal C (≥6 μM) (Figure 3. 6. 6B). But the calpain inhibitor, PD150606 (50 μM) failed to protect the cells against mal C treatment.

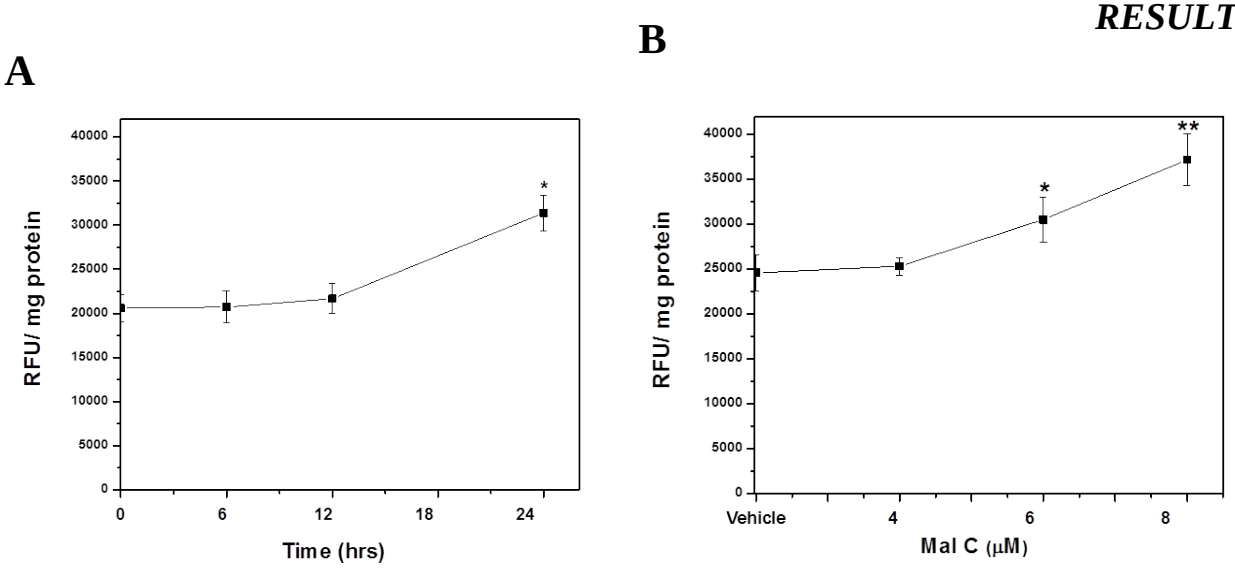

Figure 3. 6. 6. Mal C increases calpain activity in MCF-7 cells. (A) Time dependent effect. The cells were incubated for different time points (6, 12, 18, and 24 h) with mal C (6 μ M), and the calpain activity was assayed by ELISA. (B) Dose-dependent effect. This assay was carried out as above at 24 h using mal C (0–8 μM). The experiments were repeated thrice with similar results. All determinations were made in three replicates, and the values are means ± SEM. **p*<0.05, ***p*<0.01compared to vehicle control.

3. 6. 4. Mal C induces lysosomal membrane permeabilization (LMP) to release cathepsin B and activate BID in MCF-7 cells

Although not completely understood, controlled LMP has emerged as a significant inducer of MMP and apoptosis [25]. In particular, release of lysosomal cathepsins into the cytosol due to LMP can initiate apoptosis through the cleavage of BID and the degradation of the anti-apoptotic BCL-2 homologues [176]. Hence we examined LMP from the switch of the red AO fluorescence in the control cells to green in the mal C-treated cells. Fluorescent microscopy of the mal C (6 μM)-exposed cells showed marked increase in the green fluorescence with simultaneous loss of the red staining of the control cells at 1.5 h, indicating lysosomal swelling (Figure 3. 6. 7A). At 3 h, significantly enlarged lysosomes and lysosomal burst were noticed. The extensive lysosomal damage increased the acidic nature of the cytoplasm, resulting in its red staining. Quantification of these findings by flow cytometry revealed that the fluorescence ratio in the red/ green

channels was drastically reduced from 20 in the control cells to 1.2 in the mal C (6 µM)-treated cells at 1.5 h. However, the ratio increased to 3.1 at 3 h in the treated cells due to the contribution of the accumulated AO in the acidic cytosol (Figure 3. 6. 7B).

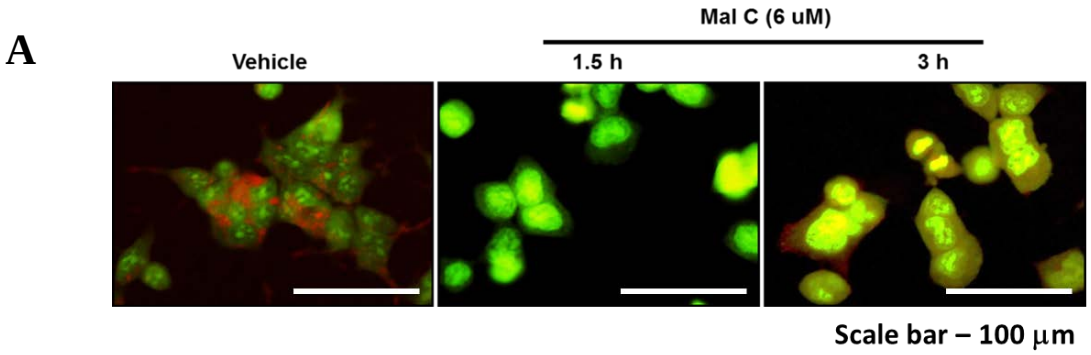

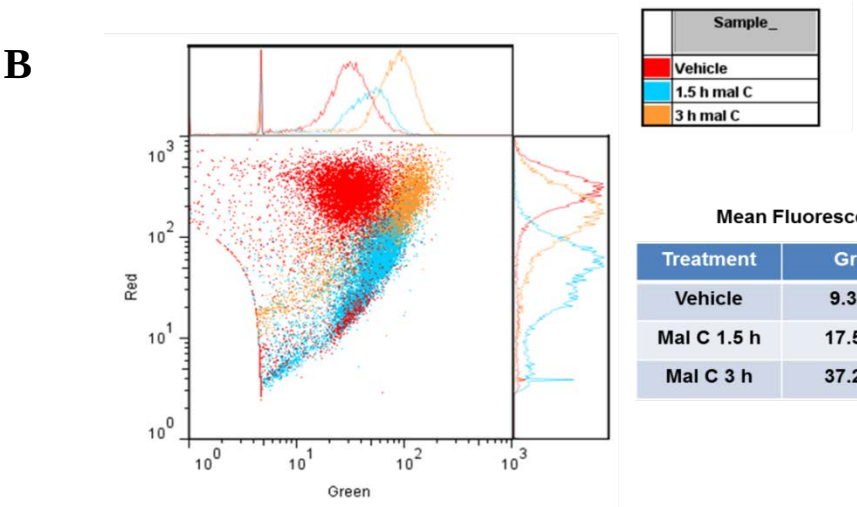

Mean Fluorescence Intensity (MFI)

Treatment	Green	Red
Vehicle	9.3±1.4	186.5±5.4
Mal C 1.5 h	17.5±2.2	21.6±1.8
Mal C 3 h	37.2±3.3	113.8±8.5

Figure 3. 6. 7. Mal C induces LMP in MCF7 cells. (A) Change in cellular morphology by fluorescence microscopy. The MCF-7 cells, stained with AO were incubated for 1.5 and 3 h with mal C (0 and 6 µ M). The AO-stained cells were visualized under a fluorescent microscope. **(B)** Quantification of LMP by flow cytometry. The AO-stained cells were analyzed by flow cytometry. Dot plots of the vehicle and 6 µM mal C (1.5 and 3 h)-treated cells are merged and shown. The adjunct histograms represent the fluorescence intensities in the green and red channels of each treatment. Representative microscopy images are shown. The experiments were repeated thrice with similar results. All determinations were made in three replicates, and the values are means ± SEM.

Next, we examined the release of the cathepsins B and L by immunoblots of the mal C (6 μM)-treated cell extracts. A time-dependent decrease of the pro-cathepsin B expression after 4 h, reaching 50% and 10% of the control value at 4 h and 16 h respectively confirmed cathepsin B release. However, the pro-cathepsin L expression was unaffected by mal C up to 24 h (Figure 3. 6. 8).

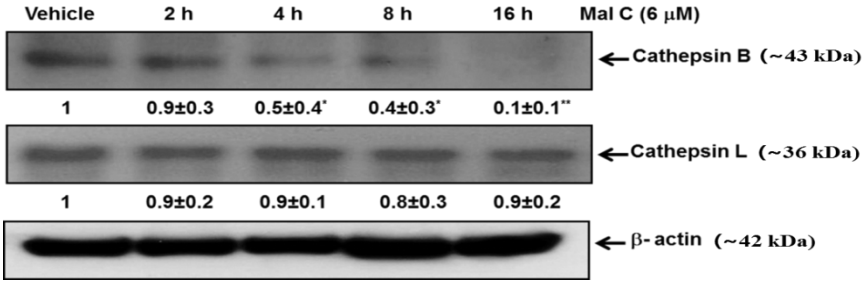

Figure 3. 6. 8. Mal C-induced LMP activates cathepsin B. The MCF-7 cells were incubated for different periods with mal C (0 and 6 μ M). The whole cell extracts were subjected to immunoblotting, using suitable antibodies against AIF and endo G. The experiments were repeated thrice with similar results and the values are means ± SEM. **p*<0.05, ***p*<0.01compared to vehicle control.

Because cathepsin B is known to process BID, we also assessed the effect of mal C on translocation of BID into mitochondria on cleavage to t-BID. A drastic reduction (50%, *p*<0.01) of BID in the whole cell extract was observed at an early time point (2 h) (Figure 3. 6. 9A). This was associated with a significant time-dependent mitochondrial accumulation of BID *viz*.3.5 and 11.5 fold at 4 h and 8 h, compared to that of the vehicle treated control cells (Figure 3. 6. 9B).

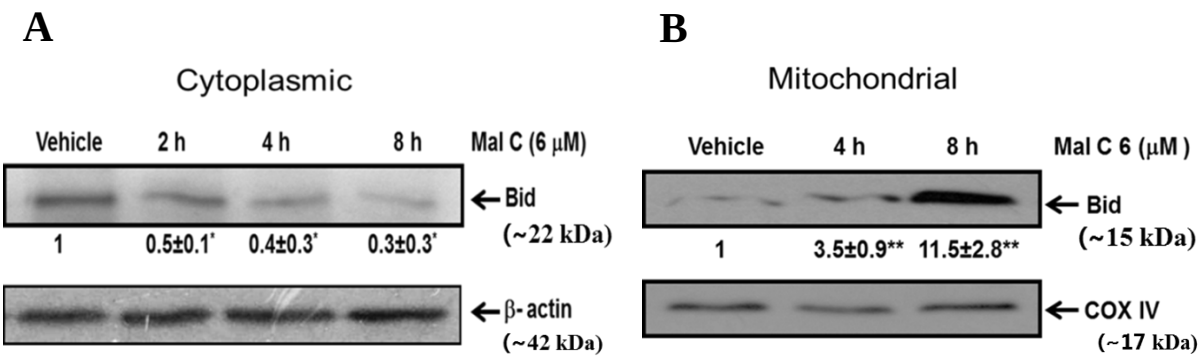

Figure 3. 6. 9. Mal C time-dependently induces BID translocation in MCF-7 cells. BID expressions in whole cell extract **(A)** and mitochondrial fraction **(B)**. The cells were incubated up to 8 h with mal C (0 and 6 μM), the whole cell extracts and the mitochondrial fractions were prepared, and subjected to immunoblotting using asuitable antibody against BID. The experiments were repeated thrice with similar results, and the representative images are shown. The values are means ± SEM. **p*<0.05, ***p*<0.01 compared to respective to vehicle controls.

3. 6. 5. Mal C arrests MCF-7 cells in S and G2-M phases of cell cycle

The cytotoxicity caused by mal C may be due to its antiproliferative and proapoptotic effects. Consequently, the effect of mal C on cell cycle progression was analyzed using flow cytometry in exponentially dividing cultures of MCF-7 cells treated with either vehicle (DMSO) or mal C, and the cell populations in the G0/G1, S, and G2-M phases were calculated. Mal C, dose-dependently caused an accumulation of cells in the S and G2-M phases of the cell cycle (Figure 3. 6. 10A, Table 3. 5). Cyclin E and cyclin A are responsible for S phase progression of cells, we also analyzed the effect of mal C on these cyclins. Our immunoblots showed markedly increased expressions of these cyclins in mal C (6 μM)-treated cells, compared to the control (Figure 3. 6. 10B). Moreover, while cyclin E was augmented at an early stage (2 h), a significant increase in the cyclin A expression was noticed at 8 h.

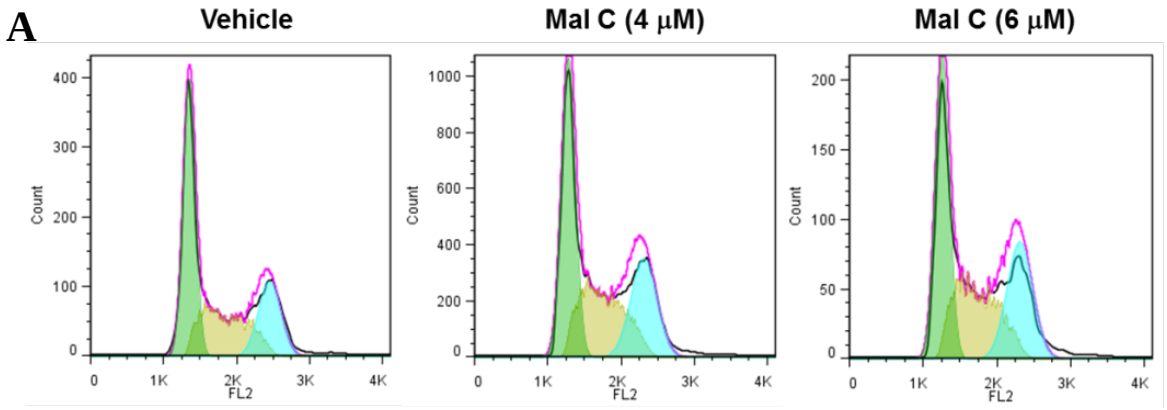

B

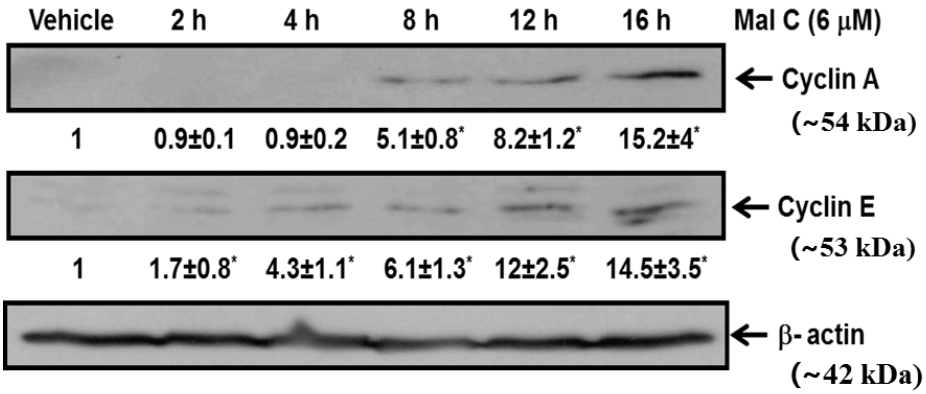

Figure 3. 6. 10. Mal C arrests MCF-7 cells in S and G2-M phase of the cell cycle. (A) Cell cycle analysis (Coloring pattern: G1 - Green, S - Yellow, G2 - Blue). **(B)** Expressions of cyclins A and E. The MCF-7 cells were incubated with mal C (0, 4, and 6 μ M) for 24 h. Twenty thousand cells in each treatment were acquired using a flow cytometer, and the DNA content of the nuclei was registered on a linear scale. Representative images are shown. The experiments were repeated thrice with similar results and the values are means ± SEM. *p<0.01 compared to vehicle control.

Table 3. 5 Mal C-induced changes in cell cycle progression of the MCF-7 cells.

Treatment	Cell population (%)		
	G1	S	G2
Vehicle	48.1 ± 2.8	30.3 ± 2.4	22.0 ± 1.5
Mal C (4 μ M)	44.4 ± 3.1	34.3 ± 2.8	26.4 ± 2.0
Mal C (6 μ M)	42.3 ± 3.0	38.5 ± 2.4 ∗	32.6 ± 2.5 ∗

All determinations were made in three replicates, and the values are means ± SEM. *p<0.05 compared to vehicle control.

3. 7. Thiol harboring antioxidants ameliorates mal C induced apoptosis in lung carcinoma cells

This section deals a novel observation that thiol antioxidants (NAC and GSH) robustly sensitize mal C-induced cell death process. Here, the mechanism by which thiol antioxidants inhibit mal-

C induced survival factors and sequester several transcription factors in the cytoplasm to switch their conventional transcription to death process will be discussed. The role played by S-glutathionylation of transcription factors in the above process will also be highlighted in this chapter.

3. 7. 1. Mal C induces oxidative stress in A549 cells

Previously we reported that mal C generates ROS *in vitro* to cause DNA damage [158]. In the light of above, we probed further to evaluate the possibility of mal C-induced generation of intracellular ROS and subsequent damage to cellular DNA. To assess the mal C induced intracellular ROS generation, we used DCFDA and DHE dyes based flow cytometry and spectrofluorimetry methods. Our result showed that mal C treatment generates ROS in both time (Figure 3. 7. 1A) and concentration dependent manner in A549 cells (Figure 3. 7. 1B). This increase was ~8.4─10.0-fold at 3-6 h with mal C (6 μM), while it was ~3.4─9.6-fold at 3 h with mal C 4-8 μM, compared to vehicle (0.1% DMSO) treated cells. The ROS induction ability of mal C (6 μM) at 6 h was almost equal to that of the positive control, H_2O_2 (25 μM). We further confirmed that the ROS produced by mal C treatment is not merely due to the interaction of mal C with fluorescent probes (Data not shown).

A

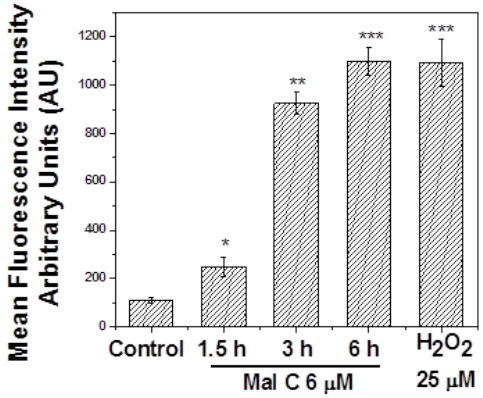

B

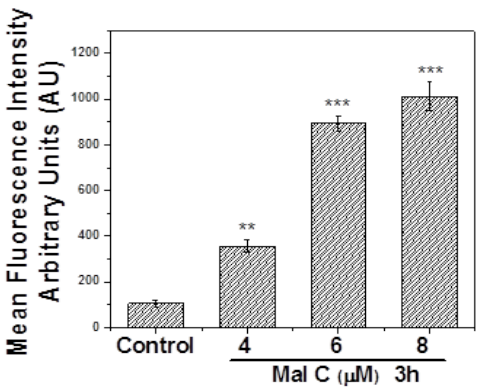

Figure 3. 7. 1. Mal C induces ROS in A549 cells. A549 cells were loaded with DCFDA (20μM) for 20 min before treating with 6 μM mal C for different time points **(A)** and different concentrations of mal C for 3 h **(B)**. After respective time of incubation with mal C, cells were trypsinised, washed and fluorescence was measured spectrofluorimetically. The experiments were repeated three times with similar results. All determinations were made in three replicates, and the values are means ± SEM. **p*<0.05, ***p*<0.01 and ****p*<0.001 compared to vehicle control.

Pretreatment of the cells with intracellular ROS scavengers like NAC, PEG-SOD, PEG-CAT, Sodium Pyruvate, tocopherol, and Trolox® abrogated this increase in ROS level by mal C to 18, 75, 81, 94, 60 and 53% respectively, compared to the mal C (6 μM) treated cells (Figure 3. 7. 2). Since, SOD and catalase enzymes are impermeable to the cells we used pegylated-SOD and –catalase, which are known to enter into the cells. Glutathione depletion is a common phenomenon during apoptosis. It is the most important non-protein thiol, and gets affected with any small change in the redox environment inside the cell. To study the mal C induced changes in the levels of total free thiol content, we used a dye monobromobimane (MBBr), wherein the free GSH content of the cells was found to decrease in time dependent manner after mal C treatment (Figure 3. 7. 3). This mal C-induced GSH depletion was prevented by NAC (5 mM) (Figure 3. 7. 3).

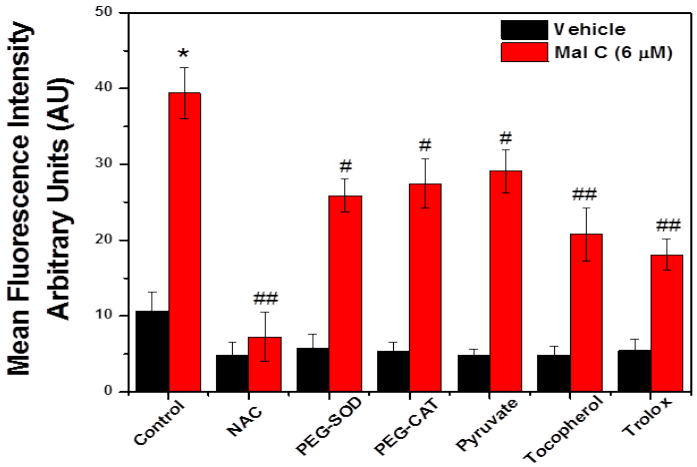

Figure 3. 7. 2. Effect of different antioxidants on mal C-induced ROS generation. The cells were pre-incubated with NAC (5 mM), PEG-SOD (1000 unit/ml), PEG-CAT (3000 unit/ml), Pyruvate (10 mM), tocopherol (100 μM) and Trolox® (100 μM) for 1 h followed by incubation with mal C (6 μM) for 3 h, and the fluorescence measured spectrofluorometrically. All determinations were made in three replicates, and the values are means ± SEM. *p<0.01 compared to vehicle control, $^{\#}p$<0.05, $^{\#\#}p$<0.01 compared to mal C (6 μM) alone treated cells.

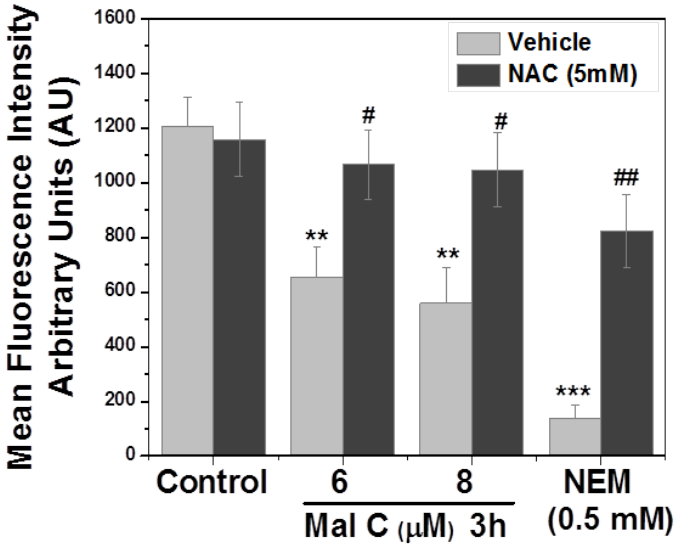

Figure 3. 7. 3. Effect of mal C on Intracellular GSH concentration. A549 cells were incubated with the indicated concentrations of mal C or for 3 h at 37°C. Monobromobimane (final concentration, 40 μM, and 30 min at 37°C) was loaded into cells, and then cells were trypsinized, washed and counted by flow cytometry, cells pretreated with NAC (5 mM) were also processed as indicated above. MFI was calculated through FloMax® software and plotted. The cells treated with NEM served as a positive control. The experiments were repeated three times with similar results. **p<0.01 and ***p<0.001 compared to vehicle, #p<0.05 and ##p<0.01 compared to respective mal C alone treatment.

3. 7. 2. Only thiol antioxidants sensitizes mal C-induced cell death process

It is well known that ROS generation and GSH depletion plays critical role in inducing cell death in cancer cells. To probe the role of ROS in mal C induced cell death process, various antioxidants were included in the mal C treatment protocol. We observed that although all the non-thiol antioxidants (trolox, α-tocopherol) reduced mal C induced ROS

generations but failed to abrogate mal C induced sub-G1 (apoptotic death process) (Figure 3. 7. 2, 3. 7. 4A). Intriguingly, only thiol harboring antioxidants like NAC (a nontoxic precursor of GSH) and GSH ameliorate the cell death process induced by mal C treatment (Figure 3. 7. 4A-C). Moreover, other non-thiol antioxidants e.g., PEG-SOD, PEG-CAT, vitamin C, and sodium pyruvate also did not change mal C induced cytotoxicity (sub-G1 population) in A549 cells. Moreover, the sub-G1 population of the mal C (6 and 8 μM)-treated cells increased by 42 and 37%, and by 40 and 29% respectively due to pretreatment with NAC (5 mM) and GSH (5 mM) respectively (Figure 3. 7. A). However, the non-thiol antioxidants (PEG-SOD, PEG-CAT, Trolox®, Tocopherol, and Pyru-Na) did not change the cytotoxicity (sub-G1 population) of mal C against the A549 cells (Figure 3. 7. A). In corroboration with the sub-G1 results, MTT and clonogenic assay result showed similar role of NAC in enhancing the cell death process in mal C-treated A549 cells. This phenomenon of thiol induced sensitization was dependent on time and concentration of mal C (Figure 3. 7. 4B, C).

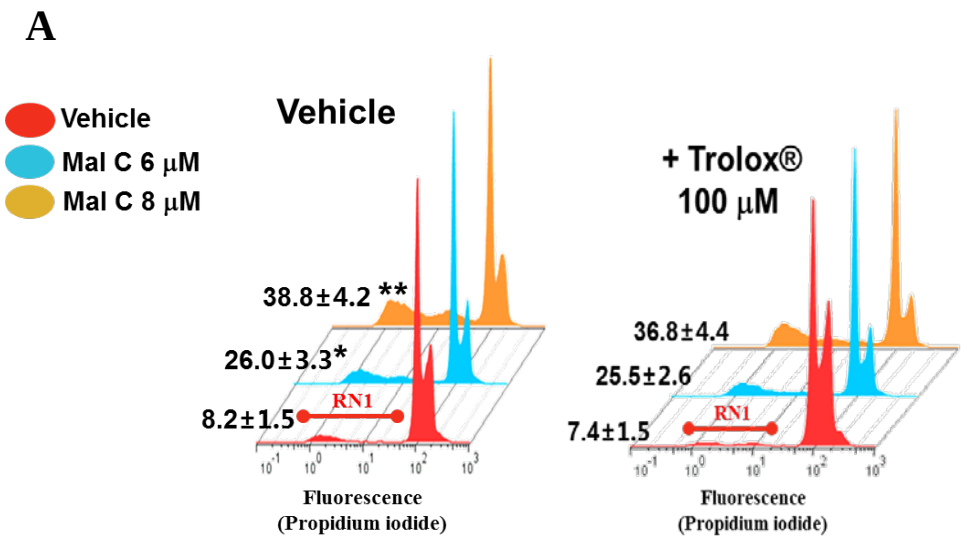

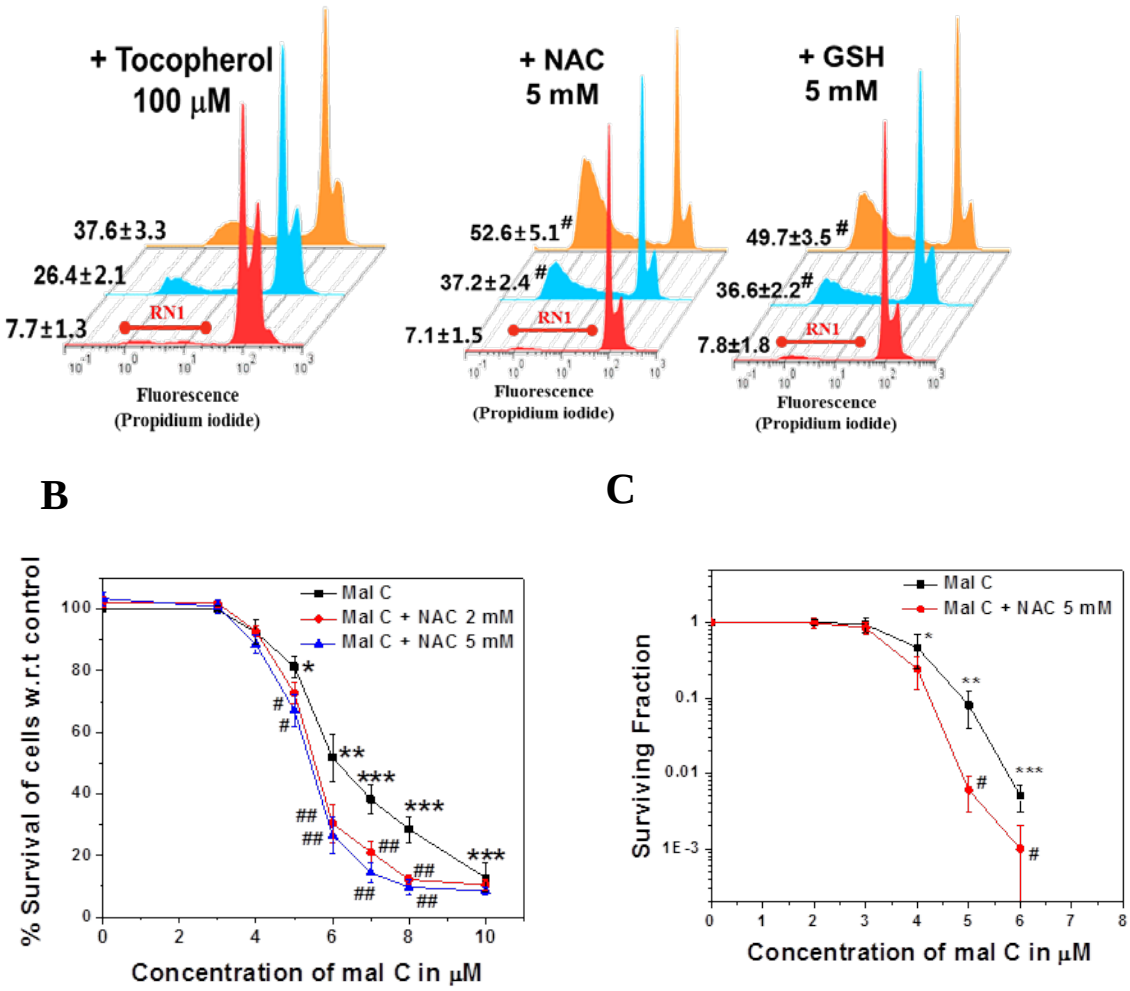

Figure 3. 7. 4. Thiols enhance mal C-induced apoptosis in A549 cells. (A) The cells were pre-incubated with Trolox® (100 µM) or Tocopherol (100 µM) or NAC (5 mM) or GSH (5mM) for 1 h followed by mal C (6 and 8 µM) treatment for 24 h. Twenty thousand cells in each treatment were acquired using a flow cytometer. The Sub-G1 region (RN1) represents the percentage of cells undergoing apoptosis.**(B)** A549 cells (10,000 cells/well), grown in 96-well plates were pre-incubated with NAC (0, 2 and 5 mM) followed by mal C (0-10 µM) treatment for 48h. The cell viability was assessed by the MTT assay and the results are expressed in percentage survival considering that of the vehicle-treated control cells as 100. (B) Clonogenic analysis of mal C and NAC-treated cells. A549 cells (1000 cell/well in 6- well plate) were incubated with NAC (0 and 5 mM) followed by mal C treatment (0-6 µM) for 14 days, colonies were counted and expressed as surviving fraction. The experiment was repeated thrice with similar results and the values are means ± S.E.M. *p<0.05, **p<0.01, **p<0.001 compared to vehicle and #p<0.05 and ##p<0.01 compared to respective mal C treated cells.

To probe the role of extracellular/intracellular interactions of mal C and NAC responsible for the sensitization process, we employed differential treatment timing, cells were pretreated with NAC: 1) for 1 h and washed off subsequently, 2) for 3 h and washed off subsequently, 3) for 3 h and allowed further to present throughout the experiment. In the former two treatment protocols, NAC remained absent extracellularly but it may boost the intracellular levels of thiol antioxidant. In contrast, NAC was available both outside and inside the cells in the third treatment. This was followed by incubation of cells with mal C (6 μM) for 24 h and % sub-G1 population analyses through flow cytometry. We found that, % sub-G1 cell population were 44.8±4.3, 48.7±5.5 and 62.8±5.2% in treatment 1, 2 and 3 respectively, *vis-à-vis* only mal C treated cells (Figure 3. 7. 5). Together, these results suggested that interaction of mal C and NAC at both extracellular and inracelluar levels might be required for the sensitization process.

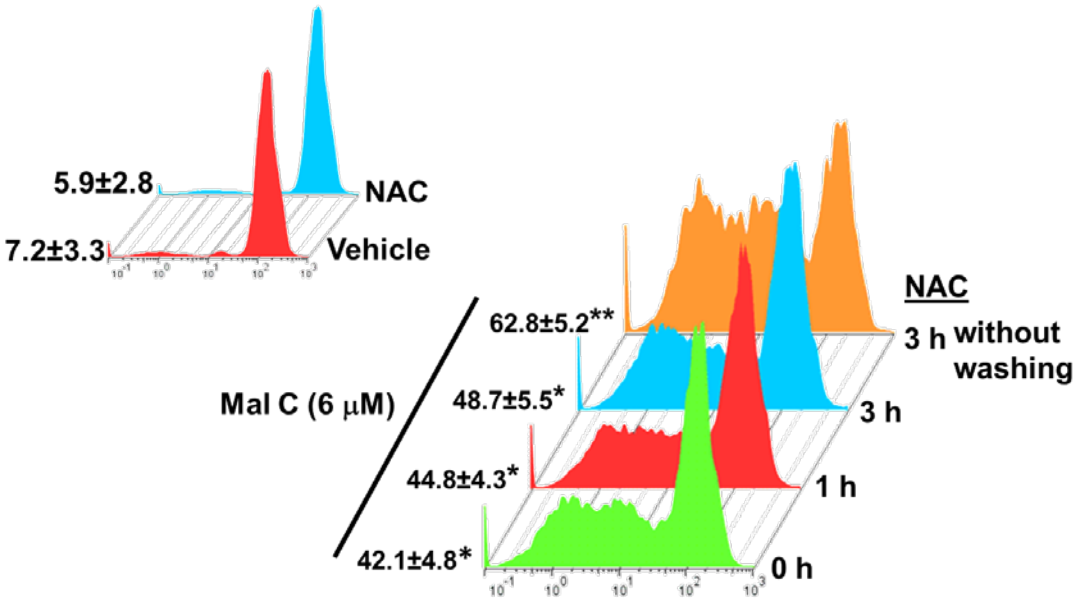

Figure 3. 7. 5. Effects of extracellular and intracellular thiol antioxidants on mal C induced cytotoxicity. A549 cells were pre-incubated with NAC for different time points (0, 1, 3 h), washed with PBS, treated with mal C in the absence or presence of NAC for 24 h, Subsequently, flow cytometry was

carried out to analyse sub-G1 population in different treatment conditions. The experiment was repeated thrice with similar results and the values are means ± S.E.M. *p<0.01, **p<0.001 compared to vehicle treated cells.

Earlier we have found that mal C induced apoptosis is dependent on caspase-3 activation (Figure 3. 1. 5C), here we probed whether thiol-antioxidants mediated sensitization might also be operated through caspase-3 and PARP1 driven apoptosis process. Our results showed that the activity of caspase-3 and PARP1, as measured in terms of their cleavage, was increased in mal C plus NAC/GSH pretreated cells *vis-à-vis* mal C alone treatment (Figure 3. 7. 6A). Further, increase in caspase-3 activity in thiol-antioxidant mediated sensitization process was confirmed by directly analyzing caspase-3 activity (Figure 3. 7. 6B). Since, NAC/GSH induced a significant increase in mal C induced death process; we have taken up further work to explain the mechanistic aspects behind this sensitization process.

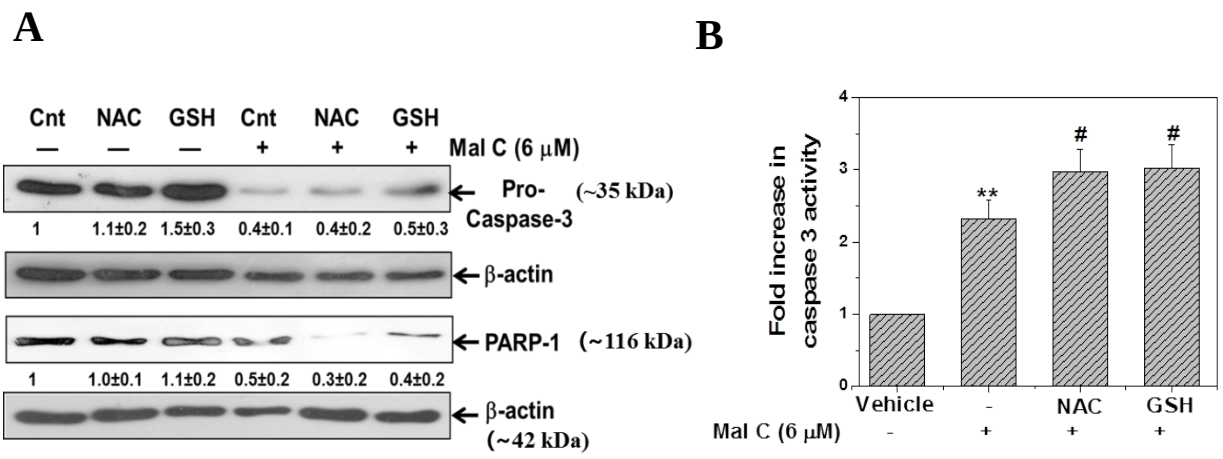

Figure 3. 7. 6. Effect of thiol antioxidants on mal C-induced apoptosis. A549 cells were pre-incubated in the absence or presence of NAC (5 mM) or GSH (5 mM) followed by mal C (6 μM) treatment for 16 h were lysed. **(A)** Caspase-3 and PARP1activation was estimated by western blotting and **(B)** Caspase-3 enzyme activity was measured. All the experiments were repeated three times with similar results, all determinations were made in four replicates, and the values are means ± S. E. M. **p<0.01 compared to vehicle and #p<0.05 compared to respective mal C treated cells.

3. 7. 3. NAC regulates the kinetics of mal C-derived quinone formation that enhances mal C-induced DSBs in A549 cells

To explore NAC mediated hypersensitization mechanism, we hypothesised initially to understand (1) whether mal C undergoes auto-oxidation which might be reversed/recycled in due process by thiol antioxidants and/or (2) whether mal C and thiols are making a stable complex, which might be more toxic *vis-à-vis* mal C itself to the cancer cells. To this end, we pre-incubated the mal C in a media in the absence or presence of NAC for different time points (0, 15, 30, 45, 60 min) and then added onto the cells. Our results showed that pre-incubation of mal C alone led to loss of potential of the mal C to kill the cancer cells. However, presence of NAC in cell free medium during the pre-incubation step of mal C led to the retention of its cell killing potential. These results suggested that the stability of mal C might be increased by NAC either by (1) forming a complex with NAC and/or (2) due to prevention of the auto-oxidation process of mal C by NAC. Further, we employed several methods to study the possibility of mal C-NAC complex formation. Spectrophotometric, HPLC, MS analysis showed no complex formation between these two molecules (data not shown). Alternatively, we tried to see the putative auto-oxidation of mal C and its recycling by NAC. Earlier, mal C induced DNA nicking in the presence of metal ion has been shown to involve the formation of quinone from its catechol moiety [158] (Figure 3. 7. 7A). To analyse the quinone formation from mal C, we recorded the time dependent absorption spectra of mal C in culture medium. Our results showed that catechol moiety in mal C undergo chemical transformation to form quinone form in the culture media, which was evident as quinone specific absorbance at 480 nm increased significantly (Figure 3. 7. 7B) [177]. Further, spectrophotometric study showed that the catechol to quinone conversion, during mal C incubation, was noticed at around 2 min, became prominent at 4 min and reached

the maxima at 6 min (Figure 3. 7. 7B). Co-incubation of mal C with NAC, concentration dependently, delayed the conversion (Figure 3. 7. 7C). Moreover, the peak quinone levels were much less in presence of NAC *vis-à-vis* in its absence. This indicated that catechol form of mal C might be an active form and required for inducing cell death. In mal C treatment alone, it was consumed fast due to oxidation/auto-oxidation process while NAC recycles the oxidized product back to catechol form of the mal C to exert sensitization process in cancer cells.

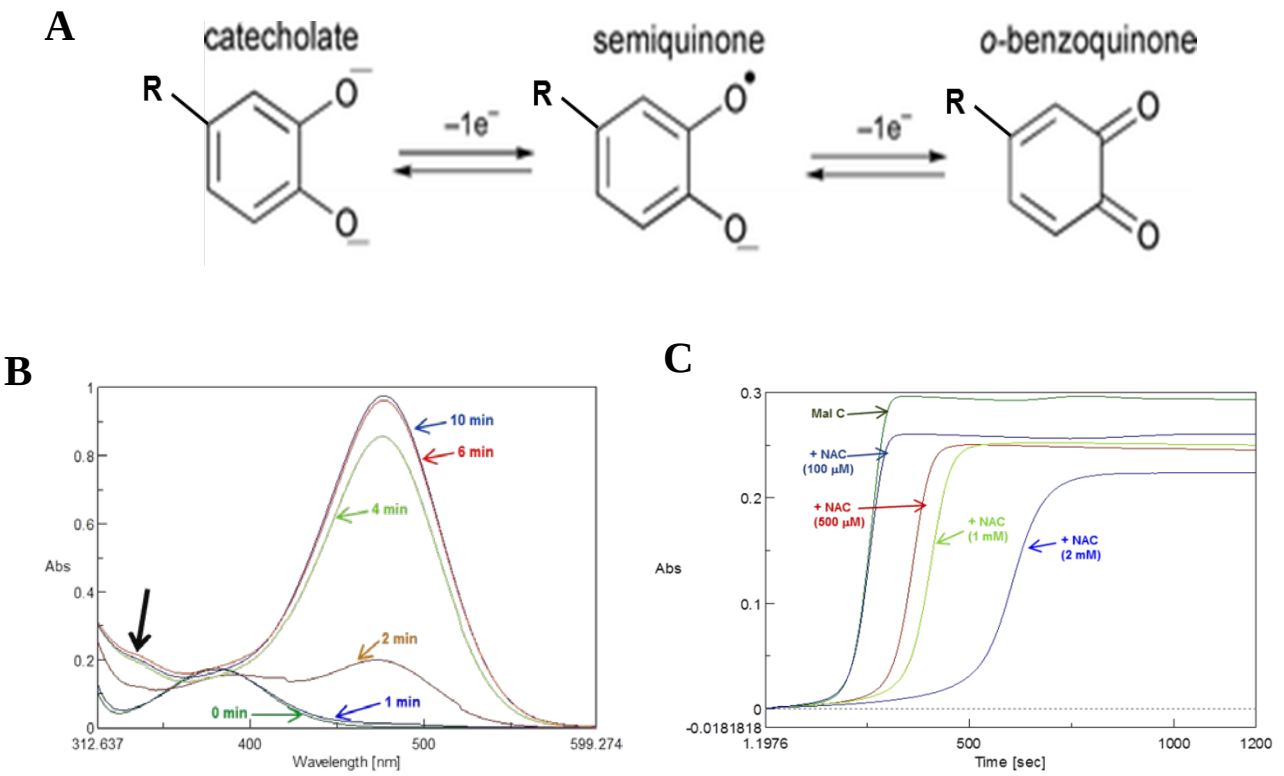

Figure 3. 7. 7. NAC regulates mal C-induced quinone generation. (A) Scheme for conversion of catechol moiety into quinone forms in mal C. "R" represents the rest of the structure in mal C (**B**) Time dependent oxidation of mal C to generate quinone form. Mal C (10 µM) was incubated in DMEM medium for different time periods (0, 1, 2, 4, 6 and 10 min). The absorption spectra of each sample were read spectrophotometrically with λ_{max} at 480 nm. **(C)** Effect of NAC on the mal C auto-oxidation process. Mal C (10 µM) in DMEM media was incubated in the absence or presence of NAC (100 µM-2 mM) and the absorption spectra was recorded for 20 min.

After confirming the recycling of mal C by NAC in cell free system, we sought to know whether NAC mediated recycling of mal C might be responsible for generating varied amount of ROS in different cellular compartments. Confocal microscopy of the DHE-stained cells revealed that mal C alone time-dependently increased DHE-fluorescence (superoxide radical) in the cells. This was significantly increased by NAC (5 mM) treatment (Figure 3. 7. 8). Intriguingly, our results showed that mal C-induced superoxide generation was several fold higher in the nucleus *vis-à-vis* cytoplasmic compartment. Moreover, NAC treatment further enhanced the DHE fluorescence time dependently in the nuclear compartment vis-à-vis cytoplasmic compartments (Figure 3. 7. 8). These results, along with our previous findings that mal C can bind with DNA in cells, suggested that NAC recycles mal C accumulated in the nucleus to generate copious amounts of ROS in the nuclear compartment.

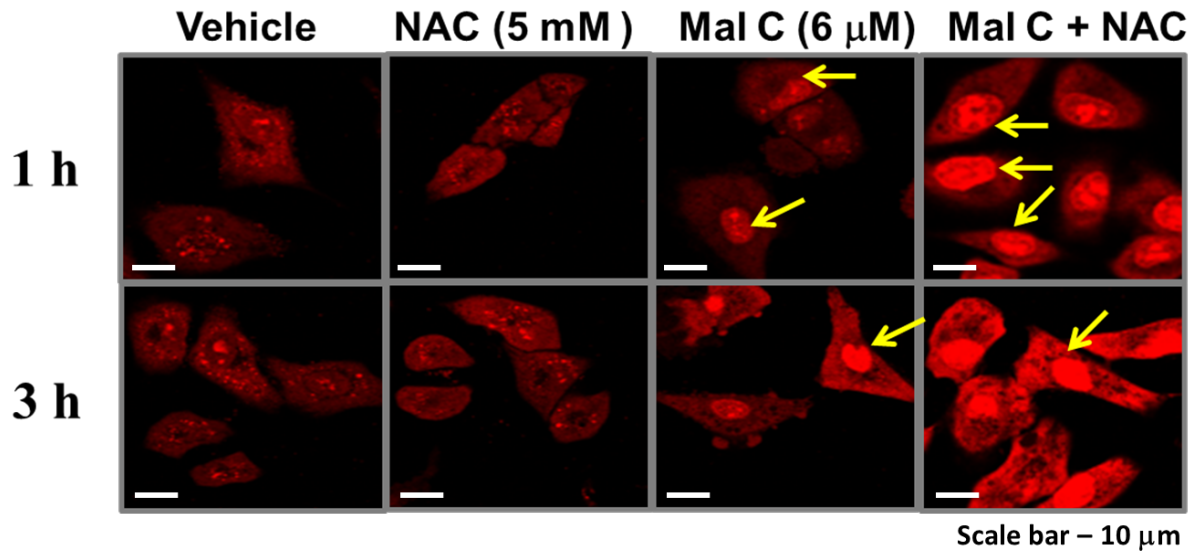

Figure 3. 7. 8. Effect of NAC on nuclear ROS induced by mal C. A549 cells pre-incubated with DHE dye (5 μM) for 30 min were treated with mal C (6 μM) or NAC (5 mM) or in combination for 1 and 3h. After respective times, cells were washed with PBS, fixed with 1% paraformaldehyde for 10 min, permeabilized with PBS containing 0.5% Triton X-100 for 30 min and then visualized under confocal microscope. Arrows marked in the images points towards higher nuclear ROS. Bar graph showed the

quantification of red fluorescence in the nucleus through imageJ software. Time points are missing in the figures

Beside a chemical basis of NAC mediated sensitization (mal C recycling and higher ROS generation in nucleus), we further sought to know whether thiol antioxidants are also involved in perturbing the cellular signalling events to exacerbate mal C induced death process. The neutral comet assay results showed that, NAC (5 mM) pretreatment increased olive tail moments by 25.8 and 33.6% after 3 h in response to mal C treatment (4 and 6 μM) (Figure 3. 7. 9A). Similarly, the NAC (5 mM) pre-incubation followed by mal C (6 μM) treatment led to further time dependent increase in the levels a DSB marker i.e. γH2AX in the cells *vis-à-vis* mal C treatment alone (Figure 3. 7. 9B).

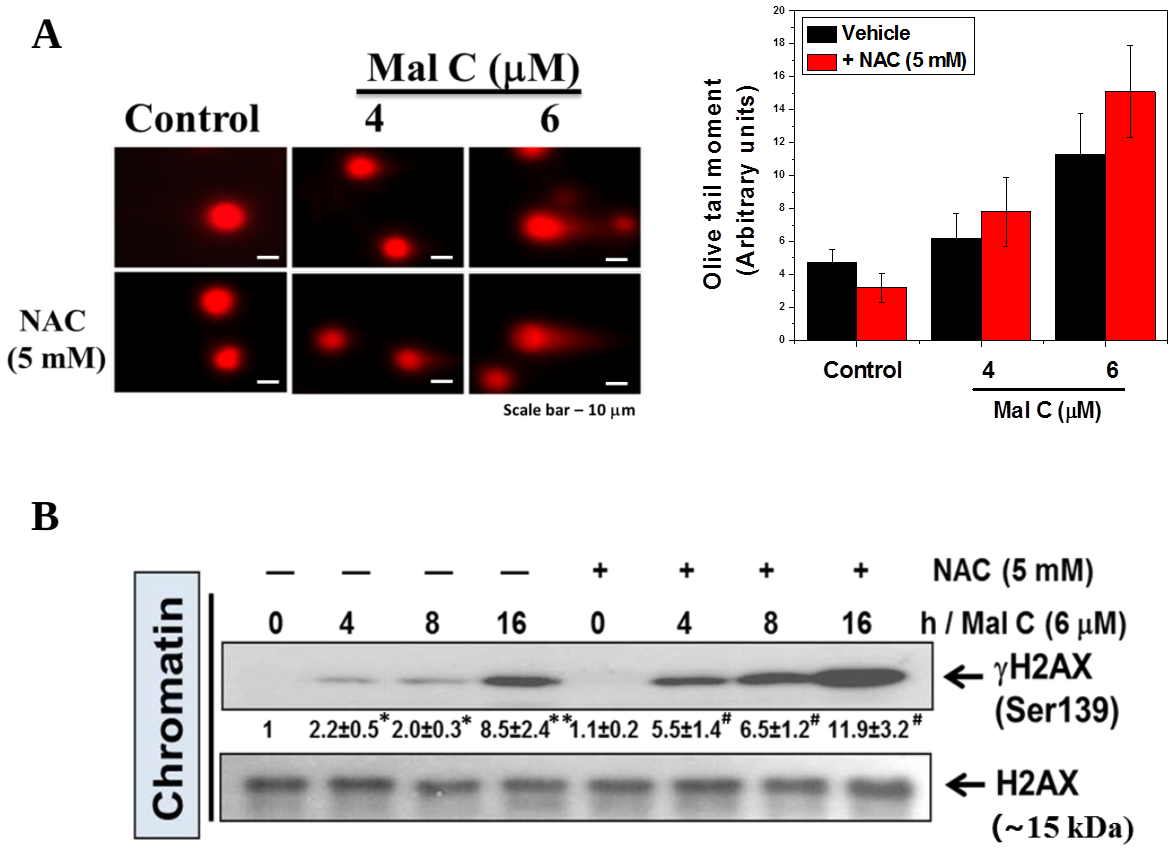

Figure 3. 7. 9. Effect of NAC on mal C-induced DNA double strand breaks (DSB) formation in the cancer cells. (A) A549 cells were incubated with NAC (0 and 5 mM) followed by mal C

treatment (0, 4 and 6 μM) for 3 h, Cells were then processed for neutral comet assay as described in materials & methods. **(B)** Effect of NAC on mal C-induced γH2AX formation. The cells pre-incubated with NAC (0 and 5 mM) followed by mal C treatment (6 μM) for 0–16 h were lysed and processed for chromatin extraction and analyzed for γH2AX through immunoblotting. All the experiments were repeated three times with similar results, and representative images are shown. All determinations were made in four replicates, and the values are means ± SEM. *p<0.05, **p<0.01 compared to vehicle control and #p<0.05 compared to respective mal C treated cells.

3. 7. 4. NAC-Sensitization to mal C induced death process in the presence of NAC is independent of ATM and CHK1

Previously, we have also shown a critical axis of signalling i.e., ATM-CHK1-p38 MAPK pathway in mal C induced cell death process. Further, we sought to know whether NAC mediated sensitization to mal C-induced death process might be due to hyper-activation of ATM-CHK1-p38 MAPK pathway. Contrary to other findings, neither NAC incubation caused further increase in phosphorylation nor did it prolong the activation of ATM and CHK1proteins in response to mal C treatment (Figure 3. 7. 10A, B). However, NAC pre-incubation induced time-dependent increase in p38 MAPK activation in the mal C-treated cells (Figure 3. 7. 10A B). Further, we used ATM-WT and ATM-KD A549 cells (with depleted ATM) and quantified the mal C (6 and 8 μM)-induced sub-G1 in the presence and absence of NAC (5 mM) (Figure 3. 7. 10C). Treatment with mal C alone caused increase in cell death, which was significantly reduced in ATM-KD cells. This result, as shown previously, suggests a role of ATM in death process (compare ATM-WT *vs* ATM-KD group, Figure 3. 7. 10D). Further mal C treatment in the presence of NAC increased apoptosis in ATM-WT cells (compare ATM-WT *vs* ATM-WT, NAC group) and ATM-KD cells (compare ATM-KD *vs* ATM-KD, NAC group) (Figure 3. 7. 8D). However, depletion of ATM in ATM-KD cells led to less sensitization in mal C plus NAC treatment (compare ATM-WT, NAC *vs* ATM-KD, NAC group) (Figure 3. 7. 10D). All these results indicated that ATM plays a critical role in both mal C-alone and mal C plus NAC induced death process.

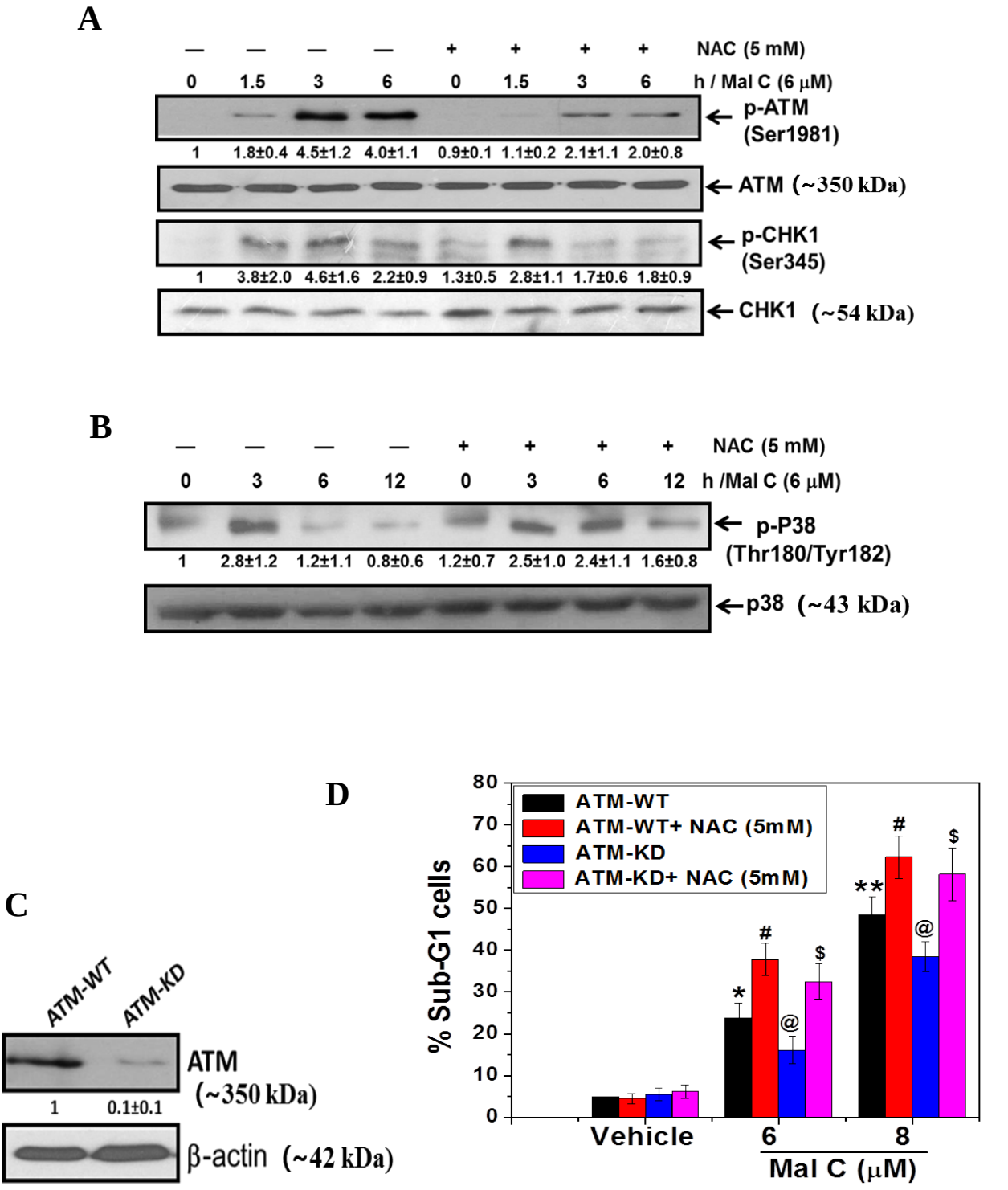

Figure 3. 7. 10. Role of ATM-CHK1 axis in NAC-mediated sensitization to mal C-induced cell death process. (A) NAC down-regulates mal C-induced activation of ATM and CHK1. The cells were pre-incubated with NAC (0 and 5 mM) followed by mal C treatment (6 μM) for different time points (1.5, 3 and 6 h), the lysate was analyzed for p-ATM and p-CHK1 levels by immunoblotting. **(B)** NAC treatment prolonged p38 activation induced by mal C. The whole cell

lysate of the cells pre-incubated with NAC (0 and 5 mM) followed by mal C treatment (6 μM) for different time points (3, 6 and 12`h) was analyzed for p-p38 level by immunoblotting. **(C)** ATM expression level in A549-WT and A549-ATM-KD cells. Cell lysates were prepared from the respective cells and ATM level was analyzed by western blotting. **(D)** The cells pre-incubated in the absence or presence of NAC (5 mM) followed by mal C treatment (6 and 8 μM) for 24 h were stained with PI and then acquired using flow cytometer. The Sub-G1 region representing the percentage of cells undergoing apoptosis was plotted in the form of bar graph. The experiments were repeated three times with similar results. All determinations were made in three replicates, and the values are means ± SEM. *p<0.01, **p<0.001 compared to vehicle control. #p<0.05 compared to respective mal C treatment, @p<0.05 compared to respective mal C treatment in A549-WT cells. \$$p$<0.05 compared to respective mal C treatment in A549-WT + NAC cells.

3. 7. 5. Thiol antioxidants modulate prosurvival and death factors signalling in mal C induced death process

Although many anti-tumor agents like camptothecin (CPT), a topoisomerase I inhibitor, ionising radiation (IR), doxorubicin, VP-16 kill cancer cells very effectively these agents are also known to activate pro-survival factors induced resistance. Amongst the pro-survival and death inducing factors, p53, NF-κB, c-FOS, cMYC, JAK-STAT transcription factors modulate the expression of several anti-apoptotic and apoptotic proteins in response to DNA damaging cancer therapeutics [9,178,179]**.** The outcomes of therapeutics mostly depend on the balance and switching between pro-survival and apoptotic signaling [83]. It is of interest to understand whether NAC plays any role in modulating mal C induced activation of death and pro-survival pathways, if any, to sensitize cancer cell death process. Initially, we sought to probe parallel activation of various pro-survival or anti-apoptotic pathways, in terms of accumulation of respective regulating transcription factors in nuclear fraction, in response to mal C treatment. Two positive controls, CPT and IR treatment, were also included in the study (Figure 3. 7. 11A). We observed that mal

C (6 μM) treatment caused an early increase in the nuclear levels of p53, cFOS and p65-Nf-κB (4-8 h), delayed increase in the expression of STAT3 (at 16 h) and no change in cMYC expression (Figure 3. 7. 11A). Next, we studied the effect of NAC (5 mM) on the mal C-induced nuclear localization of the above transcription factors. NAC treatment did not significantly alter mal C-induced nuclear accumulation of STAT3 and cFOS (Figure 3. 7. 11B, data not shown). Intriguingly however, NAC time dependently reduced the nuclear translocation of p65 and p53 proteins (Figure 3. 7. 11B).

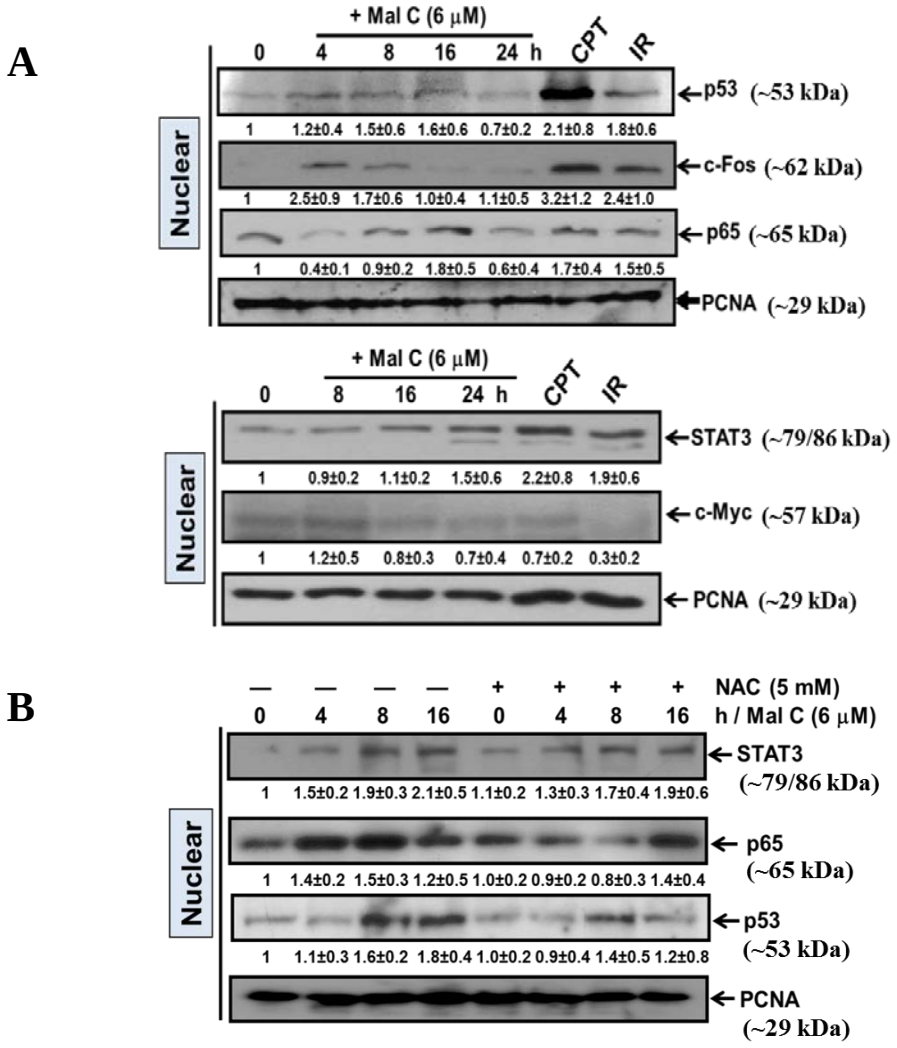

Figure 3. 7. 11. Thiol antioxidants modulate nuclear accumulation of transcription factors in mal C induced death process. **(A and B)** The cells treated for different time points (0-24 h)

with mal C (6 μM) or 3 h with camptothecin (CPT, 1 μM) and Ionising radiation (IR, 5 Gy) were lysed and their nuclear lysates was analyzed by immunoblotting. PCNA was used as loading control for nuclear lysate. The experiments were repeated three times with similar results, and representative images are shown. The values are means ± SEM.

3. 7. 6. NAC perturbs mal C induced nuclear translocation and activation of p65 and p53 proteins

Above results clearly indicated that mal C treatment causes accumulation of p53 and NF-κB, which was down regulated in the presence of NAC. Further we sought to know how thiol antioxidants modulate the apoptosis/survival function of various transcription factors. It might be possible that thiol antioxidant reduces the expression of these transcription factors which led to decreased expression of transcription regulated down-stream proteins. Alternatively, thiol antioxidants induce S-glutathionylation of these transcription factors affecting their nuclear translocation and transcription process. Imperatively, unwarranted accumulation of nuclear factors in cytoplasm may elicit death signaling pathways [180].

To this end, we analysed effects of NAC on mal C induced expression levels of p53 and p65 in whole cell extracts (WCE) and localization of these two proteins in cytosolic, nuclear and chromatin fractions. The immunoblot analysis revealed that mal C treatment increased the p65 expression by 1.5 fold vis-à-vis untreated cells. However, mal C-induced increase in p65 levels was only marginally reduced by NAC treatment (Figure 3. 7. 12A). P65 proteins remains in bound form with IκBα in cytoplasm and the later was degraded to release and translocate p65 to the nucleus during activation. Interestingly, mal C treatment time dependently increased degradation of IκBα protein, which was almost completely inhibited by NAC co-treatments (Figure 3. 7. 12A). To exert pro-survival effects through transcription, p65 subunit binds to promoter sites of the nuclear DNA. We observed that mal C induced a time dependent increase

in nuclear accumulation and concurrent chromatin binding of p65 up to 16 h while it was significantly reduced in the presence of NAC (Figure 3. 7. 12A). Further, our confocal microscopy result also showed a significant amount of p65 localization in nuclei after mal C treatment which was abrogated in the presence of NAC (Figure 3. 7. 12B). Moreover, NAC inhibited one of the NF-κB regulated gene i.e., XIAP (X chromosome-linked inhibitor of apoptosis protein), an inhibitor of caspases 3, 7 and 9 by 58%, compared to mal C alone treatment at 16 h (Figure 3. 7. 12C) [92]. Together, these results indicated that NAC mediated sensitization in cancer cells, in response to mal C treatment, might be modulated through suppressing IκBα degradation, p65 nuclear translocation and its subsequent transcriptional role.

A

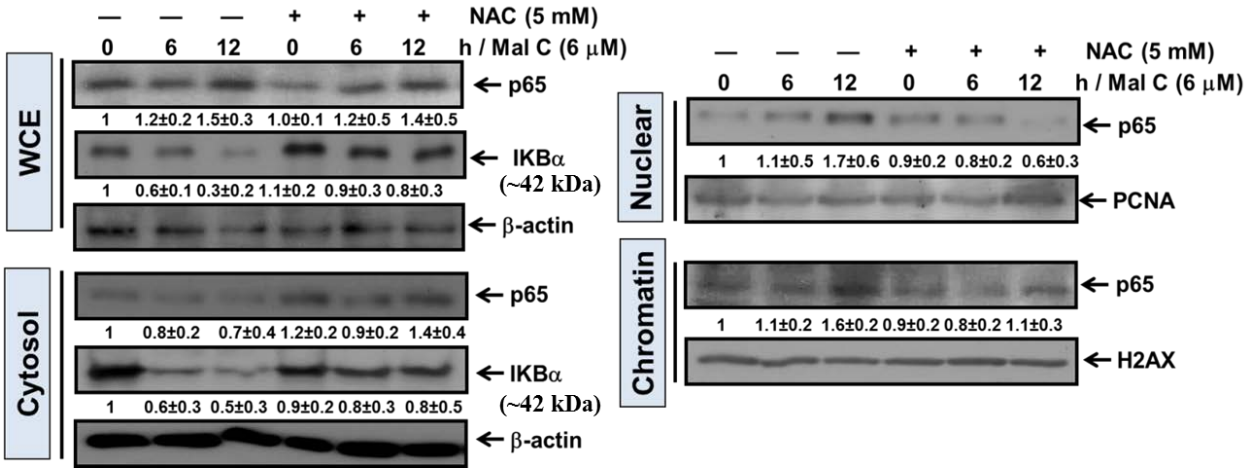

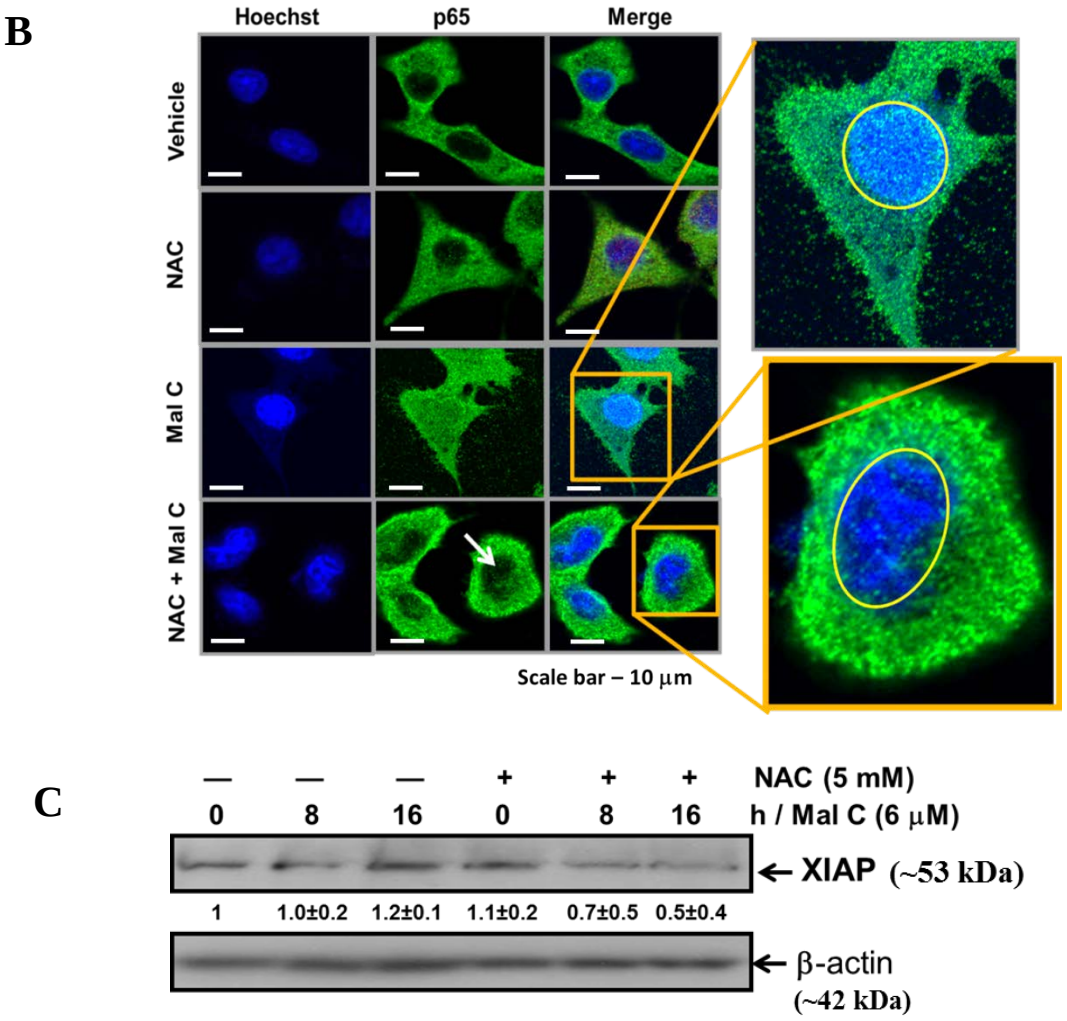

Figure 3. 7. 12. NAC induces cytoplasmic accumulation of p65 protein in response to mal C treatment. (A) Expression profile of proteins in the whole cell, cytoplasmic, nuclear and chromatin extracts. The cells pre-incubated in the absence or presence of NAC (5 mM) followed by mal C treatment (6 μM) in the continued absence or presence of NAC for 0-12 h. Cell extracts were analysed for various proteins by immunoblotting. The experiments were repeated three times with similar results, and representative images are shown. The values are means ± SEM. **(B)** Confocal microscopy showing cytoplasmic accumulation of p65 protein. The cells pre-incubated without or with NAC (5 mM) followed by mal C treatment (6 μM) for 12 h were probed with p65 antibody. P65 and nucleus was stained with Alexafluor-488 (green) and DAPI (blue). Arrow indicates for the expression/localization of p65 proteins in nucleus of A549 cells after respective treatment. The experiments were repeated three times with similar results, and representative images are shown. **(C)** The A549 cells were incubated in the absence or presence of NAC (5 mM) followed by mal C treatment (6 μM) for 0-16 h were lysed and they were analysed for expression of indicated proteins by immunoblotting. The experiments

were repeated three times with similar results, and representative images are shown. The values are means ± SEM.

Mal C (6 μM) treatment also caused a time dependent increase in the expression and phosphorylation lavels in p53 protein in A549 cells (Figure 3. 7. 13A). Interestingly, NAC treatment time dependently increased p53 expression while p53 phosphorylation level was reduced in response to mal C treatment (Figure 3. 7. 13A). Similar to p65 protein, mal C induced p53 accumulation in the cytoplasm of the NAC-pretreated cells, this increase was 67% at 12 h when compared mal C alone (Figure 3. 7. 13A). Beside, p53 protein in nuclear fraction of mal C treated cells decreased by 42% with NAC pre-incubation, while this decrease was 40% in the chromatin fraction, mal C (6 μM, 12 h) treated cells (Figure 3. 7. 13A). Further, confocal microscopy confirmed above results, wherein vehicle treated cells showed p53 localization into the cytoplasm and after 12 h of mal C treatment, p53 protein translocate to nucleus of A549 cells (Figure 3. 7. 13B). In contrast, NAC treatment caused severe reduction of p53 nuclear localization with a concurrent increase in the cytoplasm (Figure 3. 7. 13B). Moreover, p21 (a transcriptionally regulated target protein of p53, helping in cell cycle arrest and hence survival) expression decreases by 45% and 48% after 8 h and 16 h of mal C plus NAC treatment *vis-à-vis* mal C treatment alone (Figure 3. 7. 13C)

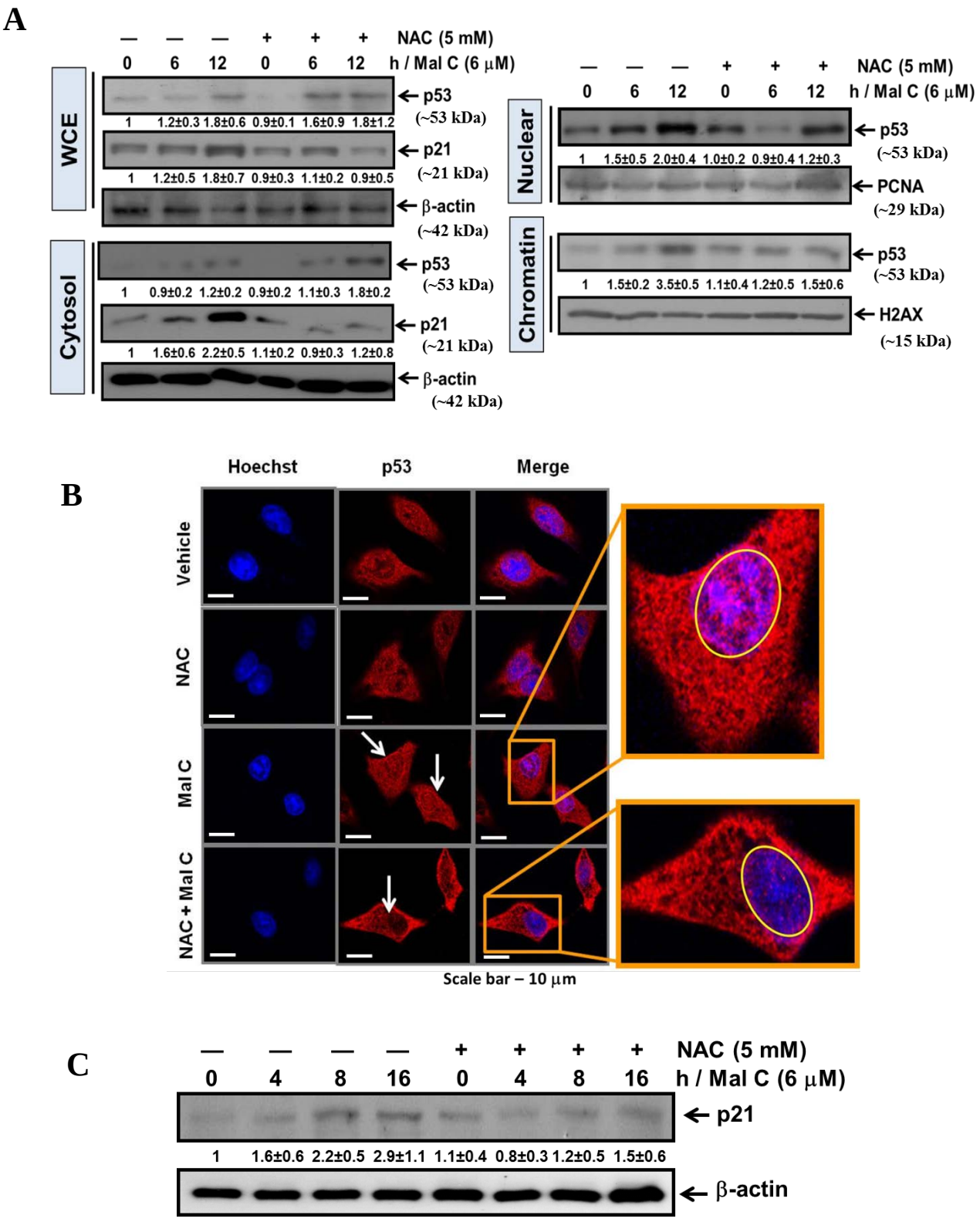

Figure 3. 7. 13. NAC induces cytoplasmic accumulation of p53 protein in response to mal C treatment. (A) Expression profile of proteins in the whole cell, cytoplasmic, nuclear and chromatin extracts. The cells pre-incubated in the absence or presence of NAC (5 mM) followed by mal C treatment

(6 μM) in the continued absence or presence of NAC for 0-12 h. Cell extracts were analysed for various proteins by immunoblotting. **(B)** Confocal microscopy showing cytoplasmic accumulation of p53 protein. The cells pre-incubated without or with NAC (5 mM) followed by mal C treatment (6 μM) for 12 h were probed with p53 antibody. P53 and nucleus was stained with Alexafluor-595 (red) and DAPI (blue). Arrow indicates for the expression/localization of p53 proteins in nucleus of A549 cells after respective treatment. The experiments were repeated three times with similar results, and representative images are shown. **(C)** The A549 cells were incubated in the absence or presence of NAC (5 mM) followed by mal C treatment (6 μM) for 0-16 h were lysed and they were analysed for expression of indicated proteins by immunoblotting. The experiments were repeated three times with similar results, and representative images are shown. The values are means ± SEM.

3. 7. 7. NAC treatment enhances S-glutathionylation of p65 and p53 proteins in response to mal C treatment

Activity of transcription factors like p65-NFkB and p53 can be regulated (inhibited) by S-glutathionylation (p65-SSG, p53-SSG) [92]. We too probed whether NAC dependent down-regulation of mal C-induced p53 and p65-NF-kB proteins involve S-glutathionylation. With the help of western blotting, initially we quantified global protein S-glutathionylation status of mal C-treated A549 cells in the presence and absence of NAC. During cell lysis and extract preparation, NEM (10 mM) was added to block free thiols and prevent alterations in thiol-disulfides [181]. Control cells (vehicle treated) were found to have a significant level of multiple proteins S-glutathionylations, which reduced time dependently with mal C-treatment (Figure 3. 7. 14). In contrast, NAC pre-incubated cells retained S-glutathionylation of multiple proteins even after mal C-treatment (Figure 3. 7. 14).

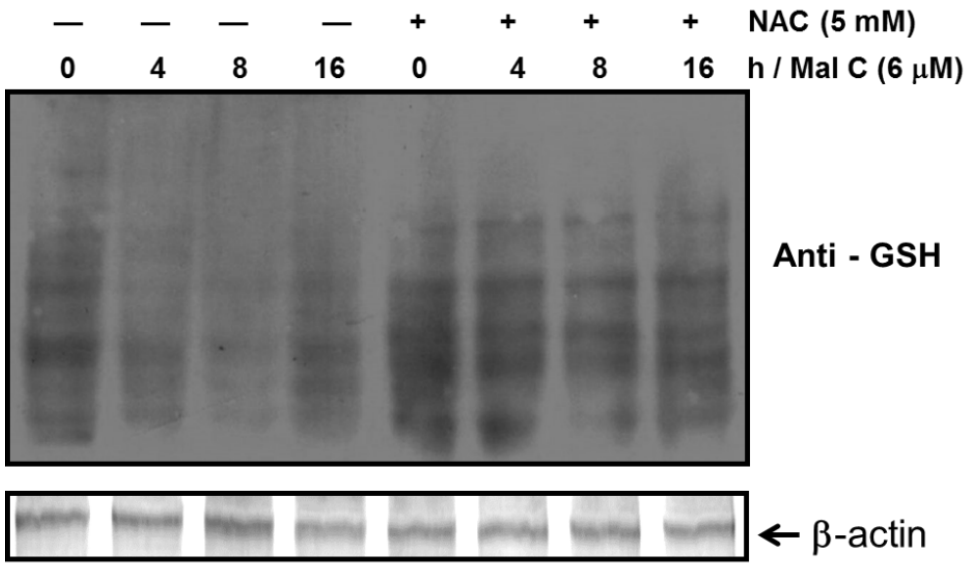

Figure 3. 7. 14. Effects of NAC on global protein S-glutathionylation in mal C treatment. The A549 cells pre-incubated without or with NAC (5 mM) followed by mal C treatment (6 μM) 0-16 h were were lysed in the presence of NEM (10 mM) to block free thiols and prevent alterations in thiol-disulfides. Lysate was boiled and subjected to SDS/PAGE under non-reducing conditions (-DTT) before detecting with anti-glutathione antibody.

For quantifying p53 and p65 proteins glutathoinylation, cytoplasmic lysates of mal C and NAC treated cells were subjected to nonreducing immunoprecipitation (-DTT, IP) using anti-p65 and anti-p53 antibody (IP: p65, IP: p53) respectively. After mal C treatment (6 μM, 8 h), glutathionylation of both p65 and p53 was reduced but in the presence of NAC, it increased ~2.3 and ~3 folds for p65 and p53 respectively (Figure 3. 7. 15A, B). These results suggested that mal C-induced p53 and p65 proteins might undergo S-glutathionylation in the presence of NAC. To validate above modification as glutathionylation, we used DTT (50 mM) as reducing agent during immune-precipitation protocol. Our results showed that mal C plus NAC-induced p65 glutathionylation was reversed in the presence of DTT (Figure 3. 7. 15C) [182].

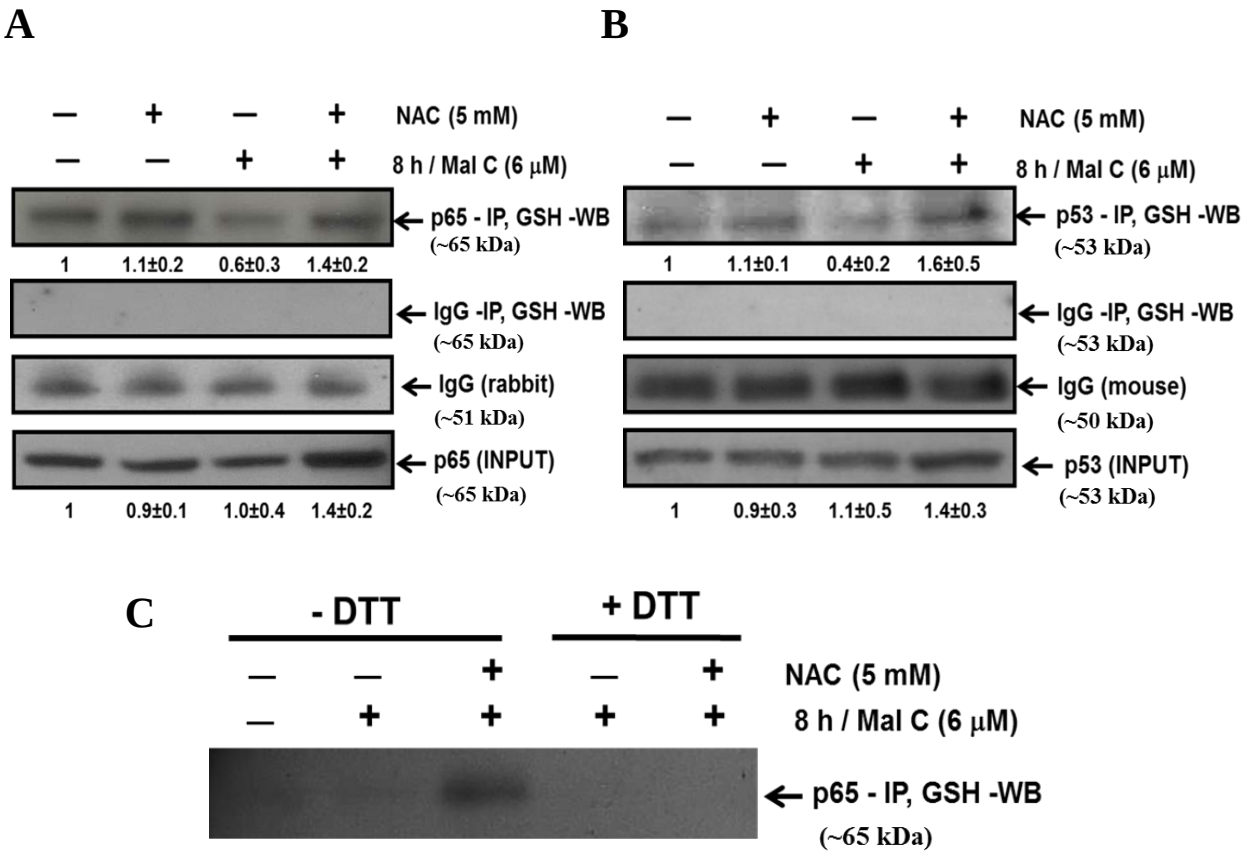

Figure 3. 7. 15. NAC induces S-glutathionylation of p65 and p53 proteins in mal C treatment. (A and B) The cytoplasmic extract of the cells pre-incubated without or with NAC (5 mM) followed by mal C treatment (6 μM) for 8 h was subjected to non-reducing IP (-DTT) using anti-p65 and anti-p53 antibody (IP: p65, IP: p53) before detecting glutathionylated proteins through western blotting using anti-glutathione antibody. **(C)** Cells were treated and IP was done in similar manner as in A except that IP solution was boiled in the presence of DTT to destabilize the p65and GSH interactions. The experiments were repeated four times with similar results. All determinations were made in three replicates, and the values are means ± SEM.

3. 7. 8. NAC induced accumulation of cytoplasmic p53 further translocates to mitochondria and releases death factors in response to mal C treatment

Cytoplasmic p53 has been shown to directly/indirectly trigger apoptosis by inducing proapoptotic BCL-2 family members [86,180,183]. In this hindsight, we quantified p53 in the mitochondrial extract of mal C-treated A549 cells in the presence/absence of NAC. As shown in

Figure 3. 7. 16A, we observed a higher accumulation of p53 protein (38% higher) in the mitochondria of mal C+NAC-treated-A549 cells *vis-à-vis* mal C treatment alone. In corroboration with this, a further decrease in cytosolic concentration of BAX protein was found with mal C + NAC treatment *vis-à-vis* mal C treatment alone (Figure 3. 7. 16B). In order to see whether NAC induced translocation of p53 into mitochondria linked to mitochondrial mediated release of cytochrome C and increase in caspase 9 activity, we used A549-WT (expressing scrambled shRNA) and A549-p53-KD cells (expressing shRNA vs p53 mRNA) to investigate release of death factors from mitochondria (Figure 3. 7. 16C). In A549-WT cells, NAC and mal C co-treatment increased the release of cytochrome c by 62% *vis-à-vis* mal C treatment alone (Figure 3. 7. 16D) while in A549-p53-KD cells, combination treatment caused only a marginal increase in cytochrome c release as compared to mal C treatment alone (Figure 3. 7. 16D). Moreover, our results showed that caspase-9 activity was also found to increase in the presence of NAC *vis-à-vis* mal C treatment alone. In contrast, caspase-9 activity increase was only marginal in mal C plus NAC treatment *vis-à-vis* mal C treatment alone in A549-p53-KD cells (Figure 3. 7. 16E), confirming the role of p53 in inducing caspase-9 activity through MPT formation. Together, this suggested that NAC plus mal C treatment enhances p53 translocation to mitochondria, leading to MPT formation, cytochrome c release into the cytoplasm and caspase-9 activation.

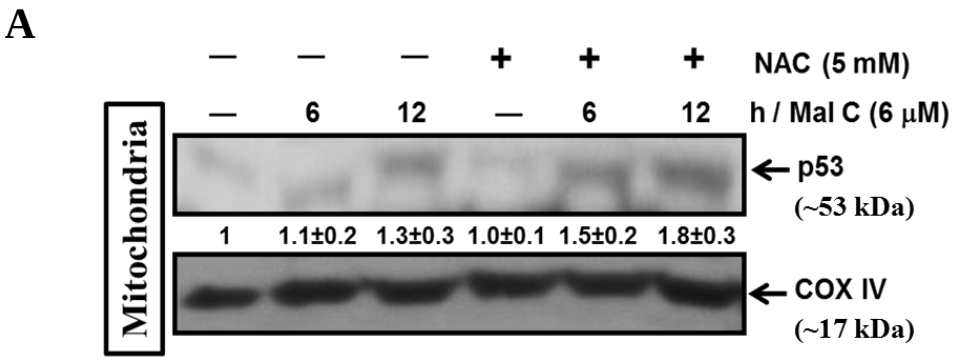

B

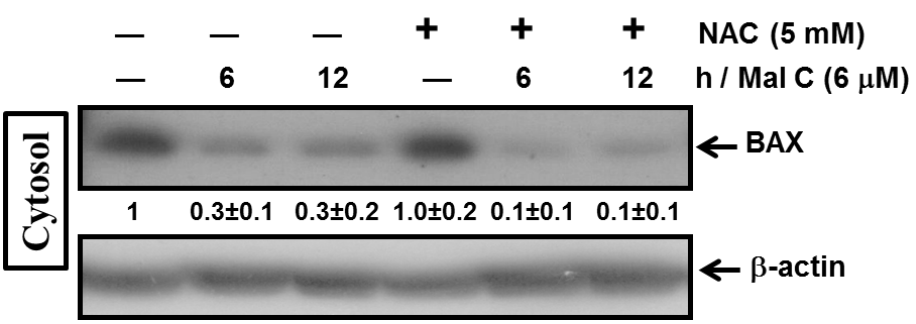
— — — + + + NAC (5 mM)
— 6 12 — 6 12 h / Mal C (6 μM)
Cytosol
BAX
1 0.3±0.1 0.3±0.2 1.0±0.2 0.1±0.1 0.1±0.1
β-actin

C

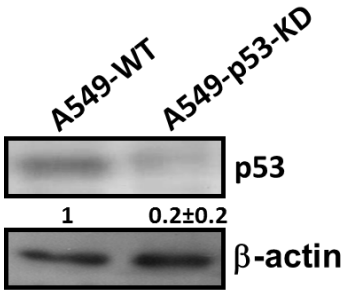
A549-WT
A549-p53-KD
p53
1 0.2±0.2
β-actin

D

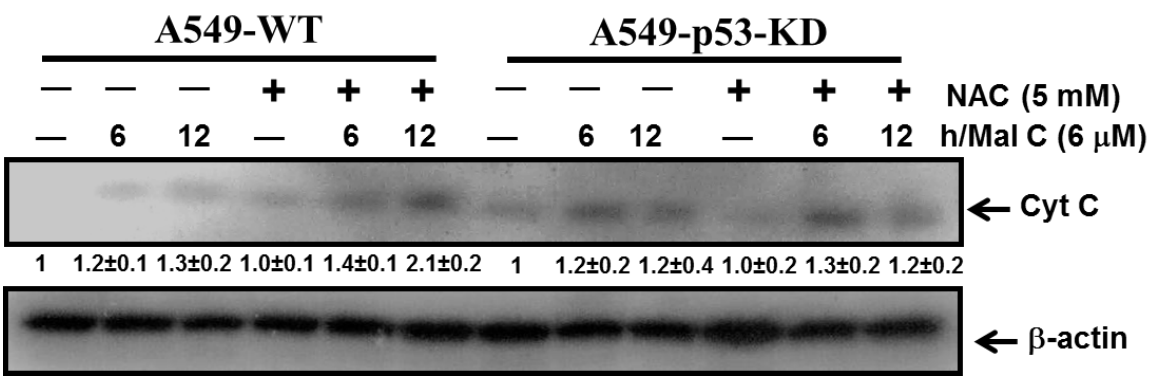
A549-WT
A549-p53-KD
— — — + + + — — — + + + NAC (5 mM)
— 6 12 — 6 12 — 6 12 — 6 12 h/Mal C (6 μM)
Cyt C
1 1.2±0.1 1.3±0.2 1.0±0.1 1.4±0.1 2.1±0.2 1 1.2±0.2 1.2±0.4 1.0±0.2 1.3±0.2 1.2±0.2
β-actin

E

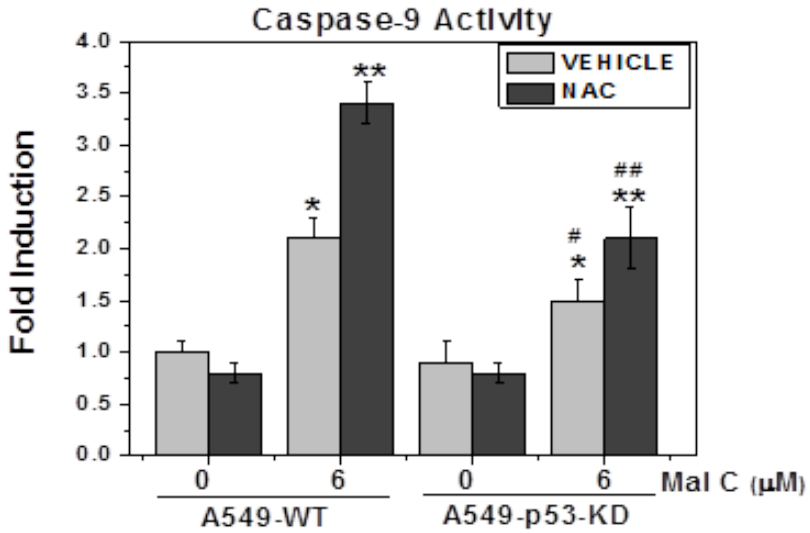
Caspase-9 Activity
VEHICLE
NAC
Fold Induction
4.0
3.5
3.0
2.5
2.0
1.5
1.0
0.5
0.0
*
**
#
*
##
**
0 6 0 6 Mal C (μM)
A549-WT
A549-p53-KD

Figure 3. 7. 16. NAC-enhances the translocation of p53 onto mitochondria and releases death factors in response to mal C treatment. (A) A549 cells were treated with vehicle, NAC (5 mM), mal C (6 μM) and NAC (5 mM) + mal C (6 μM) for 0-12 h. Mitochondrial fractions were prepared from the above treated cells and analyzed for p53 protein through immunblotting. COX IV was used as loading control for mitochondrial fraction. **(B)** A549 cells were treated similarly as mentioned in A. Cytosolic fractions were prepared from the above treated cells and analyzed for BAX protein by immunblotting. **(C)** P53 expression levels, as assessed by western blotting, in A549-WT and A549-p53-KD cells as seen through immunoblotting. **(D)** P53 plays an imperative role in enhancing the mitochondrial release of cytochrome c in NAC plus mal C treatment. A549-WT and A549-p53-KD cells treated similarly as mentioned above in A. Cytoplasmic fractions were prepared from the above treated cells and analyzed for cytochrome c by immunblotting. **(E)** Caspase-9 activation. A549-WT and A549-p53-KD cells treated similarly as mentioned above in A, except that the cells were treated for 16 h. Whole cell extracts were prepared from the above treated cells and caspase-9 activity was analyzed. All the experiments were repeated three times with similar results. All determinations were made in three replicates, and the values are means ± SEM. **p*<0.01 compared to vehicle control, ***p*<0.05 compared to respective mal C treatment without NAC, #*p*<0.05 compared to respective mal C treatment in A549-WT cells and ##*p*<0.01 compared to respective mal C+NAC treatment in A549-WT.

3. 7. 9. P53 and p65 (NF-κB) proteins play a key role in NAC induced sensitization to mal C treatment

Our results showed that NAC plus mal C treatment induces glutathionylation of p53 and p65 protein leading to their accumulation in cytoplasm and decrease in the expression of p53 and p65 regulated survival proteins e.g., p21 and XIAP respectively. Beside, cytoplasmic accumulation of p53 led to its sequestration into mitochondria and subsequent increase in the release of death factors. In the hindsight of above results, we reasoned that p53 depleted cells *vis-à-vis* p53-proficient cells may show resistance to mal C plus NAC treatment. Our results showed that, mal C plus NAC treatment significantly increased the sub-G1/apoptotic population in both A549-WT and A549-p53-KD cells in comparison to mal C treatment alone (Figure 3. 7. 17A). However,

the mal C treatment alone or its combination treatment with NAC induced lower sub-G1/apoptotic population in A549-p53-KD cells vis-à-vis A549-WT cells (Figure 3. 7. 17A).

In addition, to confirm the role of p65 (NFκB), we depleted NEMO (NEMO is a regulatory subunit required for NF-κB activation) in A549 cells by NEMO shRNA. NEMO depleted cells were designated as NEMO-KD cells while cells expressing control scrambled shRNA are designated as NEMO-WT (Figure 3. 7. 17B). Mal C treatment induced higher cell death in the NEMO-KD cells *vis-à-vis* NEMO-WT cells (Figure 3. 7. 17C). Further, NAC treatment enhances mal C-induced death process in NEMO-WT and NEMO-KD cells almost equally, suggesting a role of NF-κB in survival pathway and its down-regulation by NAC treatment (Figure 3. 7. 17C).

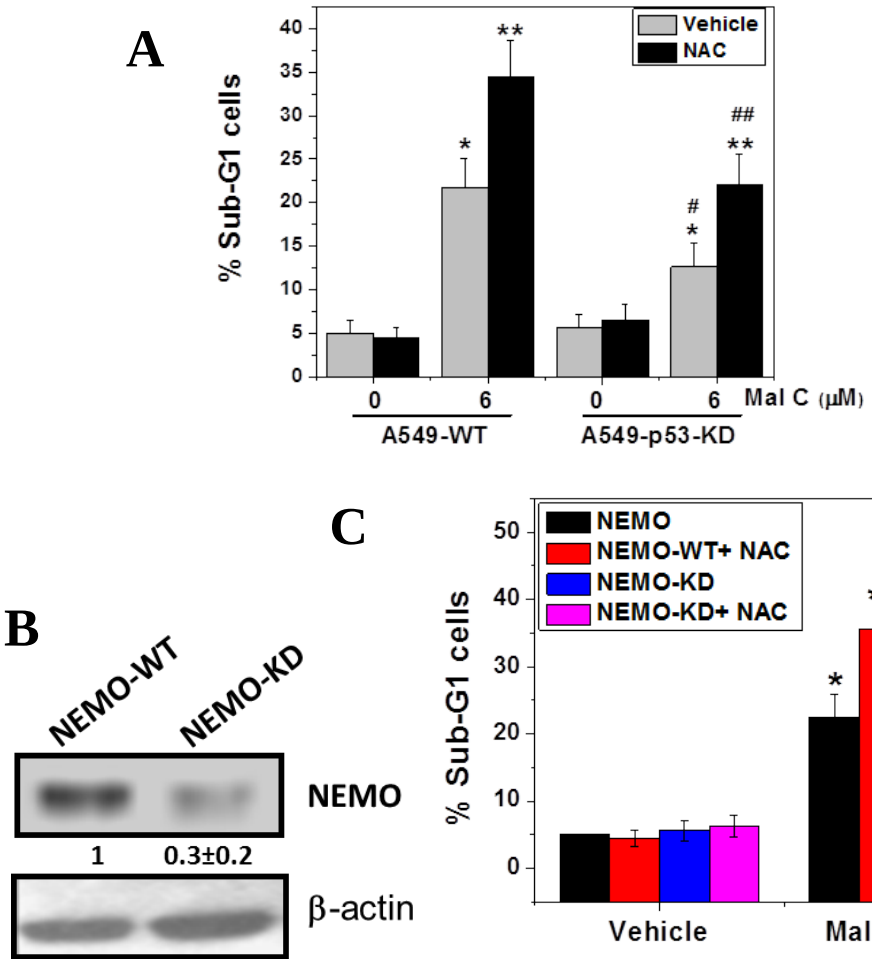

Figure 3. 7. 17. Role of p53 and NF-κB pathway in mal C-induced cell death in the presence of NAC. (A) Sub-G1 (apoptotic) analysis after mal C and NAC treatment in A549-WT and A549-p53-KD cells. The cells were pre-incubated without or with NAC (5 mM) followed by mal C treatment (6 μM) for 24 h. Twenty thousand cells in each treatment were acquired using flow cytometer. The % sub-G1 population was plotted as bar graph. **(B)** Protein expression in NEMO-WT and NEMO-KD cells as seen through immunoblotting. **(C)** The indicated cells were incubated without or with NAC (5 mM) followed by mal C treatment (6 μM) for 24 h were stained with PI and then acquired using flow cytometer. The Sub-G1 region representing the percentage of cells undergoing apoptosis was plotted in the form of bar graph. The experiments were repeated three times with similar results. All determinations were made in three replicates, and the values are means ± SEM. *p<0.01 compared to vehicle control, **p<0.05 compared to respective mal C treatment without NAC, #p<0.05 compared to respective mal C treatment in A549-WT cells and ##p<0.05 compared to respective mal C+NAC treatment in A549-WT.

3. 8. Anti-tumor efficacy of malabaricone C alone and combination treatment of mal C and NAC *in vivo* mice models

3. 8. 1. Mal C reduces lung carcinoma tumor burden in SCID mice

Male SCID mice were implanted subcutaneously with A549 xenografts and palpable tumors were allowed to grow for 7 days. The animals were then randomized into treatment groups of 5 mice each and administered 50 or 100 mg/kg of mal C or 100 mg/kg NAC or vehicle or in combination on alternate days by oral gavage up to 30 days (Figure 3. 8. 1A). Tumor volumes were measured weekly and tumor weight was quantified at the end of the study (day-30), after sacrificing the mice. The study showed significant dose dependent reduction in tumor volume/weight of mal C (50 and 100 mg/kg) compared to vehicle treated mice (Figure 3. 8. 1B-D). The efficacy of the treatment was further enhanced when mice were co-supplemented with oral gavage of NAC (100 mg/kg) (Figure 3. 8. 1B-D).

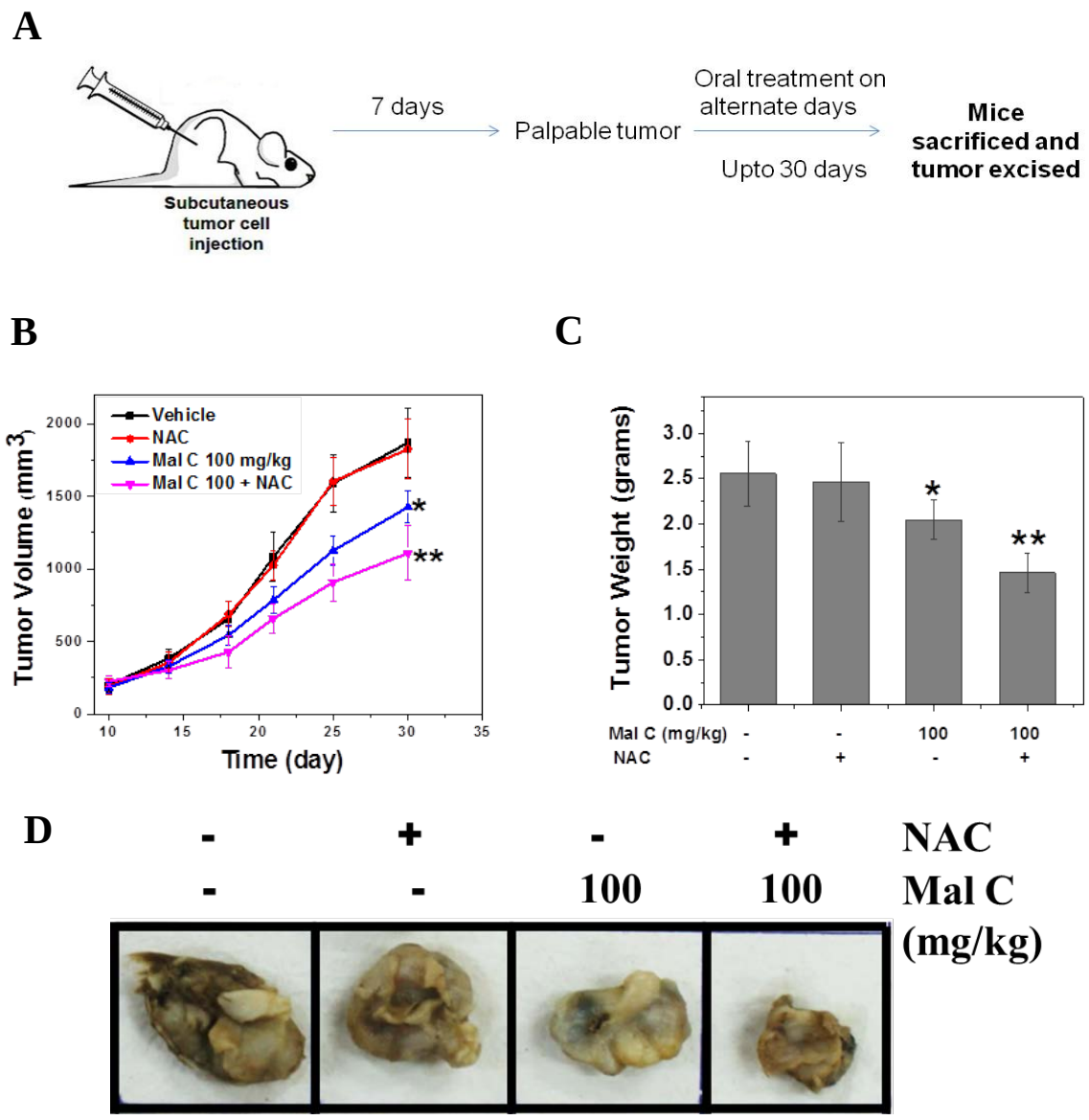

Figure 3. 8. 1. Mal C reduces lung carcinoma tumor burden in SCID mice. (A-D) Male SCID mice were inoculated subcutaneously with A549 human lung cancer cells ($8x10^6$ cells per 200 µl in DMEM media). Following implantation, tumors were allowed to grow for 7 days. Mice were randomized and assigned into six treatment groups. Animals were dosed orally with mal C or NAC or vehicle (n=5) on alternate days. Data displayed are mean ± SEM. *p<0.05, **p<0.01 compared to vehicle treated mice.

3. 8. 2. Mal C also reduces melanoma tumor burden in mice

Our investigation on the mechanism and efficacy of mal C alone and combination treatment of NAC plus mal C was exclusively based on lung adenocarcinoma cells i.e., A549 cells. We

further sought to know whether the efficacy of mal C alone and combination treatment of NAC plus mal C is limited to one types of tumor i.e., lung carcinoma or the therapeutic benefits may extendable to other types of cancers too. To this end, initially we screened A431 (human skin epithelial carcinoma), U2OS (human epithelial osteosarcoma), IMR32 (human neuroblastoma), SHSY-5Y (human neuroblastoma) and B16F10 cells (mouse melanoma) for their sensitivity towards mal C and mal C + NAC treatments. Our results showed that NAC treatment sensitized A431, U2-OS and B16F10 cells, as assessed by sub-G1 assay, to mal C treatment (Figure 3. 8. 2). Intriguingly, NAC failed to sensitize neuroblastoma tumour (IMR32 and SHSY-5Y) to mal C treatment (Figure 3. 8. 2).

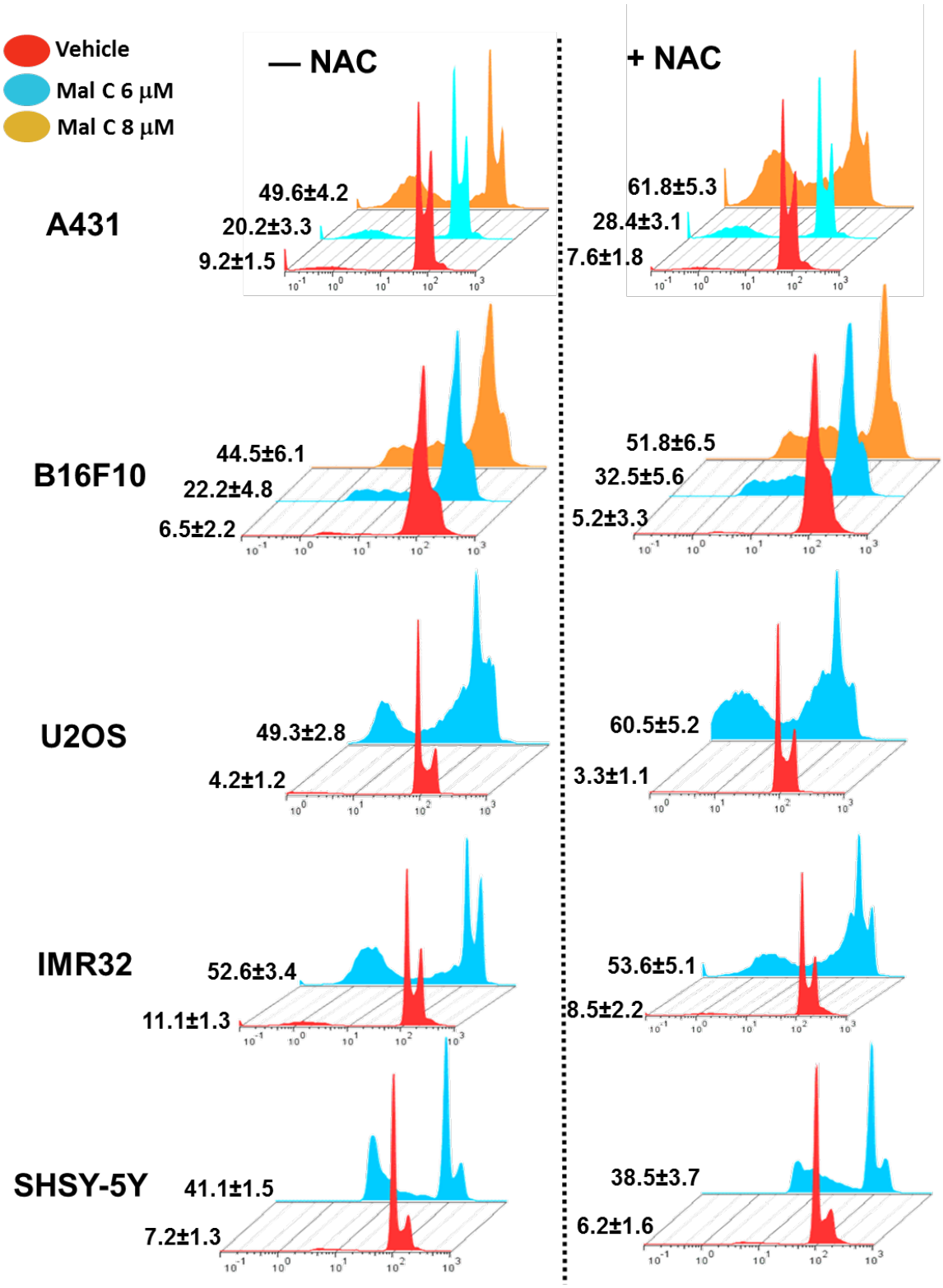

Figure 3. 8. 2. NAC treatment sensitizes A431, U2OS and B16F10 cells towards mal C-induced death process. Indicated cells were treated with mal C (6 and 8 µM) in the absence or presence of NAC

(5 mM) for 24 h. Twenty thousand cells in each treatment were acquired using a flow cytometer for analyzing the amount of sub-G1 cells. The Sub-G1 region (RN1) represents the percentage of cells undergoing apoptosis. The experiments were repeated three times with similar results and the values are mean ± SEM.

Further, *in vivo* anti-tumor efficacy of mal C in the absence and presence of NAC was also evaluated using syngeneic B16F10-C57BL/6 murine melanoma tumor model, which is well established and reported model in the literature [168,169]. Experiment was performed similarly as mentioned above for SCID mice. Animals were sacrificed after 30 days, their tumor was excised, and weight was measured (Figure 3. 8. 3A-C). Similar to lung carcinoma tumor results in SCID mice, mal C+NAC treatment was better than mal C alone treatment in inhibiting tumor growth in B16F10-C57BL/6 murine melanoma tumor model. All these data support a potential use of mal C alone or in combination with NAC (thiol antioxidants) in the management of tumors.

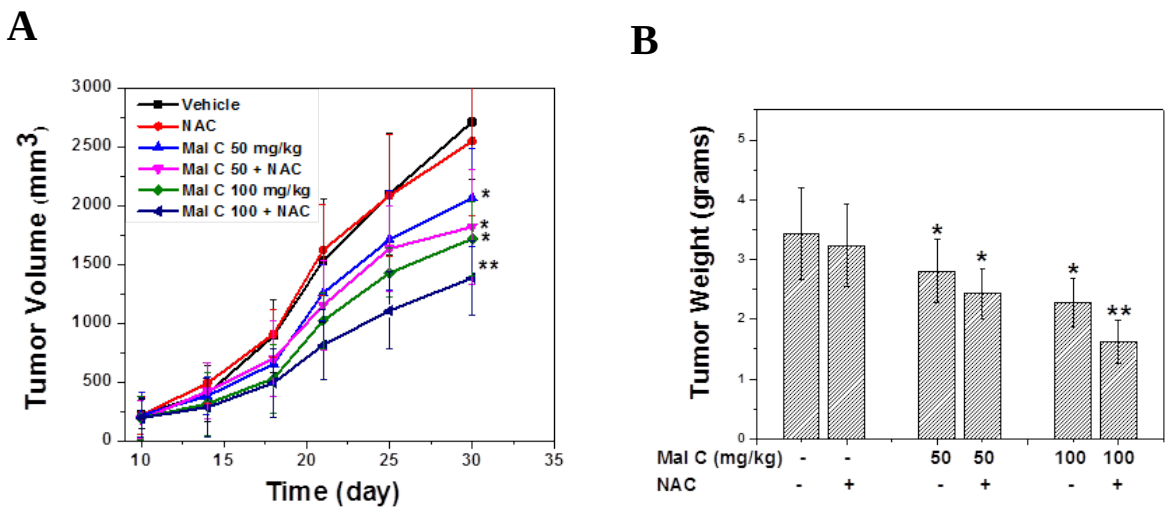

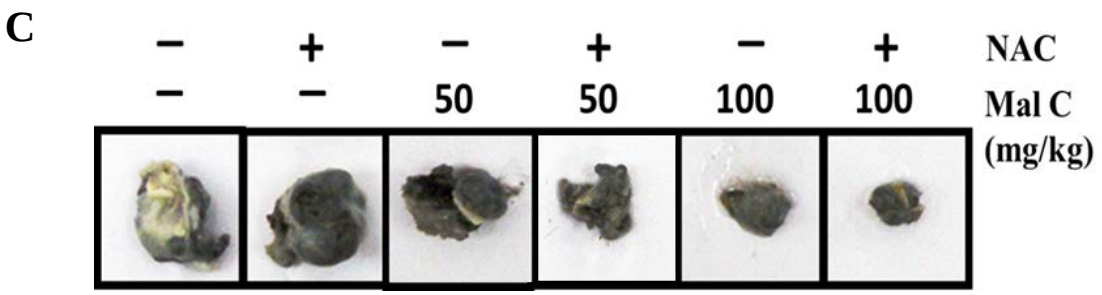

Figure 3. 8. 3. *In vivo* effect of mal C in B16F10-C57BL/6 murine model bearing B16F10 melanoma tumor. (A-C) Male C57BL/6 mice were inoculated subcutaneously with B16F10 cancer cells (7.5×104 cells/0.2 ml/mouse in DMEM media. Following implantation, tumors were allowed to grow for 7 days. The mice were assigned into six treatment groups. Animals were dosed orally with vehicle, mal C, NAC, mal C+NAC (n=5) on alternate days. Data displayed are mean ± SEM. **p*<0.05, ***p*<0.01 compared to vehicle treated mice.

3. 8. 3. Preclinical toxicity study for mal C

Rathee *et al*. [184] reported no hematologic or histopathologic toxicity associated with daily oral administration of mal C at 100 mg/kg in rats. In C57BL/6 mice also, no significant toxicity of mal C with oral dose of 500 mg/kg was reported [152]. It is also reported that histological parameters for liver and kidney remain intact after oral feeding of mal C in mice [152]. In the current study, the chronic toxicity of mal C was evaluated from the behavioral changes, observed for 1 month as well as plasma biochemistry of the mal C (300 mg/kg)-fed mice. The animals had normal food and water intake as well as stool during the experimental period. Renal and liver function tests were also carried out and analyzed for urea, creatinine, SGPT, and SGOT. The comparative plasma biochemistry profile of the normal mice and those treated with mal C revealed no hepatic and/ or renal toxicity (data not shown).

CHAPTER-IV

DISCUSSION AND CONCLUSIONS

4. 1. Discussion

Cancer remains a major burden to human health, standing second in terms of leading cause of death worldwide [185]. Most of the currently available anti-cancer drugs exhibit numerous side effects, and are too expensive for a major share of the world population. This warrants search for alternative, target-selective anti-neoplastic molecules, which are less expensive, efficacious and exhibit minimum toxicity to normal cells. Most of the these properties belongs to the compounds derived from plants "phytochemicals"[119]. More than 50% of the drugs used during the last 20 years are directly or indirectly derived from plants/plant products [133]. An ideal phytochemical is one that possesses anti-tumor properties with minimal toxicity and has a defined mechanism of action [186]. In the present study, extensive investigation was done on one of the phytochemical "malabaricone C (mal C)" a spice-derived diarylnonanoid with proven *in vitro* antioxidant activity isolated by our group from *Myristica malabarica* (rampatri), a well-known spice of Indian cuisines [151]. Initially we found mal C to be cytotoxic to various human cancer cell lines of different tissue origins and studied its detailed mechanism of action in two cancer cell lines of different tissue origin e.g., A549 (lung cancer) and MCF-7 (breast cancer) cell lines. This may further help in rationalizing the drug's action and trying different combinations in terms of established biochemical mechanisms, as done in the current study. Our extensive investigations showed that mal C induces caspase dependent apoptosis involving DNA damage dependent activation of checkpoint kinase 1 (CHK1) and mitogen activated protein kinase (MAPKs), ultimately leading to mitochondrial cell death in A549 lung carcinoma cells. In contrast, mal C induced cell death followed lysosomal and mitochondrial damage leading to calcium release and activation of cathepsin and calpains (Ca^{2+}-dependent cysteine proteases), subsequently causing cell death with apoptotic features in breast cancer cells (MCF7). Further, *in vitro* anticancer

activity of mal C was extended to establish the chemotherapeutic potentials of mal C alone and in combination with NAC in preclinical mouse tumor models.

In previous studies, the anti-cancer properties of some of the malabaricones (mal A and mal C) were evaluated in MCF-7 and U937 cells [158,187]. In these reports, mal A killed leukemic cells (non-adherent) more effectively, while mal C was more potent against adherent cancer cells, In the current investigation, we screened all the malabaricones (mal A-D) for anticancer activity by choosing all adherent cancer cell types. Mal B and mal C were found to be more potent than mal A, mal D, curcumin (diarylheptanoid, a natural product isolated from turmeric, *Curcuma longa*) and etoposide (a market available chemotherapeutic agent with the ability to inhibit topoisomerase II) (Figure 3. 1. 1, Table 3. 2). Both mal B and mal C induced caspase dependent cell death and copious amount of intracellular ROS generation (Figur 3. 1. 5, 6). Non-thiol and thiol antioxidants like trolox® and NAC drastically reduced the sensitivity of A549 cells towards mal B only while trolox® had no effect on mal C induced cell death. In contrast, thiol antioxidants like NAC/GSH enhance the apoptosis process induced by mal C.Interestingly, although structurally similar mal B mediated death process is p53 and DNA damage independent, as opposed to mal C which causes a significant and robust DNA damage with p53-dependent apoptosis (Figure 3. 1. 7, 3. 1. 8). The action of mal B was more or less similar to various ROS generating agents like curcumin and resveratrol where ROS scavangers leads to decrease in cell death [188]; while that of mal C followed non-canonical ROS-mediated cell death where non-thiol antioxidants could not protect from the cell death. Imperatively, thiol harboring antioxidants increases the mal C induced cell death indicating the involvement of site-specific and in accessible ROS. In support of this, previous reports show that some phytochemicals like EGCG make adduct with NAC/GSH leading to enhancement in anticancer

efficacy [189]. Similarly, another report show that NAC acts in synergism with doxorubicin (DOX) in reducing tumorigenicity and metastasis burden in murine models [190].

Selectivity of any cancer chemotherapeutic drug is one of the criteria for a potential candidate, which helps in reducing its side-effects too. A molecule used against cancer should have either low or no cytotoxicity towards normal/ non-cancerous cells. Cancer cells are frequently associated with enhanced cellular stress (for example, oxidative, replicative, metabolic and proteotoxic stress, and DNA damage) [24,191]. Adaptation to this stress is required for cancer cells to survive where the molecular players differs in comparison to the normal cells. Thus DNA damaging agents, causing oxidative stress are promising candidates as anti-tumor agents. A 3.5-fold higher copper concentration has been reported in cancerous tissues compared to their normal counterparts; this allows search for copper-dependent nuclease agents which can cause lethal DNA damage due to significant concentration of DNA-bound copper. In cellular system, the copper/H_2O_2 dependent damage is enhanced and generates site-specific ROS due to accumulation of high amount of DNA-bound copper [192]. Earlier, mal C is reported to damage plasmid DNA in the presence of copper [158]. Here in current investigation, we found that mal C killed lung cancer cells with higher potency than compared to their normal counterparts (L132 and WI-38) (Figure 3. 3. 1). DNA damage in normal cells was less in comparison to cancer cells (Figure 3. 3. 5). This may be attributable to the lesser uptake of mal C by normal cells as compared to cancer cells (A549) (Figure 3. 3. 4). Beside, higher amounts of copper in cancer cells might pronounce mal C induced death process in cancer cells compared to normal cells. Other reasons for selectivity can be assigned to targeting of mal C to differential expression profiles of the proteins in normal and cancer cells, which warrants further study.

Anticancer activity of most chemotherapeutics involves induction of programmed cell death like apoptosis, autophagy or mitotic catastrophe which do not induce inflammatory reaction in an organism [28]. These are dictated mostly by cell origin and the extent of specific damage induced by the drug. It has been reported that different concentration of the same drug can have variable response and thus the major cell death response pathway in a particular drug treatment needs to be verified. We established that mal C induces caspase dependent apoptosis as a major route of programmed cell death in A549 cells while lysosomal membrane permeabilization (LMP) and calpain activation was the major cause of apoptosis in MCF-7 cells (having non-functional caspase-3) [174]. However, cell lines of different tissue origins can have significant activation of other programmed cell death with or without apoptosis. To this end, our study does not overrule significance of other pathways in mal C induced death process.

Several studies have demonstrated that apoptosis plays a vital role in the treatment of cancer following chemo- and radiation therapies [9]. Apoptosis markers like chromatin condensation, nuclear fragmentation, cell shrinkage, plasma membrane blebbing, activation of caspases and generation of apoptotic bodies were detected during mal C-induced cell death in this study. In literature, apoptosis is discussed to be mediated by two strictly intertwined pathways [26]. One via death receptors, e.g., Fas mediated activation of caspase-8, wherein mitochondria is involved only later, leading to the execution phase with the cleavage of caspase-3. The other is linked primarily to mitochondrial changes, directly inducing the release of cytochrome c into the cytosol and apoptosome complex formation with the activation of caspase-9. Growing evidence implicated mitochondrion as a central integrating organelle in apoptosis, with the capacity to directly activate the execution pathways. Perhaps the most well characterized apoptotic cascade is the activation of caspases by cytochrome c and apoptosis-

activating factor-1 (apaf-1) in the presence of ATP or dATP [26,28]. Our results show significantly increased activities of the initiator (caspase-9) and executor (caspase-3) cysteine proteases in the mal C-treated A549 cells (Figure 3. 1. 5D). Furthermore, the immuno blots showed sequential induction of the upstream caspase-9 and caspase-3 with delayed activation of caspase-8 after mal C treatment (Figure 3. 1. 5C).

There is strong evidence that ROS generation can induce apoptotic process *via* damaging lipids, proteins and nucleic acid [133]. The anti-tumor activity of many agents like sulforaphane, doxorubicin, cisplatin, and emodin etc. are mediated by ROS induction [193]. Our DCFDA assay results confirmed that mal C generates a significant amount of ROS in a time-dependent fashion, compared to the control cells (Figure 3. 1. 6A). Further, mal C in the presence of copper increased the fluorescence of Dihydroethidium (DHE) (reduced form of the commonly used DNA dye ethidium bromide) confirming the generation of intracellular oxidative stress (data not shown). DHE has been used extensively in tissue culture experiments to evaluate reactive oxygen species (ROS) production specifically superoxide. DHE itself is blue fluorescent in cell cytoplasm but upon reaction with superoxide anions forms a red fluorescent product (2-hydroxyethidium) after intercalating with DNA [170].

Oxidative stress induced glutathione depletion has been shown to play an important role in apoptosis induction by a wide variety of stimuli [194]. Here, different non-thiol and thiol based ROS scavengers were employed as protective antioxidants in response to oxidative damage [105]. Although these non-thiol and thiol based antioxidants reduce the mal C-generated intracellular ROS (DCFDA sensitive) inside the cells, thiol antioxidants like NAC enhances the cytotoxic potential of mal C (Figure 3. 7. 2, 3. 7. 4). NAC is a thiol harboring extracellular and intracellular antioxidant which has emerged as a promising cancer chemopreventive agent that

can act as a source of GSH for the cell and also directly modify the activity of several enzymes [195,196]. Mal C-induced glutathione depletion was abrogated in the presence of NAC (Figure 3. 7. 3). This phenomenon of thiol mediated enhancement in mal C induced cytotoxicity was not limited to A549 cells, instead various other cell lines also showed similar enhancement, although to a different extent (Figure 3. 8. 2). It is worth noting that NAC did not show any significant enhancement of mal C induced cell death in neroblastoma cells (SHSY-5Y and IMR32) cells (Figure 3. 8. 2). We also established that the mal C-mediated cell death in the presence of NAC follows apoptotic route (caspase-3 and PARP cleavage) (Figure 3. 7. 6). Some ROS inducing compounds like doxorubicin, EGCG, HEMA, pyrroloquinoline quinone (PQQ) and leinamycin have been also documented to show enhanced apoptosis in the presence of NAC [189,190,197–199]. While dual role of glutathione in selenite-induced apoptosis in human hepatoma cells have also been discussed [200].

Mal C is a polyphenol having catechol moiety. Unlike interaction between some phenolic compounds like EGCG and thiols [189], mal C did not make any adduct with thiols (as revealed from MALDI-TOF experiments, data not shown). In addition, physical interaction between phenol and thiol groups have been reported [201,202]. We already reported mal C to generate superoxide (ROS) in the presence of metal ions like copper [158], during this process catechol form of mal C gets converted into quinone form. We found that catechol form of mal C can shuttle between the quinone form and back depending on the chemical environment. The kinetics for the formation of quinone (λ_{max}480 nm) form of mal C in the presence of copper was slowed in the presence of NAC, demonstrating that the equilibrium between catechol and quinone has shifted towards catechol (Figure 3. 7. 7). In the vicinity of cellular DNA, mal C (catechol form) might be regenerated in the presence of NAC leading to further increase in (1) superoxide

formation as quantified *via* DHE and (2) DNA damage as quantified *via* γ-H2AX and comet assay (Figure 3. 7. 8, 9) [203,204]. Our results are coherent with one of the study with doxorubicin (Dox) wherein authors reported a similar increase in DNA damage, p-ATM and p-p53 generation by Dox and NAC [205]. In another report with a DNA damaging antibiotic, leinamycin, NAC potentiates the DNA cleavage ability of leinamycin [199]. Dual role of NAC was observed in the presence of HEMA (an unreacted monomer in dental resin materials), where lower concentration of NAC (1 mM) increased ROS generation in response to HEMA while 5 and 10 mM of NAC led to its abrogation [198]. However, a detail mechanism of action in NAC induced pronunciation of death process is not known.

Intracellular ROS accumulation has been shown to cause not only MMP loss with subsequent activation of cell death but also DNA damage culminating into plethora of signaling events leading to cell cycle arrest or cell death [206]. Recent studies also provide evidence for the role of ROS induced DNA damage in potentially activating MAPK in response to a variety of different stimuli [24,207–209]. Previously, we have shown that mal C generates DNA nicks (damage plasmid DNA) in a cell free system [158]. In similar fashion, we found mal C to interact and induce DNA damage inside the cancer cells also (Figure 3. 4. 12, 13). The canonical DNA damage response (DDR) network can be divided into two major protein kinases signaling branches, which mediate checkpoint activation through the upstream kinases, ATM-CHK2 [70] and ATR-CHK1 [172]. A third checkpoint effector pathway, mediated by p38 and MAPKAP kinase-2 (MK2) operates parallel to CHK1, and is activated downstream of ATM and ATR [210,211]. The DDR-mediated sustained activation of p38 and JNK is responsible for the cisplatin-induced apoptosis *via* activation of the death receptor pathway [212,213]. Moreover, down-regulation of the CDC7 kinase activity induced ATR-mediated p38 activation to execute

apoptosis in human cancer cells [214]. Since mal C induced DNA SSBs in MCF7 breast cancer cells [158], we hypothesized that a similar mal C-mediated SSBs in A549 cells might be converted into DSBs due to the replication and/or DNA damage repair pathways which might have activated p38 MAPK. Our results of neutral comet and γH2AX assay showed that mal C binds to nuclear DNA effectively, and induces DSBs in concentration dependent manner (Figure 3. 4. 13). Furthermore, mal C also activated the DDR response proteins ATM and ATR by inducing rapid auto-phosphorylation at Ser-1981 in ATM and phosphorylation of Ser-345 in CHK1 (Figure 3. 4. 14).

The mal C-mediated apoptosis in A549 cells was also accompanied by rapid collapse of mitochondrial membrane potential (MMP), leading to the release of apoptogenic molecule, cytochrome c from the mitochondria to the cytosol (Figure 3. 4. 4). The antiapoptotic BCL-2 family members (BCL-2 and BCl-xL) play an important role in the regulation of mitochondria-mediated apoptosis by different stimuli [87]. These antiapoptotic proteins possess four conserved BCL-2 homology domains (BH1–BH4), and mainly prevent the release of apoptogenic molecules (e.g. cytochrome c) from mitochondria to the cytosol by forming heterodimer complexes with the pro-apoptotic family members such as BAX [45,46,88]. Increased expression of BCL-2 has been observed in a variety of hematologic malignancies and solid tumors, and its overexpression renders cancer cells resistant to different apoptotic stimuli including the chemotherapeutic agents [215]. Mal C treatment selectively and differentially regulated the anti- and proapoptotic BCL-2 proteins to ameliorate apoptotic stimuli. It induced a time-dependent decrease in BCL-2 level, while augmenting BAX level in the A549 cells (Figure 3. 4. 4). The mitochondria-depleted A549-ρ^o cells were extremely resistant to mal C treatment (Figure 3. 4. 5), but BCL-2 depletion conferred partial sensitization in the A549 cells to mal C (Figure 3. 4.

6). Nevertheless, a decisive role of mitochondria in mal C-induced apoptosis was inferred from these results.

Earlier, the MAPK proteins, especially JNK and p38 were suggested to activate caspases through modulating BAX, BCL-2, and mitochondrial dysfunction to execute apoptosis [80,81]. We also found mal C-induced rapid activation of JNK and p38 in the A549 cells, while ERK was activated much later (Figure 3. 4. 7). The observed dephosphorylation of the p38 and JNK proteins at a longer time point (6 h) may be due to the activation of dephosphorylating phosphatases [216]. Nevertheless, besides its transcriptional effects, transient MAPKs activation is sufficient to regulate cell behavior, as it can induce phosphorylation of the cytoplasmic target proteins, such as the apoptotic (e.g., BH3-only family) proteins [217,218].Our studies with specific MAPKs inhibitors, carried out at 3 h (whenp38 and JNK are robustly activated) revealed partial inhibition ofmal Cinducedp38 and JNK phosphorylation (Figure 3. 4. 8). This suggested that SB203580and SP600125 may be inhibiting the auto-phosphorylation of p38 and JNK, but not their phosphorylation by the upstream kinases. Moreover, the respective inhibitors also restored the normal levels of MAPKAPK and c-JUN, the downstream targets of p38 and JNK in the mal C-treated cells, without showing any effect on their own. All these results confirmed the efficacies of the chosen inhibitors. Overall, the above results suggested that these MAPKs inhibitors can inhibit upstream kinases or auto-phosphorylation of MAPKs to effectively abrogate further downstream signaling of p38, JNK and ERK in response to mal C treatment. Amongst the MAPK inhibitors, only the p38-specific inhibitor reduced the mal C-mediated apoptosis in the cells (Figure 3. 4. 9). Further, mal C increased the p38-phosphorylation almost equally in the A549-ρ^{+}/A549-ρ^{o} and BCL2-WT/BCL2-KD cells (Figure 3. 4. 10), inhibition of p38 MAPK partially attenuated the mal C-induced MMP loss (Figure 3. 4. 11A) and cytochrome

c release in the cytosol (Figure 3. 4. 11B). These implied a major role of p38 MAPK activation in the upstream, but not on the downstream in the mitochondrial damage.

The shRNA mediated silencing of ATM or ATR inhibition led to a significant reduction in p38 MAPK phosphorylation (Figure 3. 4. 15), suggesting a predominant, but redundant role of the ATM and ATR pathways in p38 MAPK activation. Intriguingly we also noticed that the mal C-induced phosphorylation of CHK1, generally an ATR target, is also partially abrogated in the ATM knock-down cells. Consistent with this, CHK1 inhibition completely abrogated the mal C-mediated p38 phosphorylation and cytochrome c release from mitochondria (Figure 3. 4. 16A). However, the mal C-induced γ-H2AX formation and CHK1 phosphorylation was not affected by the p38 MAPK inhibitor (data not shown). From this, a pivotal upstream role of the ATM/ATR-CHK1 pathway in the p38-mediated apoptosis was inferred. Although the ATM-CHK1 pathway is not activated regularly, involvement of this unscrupulous pathway in response to radiation and certain other DNA damaging agents is reported [219,220]. Overall, ATM down-regulation or inhibition of CHK1 and ATR greatly attenuated the killing effect of mal C (Figure 3. 4. 16B). This is compatible with the model that mal C induces DSB via the ATM/ATR-CHK1 pathway, which activates p38 to trigger apoptosis through mitochondrial damage. ATM, ATR and CHK1 kinases are known to regulate the phosphorylation of consensus sequence serine and threonine followed by glutamine(S/T-Q sites),while p38MAPK activation occurs through the dual phosphorylation on a tyrosine residue of T–X–Y motif in the activation loop [74]. This suggests that ATM-CHK1 kinases are not directly involved in the phosphorylation of p38 MAPK, but possibly through the activation of some other potential tyrosine phosphorylating kinase/s. It is tempting to speculate that mal C-induced ATM/ATR-CHK1 pathway might be involved in the activation of some of the upstream MAPKKKs known to participate in the activation of the p38

MAPK cascade including MEKK1/4, ASK1, and TAO kinases [74]. Further studies are needed to explore this possibility. A schematic model, explaining the mode of action of mal C in A549 cells is shown in Figure 4. 1.

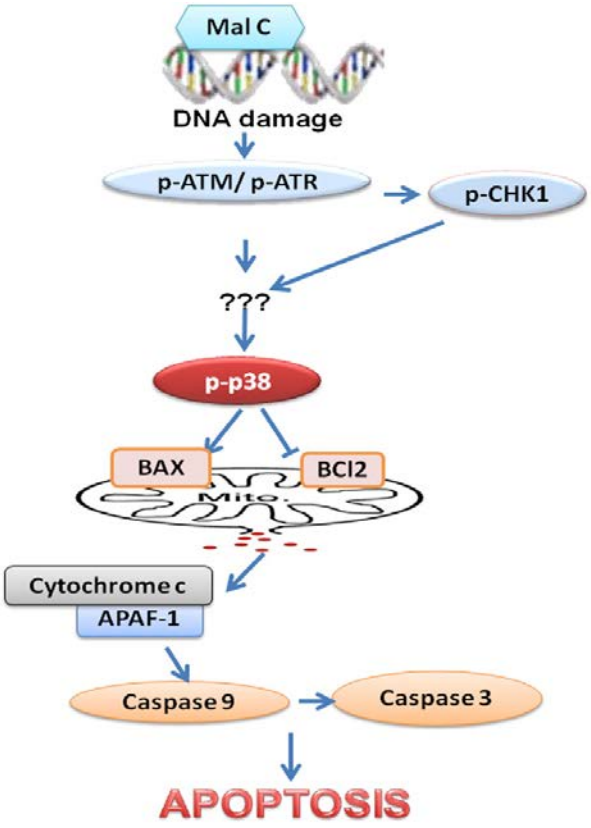

Figure 4. 1. Possible molecular mechanism of mal C-induced cell death in the A549 cells.

In A549 cells, caspase dependent apoptosis was found to be a major pathway but MCF-7 (human breast cancer) cells devoid of caspase-3 activity, also showed good sensitivity towards mal C treatment [174]. Hence we ought to explore the molecular players in its apoptotic process (Figure 3. 6. 1, 2). Similar to A549 cells, mal C induced severe mitochondrial damage in MCF-7 cells (Figure 3. 6. 3). For cells lacking functional caspase 3, translocation of the mitochondrion-specific nucleases (AIF and endo G) into the nucleus leads to cleavage of the chromatin DNA

internucleosomal fragments [42,43]. The observed nuclear translocation of AIF and endo G in mal C treated MCF-7 cells may account for its ability to induce apoptosis (Figure 3. 6. 4).

In caspase independent pathway, Ca^{2+} homeostasis may also play a vital role in apoptosis, and its modulation influences the activation of the widely expressed Ca^{2+}-dependent, apoptosis regulator, calpains [221,222]. Presently, mal C treatment resulted in a moderate increase of intracellular Ca^{2+} load, as revealed from the increased fluorescence of the intracellular Ca^{2+}-indicator, Fluo-2 AM. This was significantly attenuated by the Ca^{2+}-chelator, BAPTA-AM (Figure 3. 6. 5). The endoplasmic reticulum (ER) is a major intracellular reservoir of Ca^{2+}, and the ER-specific Ca^{2+} mobilizer, thapsigargin is known to increase Ca^{2+}level several folds. Thus, the small rise of Ca^{2+}level by mal C is very unlikely to be from ER. Possibly, the MMP loss, induced by mal C hampers the Ca^{2+}-buffering capacity of mitochondria, resulting in the release of mitochondrial Ca^{2+}. The release of Ca^{2+} could also merely reflect a change in ion pump activity. The observed mal C-induced calpain activation (Figure 3. 6. 6) may be due to the increased Ca^{2+}level. Furthermore, BAPTA-AM and Ru360, the mitochondrial Ca^{2+}-uniporter channel inhibitor produced only partial inhibition to the mal C-induced apoptosis to the MCF-7 cells. But inhibition of calpains by PD150606 did not reduce the sensitivity of the cells to mal C. It is worth noting that treatment of the cells with BAPTA-AM would also provide a low Ca^{2+} medium, because we observed a dose-dependent chelation of free Ca^{2+}ions by BAPTA-AM. Hence we used BAPTA-AM instead of the cell impermeable calcium ions chelator, BAPTA. Taken together, it appears that Ca^{2+} influx may play a minor role in the cytotoxicity of mal C towards MCF-7 cells.

Compartmentalization of proteins is an important regulatory mechanism for apoptosis signaling. Accumulating evidence suggests that the initiation steps of apoptosis are organelle-

specific and stress type-dependent [223]. Although lysosomal rupture is primarily linked to cell necrosis, selective lysosomal rupture by suitable agents can also induce apoptosis [224]. Our data with the lysosomotropic agent, Acridine orange (AO) clearly showed significant loss of red fluorescence in favor of green, clearly indicating LMP (Figure 3. 6. 7). This would release the lysosomal proteases, cathepsins B, D, and L into the cytosol, resulting in activation of the apoptotic effectors such as mitochondria and/or the caspases. Consistent with this, mal C also activated cathepsin B, but not cathepsin L in the cytosol, as revealed from our immunoblot data (Figure 3. 6. 8). Several microtubule stabilizing agents such as epothilone B, discodermolide and paclitaxel reportedly induce cathepsin B-dependent and caspase-independent apoptosis in cancer cells[225]. The ectopic presence of lysosomal proteases in the cytosol can activate various MMP inducers. Earlier, cathepsin B was reported to cleave and activate BID in camptothecin-exposed MCF-7 cells [226]. The involvement of BID in DNA damage-induced apoptosis and genotoxic stress in human cancer cells is well documented [227,228]. The extensive translocation of BID into the mitochondria in the mal C-exposed cells (Figure 3. 6. 9) may be due to cathepsin B activation. This can eventually lead to MMP, despite the insignificant role of calpains activation in the BAX mal C-induced apoptosis in the MCF-7 cells. The hypothesis is supported by the fact BID translocation was not affected by caspases or calpain [229]. The larger size of lysosomes and higher ROS generation in the cancer cells make them specifically susceptible to LMP. The copious amount of ROS, produced by mal C may induce lysosomal destabilization in the MCF-7 cells [230]. Presently, LMP occurred much earlier than MMP suggesting that the lysosomal release may be an early event for the apoptosis signaling. Thus, it is possible that the LMP, observed in the present case leads to MMP. Because of its spatially limited range of activity, ROS can induce LMP only in the proximity of mitochondria, the major ROS-generating

organelles. Hence, the distant lysosomes may not be permeabilized, excluding the possibility of any necrosis.

Overall, MCF-7 cells followed the intrinsic caspase-independent mitochondrial apoptotic pathway in response to mal C. The cytotoxic action of mal C in MCF-7 cells is summarized in Figure 4. 2. This mechanism of apoptosis may be especially relevant in tumors lacking caspase-3 activity.

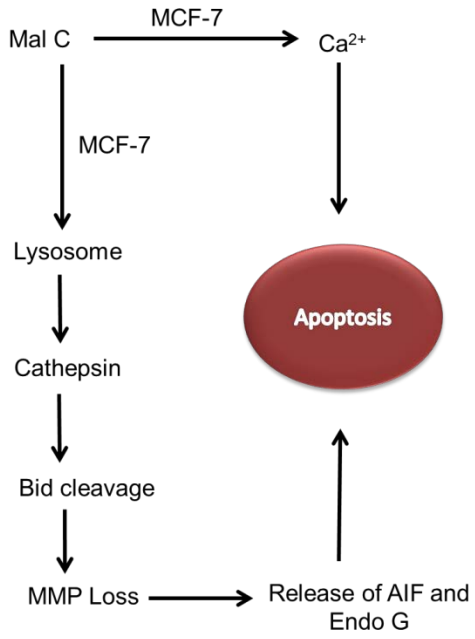

Figure 4. 2. Possible molecular mechanism of mal C-induced cell death in the MCF-7 cells.

Further, mal C enhanced the DNA damage in presence of NAC, but did not promote p-ATM and p-CHK1 activation (Figure 3. 7. 10A). This is in contrast to previous report where DNA damaging drug doxorubicin enhanced p-ATM foci formation in the presence of NAC in ovarian cancer cells [205]. In the presence of NAC, mal C-induced p38 phosphorylation was retained for a longer time (Figure 3. 7. 10B). This may be due to inactivation of de-phosphorylating enzymes due to mal C plus NAC treatment. Further in A549-ATM-KD, *vis-à-*

vis A549-ATM-WT cells, cells NAC pre-incubation partially suppressed mal C induced cell death, indicating for some role of ATM in NAC-enhanced potency of mal C (Figure 3. 7. 10D) [231].

After sufficient amount of drug has accumulated and interacted with cellular targets, the outcome of the treatment is dependent on how the cancer cell responds. Ideally, anticancer drug-induced damage to the cellular system should be tightly coupled to the induction of cell death process. However, various intrinsic adaptive responses can be triggered that promote cancer cell survival through the activation of numerous transcription factors including RAS, MEK, ERK, AP-1, NF-κB and p53 [66,82,232]. Increased expression/activation of these proteins has been observed to render cancer cells resistant to different apoptotic stimuli including the chemotherapeutic agents and their inhibition can make cells sensitive to apoptotic induction. Many studies have demonstrated that DNA damaging drugs like camptothecin and IR can activate signal transduction components including NF-κB activation [233]. With this idea we hypothesized that NAC might be regulating some of the survival factors and thus enhancing mal C-induced apoptosis.

We demonstrated mal C to activate AP-1 (c-Fos), NF-κB (p65), c-Myc, STAT3 and p53 *via* inducing their nuclear translocation (Figure 3. 7. 11) [82,234]. In the presence of NAC, mal C-induced nuclear translocation and chromatin binding of p53 and p65 reduce drastically (Figure 3. 7. 11B). This is in accordance with the earlier reports wherein NAC reduces the nuclear translocation and chromatin binding of hypoxia-induced p65 [92]. This reduction in nuclear translocation was not due to degradation of the proteins, as total p53 and p65 in whole cell extract of mal C and NAC-treated A549 cells were still increasing time-dependently (Figure 3. 7. 12, 13). Instead our results showed that the cytoplasmic accumulation of these proteins, as

confirmed by both western blotting and confocal microscopy. Reduction in chromatin binding of p53 and p65 proteins is corroborated with abrogation in the expression of their respective downstream proteins p21 and XIAP (Figure 3. 7. 12, 13). This is in accordance with previous reports where NAC abrogated hypoxia induced XIAP protein expression [235] and IR induced p21 protein expression [236].

Under pro-oxidant conditions, GSH itself can bind covalently to reactive cysteine thiols of various proteins to form mixed disulfides, a process termed S-glutathionylation, a cysteine based reversible modification *via* formation of protein sulfenic acid moieties as intermediate that subsequently react with GSH/ NAC through thiol exchange mechanism[110,237]. Numerous mechanisms involving ROS-induced thiyl radical formation have been proposed. Here thiyl radical reacts with susceptible cysteine residues present in different proteins giving rise to S-glutathionylated proteins [108]. Further, activity of transcription factors like p65 and p53 are known to be regulated (inhibited) by S-glutathionylation (p65-SSG, p53-SSG) [92,235,238]. Activities of these proteins are redox-regulated through modifications at cysteine (total nine cysteines in p65 and seven cysteines in p53) in their DNA binding domains [235,238,239]. These modifications can adversely alter the tertiary structure of proteins like p53 and p65 proteins affecting their DNA and proteins binding capabilities [240].

Our Immunoprecipitaion (IP) data confirmed that NAC is increasing S-glutathionylation of p53 and p65 proteins in the presence of mal C (Figure 3. 7. 15), thus inhibiting their activation and transport to nucleus from cytoplasm. Above results are in agreement with recent reports showing NAC and GSH can down-regulate cigarette smoke- and tumor necrosis factor-induced NF-κB activation in A549 alveolar epithelial, U937human histiocytic lymphoma, HeLa human epithelial, and MCF-7 human breast cancer cells [241,242]. Apart from preventing p65

activation, NAC also prevented the degradation of IκBα (the inhibitor of NF-κB) too (Figure 3. 7. 12A). Although we did not check the direct S-glutathionylation status of IκBα protein but considering the global protein S-glutahionylation status (Figure 3.4.21) it may be plausible that NAC might also cause S-glutathionylation of IκBα, resulting loss of its degradation.

Cytoplasmic p53 with transcriptional independent pro-apoptotic functions are emerging as an intensive area of research, here translocation of p53 on to mitochondria contributes a vital process for apoptotic induction [180,243]. Role of mitochondrial p53 in inducing BAX and BAK oligomerization, antagonizing anti-apoptotic function of BCL-X_L and BCL-2 and also complexing with cyclophilin D to disrupt mitochondrial structure has been elucidated [85,244]. A stress-stabilized cytoplasmic pool of p53 is probably the major source for p53 mitochondrial translocation; however, it is still a matter of debate on how the pool is generated. According to our results, S-glutathionylated p53 (p53-SSG) seems to be translocated onto mitochondria to induce cytochrome c release and caspase 9 activation mediated apoptosis in response to NAC plus mal C treatment (Figure 3. 7. 16). We propose S-glutahionylation as an important source of cytoplasmic pool of p53. However, it warrants further research to unravel the role of s-glutathionylated p53 in mitochondria mediated cell death.

Although, the release of cytochrome c into the cytoplasm of mal C plus NAC-treated cells increases significantly, the activity of its downstream protein caspase-9 increased to a much higher level (Figure 3.4. 24, 25). This might be due to the crosstalk of a protein called XIAP, which blocks apoptosis at a post-mitochondrial level by inhibiting caspase-9. Treatment of mal C with NAC abrogated the XIAP protein expression level and hence a small increase in cytochrome c release showed larger effect on caspase 9 activity (Figure 3. 7. 16D, E).

Understanding the role of NAC/GSH in enhancing mal C-induced apoptosis has potential clinical significance too. Cancer cells/tissues are suggested to contain higher concentration of GSH than normal cells or adjacent noncancerous tissues [245,246]. Additionally, intracellular glutathione concentration is also found to be involved in resistance arising during radio and chemo-therapy [247,248]. We also believe that apart from the differential uptake of mal C, the difference in the glutathione concentration of normal and cancer cells have a role to play in the higher sensitivity of mal C towards cancer cell than compared to normal cells. Results from this study indicate that increasing intracellular GSH concentration can make them more vulnerable to mal C treatment, further suggesting the potential usefulness of mal C in the treatment of cancer cells. A schematic model, explaining the mechanism for the GSH/NAC dependent enhancement of mal C-induced apoptosis in A549 cells is shown in Figure 4. 3.

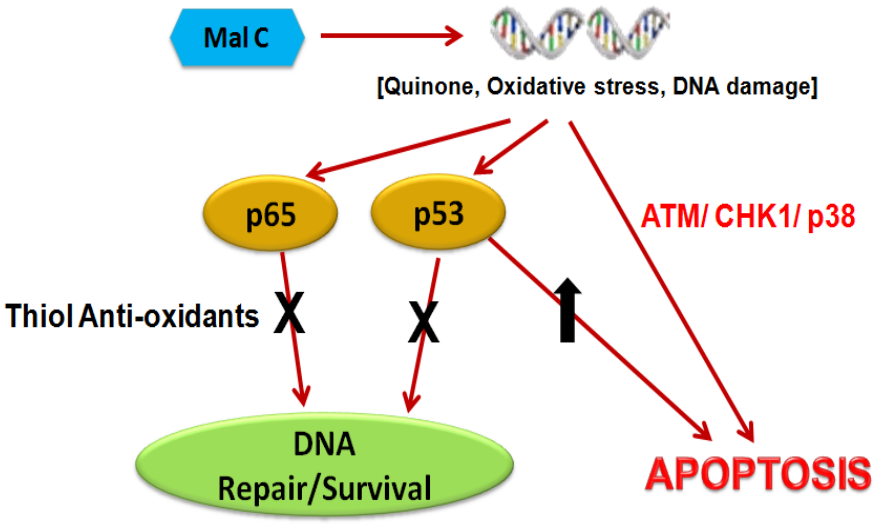

Figure 4. 3. Possible molecular mechanism of mal C-induced cell death in the presence and absence of NAC in cancer cells.

Importantly, we observed low cytotoxicity of mal C treatment in normal human lung cells, indicating that mal C may be safe for use. Besides the cellular effects, we have shown that

mal C is effective in inhibiting tumor growth in two tumor models e.g., SCID and BL/6 mice (Figure 3. 5. 1). The 100 mg/kg of mal C along with NAC, regimen reduced tumor weight in A549-SCID mice drastically. This reduction was better than the respective regimen of mal C alone. We also found an inhibitory effect of mal C and NAC on the proliferation of B16F10melanoma in BL/6 mice, confirming the antitumor activity of both mal C alone and mal C plus NAC in combination (Figure 3. 8. 1-3).

The last few decades have seen many novel anticancer agents and combinations of these with established drugs or irradiation. They range from cytoskeleton damaging agents, growth factor mimetic and metals like nickel to histone deacetylase inhibitors, topoisomerase inhibitors and checkpoint inhibitors [249–252]. This is done because the use of many anticancer drugs is limited by dose-limiting toxicities as well as the development of drug resistance in different cancer cell types. The combination of mal C with other DNA damaging agents did not show any significant additive/synergistic effect (Figure 3. 5. 1) with etoposide, mitomycin, camptothesin, topotecan and IR in A549 cells. The real explanation may not be commented from this study, but one may speculate that the pleiotropic effects of mal C may be responsible for this observation. Mal C not only acts as a DNA damaging agent but has also been reported to regulate various other signaling/pathways like inhibiting PDGF-induced proliferation and migration through induction of heme oxygenase-1 [157], healing indomethacin induced gastric ulcers [152,153], anti-inflammatory activity in LPS treated mice [155], antioxidant and hepato-protective potency *in vitro* and *in vivo* [151,253], anti-hypertensive property in DOCA-salt rats [184], and inhibiting saffrole bioactivation and DNA adduct formation both *in vitro* and *in vivo* [254]. Thus, the crosstalk between various proteins activated or/and inactivated by mal C and the chemotherapeutic drugs tested above might be responsible for the observed phenomenon.

4. 2. Conclusions

Overall, we established mal C as potential chemo-therapeutic agent against different cancers [especially A549 (human lung carcinoma) and MCF-7 (human breast adenocarcinoma)]. Our results showed that mal C possesses better cytotoxic potential than curcumin and etoposide. It was selective to cancer cells with a selectivity index of 2.1. Initially mal C induces DSB-DNA in the A549 cells, which induces p38MAPK activation, BAX translocation, mitochondrial membrane potential loss, caspase-3 activation and eventual cell death. We established a novel molecular mechanism behind thiol-based enhancement in anticancer potential of mal C. Here, mal C treatment in the presence of NAC inhibited the transcription dependent survival function of p65 and p53 proteins through S-glutathionylation. We propose that it can be used as a strategy for increasing the efficacy of other chemotherapeutic molecules also. When administered in to mice at a non-toxic dose of 50 and 100 mg/kg/oral for 30 alternate days after sub-cutaneous injection of tumor cells, mal C and mal C plus NAC showed overall good anti-tumor activity. The pro-apoptotic action of mal C against MCF-7 cells involves deregulation of lysosomes to induce LMP and release of cathepsin B to cleave BID. This eventually leads to mitochondrial membrane potential loss and release of proteins like AIF and endo G that can directly target the nuclear DNA *via* a caspase-independent intrinsic apoptotic pathway. However, this does not exclude the possibility of some additional LMP-independent MMP pathway. This mechanism of apoptosis may be especially relevant in tumors lacking caspase-3 activity. Encouraging the present findings with mice tumor models, mal C appears to be a potential anti-cancer agent for further evaluation, here our findings will aid in the development of therapeutic strategies for the use of mal C as a nontoxic alternative to conventional anticancer therapies.

4. 3. Future prospects

1. Further mechanistic studies are required to identify other putative molecular targets of mal C like growth factors and surface receptors which are known to play a crucial role in regulating chemotherapeutic responses against cancer.
2. The role of mal C in modulating angiogenesis and metastasis related proteins needs to be explored.
3. Higher ability of mal C in killing adherent cells than compared to leukemia cells needs to be studied in detail; this will help in identifying the molecular targets of mal C.
4. Interaction of mal C with NAC/GSH *via* other sensitive techniques like ESI-MS will be studied.
5. Studies on the bio-distribution of mal C in mice are being planned in our laboratory.
6. Mal C may also be considered as a model compound in the design and synthesis of more stable, active and potent diarylnonanoid having good DNA damaging activity, low cytotoxicity to normal cells, water solubility and radiosensitization capability.
7. Further mechanistic studies on the detailed role of S-glutathionylation and if possible the enzymes involved the process needs to be explored.
8. Further studies are required to identify other putative proteins, which may be getting S-glutathionylated following mal C and NAC treatment.
9. The exact mechanism of dephosphorylation of activated MAPKs in response to mal C treatment needs to be understood.

BIBLIOGRAPHY

[1] J. Ferlay, I. Soerjomataram, R. Dikshit, S. Eser, C. Mathers, M. Rebelo, D.M. Parkin, D. Forman, F. Bray, Cancer incidence and mortality worldwide : Sources , methods and major patterns in GLOBOCAN 2012, Int. J. Cancer, 136 (2015) 359–386.

[2] John S Bertram, The molecular biology of cancer, Mol. Aspects Med., 21 (2000) 167–223.

[3] A. Jemal, F. Bray, M. M, J. Ferlay, E. Ward, D. Forman, Global Cancer Statistics, CA Cancer J Clin, 61 (2011) 69–90.

[4] P. Kanavos, The rising burden of cancer in the developing world, Ann. Oncol., 17 (2006) 15–23.

[5] American cancer society, Global cancer facts & figures 3rd edition Atlanta: American cancer society, 2015.

[6] Cancer incidence to rise five-fold in India by 2025, Times of India, (2014).

[7] 1,300 Indians die of cancer every day: ICMR, Biospectrum, (2015).

[8] L.J. Kleinsmith, Principles of cancer biology, Pearson in, 2006.

[9] C.M. Croce, Oncogenes and Cancer, N. Engl. J. Med., 358 (2008) 502–511.

[10] A.G. Knudson, Two genetic hits (more or less) to cancer, Nat. Rev. Cancer, 1 (2001) 157–162.

[11] G. Danaei, S. Vander Hoorn, A.D. Lopez, C.J.L. Murray, M. Ezzati, R. Assessment, Causes of cancer in the world : comparative risk assessment of nine behavioural and environmental risk factors, Lancet, 366 (2005) 1784–93.

[12] S.P. Hussain, L.J. Hofseth, C.C. Harris, Radical causes of cancer, Nat. Rev. Cancer, 3 (2003) 276–285.

[13] D. Hanahan, R.A. Weinberg, The hallmarks of cancer, Cell, 100 (2000) 57–70.

[14] D. Hanahan, R.A. Weinberg, Hallmarks of cancer : The next generation, Cell, 144 (2011) 646–674.

[15] A. Urruticoechea, R. Alemany, J. Balart, A. Villanueva, F. Viñals, G. Capellá, Recent Advances in Cancer Therapy : An Overview, Curr. Pharm. Des., 16 (2010) 3–10.

[16] D.E. Gerber, Targeted therapies: a new generation of cancer treatments, Am. Fam. Physician., 77 (2008) 311–319.

[17] P. Soares, I. Ferreira, R. Igreja, C. Novo, J. Borges, Application of hyperthermia for cancer treatment: recent patents review, Recent Patents Anticancer Drug Discov., 7 (2012) 64–73.

[18] P. Singh M, V. Raina, Lung cancer: Prevalent trends & emerging concepts, Indian J. Med. Res., 141 (2015) 5–7.

[19] F. Leo, L. Cagini, P. Rocmans, M. Cappello, A.N. Van Geel, G. Maggi, P. Goldstraw, U. Pastorino, Lung metastases from melanoma : when is surgical treatment warranted ?, Br. J. Cancer, 83 (2000) 569–572.

[20] F. Tas, Metastatic behavior in melanoma : timing , pattern , survival , and influencing factors, J. Oncol., 647684 (2012) 1–9.

[21] S.-J. Soong, R.A. Harrison, W.H. McCarthy, M.M. Urist, C.M. Balch, Factors affecting survival following local, regional, or distant recurrence from localized melanoma, J. Surg. Oncol., 67 (1998) 228–233.

[22] R.S. Hotchkiss, A. Strasser, J.E. Mcdunn, P.E. Swanson, Cell death in disease: mechanisms and emerging therapeutic concepts, N. Engl. J. Med., 361 (2009) 1570–1583.

[23] J.F.R. Kerr, A.H. Wyllie, A.R. Currie, Apoptosis : A Basic Biological Phenomenon With Wide-Ranging Implication In Tissue Kinetics, Br. J. Cancer, 26 (1972) 239–257.

[24] S. Fulda, A.M. Gorman, O. Hori, A. Samali, Cellular stress responses : cell survival and cell death, Int. J. Cell Biol., 214074 (2010) 1–23.

[25] G. Melino, The sirens ' song, Nature, 412 (2001) 23.

[26] J.C. Reed, Mechanisms of apoptosis, Am. J. Pathol., 157 (2000) 1415–1430.

[27] Hacker G, The morphology of apoptosis, Cell Tissue Res., 301 (2000) 5–17.

[28] S. Elmore, Apoptosis : a review of programmed cell death, Toxicol. Pathol., 35 (2007) 495–516.

[29] J. Savill, V. Fadok, Corpse clearance defines the meaning of cell death, Nature, 407 (2000) 784–788.

[30] S. Fulda, L. Galluzzi, G. Kroemer, Targeting mitochondria for, Nat. Rev. Drug Discov., 9 (2010) 447–464.

[31] M.J. Pinkoski, N.J. Waterhouse, J.A. Heibein, B.B. Wolf, T. Kuwana, J.C. Goldstein, D.D. Newmeyer, R.C. Bleackley, D.R. Green, Granzyme B-mediated apoptosis proceeds predominantly through a Bcl-2-inhibitable mitochondrial pathway, J. Biol. Chem., 276 (2001) 12060–12067.

[32] R.M. Locksley, N. Killeen, M.J. Lenardo, S. Francisco, S. Francisco, The TNF and TNF receptor superfamilies : integrating mammalian biology, Cell, 104 (2001) 487–501.

[33] A. Ashkenazi, V.M. Dixit, Death receptors : Signaling and modulation, Science (80-.)., 281 (1998) 1305–1308.

[34] A. Suliman, A. Lam, R. Datta, R.K. Srivastava, Intracellular mechanisms of TRAIL : apoptosis through mitochondrial-dependent and -independent pathways, Oncogene, 20 (2001) 2122–2133.

[35] S.G. Hymowitz, H.W. Christinger, G. Fuh, M. Ultsch, M.O. Connell, R.F. Kelley, A. Ashkenazi, A.M. De Vos, D.N.A. Way, S.S. Francisco, Triggering cell death : the crystal structure of Apo2L / TRAIL in a complex with death receptor 5, Mol. Cell, 4 (1999) 563–571.

[36] K. Kim, Multifunctional role of Fas-associated death domain protein in apoptosis, J. Biochem. Mol. Biol., 35 (2002) 1–6.

[37] C. Scaffidi, I. Schmitz, P.H. Krammer, M.E. Peter, The role of c-FLIP in modulation of CD95-induced apoptosis, J. Biol. Chem., 274 (1999) 1541–1548.

[38] C. Du, M. Fang, Y. Li, L. Li, X. Wang, Smac , a Mitochondrial Protein that Promotes Cytochrome c – Dependent Caspase Activation by Eliminating IAP Inhibition, 102 (2000) 33–42.

[39] C. Garrido, L. Galluzzi, M. Brunet, P.E. Puig, C. Didelot, Mechanisms of cytochrome c release from mitochondria, (2006) 1423–1433.

[40] M.M. Hill, C. Adrain, P.J. Duriez, E.M. Creagh, S.J. Martin, Analysis of the composition , assembly kinetics and activity of native Apaf-1 apoptosomes, EMBO J., 23 (2004) 2134–2145.

[41] A.D. Schimmer, Inhibitor of apoptosis proteins : translating basic knowledge into clinical practice, Cancer Res., 64 (2004) 7183–7190.

[42] N. Joza, S.A. Susin, E. Daugas, W.L. Stanford, S.K. Cho, C.Y.J. Li, T. Sasaki, A.J. Elia, H.M. Cheng, L. Ravagnan, K.F. Ferri, N. Zamzami, A. Wakeham, R. Hakem, H. Yoshida, G. Kroemer, J.M. Penninger, Y. Kong, T.W. Mak, J.C. Zu, Essential role of the mitochondrial apoptosis-inducing factor in programmed cell death, Nature, 410 (2001) 549–554.

[43] L.Y. Li, X. Luo, X. Wang, Endonuclease G is an apoptotic DNase when released from mitochondria, Nature, 412 (2001) 95–99.

[44] M. Enari, H. Sakahira, H. Yokoyama, K. Okawa, A. Iwamatsu, S. Nagata, A caspase-activated DNase that degrades DNA during apoptosis, and its inhibitor ICAD, Nature, 391 (1998) 43–50.

[45] S. Cory, J.M. Adams, The Bcl2 family: regulators of the cellular life-or-death switch, Nat. Rev. Cancer, 2 (2002) 647–656.

[46] F. Liu, A.C. Newland, L. Jia, Bax conformational change is a crucial step for PUMA-mediated apoptosis in human leukemia, Biochem. Biophys. Res. Commun., 310 (2003) 956–962.

[47] J.A. Trapani, M.J. Smyth, Functional significance of the perforin/granzyme cell death pathway, Nat. Rev. Immunol., 2 (2002) 735–747.

[48] H. Sakahira, M. Enari, Cleavage of CAD inhibitor in CAD activation and DNA degradation during apoptosis, Nature, 391 (1998) 96–99.

[49] S. Kothakota, T. Azuma, C. Reinhard, A. Klippel, J. Tang, K. Chu, T.J. Mcgarry, M.W. Kirschner, K. Koths, D.J. Kwiatkowski, L.T. Williams, Caspase-3 – Generated fragment of gelsolin : effector of morphological change in apoptosis, Science (80-.)., 278 (1997) 294–298.

[50] P. Martin, N. Schill, L. Jo, M. Berg, C.J. Froelich, R. Wallich, M.M. Simon, Granzyme B-induced and Caspase 3-dependent cleavage of gelsolin by mouse cytotoxic T cells modifies cytoskeleton, J. Biol. Chem., 285 (2010) 18918–18927.

[51] R.L. Deter, C. De Duve, Influence of glucagon, an inducer of cellular autophagy, on some pjysical propeties of rat liver lysososmes, J. Cell Biol., 33 (1967) 437–449.

[52] V. Nikoletopoulou, M. Markaki, K. Palikaras, N. Tavernarakis, Crosstalk between apoptosis , necrosis and autophagy, Biochim. Biophys. Acta - Mol. Cell Res., 1833 (2013) 3448–3459.

[53] N. Mizushima, B. Levine, A.M. Cuervo, D.J. Klionsky, Autophagy fights disease through cellular self-digestion, Nature, 451 (2008) 1069–1075.

[54] T. Vanden Berghe, A. Linkermann, S. Jouan-lanhouet, Regulated necrosis: the expanding network of non-apoptotic cell death pathways, Nat. Rev. Mol. Cell Biol., 15 (2014) 135–147.

[55] W. Zong, D. Ditsworth, D.E. Bauer, Z. Wang, C.B. Thompson, Alkylating DNA damage stimulates a regulated form of necrotic cell death, Genes Dev., 18 (2004) 1272–1282.

[56] G. Majno, I. Joris, Apoptosis, oncosis, and necrosis an overview of cell death, Am. J. Pathol., 146 (1995) 3–15.

[57] J. Sosna, S. Voigt, S. Mathieu, A. Lange, L. Thon, P. Davarnia, T. Herdegen, A. Linkermann, A. Rittger, F. Ka, M. Chan, D. Kabelitz, S. Schütze, D. Adam, TNF-induced necroptosis and PARP-1-mediated necrosis represent distinct routes to programmed necrotic cell death, Cell. Mol. Life Sci., 71 (2014) 331–348.

[58] B.D. Vercammen, R. Beyaert, G. Denecker, V. Goossens, G. Van Loo, W. Declercq, J. Grooten, W. Fiers, P. Vandenabeele, Inhibition of caspases increases the sensitivity of L929 cells to necrosis mediated by tumor necrosis factor, J. Exp. Med., 187 (1998) 1477–1485.

[59] R.A. Lockshin, Z. Zakeri, Caspase-independent cell death?, Oncogene, 23 (2004) 2766–2773.

[60] Y. Cho, S. Challa, D. Moquin, R. Genga, T.D. Ray, M. Guildford, F.K. Chan, Phosphorylation-driven assembly of the RIP1-RIP3 complex regulates programmed necrosis and virus-induced inflammation, Cell, 137 (2009) 1112–1123.

[61] S. Gobeil, C.C. Boucher, D. Nadeau, G.G. Poirier, Characterization of the necrotic cleavage of poly (ADP-ribose) polymerase (PARP-1): implication of lysosomal proteases, Cell Death Differ., 8 (2001) 588–594.

[62] A. Oberst, C.P. Dillon, R. Weinlich, L.L. Mccormick, P. Fitzgerald, C. Pop, R. Hakem, G.S. Salvesen, D.R. Green, Catalytic activity of the caspase-8-FLIP complex inhibits RIPK3-dependent necrosis, Nature, 471 (2011) 363–366.

[63] W. Zong, C.B. Thompson, Necrotic death as a cell fate, Genes Dev., 20 (2006) 1–15.

[64] H. Vakifahmetoglu, M. Olsson, B. Zhivotovsky, Death through a tragedy : mitotic catastrophe, Cell Death Differ., 15 (2008) 1153–1162.

[65] G. Housman, S. Byler, S. Heerboth, K. Lapinska, M. Longacre, N. Snyder, S. Sarkar, Drug resistance in cancer : An overview, Cancers (Basel)., 6 (2014) 1769–1792.

[66] C. Holohan, S. Van Schaeybroeck, D.B. Longley, P.G. Johnston, Cancer drug resistance : an evolving paradigm, Nat. Rev. Cancer, 13 (2013) 714–726.

[67] H. Zahreddine, K.L.B. Borden, Mechanisms and insights into drug resistance in cancer, Front. Pharmaology, 4 (2013) 1–8.

[68] J.W. Harper, S.J. Elledge, The DNA damage response : Ten years after, Mol. Cell, 28 (2007) 739–745.

[69] Y. Shiloh, Y. Ziv, The ATM protein kinase: regulating the cellular response to genotoxic stress, and more, Nat. Rev. Mol. Cell Biol., 14 (2013) 197–210.

[70] C.A. Cremona, A. Behrens, ATM signalling and cancer, Oncogene, 33 (2014) 3351–3360.

[71] S. Matsuoka, B.A. Ballif, A. Smogorzewska, E.R.M. Iii, K.E. Hurov, J. Luo, C.E. Bakalarski, Z. Zhao, N.

Solimini, Y. Lerenthal, Y. Shiloh, S.P. Gygi, S.J. Elledge, RESEARCH ARTICLE ATM and ATR Substrate Analysis Reveals Extensive Protein Networks Responsive to DNA Damage, Science (80-.)., 316 (2007) 1160–1166.

[72] Y. Zhang, T. Hunter, Roles of Chk1 in cell biology and cancer therapy, Int. J. Cancer, 134 (2014) 1013–1023.

[73] A. Bensimon, R. Aebersold, Y. Shiloh, Beyond ATM : The protein kinase landscape of the DNA damage response, FEBS Lett., 585 (2011) 1625–1639.

[74] H.C. Reinhardt, M.B. Yaffe, Kinases that control the cell cycle in response to DNA damage : Chk1, Chk2, and MK2, Curr. Opin. Cell Biol., 21 (2009) 245–255.

[75] E.K. Kim, E. Choi, Pathological roles of MAPK signaling pathways in human diseases, Biochim. Biophys. Acta - Mol. Basis Dis., 1802 (2010) 396–405.

[76] Y. Yan, C.P. Black, K.H. Cowan, Irradiation-induced G2 / M checkpoint response requires ERK1 / 2 activation, Oncogene, 26 (2007) 4689–4698.

[77] F. Wei, Y. Xie, L. Tao, D. Tang, Both ERK1 and ERK2 kinases promote G2 / M arrest in etoposide-treated MCF7 cells by facilitating ATM activation, Cell. Signal., 22 (2010) 1783–1789.

[78] H.C. Reinhardt, P. Hasskamp, I. Schmedding, S. Morandell, M.A.T.M. Van Vugt, X. Wang, R. Linding, S. Ong, D. Weaver, S.A. Carr, M.B. Yaffe, DNA damage activates a spatially distinct late cytoplasmic cell-cycle checkpoint network controlled by MK2-mediated RNA stabilization, Mol. Cell, 40 (2009) 34–49.

[79] T.M. Thornton, M. Rincon, Non-classical P38 MAP kinase functions : cell cycle checkpoints and survival, Int. J. Biol. Sci., 5 (2009) 44–52.

[80] B. Kim, S. Ryu, B. Song, JNK- and p38 Kinase-mediated phosphorylation of Bax leads to its activation and mitochondrial translocation and to apoptosis of human hepatoma HepG2 Cells, J. Biol. Chem., 281 (2006) 21256–21265.

[81] A. Cuadrado, A.R. Nebreda, Mechanisms and functions of p38 MAPK signalling, Biochem. J., 429 (2010) 403–417.

[82] M.L. Agarwal, W.R. Taylor, M. V Chernov, O.B. Chernova, G.R. Stark, The p53 network, J. Biol. Chem., 273 (1998) 1–4.

[83] F. Kruiswijk, C.F. Labuschagne, K.H. Vousden, p53 in survival, death and metabolic health : a lifeguard with a licence to kill, Nat. Rev. Mol. Cell Biol., 16 (2015) 393–405.

[84] X. Zhang, Y. He, K. Lee, W. Dubois, Z. Li, X. Wu, A. Kovalchuk, Rap2b , a novel p53 target , regulates p53-mediated pro-survival function, Cell Cycle, 12 (2013) 1279–1291.

[85] J.E. Chipuk, L. Bouchier-hayes, T. Kuwana, PUMA couples the nuclear and cytoplasmic proapoptotic function of p53, Science (80-.)., 309 (2005) 1732–1735.

[86] M. Schuler, E. Bossy-wetzel, J.C. Goldstein, P. Fitzgerald, D.R. Green, p53 induces apoptosis by caspase activation through mitochondrial cytochrome c release, J. Biol. Chem., 275 (2000) 7337–7342.

[87] D.T. Chao, S.J. Korsmeyer, BCL-2 family: Regulators of cell death, Annu. Rev. Immunol., 16 (1998) 395–419.

[88] A. Gross, J.M. Mcdonnell, S.J. Korsmeyer, BCL-2 family members and the mitochondria in apoptosis, Genes Dev., 13 (1999) 1899–1911.

[89] P. Hauck, B.H. Chao, J. Litz, G.W. Krystal, Alterations in the Noxa / Mcl-1 axis determine sensitivity of small cell lung cancer to the BH3 mimetic ABT-737, Mol. Cancer Ther., 8 (2009) 883–893.

[90] B. Hoesel, J.A. Schmid, The complexity of NF- κ B signaling in inflammation and cancer, Mol. Cancer, 12:86 (2013) 1–15.

[91] K.J. Campbell, S. Rocha, N.D. Perkins, Active repression of antiapoptotic gene expression by RelA (p65) NFkB, Mol. Cell, 13 (2004) 853–865.

[92] S. Qanungo, D.W. Starke, H. V. Pai, J.J. Mieyal, A.L. Nieminen, Glutathione supplementation potentiates hypoxic apoptosis by S-glutathionylation of p65-NFkB, J. Biol. Chem., 282 (2007) 18427–18436.

[93] S. Janssens, J. Tschopp, Signals from within : the DNA-damage-induced NF-kB response, Cell Death Differ., 13 (2006) 773–784.

[94] T. Kato, M. Delhase, A. Hoffmann, M. Karin, CK2 Is a C-terminal IkB kinase responsible for NF-kB activation during the UV response, Mol. Cell, 12 (2003) 829–839.

[95] B. Lin, C. Williams-skipp, Y. Tao, M.S. Schleicher, L.L. Cano, R.C. Duke, R.I. Scheinman, NF-kB functions as both a proapoptotic and antiapoptotic regulatory factor within a single cell type, Cell Death Differ., 6 (1999) 570–582.

[96] S. Kasibhatla, T. Brunner, L. Genestier, F. Echeverri, A. Mahboubi, D.R. Green, DNA damaging agents induce expression of Fas ligand and subsequent apoptosis in T lymphocytes via the activation of NF-kB and AP-1, Mol. Cell, 1 (1998) 543–551.

[97] K.M.O. Galenkamp, P. Carriba, J. Urresti, L. Planells-ferrer, E. Coccia, J. Lopez-soriano, B. Barneda-zahonero, R.S. Moubarak, M.F. Segura, J.X. Comella, TNF α sensitizes neuroblastoma cells to FasL-, cisplatin- and etoposide-induced cell death by NF-κB-mediated expression of Fas, Mol. Cancer, 14:62 (2015) 1–14.

[98] W. Chen, Z. Li, L. Bai, Y. Lin, NF-kappaB, a mediator for lung carcinogenesis and a target for lung cancer prevention and therapy, Front Biosci, 16 (2012) 1172–1185.

[99] J.C. Cusack, R. Liu, M. Houston, K. Abendroth, P.J. Elliott, J. Adams, A.S. Baldwin, Advances in brief enhanced chemosensitivity to CPT-11 with proteasome inhibitor PS-341 : Implications for systemic Nuclear Factor-k B inhibition, Cancer Res., 61 (2001) 3535–3540.

[100] J.C. Cusack, R. Liu, A.S. Baldwin, NF-kB and chemoresistance : potentiation of cancer chemotherapy via inhibition of NF- κ B, Drug Resist. Updat., 2 (1999) 271–273.

[101] D.P. Jones, Redox potential of GSH/GSSG couple: assay and biological significance, in: H. Sies, L. Packer (Eds.), Methods Enzymol. Vol 348., Elsevier Inc, 2002: pp. 93–112.

[102] B. Halliwell, J.M.C. Gutteridge, Free radicals in biology and medicine, Clarendon Press,Oxford, UK,

1989.

[103] V.I. Lushchak, Glutathione homeostasis and functions : potential targets for medical interventions, J. Amino Acids, 736837 (2012) 1–26.

[104] Y. Higuchi, Glutathione depletion-induced chromosomal DNA fragmentation associated with apoptosis and necrosis, J. Cell. Mol. Med., 8 (2004) 455–464.

[105] R. Franco, M.I. Panayiotidis, J.A. Cidlowski, Glutathione depletion is necessary for apoptosis in lymphoid cells independent of reactive oxygen species formation, J. Biol. Chem., 282 (2007) 30452–30465.

[106] K.D. Tew, Glutathione S - transferases and S - glutathionylation in cancer, Biomed. Pharmacother., 62 (2008) 513.

[107] R. Franco, J.A. Cidlowski, Apoptosis and glutathione : beyond an antioxidant, Cell Death Differ., 16 (2009) 1303–1314.

[108] I. Dalle-donne, G. Colombo, N. Gagliano, R. Colombo, D. Giustarini, R. Rossi, A. Milzani, S-Glutathiolation in life and death decisions of the cell, Free Radic. Res., 45 (2011) 3–15.

[109] S. Pan, B.C. Berk, Caspase-3 Cleavage and Apoptosis Key Role for Glutaredoxin in the Death Pathway, Circ. Res., 100 (2007) 213–219.

[110] V. Anathy, E.C. Roberson, A.S. Guala, K.E. Godburn, R.C. Budd, Y.M.W. Janssen-heininger, Redox-based regulation of apoptosis : S-glutathionylation as a regulatory mechanism to control cell death, Antioxid. Redox Signal., 16 (2012) 496–505.

[111] J. Scotcher, D.J. Clarke, C.L. Mackay, T. Hupp, P.J. Sadler, P.R.R. Langridge-Smith, Redox regulation of tumour suppressor protein p53: identification of the sites of hydrogen peroxide oxidation and glutathionylation, Chem. Sci., 4 (2013) 1257.

[112] D. Kakde, D. Jain, V. Shrivastava, R. Kakde, a T. Patil, Cancer therapeutics-opportunities, challenges and advances in drug delivery, J. Appl. Pharm. Sci., 1 (2011) 1–10.

[113] P. Anand, A.B. Kunnumakara, C. Sundaram, K.B. Harikumar, S.T. Tharakan, O.S. Lai, B. Sung, B.B. Aggarwal, Cancer is a preventable disease that requires major lifestyle changes, Pharm. Res., 25 (2008) 2097–2116.

[114] J. Mann, Natural products in cancer chemotherapy: past, present and future, Nat. Rev. Cancer, 2 (2002) 143–148.

[115] S.K. Chauthe, S.B. Bharate, G. Periyasamy, A. Khanna, K.K. Bhutani, P.D. Mishra, I.P. Singh, One pot synthesis and anticancer activity of dimeric phloroglucinols, Bioorg. Med. Chem. Lett., 22 (2012) 2251–2256.

[116] P.H. Johnson, Global use of complementary and alternative medicine and treatments, in: C. Holtz (Ed.), Glob. Heal. Care, Second, 2013: pp. 207–238.

[117] B. Ballabh, O.P. Chaurasia, Traditional medicinal plants of cold desert ladakh —used in treatment of cold , cough and fever, J. Ethnopharmacol., 112 (2007) 341–349.

[118] V.P. Kamboj, Herbal medicine, Curr. Sci., 78 (2000) 35–51.

[119] J.G. Graham, M.L. Quinn, D.S. Fabricant, N.R. Farnsworth, Plants used against cancer – an extension of the work of Jonathan Hartwell, J. Ethnopharmacol., 73 (2000) 347–377.

[120] G.M. Cragg, D.J. Newman, Nature: a vital source of leads for anticancer drug development, Phytochem. Rev., 8 (2009) 313–331.

[121] F. Gueritte, J. Fahy, The vinca alkaloids, in: G. Cragg, D. Kingston, D. Newman (Eds.), Anticancer Agents from Nat. Prod., Brunner-Routledge Psychology Press, 2005: p. 23.

[122] G.M. Cragg, D.J. Newman, Plants as a source of anti-cancer agents, J. Ethnopharmacol., 100 (2005) 72–79.

[123] P. Kovács, G. Csaba, E. Pállinger, R. Czaker, Effects of taxol treatment on the microtubular system and mitochondria of Tetrahymena, Cell Biol. Int., 31 (2007) 724–732.

[124] M.C. Wani, H.L. Taylor, M.E. Wall, P. Coggon, A.T. McPhail, plant antitumor agents VI The isolation and structure of taxol, a novel antileukemic and antitumor agent from Taxus brevifolia, J. Am. Chem. Soc., 93 (1971) 2325–2327.

[125] D.G.I. Kingston, Taxol and its analogs, in: G. Cragg, D. Kingston, D. Newman (Eds.), Anticancer Agents from Nat. Prod., Brunner-Routledge Psychology Press, 2005: p. 89.

[126] G.M. Cragg, P.G. Grothaus, D.J. Newman, Impact of natural products on developing new anti-cancer agents, Chem. Rev., 109 (2009) 3012–3043.

[127] K. Scharfenberg, R. Wagner, K.G. Wagner, The cytotoxic effect of ajoene, a natural product from garlic, investigated with different cell lines, Cancer Lett., 53 (1990) 103–108.

[128] M. Thomson, M. Ali, Garlic [Allium sativum]: a review of its Potential Use as an anti-cancer agent, Curr. Cancer Drug Targets, 3 (2003) 67–81.

[129] E.A. Sausville, D. Zaharevitz, R. Gussio, L. Meijer, M. Louarn-leost, C. Kunick, R. Schultz, T. Lahusen, D. Headlee, S. Stinson, S.G. Arbuck, A. Senderowicz, Cyclin-dependent kinases : initial approaches to exploit a novel therapeutic target, Pharmacol. Ther., 82 (1999) 285–292.

[130] R.H. Cichewicz, S.A. Kouzi, Chemistry, biological activity, and chemotherapeutic potential of betulinic acid for the prevention and treatment of cancer and HIV infection, Med. Res. Rev., 24 (2004) 90–114.

[131] R.. Couch, R.. Browning, T. Honda, G.. Gribble, D.. Wright, M.. Sporn, A.. Anderson, Studies on the reactivity of CDDO, a promising new chemopreventive and chemotherapeutic agent: implications for a molecular mechanism of action, Bioorg. Med. Chem. Lett., 15 (2005) 2215–2219.

[132] K. Min, T.K. Kwon, Anticancer effects and molecular mechanisms of epigallocatechin-3-gallate, Integr. Med. Res., 3 (2014) 16–24.

[133] A. Amin, H. Gali-muhtasib, M. Ocker, R. Schneider-stock, Overview of major classes of plant-derived anticancer drugs, Int. J. Biomed. Sci., 5 (2009) 1–11.

[134] H. Gali-muhtasib, M. Ocker, D. Kuester, S. Krueger, Z. El-hajj, A. Diestel, M. Evert, N. El-najjar, B.

Peters, A. Jurjus, A. Roessner, R. Schneider-stock, Thymoquinone reduces mouse colon tumor cell invasion and inhibits tumor growth in murine colon cancer models, J. Cell. Mol. Med., 12 (2008) 330–342.

[135] C. Kao, L. Chen, Y. Chang, M. Yung, C. Hsu, Resveratrol protects human endothelium from H2O2-induced oxidative stress and senescence via SirT1 activation, J. Atheroscler. Thromb., 17 (2010) 970–979.

[136] Q.N. Tona, T. Trana, A.E. Yanga, H.B. Gottlieba, R.A. Bellangera, Resveratrol: Potential as anticancer agent, J. Diet. Suppl., 9 (2012) 45–56.

[137] D. Delmas, E. Solary, N. Latruffe, Resveratrol, a phytochemical inducer of multiple cell death pathways: apoptosis, autophagy and mitotic catastrophe, Curr. Med. Chem., 18 (2011) 1100–1121.

[138] J. Tomé-Carneiro, M. Larrosa, A. González-Sarrías, F.A. Tomás-Barberán, M.T. García-Conesa, J.C. Espín, Resveratrol and clinical trials: the crossroad from in vitro studies to human evidence, Curr. Pharm. Des., 19 (2013) 6064–6093.

[139] Y.P. Palve, P.L. Nayak, Curcumin : A wonder anticancer drug, Int. J. Pharm. Biomed. Sci., 3 (2012) 60–69.

[140] G. Sa, T. Das, S. Banerjee, J. Chakraborty, Curcumin : From exotic spice to modern anticancer drug, Al Ameen J. Med. Sci., 3 (2010) 21–37.

[141] A. Barik, B. Mishra, A. Kunwar, R.M. Kadam, L. Shen, Comparative study of copper (II) e curcumin complexes as superoxide dismutase mimics and free radical scavengers, Eur. J. Med. Chem., 42 (2007) 431–439.

[142] R. Wilken, M.S. Veena, M.B. Wang, E.S. Srivatsan, Curcumin : A review of anti-cancer properties and therapeutic activity in head and neck squamous cell carcinoma, Mol. Cancer, 10:12 (2011) 1–19.

[143] S.C. Gupta, S. Prasad, J.H. Kim, S. Patchva, L.J. Webb, I.K. Priyadarsini, B.B. Aggarwal, Multitargeting by curcumin as revealed by molecular interaction studies, Nat. Prod. Rep., 28 (2011) 1937.

[144] A. Barik, B. Mishra, A. Kunwar, K.I. Priyadarsini, Interaction of curcumin with human serum albumin : Thermodynamic properties , fluorescence energy transfer and denaturation effects, Chem. Phys. Lett., 436 (2007) 239–243.

[145] A. Kunwar, A. Barik, R. Pandey, K.I. Priyadarsini, Transport of liposomal and albumin loaded curcumin to living cells : An absorption and fluorescence spectroscopic study, Biochim. Biophys. Acta - Gen. Subj., 1760 (2006) 1513–1520.

[146] P. Anand, S.G. Thomas, A.B. Kunnumakkara, C. Sundaram, K.B. Harikumar, B. Sung, S.T. Tharakan, K. Misra, I.K. Priyadarsini, K.N. Rajasekharan, B.B. Aggarwal, Biological activities of curcumin and its analogues (Congeners) made by man and Mother Nature, Biochem. Pharmacol., 76 (2008) 1590–1611.

[147] V. Palani, R.K. Senthilkumaran, S. Govindasamy, Biochemical evaluation of antitumor effect of

Muthu Marunthu (a herbal formulation) on experimental fibrosarcoma in rats, J. Ethnopharmacol., 65 (1999) 257–265.

[148] S.P. Duggal, A.R.S. Kartha, Antioxidants for edible oils and fats from seeds of Myristica species, Indian J. Agric. Sci, 26 (1956) 391–399.

[149] A.S. and J.D.C. Kozhiparambil K. Purushothaman, Malabaricones A–D, novel diarylnonanoids from Myristica malabarica Lam (Myristicaceae), J. Chem. Soc., Perkin Trans., 6 (1977) 587–588.

[150] F. Khandom, H. Kayahara, K. Tadasa, Superoxide-scavanging and prolyl endopeptidase inhibitory activities of Bangladeshi indigenous medicinal plants, Biosci. Biotechnol. Biochem., 64 (2000) 837–840.

[151] B.S. Patro, A.K. Bauri, S. Mishra, S. Chattopadhyay, Antioxidant activity of Myristica malabarica extracts and their constituents, J. Agric. Food Chem., 53 (2005) 6912–6918.

[152] D. Banerjee, B. Maity, A.H. Bandivdeker, S.K. Bandyopadhyay, S. Chattopadhyay, Angiogenic and cell proliferating action of the natural diarylnonanoids, malabaricone B and malabaricone C during healing of indomethacin-induced gastric ulceration, Pharm. Res., 25 (2008) 1601–1609.

[153] D. Banerjee, B. Maity, A.K. Bauri, S.K. Bandyopadhyay, S. Chattopadhyay, Gastroprotective properties of Myristica malabarica against indomethacin-induced stomach ulceration : a mechanistic exploration, J. Pharm. Pharmacol., 59 (2007) 1–11.

[154] Y.M. Chong, W.F. Yin, C.Y. Ho, M.R. Mustafa, A.H.A. Hadi, K. Awang, P. Narrima, C. Koh, D.R. Appleton, K. Chan, Malabaricone C from Myristica cinnamomea exhibits anti-quorum sensing activity, J. Nat. Prod., 74 (2011) 2261–2264.

[155] B. Maity, S.K. Yadav, B.S. Patro, M. Tyagi, S.K. Bandyopadhyay, S. Chattopadhyay, Molecular mechanism of the anti-inflammatory activity of a natural diarylnonanoid, malabaricone C, Free Radic. Biol. Med., 52 (2012) 1680–1691.

[156] J. Kang, N. Tae, B. Sun, J. Choe, J. Lee, Malabaricone C suppresses lipopolysaccharide-induced in fl ammatory responses via inhibiting ROS-mediated Akt / IKK / NF- κ B signaling in murine macrophages, Int. Immunopharmacol., 14 (2012) 302–310.

[157] S. Lee, J. Seo, S. Ryoo, T.D. Cuong, B. Min, J. Lee, Malabaricone C inhibits PDGF-induced Proliferation and migration of aortic smooth muscle cells through induction of heme oxygenase-1, J. Cell. Biochem., 113 (2012) 2866–2876.

[158] B.S. Patro, M. Tyagi, J. Saha, S. Chattopadhyay, Comparative nuclease and anti-cancer properties of the naturally occurring malabaricones, Bioorganic Med. Chem., 18 (2010) 7043–7051.

[159] M. King, G. Attadi, Mitochondria-mediated transformation of human rho(0) cells, Methods Enzym., 264 (1996) 313–334.

[160] J. Cao, Y. Liu, L. Jia, H. Zhou, Y. Kong, G. Yang, L. Jiang, Curcumin induces apoptosis through mitochondrial hyperpolarization and mtDNA damage in human hepatoma G2 cells, Free Radic. Biol. Med., 43 (2007) 968–975.

[161] P. Desjardins, E. Frost, R. Morais, Ethidium bromide-induced loss of mitochondrial DNA from

primary chicken embryo fibroblasts, Mol. Cell. Biol., 5 (1985) 1163–1169.

[162] B. Kalyanaraman, V. Darley-Usmar, K.J.A. Davies, P.A. Dennery, H.J. Forman, M.B. Grisham, G.E. Mann, K. Moore, L.J. Roberts, H. Ischiropoulos, Measuring reactive oxygen and nitrogen species with fluorescent probes: Challenges and limitations, Free Radic. Biol. Med., 52 (2012) 1–6.

[163] A. Gomes, E. Fernandes, J.L.F.C. Lima, Fluorescence probes used for detection of reactive oxygen species, J. Biochem. Biophys. Methods, 65 (2005) 45–80.

[164] D.W. Hedley, S. Chow, Evaluation of methods for measuring cellular glutathione content using flow cytometry, Cytometry, 15 (1994) 349–58.

[165] P.L. Olive, J.P. Banáth, The comet assay: a method to measure DNA damage in individual cells, Nat. Protoc., 1 (2006) 23–29.

[166] J. Mendez, B. Stillman, Chromatin Association of Human Origin Recognition Complex , Cdc6 , and Minichromosome Maintenance Proteins during the Cell Cycle : Assembly of Prereplication Complexes in Late Mitosis, Mol. Cell. Biol., 20 (2000) 8602–8612.

[167] B.S. Patro, R. Frohlich, V. a. Bohr, T. Stevnsner, WRN helicase regulates the ATR-CHK1-induced S-phase checkpoint pathway in response to topoisomerase-I-DNA covalent complexes, J. Cell Sci., 124 (2011) 3967–3979.

[168] L. Huo, H. Yao, X. Wang, G.W. Wong, H.F. Kung, M.C. Lin, Inhibition of melanoma growth by subcutaneous administration of hTERTC27 viral cocktail in C57BL/6 mice, PLoS One, 5 (2010) 1–9.

[169] W.W. Overwijk, N.P. Restifo, B16 as a Mouse Model for Human Melanoma, in: Curr. Protoc. Immunol., 39:20.1:20 ed., 2001: pp. 1–33.

[170] S. Shrotriya, G. Deep, M. Gu, M. Kaur, a. K. Jain, S. Inturi, R. Agarwal, C. Agarwal, Generation of reactive oxygen species by grape seed extract causes irreparable DNA damage leading to G2/M arrest and apoptosis selectively in head and neck squamous cell carcinoma cells, Carcinogenesis, 33 (2012) 848–58.

[171] M.F. Favata, K.Y. Horiuchi, E.J. Manos, A.J. Daulerio, D.A. Stradley, W.S. Feeser, D.E. Van Dyk, W.J. Pitts, R.A. Earl, F. Hobbs, R.A. Copeland, R.L. Magolda, P.A. Scherle, J.M. Trzaskos, P.D. Dudley, A.R. Proc, N.A.S.U.S. A, Identification of a novel inhibitor of mitogen-activated protein kinase kinase, J. Biol. Chem., 273 (1998) 18623–18632.

[172] A.M. Weber, A.J. Ryan, Pharmacology & Therapeutics ATM and ATR as therapeutic targets in cancer, Pharmacol. Ther., 149 (2015) 124–138.

[173] H. Nishida, N. Tatewaki, Y. Nakajima, T. Magara, K.M. Ko, Y. Hamamori, T. Konishi, Inhibition of ATR protein kinase activity by schisandrin B in DNA damage response, Nucleic Acid Res., 37 (2009) 5678–5689.

[174] Janicke Reiner U., MCF-7 breast carcinoma cells do not express caspase-3, Breast Cancer Res Treat, 117 (2009) 219–221.

[175] A. Görlach, K. Bertram, S. Hudecova, O. Krizanova, Redox Biology Calcium and ROS : A mutual interplay, 6 (2015) 260–271.

[176] A. Degterev, M. Boyce, J. Yuan, A decade of caspases, (2003) 8543–8567.

[177] S. Jana, M. Sinha, D. Chanda, T. Roy, K. Banerjee, S. Munshi, B.S. Patro, S. Chakrabarti, Mitochondrial dysfunction mediated by quinone oxidation products of dopamine: Implications in dopamine cytotoxicity and pathogenesis of Parkinson's disease, Biochim. Biophys. Acta - Mol. Basis Dis., 1812 (2011) 663–673.

[178] E. Shaulian, M. Karin, AP-1 in cell proliferation and survival, Oncogene, 20 (2001) 2390–2400.

[179] N. Meyer, S.S. Kim, L.Z. Penn, The Oscar-worthy role of Myc in apoptosis, Semin. Cancer Biol., 16 (2006) 275–287.

[180] A. V Vaseva, U.M. Moll, The mitochondrial p53 pathway, BBA - Bioenerg., 1787 (2009) 414–420.

[181] T. Söderdahl, M. Enoksson, M. Lundberg, A. Holmgren, O.P. Ottersen, S. Orrenius, G. Bolcsfoldi, I. a. Cotgreave, Visualization of the compartmentalization of glutathione and protein-glutathione mixed disulfides in cultured cells, FASEB J., 17 (2003) 124–126.

[182] S.W. Aesif, Y.M.W. Janssen-heininger, N.L. Reynaert, Protocols for the Detection of S -Glutathionylated and S -Nitrosylated Proteins In Situ, in: Methods Enzymol., 1st ed., Elsevier Inc., 2010: pp. 289–296.

[183] M. Mihara, S. Erster, A. Zaika, O. Petrenko, T. Chittenden, P. Pancoska, U.M. Moll, S. Brook, N. York, S. Street, p53 has a direct apoptogenic role at the mitochondria, Mol. Cell, 11 (2003) 577–590.

[184] J.S. Rathee, B.S. Patro, L. Brown, S. Chattopadhyay, Mechanism of the anti-hypertensive property of the naturally occurring phenolic , malabaricone C in DOCA-salt rats, Free Radic. Res., 50 (2016) 111–121.

[185] R.L. Siegel, K.D. Miller, A. Jemal, Cancer Statistics, 2015, CA. Cancer J. Clin., 65 (2015) 5–29.

[186] H. Wang, T.O. Khor, L. Shu, Z. Su, F. Fuentes, J.-H. Lee, K. Tony Ah-Ng, Plants Against Cancer: A Review on Natural Phytochemicals in Preventing and Treating Cancers and Their Druggability, Anticancer Agents Med Chem, 12 (2012) 1281–1305.

[187] A. Manna, P. Saha, A. Sarkar, D. Mukhopadhyay, A.K. Bauri, D. Kumar, P. Das, S. Chattopadhyay, M. Chatterjee, Malabaricone-A induces a redox imbalance that mediates apoptosis in U937 cell line, PLoS One, 7 (2012) e36938.

[188] S. Wu, L. Hang, J. Yang, H. Chen, H. Lin, J. Chiang, C. Lu, J. Yang, Curcumin Induces Apoptosis in Human Non-small Cell Lung Cancer NCI-H460 Cells through ER Stress and Caspase Cascade- and Mitochondria-dependent Pathways, Anticancer Res., 30 (2010) 2125–2133.

[189] J.D. Lambert, S. Sang, C.S. Yang, N- Acetylcysteine enhances the lung cancer inhibitory effect of epigallocatechin-3-gallate and forms a new adduct, Free Radic. Biol. Med., 44 (2008) 1069–1074.

[190] S. DE Flora, F. D'Agostini, L. Masiello, D. Giunciuglio, Adriana Albini, Synergism between N-acetylcysteine and doxorubicin in the prevention of tumorigenicity and metastasis in murine models, Int J Cancer., 67 (1996) 842–848.

[191] L. Raj, T. Ide, A.U. Gurkar, M. Foley, M. Schenone, X. Li, N.J. Tolliday, T.R. Golub, S.A. Carr, A.F.

Shamji, A.M. Stern, A. Mandinova, S.L. Schreiber, S.W. Lee, Selective killing of cancer cells by a small molecule targeting the stress response to ROS, Nature, 475 (2011) 231–234.

[192] Q. Liang, P.C. Dedon, Cu(II)/H2O2-induced DNA damage is enhanced by packaging of DNA as a nucleosome, Chem. Res. Toxicol., 14 (2001) 416–422.

[193] S. V Singh, S.K. Srivastava, S. Choi, K.L. Lew, J. Antosiewicz, D. Xiao, Y. Zeng, S.C. Watkins, C.S. Johnson, D.L. Trump, Y.J. Lee, H. Xiao, A. Herman-antosiewicz, Sulforaphane-induced Cell Death in Human Prostate Cancer Cells Is Initiated by Reactive Oxygen Species *, J. Biol. Chem., 280 (2005) 19911–19924.

[194] R. Franco, C. Bortner, I. Schmitz, J.A. Cidlowski, Glutathione depletion regulates both extrinsic and intrinsic apoptotic signaling cascades independent from multidrug resistance protein 1, Apoptosis, 19 (2014) 117–134.

[195] Zandwijk N. V., N-acetylcysteine (NAC) and glutathione (GSH): antioxidant and chemopreventive properties, with special reference to lung cancer, J. Cell. Biochem. Suppl., 22 (1995) 24–32.

[196] M. Zafarullah, J.S. W. Q. Li, M. Ahmad, Molecular mechanisms of N-acetylcysteine actions, Cell. Mol. Life Sci., 60 (2003) 6–20.

[197] B.S. Shankar, R. Pandey, P. Amin, H.S. Misra, K.B. Sainis, Role of glutathione in augmenting the anticancer activity of pyrroloquinoline quinone (PQQ), Redox Rep., 15 (2010) 146–154.

[198] C. Cosentino, G. Schmalz, G. Spagnuolo, V.D. Anto, H. Schweikl, S. Rengo, Effect of N -acetyl- L -cysteine on ROS production and cell death caused by HEMA in human primary gingival fibroblasts, Biomaterials, 27 (2006) 1803–1809.

[199] P. Sinha, Y. Shin, A.M. Hays, K. Gates, D. Sun, Cellular responses to the DNA damaging natural compound Leinamycin, J. Cancer Sciecnce Ther., S8:003 (2012) 1–7.

[200] H. Shen, C. Yang, J. Liu, C. Ong, Dual role of glutathione in selenite-induced oxidative stress and apoptosis in human hepatoma cells, Free Radic. Biol. Med., 28 (2000) 1115–1124.

[201] S. Awasthi, U. Pandya, S.S. Singhal, J.T. Lin, V. Thiviyanathan, W.E. Seifert, Y.C. Awasthi, G.A.S. Ansari, Curcumin – glutathione interactions and the role of human glutathione S -transferase P1-1, Chem. Biol. Interact., 128 (2000) 19–38.

[202] R. Checker, D. Sharma, S.K. Sandur, N.M. Khan, Vitamin K3 suppressed infl ammatory and immune responses in a redox-dependent manner, Free Radic. Res., 45 (2011) 975–985.

[203] M.A. Garcia, S. Alvarez, H. Sailem, V. Bousgouni, J. Sero, C. Bakal, Differential RNAi screening provides insights into the rewiring of signalling networks during oxidative stress w z, Mol. Biosyst., 8 (2012) 2605–2613.

[204] M.A.H. Talukder, W.M. Johnson, S. Varadharaj, J. Lian, P.N. Kearns, M.A. El-mahdy, X. Liu, J.L. Zweier, E. Ma, X. Liu, Z. Jl, Chronic cigarette smoking causes hypertension , increased oxidative stress , impaired NO bioavailability , endothelial dysfunction , and cardiac remodeling in mice, (2011) 388–396.

[205] G. Brum, T. Carbone, E. Still, V. Correia, K. Szulak, D. Calianese, C. Best, G. Cammarata, K. Higgins,

F. Ji, W. Di, Y. Wan, N-acetylcysteine potentiates doxorubicin-induced ATM and p53 activation in ovarian cancer cells, Int. J. Oncol., 42 (2013) 211–218.

[206] H.U. Simon, A. Haj-Yehia, F. Levi-Schaffer, Role of reactive oxygen species (ROS) in apoptosis induction, Apoptosis, 5 (2000) 415–418.

[207] Y. Li, C.R. Goodwin, Y. Sang, E.M. Rosen, J. Laterra, S. Xia, Camptothecin and Fas receptor agonists synergistically induce medulloblastoma cell death: ROS-dependent mechanisms, Anticancer. Drugs, 20 (2009) 770–778.

[208] P. Zou, J. Zhang, Y. Xia, K. Kanchana, G. Guo, ROS generation mediates the anti-cancer effects of WZ35 via activating JNK and ER stress apoptotic pathways in gastric cancer, Oncotarget, 6 (2014) 5860–5876.

[209] R. Marullo, E. Werner, N. Degtyareva, B. Moore, G. Altavilla, S. Suresh, P.W. Doetsch, Cisplatin induces a mitochondrial-ROS response that contributes to cytotoxicity depending on mitochondrial redox status and bioenergetic functions, PLoS One, 8 (2013) e81162.

[210] I.A. Manke, A. Nguyen, D. Lim, M.Q. Stewart, A.E.H. Elia, M.B. Yaffe, MAPKAP Kinase-2 is a cell cycle checkpoint kinase that regulates the G2/M transition and S phase progression in response to UV irradiation, Mol. Cell, 17 (2005) 37–48.

[211] C. Huang, W. Ma, A. Maxiner, Y. Sun, Z. Dong, p38 Kinase Mediates UV-induced Phosphorylation of p53 Protein at Serine 389, J. Biol. Chem., 274 (1999) 12229–12235.

[212] A. Mansouri, L.D. Ridgway, A.L. Korapati, Q. Zhang, L. Tian, Y. Wang, Z.H. Siddik, G.B. Mills, X. Claret, Sustained Activation of JNK / p38 MAPK Pathways in Response to Cisplatin Leads to Fas Ligand Induction and Cell Death in Ovarian Carcinoma Cells *, J. Biol. Chem., 278 (2003) 19245–19256.

[213] W.P. Roos, B. Kaina, DNA damage-induced cell death by apoptosis, Trends Mol. Med., 12 (2006) 440–450.

[214] J. Im, J. Lee, ATR-dependent activation of p38 MAP kinase is responsible for apoptotic cell death in cells depleted of Cdc7, J. Biol. Chem., 283 (2008) 25171–25177.

[215] L. Vela, I. Marzo, Bcl-2 family of proteins as drug targets for cancer chemotherapy : the long way of BH3 mimetics from bench to bedside, Curr. Opin. Pharmacol., 23 (2015) 74–81.

[216] M.R. Junttila, S. Li, J. Westermarck, M. Mapk, Phosphatase-mediated crosstalk between MAPK signaling pathways in the regulation of cell survival, FASEB J., 22 (2008) 954–965.

[217] X. Wang, L. Cui, J. Joseph, B. Jiang, D. Pimental, D.E. Handy, R. Liao, J. Loscalzo, Journal of molecular and cellular Cardiology Homocysteine induces cardiomyocyte dysfunction and apoptosis through p38 MAPK-mediated increase in oxidant stress, J. Mol. Cell. Cardiol., 52 (2012) 753–760.

[218] H.J. Cho, S. Park, E.M. Hwang, K.E. Baek, I. Kim, I. Nam, M. Im, S. Park, S. Bae, J. Park, J. Yoo, Gadd45b mediates Fas-induced apoptosis by enhancing the interaction between p38 and retinoblastoma tumor suppressor, J. Biol. Chem., 285 (2010) 25500–25505.

[219] M. Gatei, K. Sloper, C. So, R. Syljua, J. Falck, K. Hobson, K. Savage, J. Lukas, B. Zhou, J. Bartek, K. Kum, Ataxia-telangiectasia-mutated (ATM) and NBS1-dependent phosphorylation of Chk1 on Ser-317 in response to ionizing radiation, J. Biol. Chem., 278 (2003) 14806–14811.

[220] C.S. Sørensen, R.G. Syljua, J. Falck, T. Schroeder, L. Ro, Chk1 regulates the S phase checkpoint by coupling the physiological turnover and ionizing radiation-induced accelerated proteolysis of Cdc25A, Cancer Cell, 3 (2003) 247–258.

[221] T. Nakagawa, J. Yuan, Cross-talk between two cysteine protease families : activation of caspase-12 by calpain in apoptosis, J. Cell Biol., 150 (2000) 887–894.

[222] S. Orrenius, B. Zhivotovsky, P. Nicotera, Regulation of cell death : The Calcium – Apoptosis link, Nat. Rev. Mol. Cell Biol., 4 (2003) 552–565.

[223] K.F. Ferri, G. Kroemer, Organelle-specific initiation of cell death pathways, Nat. Cell Biol., 3 (2001) E255–E263.

[224] A. Johansson, H. Appelqvist, C. Nilsson, K. Kagedal, K. Roberg, K. Ollinger, Regulation of apoptosis-associated lysosomal membrane permeabilization, Apoptosis, 15 (2010) 527–540.

[225] L.E. Bro, C. Huisman, S.W. Span, A. Rodriguez, F.A.E. Kruyt, G. Giaccone, Cathepsin B mediates caspase-independent cell death induced by microtubule stabilizing agents in non-small cell lung cancer cells, Cancer Res., 64 (2004) 27–30.

[226] M. Lamparska-przybysz, B. Gajkowska, T. Motyl, M. Lamparska-przybysz, B. Gajkowska, T. Motyl, BID-deficient breast cancer MCF-7 cells as a model for the study of autophagy in cancer therapy, Autophagy, 8627 (2016) 3–5.

[227] S.S. Zinkel, K.E. Hurov, C. Ong, F.M. Abtahi, A. Gross, S.J. Korsmeyer, A role for proapoptotic BID in the DNA-damage response, Cell, 122 (2005) 579–591.

[228] S.N. Shelton, M.E. Shawgo, J.D. Robertson, Cleavage of Bid by executioner caspases mediates feed forward amplification of mitochondrial outer membrane permeabilization during genotoxic stress-induced apoptosis in jurkat cells, 2009, 284 (2009) 11247–11255.

[229] S. Anguissola, B. Ko, R.O. Byrne, H. Du, M.D. Cannon, F.E. Murray, C.G. Concannon, M. Rehm, D. Ko, Bid and calpains cooperate to trigger oxaliplatin-induced apoptosis of cervical carcinoma HeLa cells, Mol. Pharmacol., 76 (2009) 998–1010.

[230] A. Terman, T. Kurz, B. Gustafsson, U.T. Brunk, Lysosomal Labilization, IUBMB Life, 58 (2006) 531–539.

[231] M. Tyagi, R. Bhattacharyya, A.K. Bauri, B.S. Patro, S. Chattopadhyay, DNA damage dependent activation of checkpoint kinase-1 and mitogen-activated protein kinase-p38 are required in malabaricone C-induced mitochondrial cell death, Biochim. Biophys. Acta - Gen. Subj., 1840 (2014) 1014–1027.

[232] B. Piret, S. Schoonbroodt, J. Piette, The ATM protein is required for sustained activation of NF-kappaB following DNA damage, Oncogene, 18 (1999) 2261–2271.

[233] T.T. Huang, S.M. Wuerzberger-davis, B.J. Seufzer, S.D. Shumway, T. Kurama, D.A. Boothman, S.

Miyamoto, NF-kappaB activation by camptothecin A linkage between nuclear DNA damage and cytoplasmic signaling events, J. Biol. Chem., 275 (2000) 9501–9509.

[234] T.T. Huang, S.M. Wuerzberger-davis, B.J. Seufzer, S.D. Shumway, T. Kurama, D.A. Boothman, S. Miyamoto, NF- B Activation by Camptothecin, 275 (2000) 9501–9509.

[235] S. Qanungo, M. Wang, A. Nieminen, N -Acetyl- L -cysteine enhances apoptosis through inhibition of Nuclear Factor-kB in hypoxic murine embryonic fibroblasts, J. Biol. Chem., 279 (2004) 50455–50464.

[236] A.L. Fitzgerald, A.A. Osman, T. Xie, A. Patel, H. Skinner, V. Sandulache, J.N. Myers, Reactive oxygen species and p21 Waf1 / Cip1 are both essential for p53-mediated senescence of head and neck cancer cells, Cell Death Dis., 6 (2015) e1678–10.

[237] M.D. Shelton, P.B. Chock, J.J. Mieyal, Glutaredoxin: Role in reversible protein S-glutathionylation and regulation of redox signal transduction and protein translocation, Antioxid. Redox Signal., 7 (2005) 348–366.

[238] C.S. Velu, S.K. Niture, C.E. Doneanu, N. Pattabiraman, K.S. Srivenugopal, Human p53 is inhibited by glutathionylation of cysteines present in the proximal DNA-Binding domain during oxidative stress, Biochemistry, 46 (2007) 7765–7780.

[239] S. Qanungo, J.D. Uys, Y. Manevich, A.M. Distler, B. Shaner, E.G. Hill, J.J. Mieyal, J.J. Lemasters, D.M. Townsend, A.-L. Nieminen, N-acetyl-l-cysteine sensitizes pancreatic cancers to gemcitabine by targeting the NFκB pathway, Biomed. Pharmacother., 68 (2014) 855–864.

[240] J. Markovic, C. Borrás, Á. Ortega, J. Sastre, J. Viña, F. V. Pallardó, Glutathione is recruited into the nucleus in early phases of cell proliferation, J. Biol. Chem., 282 (2007) 20416–20424.

[241] A. Sarkar, Y. Sreenivasan, G.T. Ramesh, S.K. Manna, beta-D-Glucoside suppresses tumor necrosis factor-induced activation of nuclear transcription factor k B but potentiates apoptosis, J. Biol. Chem., 279 (2004) 33768–33781.

[242] F.M. Moodie, J.A. Marwick, C.S. Anderson, P. Szulakowski, S.K. Biswas, M.R. Bauter, I. Kilty, I. Rahman, Oxidative stress and cigarette smoke alter chromatin remodeling but differentially regulate NF- κ B activation and proinflammatory cytokine release in alveolar epithelial cells, FASEB J, 18 (2004) 1897–1899.

[243] D. Speidel, Transcription-independent p53 apoptosis: an alternative route to death, Trends Cell Biol., 20 (2010) 14–24.

[244] S. Wolff, S. Wolff, S. Erster, G. Palacios, U.M. Moll, p53's mitochondrial translocation and MOMP action is independent of Puma and Bax and severely disrupts mitochondrial membrane integrity, Cell Res., 18 (2008) 733–744.

[245] R.R. Perry, J. Mazetta, M. Levin, Glutathione levels and variability in breast tumors and normal tissue, Cancer, 72 (1993) 783–787.

[246] T.C. Chang, M.J. Chang, S. Hsueh, Glutathione concentration and distribution in cervical cancers and adjacent normal tissues, Gynecol Obs. Invest., 36 (1993) 52–55.

[247] C.R. Wolf, A.D. Lewis, J. Carmichael, D.J. Adams, S.G. Allan, D.J. Ansell, The role of glutathione in determining the response of normal and tumor cells to anticancer drugs, Biochem. Soc. Trans., 15 (1987) 728–30.

[248] L.K. Hosking, R.D.H. Whelan, S.A. Shellard, P. Bedford, B.T. Hill, An evaluation of the role of glutathione and its associated enzymes in the expression of differential sensitivities to antitumour agents shown by a range of human tumour cell lines, Biochem. Pharmacol., 40 (1990) 1833–1842.

[249] N.T. Christie, The synergistic interaction of Nickel(II) with dna damaging agents, Toxicol. Environ. Chem., 22 (1989) 51–59.

[250] X. Shang, Y. Shiono, Y. Fujita, Y. Oka, S. Yamazaki, Synergistic enhancement of apoptosis by DNA- and cytoskeleton-damaging agents: a basis for combination chemotherapy of cancer, Anticancer Res., 21 (2001) 2585–2589.

[251] M. Stiborová, T. Eckschlager, J. Poljaková, J. Hrab, V. Adam, R. Kizek, E. Frei, The synergistic effects of DNA-targeted chemotherapeutics and histone deacetylase inhibitors as therapeutic strategies for cancer treatment, Curr. Med. Chem., 19 (2012) 4218–4238.

[252] M.J. Kelner, T.C. Mcmorris, R.J. Rojas, L.A. Estes, P. Suthipinijtham, Synergy of irofulven in combination with other DNA damaging agents : synergistic interaction with altretamine , alkylating , and platinum-derived agents in the MV522 lung tumor model, Cancer Chemother. Pharmacol., 63 (2008) 19–26.

[253] B.K. Manjunatha, V. Hegde, N. Abhilash, R. Divakara, Research Journal of Pharmaceutical , Biological and Chemical Sciences Evaluation of Invitro Antioxidant and Invivo Hepatoprotective Potency of Myristica Malabarica, Res. J. Pharm. Biol. Chem. Sci., 3 (2012) 1044–1052.

[254] E. Martati, R. Boonpawa, J.H.J. Van Den Berg, A. Paini, A. Spenkelink, A. Punt, J. Vervoort, P.J. Van Bladeren, I.M.C.M. Rietjens, Malabaricone C-containing mace extract inhibits safrole bioactivation and DNA adduct formation both in vitro and in vivo, Food Chem. Toxicol., 66 (2014) 373–384.